Neuroimaging Working Group Summary Report

June 18, 2015

Fort Detrick, MD

Booz | Allen | Hamilton

Table of Contents

List of Tables

List of Figures

Acronyms and Abbreviations

3D	Three Dimensional
ACC	Anterior Cingulate Cortex
ACR	American College of Radiology
ADC	Apparent Diffusion Coefficient
AIF	Apoptosis-inducing Factor
ANTs	Advanced Normalization Tools
ApoE	Apolipoprotein E
APP	Amyloid Precursor Protein
ASDH	Acute Subdural Hemorrhage
ASL	Arterial Spin Labeling
ATP	Adenosine Triphosphate
BBB	Blood-brain barrier
Bcl-2	B-cell lymphoma 2
BOLD	Blood Oxygenation Level-Dependent
C	Carbon
CAA	Cerebral Amyloid Angiopathy
CBF	Cerebral Blood Flow
CCHR	Canadian Computed Tomography Head Rules
CCCRP	Combat Casualty Care Research Program
CD68	Cluster of Differentiation 68
CDC	U.S. Centers for Disease Control and Prevention
Cho	Choline
CMB	Cerebral Microbleeds
$CMRO_2$	Cerebral Metabolic Rate of Oxygen
CNS	Central Nervous System
CPP	Cerebral Perfusion Pressure
Cr	Creatine
CSD	Cortical Spreading Depression
CSI	Chemical Shift Imaging
CT	Computed Tomography
CTA	Computed Tomography Angiography
CTE	Chronic Traumatic Encephalopathy
CTP	CT Perfusion
CVR	Cerebrovascular Reactivity
DCoE	Defense Centers of Excellence for Psychological Health and Traumatic Brain Injury
DCS	Diffuse Correlation Spectroscopy
DECT	Dual-Energy Computed Tomography
DKI	Diffusion Kurtosis Imaging
DLPFC	Dorsolateral Prefrontal Cortex
DMN	Default Mode Network
dMRI	Diffusion MRI

DoD	Department of Defense
DSI	Diffusion Spectrum Imaging
DSWA	Temporal Lobe Slow Waves
DTI	Diffusion Tensor Imaging
DVI	Diffuse Vascular Injury
ECD	Equivalent Current Dipole
EDH	Epidural (extradural) hemorrhage
ERF	Event Related Field
FA	Fractional Ansiotropy
FD	Frequency Domain
FDR	False Discovery Rate
FDG	fluorodeoxyglucose
FDG-PET	Flurodeoxyglucose Positron Emission Tomography
FITBIR	Federal Interagency for Traumatic Brain Injury Research
FLAIR	Fluid Attenuation Inversion Recovery
fMRI	Functional Magnetic Resonance Imaging
FNA	Functional Needs Assessment
FQ	Flow Quantification
FSL	FMRIB Software Library
GABA	Gamma-aminobutyric Acid
Glx	Glutamine
GM	Grey Matter
GRE	Gradient Echo
HARDI	High Angular Resolution Diffusion Imaging
HbO	Oxygenated Hemoglobin
HbR	Deoxygenated Hemoglobin
Hct	Hematocrit
H&E stain	Hematoxylin and Eosin Stain
HU	Hounsfield's Units
IADSA	Intra-arterial Digital Subtraction Angiography
ICA	Independent Component Analysis
ICAM-1	Intercellular Adhesion Molecule 1
ICH	Intracerebral Hemorrhages
ICP	Intracranial Pressure
IPR	In-Process Review
JCD	Joint Capabilities Document
JFHP	Joint Forces Health Protection
JPC-6	Joint Program Committee for Combat Casualty Care
kVp	Tube Voltage
L1	Longitudinal Diffusivity
Lt	Transverse Diffusivity
MABP	Mean Arterial Blood Pressure
MACE	Military Acute Concussion Evaluation
MAP-2	Microtubule Associated Protein
MCA	Middle Cerebral Artery

MD	Mean Diffusivity
MEG	Magnetoencephalography
MHC	Major Histocompatibility Complex
MHz	Megahertz
mI	Myo-inositol
MIP	Maximum Intensity Projection
MPR	Multiplanar Reformatting
MRA	Magnetic Resonance Angiography
MRS	Magnetic Resonance Spectroscopy
MRI	Magnetic Resonance Imaging
mRNA	Messenger RNA
MTC	Magnetization Transfer Contrast
Na	Sodium
NAA	N-Acetyl Aspartate
nAChR	Nicotinic acetylcholine receptor
NCCT	Non-contrast Head Computed Tomography
NEXUS	National Emergency X-ray Utilization Study
NFPs	Neurofilament Proteins
NFTs	Neurofibrillary Tangles
NIRS	Near Infrared Spectroscopy
NO	Nitric Oxide
OCT	Optical Coherence Tomography
P	Phosphorus
PC	Phase Contrast
PCS	Post-concussive Syndrome
PDHA	Post-deployment Health Assessment
PDHRA	Post-deployment Health Reassessment Program
PET	Positron Emission Tomography
PGP	Protein Gene Product
PRESS	Point-resolved Spectroscopy
PS	Phosphatidylserine
PTP	Pharmacological Thromboprophylaxis
PTSD	Post-Traumatic Stress Disorder
QSM	Quantitative Susceptibility Mapping
ROI	Region of Interest
Rs-fMRI	Resting State Functional Magnetic Resonance Imaging
SAH	Subarachnoid hemorrhage
SDH	Subdural Hemorrhage
SMS	Simultaneous Multi-Slice
SPECT	Single-Photon Emission Computed Tomography
SPM	Statistical Parametric Mapping
SQI	Signal Quality Index
SQUIDS	Superconducting Quantum Interface Devices
SRC	Sports Related Concussions
SWI	Susceptibility-weighted Imaging

TAI	Traumatic Axonal Injury
TBI	Traumatic Brain Injury
TBSS	Tract-based Spatial Statistics
TCD	Transcranial Doppler
tCMB	Trauma Cerebral Microbleeds
TD	Time Domain
TOF	Time-of-Flight
TRUST	T(2)-Relaxation-Under-Spin-Tagging
TSR	Time to Symptom-Resolution
USAMRMC	U. S. Army Medical Research and Materiel Command
VESTAL	VEctor-based Spatio-Temporal analysis using L1-minimum norm
WM	White Matter
Ya	Arterial Blood
Yv	Venous Blood

Executive Summary

The Department of Defense (DoD) Combat Casualty Care Research Program (CCCRP) neurotrauma portfolio contains research projects that aim to develop biomarkers (e.g., neuroimaging approaches, serum molecule detection methods) to improve the diagnosis, assessment, and study of traumatic brain injury (TBI) and its associated comorbidities. Neuroimaging is of particular interest as it is noninvasive and may provide important structural, physiological, and molecular information related to the injury.

The Joint Program Committee for Combat Casualty Care (JPC-6) recognizes that a strategic, forward-thinking plan is required to advance the effective use of neuroimaging in individuals with TBI. A step in the development of this strategic plan involves a working group analysis of the state of the field in the neuroimaging of TBI and discussion of critical issues that should be addressed to advance the field. The strategic approach was developed by: (i) assessing the current state of the science and ongoing research, (ii) identifying critical research gaps, and (iii) defining the essential priority areas for advancing clinical care.

The following critical issues related to the neuroimaging of TBI were identified by the group:

- Collection of large-scale normative neuroimaging data utilizing techniques and sequences relevant to TBI

- Public availability of large, longitudinal TBI-specific data sets containing high quality multimodal neuroimaging

- Standardization of neuroimaging acquisition parameters and development of data harmonization approaches to address vendor specific, scanner specific, and institution specific sources of variability

- Identification of neuroimaging features predictive of diagnosis and prognosis, along with optimal injury recovery and return to duty/work/play

- Development of FDA approved machine-learning based diagnostic platforms for the computational evaluation of advanced neuroimaging in a patient care setting

- Development of standardized, structured reporting methods for the clinical interpretation of neuroimaging studies

- Discovery, development, and validation of radiopharmaceuticals for the molecular neuroimaging of TBI

- Development neuroimaging approaches that may be deployed at echelons 1 or 2 of care for the diagnosis of TBI

- Improved understanding of anatomic and functional networks of the brain

- Improved understanding of TBI pathobiology to guide development of future imaging methods

The next step for the efficient and effective management of the neurotrauma research portfolio will be to mitigate these critical issues through prioritization of future research investments. The accumulation of these efforts holds the potential impact how TBI is managed by providing clinical neuroimaging data that would inform: (i) achieving a diagnosis, (ii) determining prognosis, and (iii) utilizing interventions to improve recovery and mitigate further injury.

Introduction

Traumatic brain injury (TBI) is a significant threat to warfighter health, performance, and survivability, and advances are needed to prevent and mitigate the effects of this threat. To target the needs of warfighters at risk of, or who sustain, a TBI, the Combat Casualty Care Research Program (CCCRP) at the U.S. Army Medical Research and Materiel Command (USAMRMC) manages a neurotrauma research portfolio of studies that spans the eight phases of the TBI continuum of care: basic science and epidemiology; prevention, education, and training; blast TBI; TBI screening; TBI assessment; TBI treatment; TBI recovery; and return to duty. The purpose of this research portfolio is to close high priority capability gaps in the TBI continuum of care areas and transition science and technology information and approaches to solutions for improving survivability and readiness of warfighters.

The current research strategy of the neurotrauma portfolio is shaped by directive requirements. These requirements are informed by TBI capability gaps and priorities identified by multiple sources, including the TBI gaps described in the Joint Forces Health Protection (JFHP) Joint Capability Document (JCD) and Functional Needs Assessment (FNA) requiring medical research and development efforts.[1]

The TBI gaps described in these requirements served as guidance for the identification of specific capability gaps to be addressed by the neurotrauma research portfolio. In November 2011, 25 neurotrauma portfolio capability gaps were identified through collaborative efforts between the USAMRMC and the Defense Centers of Excellence for Psychological Health and Traumatic Brain Injury (DCoE). Many of these gaps focus on developing biomarkers (e.g., neuroimaging data, neural proteins) to improve the diagnosis, assessment, and study of TBI and its associated comorbidities. Specifically, the JFHP capability gaps relevant to diagnosis, assessment, and study of TBI led to the development of 14 specific JPC-6 neurotrauma portfolio screening and assessment capability gaps that address these issues (Table 1.).

Table 1. Neurotrauma Portfolio Capability Gaps Specifically Relevant to TBI Diagnosis, Assessment, and Study

TBI Capability Gap
Return to Duty: Reliable, objective return to duty assessment (time for brain recovery, single mild TBI versus recurrent mild TBI, permissible activity following TBI)
Epidemiology: Long-term effects of TBI (including role of Tau protein, role of multiple TBIs, chronic traumatic encephalopathy)
TBI from Head Impact and Blast Exposure: Cumulative measurement of blast exposure/effects of repeated exposures
TBI Screening: Noninvasive, field-deployable, objective screening tool and/or biomarkers of TBI
TBI from Head Impact and Blast Exposure: Objective measures of exposure/impact (sensors) and injury threshold (validation of exposure criteria ["50m Rule"])
TBI Screening: Standardized diagnostic definition of TBI
TBI Screening: Validation of screening tests (MACE/PDHA/PDHRA)
Basic Science: Pathophysiology and genetic risk factors of TBI (including traumatic cerebral vasospasm; cell protein isoforms as targets for neuroprotection; and genomic, epigenetic, and proteomic risk factors)
TBI Recovery: Standardized outcomes measurement and tracking

TBI Assessment: Improved neurocognitive assessment (validation of NCATs, effective differential diagnosis methods to distinguish concussion from psychological health disorders)
TBI Assessment: Validation and standardization of balance, vision, auditory, and functional assessments
TBI Assessment: Correlation of neurobehavioral, neuroimaging, and sensorimotor assessments with clinical disposition and follow-up procedures
TBI Assessment: Standardized clinical prediction algorithms
Prevention, Education, and Training: Identification of risk factors to predict outcomes and course of recovery (validation of environmental, biological, psychological, and other risk factors)

The use of neuroimaging is of particular interest for determining diagnosis, prognosis, and potential intervention for TBI as it is noninvasive and may provide important structural, physiological and molecular information related to the injury. Several working group meetings were held from June through October 2014 to discuss the state of the field, and identify the critical issues related to the neuroimaging of TBI. The findings of the working group meetings are summarized in the next section.

Background

TBI is a leading cause of morbidity and mortality in service members deployed in Iraq and Afghanistan, an assertion supported by TBI accounting for almost 25% of medical evacuations from these recent armed conflicts.[2] Additionally, in the civilian population, mild TBI, also known as concussion, has been termed the "silent epidemic" and has been identified as a major public health concern by the U.S. Centers for Disease Control and Prevention. Despite the significant societal importance of this disease process, achieving diagnosis and determining prognosis in patients with TBI has been problematic for a variety of reasons. Some of these include: (i) difficulties in obtaining a clear history from an individual with TBI, (ii) overlap of TBI symptoms with other neurological and psychiatric conditions, (iii) lack of clear objective assessments predictive of diagnosis and prognosis.

Neuroimaging biomarkers have garnered significant interest as a potential method for providing objective data related to determining diagnosis and achieving prognosis for TBI. However, there currently exists a gap between powerful research neuroimaging techniques that are capable of revealing subtle details in TBI and those approaches that are available for use in clinical practice. At present, neuroimaging has little utility in the clinical neuroimaging of mild TBI. Often there is no easily measurable or objective radiological evidence of brain injury from current clinical neuroimaging techniques. Mild TBI is subtle and involves structural, physiological, and molecular alterations that cannot be readily detected with either conventional computed tomography (CT) or magnetic resonance imaging (MRI) scans. Subtle volume loss, damage to white matter tracts, clinically meaningful alterations in blood flow, alterations in proteins, and overall changes in neuronal connectivity are difficult to detect utilizing current clinical neuroimaging approaches.

Although the damage may escape detection with current routine imaging techniques, the effects certainly are not. Patients often suffer from a multitude of symptoms including headaches, dizziness, balance problems, fatigue, attention deficits, and memory difficulties. These symptoms are often incapacitating and take service members out of their mission, handicapping not only the service member, but often the entire mission at hand.

A critical need for the field of TBI is an objective, consistent way of performing measurements of the brain in injured patients. Over the past decade, a number of advanced neuroimaging approaches have emerged which have shown promise in the detection of the subtle alterations in patients with TBI. Most of these approaches remain confined to population based research studies. Other approaches require continued refinement towards methodologies that may be transformative for this disease process. New platforms may be required for bridging the gap between advanced research imaging and advanced clinical imaging. Additionally, the field has a present critical need for sequence standardization and collection of normative information. The sections below have been designed to lay out: (i) what is known concerning the pathobiology of TBI, (ii) current clinical imaging approaches for TBI, (iii) advanced methods for the imaging of TBI, and (iv) potentially transformative approaches for the field. It is hoped this information will serve as a reference as the community works to close critical gaps related to the neuroimaging of TBI.

Pathological Hallmarks of Neurotrauma

The pathobiology of TBI may be categorized as primary or secondary types of injury. Primary TBI is the consequence of mechanical forces producing tissue deformation at the moment of injury and results in direct injury to blood vessels, axons, neurons, and glia. The pattern of damage may be focal, multifocal, or diffuse and may initiate an evolving cascade of injury. Secondary traumatic brain damage is a sequelae of primary injury and may include hypoxic/ischemic changes, cerebral swelling, and consequences of raised intracranial pressure, hydrocephalus, and infection. Additionally, secondary traumatic brain damage may occur due to delayed injury cascades that evolve in the hours to months following the initial insult. Secondary brain damage is potentially reversible with adequate treatment. Traumatic head injury consists of different types of lesions that may occur in combination.[3] Lesions caused by blunt head trauma include contusions and/or lacerations of the brain parenchyma at the site of the impact (coup lesion), the site opposite to the impact (contra coup lesion). Lesions caused by acceleration/deceleration injury or heavy falling objects are accompanied by multifocal petechial hemorrhages in the parasagittal white matter, corpus callosum, and rostral brainstem. Projectile and explosive injuries of the central nervous system (CNS) are large kinetic energy injuries, which follow several basic laws of physics. Blunt force injuries are caused by relatively low velocity kinetic energy, and with objects larger than typical missile injuries.

The primary insult to the CNS, the direct mechanical damage, may represent injury that cannot be mitigated following trauma given its proximity to the injury. However, the delayed non-mechanical damage may represent a target for therapeutic intervention. This secondary damage may be influenced by changes in cerebral blood flow (hypo- and hyperperfusion), impairment of cerebrovascular autoregulation, cerebral metabolic dysfunction and inadequate cerebral oxygenation. Excitotoxic cell damage and inflammation may lead to apoptotic and necrotic cell death. Understanding the complexity of secondary brain injury is essential to apply differentiated therapeutic options.

The brain is covered by the scalp, skull dura matter and meninges, which constitute a natural barrier against trauma. Cerebrospinal fluid may provide additional protection, although this concept has not been well studied. The rigid nature of the skull, however, is a limitation, as brain parenchyma cannot expand in the event of edema or other space occupying lesions, such as hemorrhage, which may lead to herniation and death. The bony structures may also become the source of injury, inflicting contusions, and/or contrecoup injuries.[3,4]

Macroscopic Pathological Hallmarks of Neurotrauma

Hemorrhages of the dura mater:

- Epidural (extradural) hemorrhage (EDH): EDH is defined by the presence of blood in the epidural space. Usually located under an impact lesion of the scalp, and accompanied by linear fractures of the skull that lacerates a major meningeal artery. EDHs dissecting the dura from the skull and stop where the dura is tightly attached to the inner surface of the skull (sutures, insertion of the falx cerebri and tentorium). EDHs commonly represent a life threatening condition because the mass effect may cause increased intracranial

pressure and herniation of brain matter through the foramen magnum. When the hemorrhage is expanding in volume (more than 1 cm deep or more than 25 ml in volume), EDH is usually clinically significant and an indication for prompt surgical evacuation.[3,4] Of note, EDHs are frequently seen without significant parenchymal brain injuries; consequently, timely treatment, usually neurosurgical evacuation of hematoma, may result in full functional recovery. CT of the head is an excellent screening tool for this condition.

- Subdural hemorrhage (SDH): Common to many types of head trauma is the collection of blood in the potential space between the dura mater and the arachnoid. SDH may develop from capillary hemorrhages in cortical contusions, laceration of cortical arteries, and/or tears of bridging vessels. In most instances, SDH is the consequence of an impact injury with or without fracture of the skull. The risk of developing SDHs is enhanced in conditions of severe brain atrophy, anticoagulant treatment, arachnoid cysts, etc. Frequently, SDH accumulates at a slower rate than EDH, which allows compensatory mechanism to occur. SDH may evolve into organized subacute or chronic lesions that can be monitored by imaging and do not require immediate evacuation. Chronic SDHs (3 weeks or more) may expand/rebleed, which represents a significant risk for the patient. Inflammatory mediators (cytokines), fibrinolytic factors, angiogenic molecules and coagulation system factors is increased in the hematoma compared with serum, suggesting that the chronic subdural hematoma is a chronic inflammatory process.[5] The volume of SDHs should be measured or estimated with appropriate imaging studies. Most small acute subdural hemorrhage (ASDH) may resolve spontaneously, however a hematoma volume of 50-75 ml is potentially life threatening due to displacement of the brain parenchyma and associated herniations. Of note, nontraumatic SDH has been described in patients with spontaneous intracranial hypotension, and as a complication of meningiomas, metastatic dural neoplasms and hemodialysis.

Traumatic lesions of the brain:

- Subarachnoid hemorrhage (SAH): Bleeding into the subarachnoid space is one of the most common pathologic finding in head trauma. SAH is frequently multifocal and more prominent over the convexity of the hemispheres. The accumulation of blood may be so considerable that it acts as a local space-occupying lesion. The sequelae of traumatic SAH include obstruction of cerebrospinal fluid pathways, ventricular enlargement and fibrous scarring of the subarachnoid space, eventually leading to a delayed progressive communicating hydrocephalus. In TBI cases, SAH is a common neuroimaging finding. Traumatic subarachoid hemorrhage associated with parenchymal damage may have a less favorable outcome.

- Intracerebral hemorrhages (ICH): Traumatic parenchymal hemorrhages of the brain are usually associated with other traumatic brain lesions; however, hemorrhage can sometimes be the only sign of injury. The site of predilection is the cerebral white matter and occasionally the ventricular system. The pathogenesis of ICH is likely related to the deformation and rupture of the parenchymal blood vessels at the time of the injury. Large hematomas that act as space-occupying lesions result in increased intracranial pressure and may lead to subsequent transtentorial herniation. Traumatic parenchymal hematomas

may develop hours to days after the injury and may be not seen on imaging studies obtained immediately after the injury. Delayed traumatic intracerebral hematoma should be suspected in patients with secondary neurological deterioration after head injury.

- Cerebral contusions: Cerebral contusions are focal parenchymal injuries that result when mechanical forces damage small blood vessels, and other tissue components including nerve and glial cells of the CNS parenchyma. Most but not all contusions are hemorrhagic and represent bruising of the brain/cerebral tissue beneath the site of the impact, opposite or away from the site of the impact, deep in the parenchyma or as a result of displacement of the brain (herniation). Neurological deficits generally correlate with the size and location of contusions. Quantitation of the contusional injury and total vascular damage of the traumatized brain has been reported as the contusion index and vascular injury score, respectively.[6,7] Cerebral contusions may be classified as a) Coup contusions, when they occur underneath the site of impact as a result of contact traumatic forces), b) Contrecoup contusions, when they occur opposite or away from the site of the impact as a result the moving brain hitting the underlying bone), and c) Intermediate coup ontusions, when the lesion is seen in CNS parenchyma between the site of the impact and opposite side. Fracture contusions are found beneath a fracture, gliding contusions are seen in the parasagittal areas of the cerebrum as a result of acceleration/deceleration impulsive forces, herniation contusions result when the brain displaced against the bony skull, burst lobe refers to acerebral contusion combined with hematoma and an overlying acute SDH. Contusions may evolve with time and the progression/expansion can be demonstrated with CT and MRI imaging.

- Lacerations of the brain: Lacerations are parenchymal tears from high mechanical stress, frequently from skull fractures, but may also consequence from shearing forces secondary to acceleration/deceleration injuries. Traumatic hyperextension of the head and neck may cause lacerations of the brainstem, in particular at the pontomesencephalic or pontomedullary junctions.

- Cerebral edema: Edema or increased water content of the brain parenchyma is seen with traumatic brain injury represents a combination of cytotoxic (increased water content within the neurons and astrocytes) and vasogenic (increased extracellular water content secondary to disruption of the blood-brain barrier (BBB)) components. Brain edema may present grossly as diffuse flattening of the gyri, collapse of the ventricular system, and a narrowed or compressed aqueduct of Sylvius. Brain weight is not a reliable indicator of brain edema, because of the great variability in normal brain weights (1,200 to 1,800 g). Patterns of traumatic brain swelling may be characterized as swelling around the focal lesions (contusions, hemorrhages etc.), diffuse and unilateral hemispheric swelling of the brain. MR imaging in experimental models of TBI demonstrate the importance of cytotoxic edema and the persistence of such edema even after restoration of blood-brain barrier.[8]

- Brain herniations: Raised intracranial pressure (ICP) is one of the most important secondary complications of TBI that may lead to herniations. The spectrum encompasses cingulate (subfalcine), transtentorial, uncal and parahippocampal, central, tonsillar

cerebellar, rostral or upward cerebellar herniations and cerebral herniations through a craniotomy site. Herniated brain may show poor demarcation of the cortical mantle from the subjacent white matter and multifocal dusky discoloration, reflecting global or multifocal hypoxic-ischemic changes.

- Enlarged Virchow-Robin spaces, pituitary atrophy, cavum septum: As described in dementia pugilistica traumatic brain injuries are sometimes accompanied by widened Virchow-Robin spaces, pituitary atrophy and cavum septum pellucidum. Occasionally, the hypothalamus and pituitary can be affected in traumatic injuries.[9]

Projectile and explosive injuries of the CNS:

- Kinetic injury, cavitation**:** When a **projectile such as a bullet** passes through brain tissue characterized by high water content and lack of elasticity, a hydrodynamic effect is created, in which energy is passed into the fluid compartment and then accelerated in a radial direction. The permanent cavity created by a penetrating object is similar in size to the object itself. Temporary cavitation is the result of hydrodynamic forces seen with higher velocity bullets and will approximate the permanent cavity once the energy has been dissipated. However, it is significant because the concussive effect and tissue injury can be observed at some distance from the projectile path. Characteristic features are observed in distant, close-range and contact entrance gunshot wounds; exit wounds usually appear as lacerations. Orbital plate fractures are a common feature of facial trauma and may entrap extraocular muscles.[4]

- Explosive/blast related injury: The biomechanics of blast related injuries are very complex. In fact, there are three kinetic energy mechanisms and one thermal mechanism that can cause injury. **Primary blast injury** is caused by a positive pressure blast wave with the intensity and duration related to the type and size of the explosive. Although solid organs are less vulnerable than hollow, gas-filled organs, injury to the respiratory system can cause secondary effects such as multiple small air emboli that can travel to all organs including the CNS. As a result, multiple-infarcts can be seen in the brain, spinal cord and retina. The transfer of kinetic energy from the explosion of objects at the blast site causes **secondary blast injury**. For example, bomb fragments, and debris may behave as projectiles and cause variable injuries including penetration of the skull, similar to a firearm projectile. In **tertiary blast injury**, the victim is thrown by the energy from the explosion. Sudden acceleration and corresponding deceleration phases of this process. The brain and other solid organs are vulnerable to this type of injury, which is similar to those caused blunt force injury and falls (see above).[3,5]

- Ischemic damage in traumatic brain injury**:** Neuropathologic evidence of ischemic brain damage is observed in approximately 90% of patients who survived several hours after severe TBI. Areas of the brain that are selectively vulnerable include the hippocampus (81%), basal ganglia (79%), cerebral cortex (46%), and cerebellum (44%).[10,11] The mechanisms of ischemic damage are heterogeneous and complex and include raised intracranial pressure, global ischemia (ICP = CPP), global oligemia, and vascular pathology. Most ischemic changes can only be identified with comprehensive histological analysis.

Based on early blood flow studies, only about one-third of severe head injury patients showed reduced cerebral blood flow to ischemic levels (CBF<18ml/100g/min) 206 hours after injury with subsequent return to non-ischemic levels.[12] Recent studies with Xenon SPECT have shown correlation between the estimated volume of ischemic tissue and outcome.[13] In another report, positron-emission tomography (PET) scanning showed regional ischemia in patients with adequate cerebral perfusion pressure and ICP control.[14] Of note, PET abnormalities may be observed in brain with normal MR imaging.[15]

Cerebral vasospasm and ischemic damage in traumatic brain injury: Cerebral vasospasm has been documented angiographically and correlated with ischemic damage in patients with severe traumatic brain injury. These changes are predominantly observed in the distribution of the middle and/or the anterior cerebral arteries.[16,17] It has also been reported that transcranial Doppler ultrasonography can document changes consistent with vasospasm.[18]

Microscopic Pathological Hallmarks of Neurotrauma

TBI may be divided into primary and secondary types of injury. Primary TBI is the consequence of mechanical forces producing tissue deformation that may directly damage axons, neurons, glia and blood vessels. The damage may be diffuse, focal and/or multifocal. Secondary TBI develops as a complication of different types of primary brain damage and appears as ischemic/hypoxic damage and cerebral swelling. Patients who survive head injury long enough to be admitted to the hospital are usually present with diffuse/traumatic axonal injury (TAI), hypoxic/ischemic damage, and diffuse brain swelling. Diffuse vascular injury (DVI) consists of multiple small hemorrhages and is seen in patients who die soon after the head injury. TAI and DVI are initiated by mechanical forces at the time of the injury and evolve over time. Hypoxic/ischemic brain damage and diffuse brain swelling develop secondary to raised intracranial pressure with global and focal ischemia, and/or DVI or hypoxemia and also exhibit temporal progression. It is important to emphasize that in any given brain injury, primary and secondary forms of brain damage may have a complex and dynamic interplay resulting in lesions that are unique in anatomical site and number. It is also important to consider factors such as age, genetic predisposition, pre-existing disease, drugs, alcohol, and nutritional status among others.

The delayed consequences of TBI may continue to develop even years after the initial event. The spectrum of findings encompasses gray and white matter atrophy, gliosis, cavity formation, loss of neural tissue, selective or pan-necrosis, neural deinnervation/reinnervaton, trans-synaptic degeneration, and immune reactions. The evolving consequences of primary injury and the delayed consequences of secondary injury cumulatively interact over time (up to years).

Traumatic axonal injury may be focal, multifocal or diffuse: Traumatic axonal injury (TAI) refers to axonal damage caused by trauma. Experimental investigations have reported a spectrum of axonal damage including axonal swellings and axonal bulbs. The majority of changes are progressive occurring over several hours to days following injury. Axonal changes comprise axonal deformation at the moment of injury resulting focal axonal swelling, focal disruption of the axonal membrane, and over the next 6-12 hours, the proximal axonal segment disconnects from the distal segment, which undergoes Wallerian degeneration. The heterogeneity of TAI is assessed using any combination of techniques, which may include H&E stained sections, silver

impregnation techniques, immunohistochemistry for beta-amyloid precursor protein (APP), neurofilament proteins (NFPs), synaptophysin, ubiquitin, tau, protein gene product 9.5 (PGP 9.5). The morphological quantitation of the severity of axonal injury is challenging because the distribution and extent of axonal damage is not uniform. Experimental studies have also found that phosphorylated tau (a microtubule-associated protein) accumulates in injured axons and cell bodies.[19,20] Measurement of the cleaved forms of tau proteins in the cerebrospinal fluid is another approach to quantify TAI. Loss of microtubule-associated protein 2 (MAP-2) immunolabeling has been reported as an acute and persistent finding in trauma experiments in animals, and could also be a useful marker of dendritic pathology in cerebral ischemia and neuronal injury. Microglial activation (CD68 and MHC class II antigen immunolabeling) has also been detected in TAI.[21] The presence of microglial activation have been reported in the white matter following TBI with survival times up to 17 years.[22–24] Of note, increased number of microglia may be seen in CNS infections, neoplasms among others; it is not specific for TBI.

Diffuse/multifocal axonal injury is directly proportional to the duration of coma. The severity of TAI is graded on the basis of macroscopic findings and microscopic markers such as silver impregnation techniques to identify axonal swellings and bulbs. Neuroimaging of focal hemorrhagic and non-hemorrhagic lesions in the deep white matter, corpus callosum, and rostral brain stem represent a surrogate marker of traumatic axonal injury.

Raised intracranial pressure with brain herniation shows a non-hemorrhagic necrosis. APP immunostaining demonstrates a characteristic zigzag pattern, the so-called vascular axonal injury, which is attributed to hypoxic/ischemic injury. These changes along with other post-traumatic changes can be identified only in the properly fixed, sectioned and sampled autopsy brains employing comprehensive neurohistologic evaluation. Of note, APP reactivity may be difficult to interpret and is not specific for trauma. Reportedly, APP-positive axonal injury (AI) of fatal human cases mainly comprises AI secondary to ischemia.[25] An altered metabolic response with upregulation of APP messenger RNA (mRNA) has been reported in situ hybridization studies.
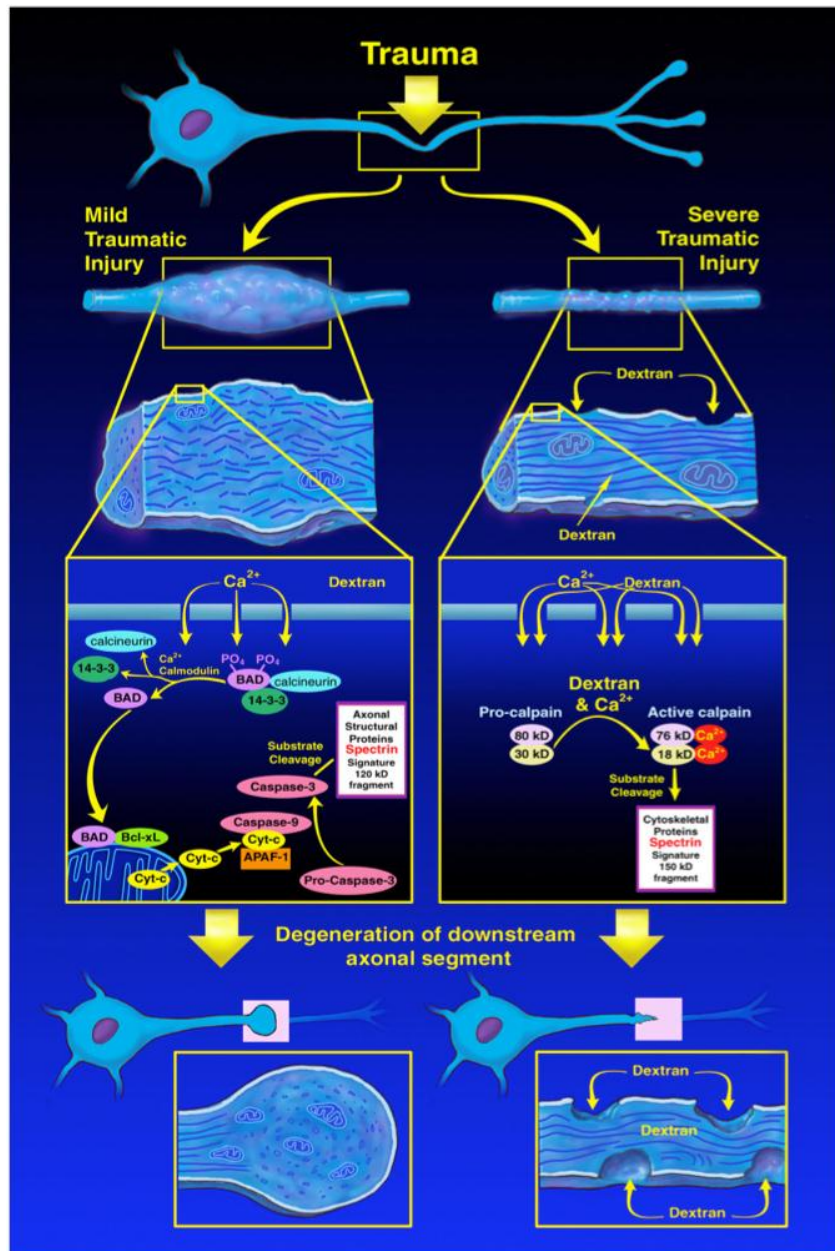
Figure 1. Traumatic axonal injury results from shearing forces across white matter tracts. An initial physical perturbation results in evolution of injury across distinct pathways of axonal degeneration.[26,27] Axons may demonstrate impaired axonal transport, resulting in axonal disconnection over hours to days following injury. Alternatively, axons may undergo rapid alteration of axolemmal integrity, resulting in rapid disconnection and dissolution of the affected axonal segment. It is believed the mechanisms associated with these distinct phenotypes may share similarities with apoptosis and necrosis occurring in neuronal cell bodies. Both of these are believed to result in alterations in water diffusion characteristics across white matter tracts that may be detected with diffusion based neuroimaging approaches. (Figure provided by J.R. Stone)

Cell necrosis—apoptosis in traumatic brain injury: Cell necrosis is characterized by the loss of cell membrane integrity, cellular swelling, damage to subcellular organelles, nuclear changes (karyolysis, pyknosis, karyorrhexis) and finally cell lysis, which may elicit an inflammatory response. Necrosis affects otherwise normal cells that happen to be in a hostile micro-environment like ischemia, acidosis or hypoglycemia, etc.

Apoptotic cells show preserved membrane integrity, cell shrinkage, plasma membrane blebbing, nuclear condensation and fragmentation resulting in the formation of apoptotic bodies, which are engulfed by other cells without an inflammatory response. Apoptosis is an active form of cell death that follows the launch of series of programmed biochemical processes (programmed cell death).

Apoptosis and necrosis share common signal transduction pathways leading to cell death. It has been reported that intracellular Ca^{2+} and adenosine triphosphate (ATP) levels (depleted as a result to damage to the mitochondria) determine the mode of cell death and inhibition one pathway may lead to death in an alternative pathway.[28] Reportedly, cyclosporin A treatment inhibits experimental traumatic cortical cell loss and axonal injury [29,30], and can be used to prevent trauma-induced mitochondrial damage.

In neuronal apoptosis, Caspase-3 is the major effector caspase and the Bcl-2 family of proteins modulates its activation. It has been reported that transgenic mice overexpressing human Bcl-2 exhibit considerably less neuronal loss in the injured cortex and hippocampus than wild-type controls following experimental TBI. Release of cytochrome C, mitochondria and caspase activation has been noted in both neuronal cell bodies and axons following experimental brain trauma and may be influenced by upregulation of Bcl-2 family members.[31] Caspase-independent cell death/apoptosis involving apoptosis-inducing factor (AIF) also have been reported.[23,24]

Experimental studies support the theory that calcium-mediated mechanisms represent the final common pathway of cell death following CNS injury.[24,25]

Oxidative or other damage to the DNA results either in growth arrest and apoptosis or repair due to activation of intracellular pathways.[29,30]
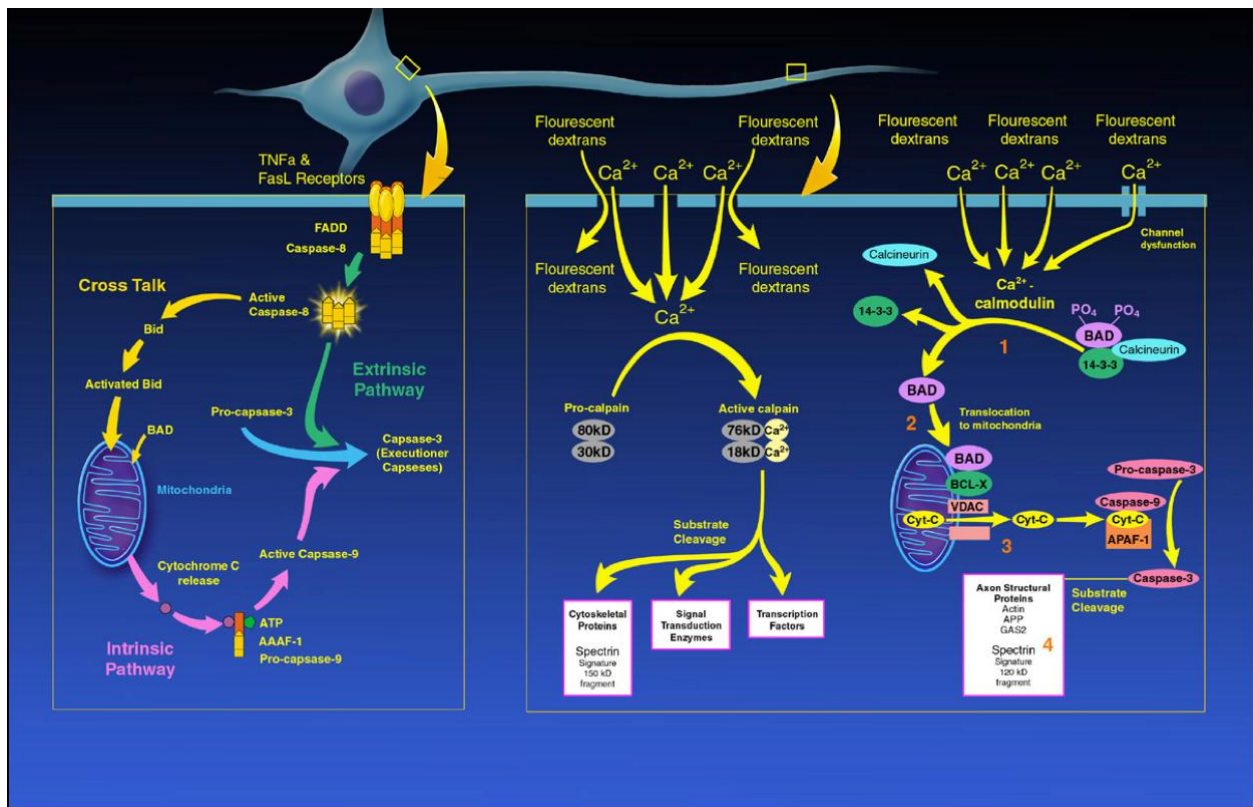
Figure 2. TBI results in the activation of secondary injury cascades across the neuronal cell body and axonal segment. Apoptosis may be activated within the neuronal cell body through either intrinsic or extrinsic pathways. Many of these non-nuclear based pathways are believed to also occur within injured axonal segments. Loss of neurons through cell death in aggregate may be detected with cortical volumetric imaging. Secondary injury cascades resulting in the evolution of injury may be seen within PET imaging methods target neuroinflammation, caspase activity, or membrane changes associated with apoptosis. (Figure provided by J.R. Stone).

Inflammation and traumatic brain injury: Disruption of the blood-brain barrier after TBI allows leakage of the serum components and blood cells, including neutrophils, into the cerebral tissue. Neutrophils secrete a large number of proinflammatory cytokines, oxygen radicals, NO and proteinases. The upregulation of ICAM-1 is involved in mediating the extravasation of leukocytes across cerebral vessels. Cerebral ICAM-1 levels correlate with the size of cerebral contusion and degree of blood-brain barrier dysfunction after human TBI.

Blood-brain barrier and traumatic brain injury: Regulation of blood-brain barrier permeability is a complex process involving inter- and intracellular signaling in the arrangement of tight junction. Disruption of the blood-brain barrier may lead to vasogenic edema, with increased extracellular water.

Cerebral endothelial injury and traumatic brain injury: There are many direct and indirect factors, including mechanical deformation of cerebral vessels, hemodynamic stress hypoxemia, ischemia and brain edema that contribute to cerebral endothelial injury. The mechanisms of endothelial injury in TBI are poorly understood. Minor degrees of mechanical deformation may

lead to microscopic perivascular hemorrhages, possibly due to partial tears of the blood vessels resulting in loss of contact of perivascular astrocytic foot processes with the micro-vessels. Surgically obtained pericontusional tissue of human cerebral cortex demonstrates marked endothelial cell swelling, increased pinocytic activity and intact tight junction on ultrastructural examination.[32,33] Endothelial damage in TBI can be characterized with a series of markers including thrombomodulin, Von Willebrand factor, laminin, fibronectin, glucose transporter, endothelial barrier antigen, cyclo-oxygenase 1, and endothelin 1, among others. Pericytes have also been implicated in playing a pivotal role in the effects of vascular injury. The complex structure, and regulation of tight junctions of the blood-brain barrier is extensively studied. The interendothelial junctional complexes of microvessels in human brain contain transmembrane proteins (occluding, junctional adhesion molecule 1, and claudin-5); adherens junctions proteins (cadherins); ZO proteins and catenins, which connect transmembrane proteins with the cytoskeleton.[34–39] Experimental studies demonstrate that matrix metalloproteinase may be involved in the pathophysiological cascade of neuronal damage after TBI.[40–42]

Brain swelling in head injury: The causes of brain swelling associated with trauma are multifactorial and poorly understood. Swelling may be due to the increased tissue water content of brain known as "cerebral edema" or increased intravascular blood volume referred to as congestive brain swelling or a combination. In 85% of affected patients, **massive swelling of one cerebral hemisphere** is associated with an ipsilateral subdural hematoma, with a large epidural hematoma in 9% of cases and in 5.4%, an isolated lesion studied with CT.[43,44] Rapidly occurring swelling suggests congestive type swelling; however, subsequent increased ICP may cause ischemic cytotoxic edema. Craniectomy to evacuate the ASDH may result in rapid herniation of the brain through the operative site, referred to as fungal herniation. Cytotoxic edema (shift of water from the extracellular space into the intracellular space) appear histologically as parenchymal vacuolation and neuronal red cell change in the gray matter and myelin loss and extracellular space enlargement in the white matter.

Diffuse cerebral swelling: Based on neuroimaging techniques, cerebral edema is observed in 87% of the head –injured cases included in that particular study.[45]

Ischemic cell processes in traumatic brain injury:

- Selective neuronal necrosis: Commonly seen in TBI, however, selective neuronal necrosis is also often noted after resuscitation in cardiac arrest and other global hypoxic changes. As the name designates, necrosis is limited to neurons and spares glia, blood vessels, and is believed to be a type of excitotoxic injury caused by the uncontrolled release of the excitatory neurotransmitter glutamate. The neurotransmitter glutamate selectively damages the dendrites and initially spares axons and the perikaraya. The selective neuronal loss may be present despite the lack of structural imaging changes following head injury.[46]

- Ischemic neuronal cell process (red dead neurons): Irreversibly damaged neurons (hyperchromatic pyknotic nucleus and acidophilic cytoplasm) may be seen 1-2 hours after the insult. In the next 1-6 hours, cytoplasmic incrustation occurs, definitive evidence of true irreversible neuronal damage. 15-18 hours after the insult homogenizing cell change takes place. Based on this relatively constant time –course of ischemic neuronal

change, the interval between the insult and death can be assessed with reasonable accuracy, provided the time since the insult is not less than 2 hours and not more than 24 hours.[3]

- **Mitochondrial failure, neuronal red cell change:** Mitochondrial damage due to TBI leads to failure of generation of ATP by mitochondrial oxidative phosphorylation critical for the maintenance of ionic homeostasis. The subcellular failure of appropriate utilization of oxygen manifests as a neuronal red cell change. It has been suggested that mitochondrial failure may result from the primary deformation related to injury or may be secondary to the failure of delivery of oxygen and essential nutrients by the cerebral blood flow. The finding of high cerebral extracellular lactate concentration with maintained regional blood flow and brain tissue oxygen tension supports the concept of mitochondrial damage in TBI.[47]

- **Long-term effects of traumatic brain injury:** The pathological substrate of persisting mental, a physical and social disability is the aggregate of all-different types primary and secondary brain damage. The Glasgow Outcome Scale, which provides a four-tiered survival scale to assess the recovery potential of patients: good recovery, moderate disability, severe disability, and vegetative state.

- Patients with **post-traumatic vegetative state** show widespread damage to gray and white matter and extensive thalamic damage. Although the brain may appear macroscopically normal, diffuse axonal injury, raised intracranial pressure, skull fractures, intracranial hematomas and secondary brainstem damage has been reported.[48,49,50] The main neuropathological change **in severely disabled patients** following traumatic brain injury is the presence of focal damage resulting from intracranial hemorrhage, contusions, ischemic brain damage or brain stem lesions.[51] Patients with **moderate disability** show mainly residual effects of local brain damage and lack evidence of severe diffuse damage**.** ApoE a 34-KDa glycoprotein involved in cholesterol transport and the regulation of multiple metabolic pathways is synthesized mainly by astrocytes.[52] After brain injury, there is a marked increase in neuronal ApoE immunoreactivity.[53] APOE e4 polymorphism has been reported to be associated with adverse effects in severe head injury. A prospective clinical study found that e4 carriers were likely to have poor outcome at 6 months after TBI than non-carriers.[54]

- **Markers of chronic neurodegeneration:** Epidemiological studies demonstrate an increased risk of Alzheimer's disease in patients after severe head injury.[55,56] Accelerated cognitive decline is well documented in aged subjects with a history of TBI.[57] However, a large community based prospective study failed to find an association between TBI and Alzheimer's disease.[58] Diffuse cortical beta amyloid deposits without dense core plaques, neurofibrillary tangles (NFTs) and/or neuropil threads are seen in the temporal cortex following TBI in one-third of patients as early as 2 hours after injury.[59]

- Tau immunopositive neurofibrillary tangles (NFT) and neuropil threads are important features of Alzheimer's disease and have been studied extensively. Age related changes were reported with anti-tau monoclonal antibody labeling both phosphorylated and unphosphorylated tau.[60] Tau immunoreactivity in oligodendrocytes was found in patients

dying after stroke and TBI.[59] In addition, unusual NFT with perivascular predilection were described in the neocortex of four young adults (aged 23-28 years) following minor repetitive head injury.[61] NFTs are not typically found after single episodes of TBI. Elevated CSF concentrations of cleaved forms of tau protein have been documented in brain injury.[21]

Physiological Hallmarks of Neurotrauma

Although our understanding of the biomechanics of concussion is still in progress, it is generally accepted that a concussion results from rotational or angular motion of the brain. The resulting shear strain on the soft tissue of the brain is believed to cause a disruption of the membrane resting potentials by altering axonal membrane permeability and ionic shifts that result in a metabolic cascade of events. Sodium, which lies outside the neuronal membrane in the resting state, moves into the cell, causing an efflux of potassium into extracellular space. This is followed by a calcium-dependent release of excitatory amino acids such as glutamate, further depolarizing the neuron, causing a spreading depression-like phenomenon throughout the brain. In order to restore homeostasis, the sodium-potassium pump requires ATP. This need for ATP results in increased glycolysis and lactate accumulation. Additive effects may include a decrease in total cerebral blood flow, activation of N-methyl-D-aspartate receptors, and a decrease in gamma-aminobutyric acid and other inhibitory neurotransmitters.[62–64] Trauma-induced metabolic changes, however, may return to baseline within a relatively short period of time. This sequence of events is especially pertinent to this report as it is these changes that often occur prior to what can be visualized using CT or conventional MRI but can be visualized using advanced neuroimaging methods such as PET, SPECT, DTI, MRS, MEG, ultrasound, etc.[65]

Brain energetics as measured through glucose metabolism has been shown to significantly increase within the first 30 minutes after injury as a result of the disruption of ionic gradients across the cell membrane. The length of hyperglycolysis is dependent on the severity of injury however after this acute phase of injury, glucose levels drop below normal and can be seen to persist chronically for weeks or months. PET can observe these changes by using flourodeoxyglucose (see Metabolic Imaging Overview and Positron Emission Tomography section for more details) as a marker of glucose metabolism.

Blood flow also changes upon injury and these hemodynamics are also dependent upon type and severity of the brain injury. As described above, the changes in blood flow may evolve from ischemic injury. These changes can be detected by blood-flow sensitive imaging techniques such as single photon emission computed tomography methods (SPECT), or perfusion weighted MRI (see Single-Photon Emission Computed Tomography (SPECT)] and Magnetic Resonance Imaging (MRI)]). Acute injury also results in a rapid release of glutamate as result of neurotransmitter release, membrane disruption, and action potentials. While intracellular and extracellular concentrations of glutamate cannot be measured, method such as magnetic resonance spectroscopy (MRS) can measure the static pools of glutamate in the brain non-invasively (see Magnetic Resonance Spectroscopy).

There are also secondary mechanisms of injury that can be detected with neuroimaging techniques. Neuroinflammation is one such mechanism that may contribute to the long-term effects of brain injury. After injury, glial cells are activated and leukocytes are recruited along with macrophages to repair tissue in an effort to protect the brain. However this neuroprotective response can be a double-edge sword as the activation of microglia can result in the release of pro-inflammatory cytokines that may induce neurotoxic effects. It is thus key to be able to monitor these inflammatory changes and where neuroimaging can play a key role. Metabolic imaging methods such as PET can target some of these inflammatory markers to quantify the degree of neuroinflammation (see Positron Emission Tomography). MRS can also measure the concentration of metabolites involved in inflammation such as glutathione, an important anti-oxidant in the brain that binds to reactive oxidative species (see Magnetic Resonance Spectroscopy).

Imaging Overview

Neuroimaging in the setting of TBI is important for diagnosing the extent of injury and prompt recognition of treatable injuries such as an epidural hematoma, a large subdural hematoma, or significantly depressed skull fracture. To this end, a stratagem for evaluation of the TBI patient in the clinical setting should follow current guidelines and recommendations such as those published by the Defense Centers of Excellence for both garrison and combat TBI imaging evaluation. In addition to the known clinical utility of the imaging methods described below, these techniques play a key role in the objective evaluation of TBI outcomes in the laboratory or clinical research setting. Each section below deals with a different approach to imaging, with some significant overlap between modalities, but in total allow an unprecedented look into the structural, functional, and molecular changes that occur in TBI.

Structural Imaging Overview

Computed Tomography (CT): CT is the imaging modality of choice to triage patients with acute head trauma because of its widespread availability, speed, and compatibility with life support and monitoring devices. CT is very sensitive in the detection of acute hemorrhage and in the evaluation of skull fractures. The limitations of CT are related to metallic streak artifacts, patient motion, partial volume averaging, beam hardening artifact in the posterior fossa, inferior temporal and inferior frontal regions, and the fact that it uses an ionizing radiation. Despite these limitations, a non-contrast head CT (NCCT) is the standard of care for moderate and severe TBI. CT is not of significant utility in mild TBI and multiple guidelines[66–68] such as the New Orleans Criteria (NOC), the Canadian CT Head Rules (CCHR), and the National Emergency X-ray Utilization Study (NEXUS)-II studies provide patient selection guidelines for the use of NCCT in the setting of mild TBI.

A non-contrast CT is highly sensitive and specific for demonstrating intracranial hemorrhage, extra-axial collections, edema, swelling, midline shift, herniation, and fracture.[69] Its widespread availability, speed of acquisition, and lack of contraindications make it the first line modality in the management of TBI. Nonetheless, when subjecting patients to repeated NCCT exams, the risks and benefits should be carefully considered because of the radiation exposure.

Magnetic Resonance Imaging (MRI): MRI is an alternative initial imaging modality that provides multi-planar capability. It is helpful for the characterization and timing of hemorrhage, and is better for the evaluation of intraparenchymal injury such as intraparenchymal hematoma, contusion, diffuse axonal injury, and cerebral edema. Unlike CT, MRI provides excellent visualization of the inferior frontal and temporal lobes and the posterior fossa. Susceptibility-weighted imaging (SWI) is a newer imaging technique that maximizes sensitivity to magnetic susceptibility effects, and is more sensitive than conventional gradient echo images for the detection of blood products. In uncooperative, unstable, or claustrophobic patients, ultrafast sequences may provide answers to crucial questions in the shortest time possible. Limitations of MRI are related to the long imaging time, the cumbersome nature of imaging and monitoring the trauma patient and the location of most MRI's outside of the emergency department. MRI is also less sensitive than CT in detecting fractures.

While considerable research is being conducted in the use of MRI for characterizing TBI, it is not presently a primary tool for investigation for acute TBI. This limitation is in large part due to the lack of normative neuroimaging data to determine the variability of normal imaging findings across the population. In research studies, aggregate pools of patients or research subjects may be compared to each other to determine statistical significance between groups. However, in patient care, the individual patient must be assessed and a determination must be made concerning whether that individual varies from normal. In the absence of available normative neuroimaging data, that comparison cannot be conducted. As such, there will remain a gap between advanced quantitative MRI and clinical MRI until that data is available.

As compared to NCCT, an MRI is more sensitive in demonstrating certain pathologies such as diffuse axonal injury, edema, and temporal course of hemorrhage. At the present time, MRI should be obtained in a patient where the CT findings fail to explain the neurological deficits. MRI may also provide prognostic information about long-term outcome.[70] MRI is also better suited for grading stages of intracranial hemorrhage and for detecting contusions, diffuse axonal injury, micro hemorrhages, edema, and brainstem injuries.[71]

Drawbacks of MRI include multiple contraindications such as pacemakers, need for careful patient screening in an acute setting, long exam times, and the relative unavailability of MRI compared to CT.

Functional Imaging Overview

Functional MRI (fMRI) uses much of the same technology that routine MRI employs. However, the primary goal of fMRI is not anatomic or morphologic imaging; the primary goal is functional information (this functional information will be overlaid or registered with anatomic CT or MR or PET to provide localization). There are two different versions of fMRI. The first is "stimulus driven" fMRI, while the second is resting state MRI (rs-fMRI). Both types of fMRI use the principle of BOLD (Blood Oxygen Level Dependent) contrast, the state of oxygenation of hemoglobin is used as an endogenous contrast agent. Hemoglobin provides this type of contrast as there is a difference in magnetic susceptibility between oxyhemoglobin and deoxyhemoglobin.

Magnetoencephalography (MEG) is a technique for measuring the electromagnetic field produced by the brain. It employs superconducting quantum interface devices (SQUIDs), which are liquid helium cooled detectors, sensitive to electromagnetic events at the quantum level. Early MEG scanners employed a single detector, which was scanned over the head, in much the same way as early rectilinear nuclear medicine scanners. However, current scanners employ fixed hemispherical arrays that encompass the majority of the cranial cavity. A MEG system is capable of time resolution of less than a millisecond, and a maximal spatial resolution of 2-3 mm (the best resolution occurs on the surface of the hemispheres, closest to the detectors), but does require a fully magnetic and electrically shielded room.

MEG and fMRI are two different techniques, both of which can be performed in an event-driven stimulus mode, or in a resting state environment. The first method is useful in locating specific eloquent regions of brain and their relation to injury foci. The resting state techniques look at coordinated functioning of different brain areas, rs-fMRI by creating functional connectivity networks identified by synchronous BOLD signal; rs-MEG by looking at voxel-to-voxel pairwise synchronous electrical signal, or at regional variations of cyclical brain activity within different frequency ranges. Comparing the two techniques – MEG has good temporal resolution and average spatial resolution, fMRI has poor temporal resolution, but much better spatial resolution.

Molecular Imaging Overview

Unlike other imaging methods that focus on brain morphology, molecular imaging methods provide information about brain biochemistry.

Positron Emission Tomography (PET) utilizes radioactive materials that produce two gamma rays that move in opposite directions. The PET scanner then uses rings of radiation detectors to detect the coincidence event of the positron emission decay, which is then used to calculate the location and concentration of the PET tracer within the brain, generating an image. It is highly sensitive, requiring tracer amounts of a radio-nuclide for image formation. The high sensitivity also allows for relatively short scan times, important for dynamic PET studies and in the clinical setting. Moreover, positron-emitting isotopes include carbon, nitrogen, oxygen and fluorine; these are found in many biological compounds of interest and can be readily incorporated into radiopharmaceutical analogs for imaging of physiological function. The most common radioisotope used in clinical PET imaging is fluorine-18 that has a half-life of 110 minutes. By radiolabeling glucose with 18F, the radiotracer 2-deoxy-2-(18F)-fluoro-D-glucose (FDG) is created. FDG is analogous to glucose in the body and, as glucose is the primary fuel for the brain, it is rapidly crosses the blood brain barrier and is taken up into brain cells and trapped in the tissue. Other PET tracers can be created by fusing a radionucleotide to a biological ligand. Finally, in the context of repetitive brain trauma, PET is a quantitative technique, enabling longitudinal studies on the same subject to be performed. However, these benefits are tempered by the relatively high cost of PET and concerns about elevated ionizing radiation exposure to the patient.

Magnetic Resonance Spectroscopy (MRS) is a non-invasive technique that examines physiological metabolism in vivo. Using standard MR scanners, chemical metabolites from

tissue regions of interest (ROI) are detected and shown as a spectrum depicting the type and concentration of the metabolites present. Localization of the signal can be from a single cubic volume (single voxel spectroscopy) or may utilize additional excitations pulses and scan time to provide information regarding spatial variations of these metabolites within a large ROI (chemical shift imaging). The choice of echo time can influence which metabolites are detected based on their relaxation properties. Some MRS methods take advantage of this property to provide greater chemical specificity such as spectral editing methods or two-dimensional correlated spectroscopy which obtains spectra at multiple echo times, which upon Fourier transform provides spectral information in two dimensions (as opposed to spatial information in CSI). Furthermore, MRS can detect the presence of metabolites via a variety of isotopes such as hydrogen (^{1}H), phosphorus (^{31}P), sodium (^{23}Na) and carbon (^{13}C). MRS has been demonstrated to be useful in multiple body systems, but its greatest application has been in the study of neurological disorders including neuro-inflammatory diseases, dementia and brain cancers.

Analysis and Interpretation of Neuroimaging Data Overview

Established neuroimaging analysis techniques are often employed in TBI research despite having been originally developed for neuroscience investigations outside of a TBI-specific domain. Many of these standard techniques involve regression analysis on image features in corresponding brain regions despite the fact that a fundamental assumption underlying these techniques (viz., that comparison of corresponding anatomy will yield insight into population trends of TBI effects on the structural and functional components of the brain) is often flawed given the spatial heterogeneity of TBI effects. However, given the widespread availability of these methods in publicly available and vetted implementations, they continue to be employed for TBI research.

Although certain commonalities exist between these existing analysis methods, they are highly variable in terms of operator-selected anatomical locality, preprocessing and data transformations, and subsequent statistical analysis. Regional locality considerations for these traditional analysis methods are typically voxelwise or anatomical region-based or some hybrid thereof. Preprocessing and other data preparation steps also contribute to the variability between analysis approaches. Data cleaning methods such as denoising and MR inhomogeneity correction as well as fundamental data transformation methods such as image segmentation and spatial normalization (i.e., image registration) all factor into composition of the analysis pipeline. Also, statistical testing choices (parametric vs. non-parametric regression testing and/or machine learning techniques for diagnosis/prediction) can also have a significant impact on the interpretation of results. Finally, performance of the available softwares used to perform the same analyses must be considered. Although many of these factors causing such variations are hidden, or at least obscured, from the average user, understanding these issues are of vital importance for ensuring the integrity of reported findings.

Voxel-based analysis: A primary processing consideration regards the spatial locality of hypothesized TBI effects. One of the earliest techniques and one that continues to be widely used within neuroimaging research today is the statistical parametric mapping (SPM) technique originally developed for use in functional neuroimaging.[72] Although variations exist, the core procedures are essentially the same. A template (i.e., brain image which is representative of the

study data) serves as the standard coordinate space to which all other brain images are normalized, or registered. These normalized images are then smoothed to account for local residual misalignments in the data followed by some form of statistical testing or partitioning of the data. Statistical testing typically involves mass univariate regression analysis (i.e., a statistical test at each voxel) with post processing steps including corrections for multiple testing using random field theory[73] or false discovery rate (FDR).[74] Interpretation of results involves identification of statistically significant regions and their relationship to study hypotheses. Although, as mentioned previously, SPM was originally developed for functional neuroimaging studies, it has been readily adapted to investigating effects in structural gray matter[75] and white matter from DTI.[76] In TBI, voxel-based analysis has been used in studies involving white matter integrity between veteran groups with and without blast exposure[77], gray matter concentration between TBI patients and controls[78], and thalamic metabolic differences using FDG-PET.[79] Derived cortical thickness maps can also be analyzed using the voxel-based paradigm such as in[80] involving children with TBI where such maps were produced using the FreeSurfer package.

However, the use of voxel-based analysis is not without its caveats. In two recent studies[81,82] it was shown that certain preprocessing steps which are integral to common voxel-based analysis protocols are susceptible to a type I error-inducing selection bias. Specifically, a common data preparation step for group analysis is the alignment of the cohort to a pre-existing or population-specific template. However, depending on the images being spatially normalized and the subsequent statistical analysis, such processing steps could explicitly generate false positives. This issue affects some of the most popular tools in contemporary use for both white matter[83] and gray matter voxel-based population studies[84] which are applied routinely in TBI studies. These findings complement other work which illustrates the presence of methodological selection bias in the use of fMRI and, more generally, in experimental design.[85] Aside from the issues mentioned previously and the, other examples of specific confounds affecting the integrity of findings include small sample sizes[86–88] and motion correction in DTI[89] and fMRI.[90]

ROI-analysis: A similar framework uses corresponding anatomical regions for inferring statistical relationships between TBI effects and neuroimaging.[91] This approach relaxes the requisite precision for establishing anatomical correspondence and reduces the number of statistical tests performed. However, delineation of anatomical regions is often done manually which is time-consuming, tedious, and susceptible to intra- and inter-rater bias. These problems have been mitigated by recent research into computational algorithms for "atlas-based label fusion" (e.g.,[92]) and publicly available labeled brain atlas resources based on accepted parcellation protocols (e.g.,[93]).

Tract-based spatial statistics: White matter-specific regional analysis has also figured prominently in the TBI literature. One of the most widely used techniques is the well-known tract-based spatial statistics (TBSS).[82] The methodology involves the generation of fractional anisotropy image from DTI for each individual subject which are then registered to a standard space. Skeletonization of the mean FA image represents the common centers of all white matter tracts on which all white matter voxels for all subjects are projected and statistically compared. Given the widespread usage of TBSS, several studies have been performed to investigate various aspects of its reliability. TBSS was shown to be reliable in a multi-site DTI study across a variety

of 3T scanners.[94] However, output has also shown to be significantly dependent on chosen parameters such as smoothing[95], normalization protocol[96], and template selection[97].

Spatially agnostic methods: Given the potentially problematic assumption of hypothesized common spatial effects in populations in the context of TBI[98], many researchers have found the aforementioned techniques deficient and have proposed modified metrics accordingly. For example, TBSS was used in[99] to determine white matter differences in a cohort of acute mild TBI versus a control population. This particular study showed no white matter differences although previous studies have reported otherwise. Possible explanations include study design flaws but could also be the result of the spatial heterogeneity of effects. As a remedy, location-independent measures quantifying deviations from a normal population distribution have been proposed thus leading to subject-specific assessments. In[100], FA-based metrics ("load" and "severity") were calculated in GM regions of each subject using deviations from a template describing the regional distribution of a normal population. Similarly, a voxel-based study showed no differences in FA in mild TBI and normal cohorts although modification of the study to a spatially agnostic metric (described as the number of "potholes") did show FA differences in said groups.[77]

Connectivity methods: Related to methods investigating the integrity of white matter indicating possible compromise of structural connectivity in the brain, the use of fMRI has been used to assess functional connectivity between anatomical regions. Given the characteristic small-world topology of normal brain networks[101], the authors of[102] investigated functional connectivity in the presence TBI using graph theoretical metrics. Twenty TBI patients and 21 age-matched normals underwent resting state fMRI acquisition. Network analysis demonstrated impaired connectivity, specifically a deviation from small world topology, with the TBI cohort which was confirmed with visual inspection of DTI-derived FA images. Similar to the previous study, the authors of[103] also looked at the effects of diffuse TBI on functional connectivity in a cohort of 20 patients and 17 age-matched controls. Using independent component analysis (ICA) of the default mode network (DMN), group differences of functional connectivity were assessed. It was postulated that decreased FA in the cingulate tract of patients was compensated by increased functional connectivity in the DMN.

Current Capabilities

Neuroimaging modalities and their ability to measure pathological hallmarks of TBI were reviewed at the working group meeting. The current state of clinical neuroimaging and current research capabilities discussed by the working group are summarized below.

Current Clinical Capabilities:

Computed Tomography (CT)

This section will discuss the capabilities of current clinical neuroradiological CT techniques, specifically in relation to traumatic brain injury. Non-contrasted CT, contrasted CT, CT perfusion and CT angiography will each be described; then each technique's advantages, disadvantages, and clinical indications will be enumerated. At the outset, it should be stated that the place of CT in the overall assessment of TBI is unique: part of the diagnosis of mild TBI is the requirement that the initial non-contrasted head CT is negative. Hence part of the reason for ordering a CT is to assist in making the diagnosis of mild TBI (by a negative exam), but the second, equally important reason for an initial CT scan is to detect evidence of more serious brain injuries, for which emergent therapy may be indicated.

The role of the initial non-contrasted head CT in prognosis, both in cases of mild TBI, and in cases of moderate or severe TBI, is important. In one study, using the Canadian CT Head rules to clinically select which patients were to be scanned (these patients would all be considered mild TBI), less than 5% of over 3000 people had an initial intracranial bleed, and of the few who did none deteriorated or died.[104] In a second study, after an initial negative head CT in clinical mild TBI, 74% of 2444 patients were discharged and only 1% returned – and of these 44% had scans, of which all were negative. Of the 26% who were admitted, only 7% had a repeat CT – and all were negative. The implication is that complications are negligible with an initial negative head CT in mild TBI.[105] Further, in the setting of mild traumatic brain injury the CT findings have little impact on the prognosis, and the clinical outcome at six months.[106] Lannsjo (2013) reported that pathology on an acute CT scan in mild TBI has no effect on self-reported symptoms at 3 months post injury – although factors including gender and age do correlate.[107]

However, the situation is not the same in the setting of moderate or severe traumatic brain injury. In this setting, some CT observations (e.g. status of the ambient cisterns, fourth ventricle location, size of largest hemorrhage) do correlate within clinical outcome at 6 months, although other factors (e.g. age, pupil responses, Glasgow Coma Scale score, hypo-tensive episode) also correlate as well.[108] To summarize, an initial CT scan in the setting of mild traumatic brain injury provides little prognostic value for the recovery; whereas the initial CT scan in the setting of moderate or severe traumatic brain injury does provide prognostic information, although other factors are still important.

Non-contrasted head CT: Non-contrasted head CT is performed by obtaining CT scan slices through the head without the use of intravenous iodinated contrast material. With the current multi slice helical scanners, the entire head can be scanned in less than several seconds.

The advantages of non-contrasted head CT are many, especially in the initial evaluation of the injury. CT is the most available technology for the initial assessment, so that whether in mild or moderate or severe cases of TBI it can quickly and accurately locate any severe acute problems that demand immediate medical and/or surgical attention. Large parenchymal (within the brain substance) bleeds, and large space-occupying extra axial (within the skull, but outside of the brain substance) bleeds - subdural hematomas and epidural hematomas, for example - can be identified and appropriate surgical management performed. Other acute hemorrhagic injuries - shear injuries occurring throughout the brain but specifically at the gray white junction (the junction between neurons (grey matter) and the processes of neurons called axons (white matter), are visible on a non-contrasted head CT, even though surgical treatment is usually not required. Extensive subarachnoid hemorrhage is easily visible, but is not, in and of itself, considered a surgical condition. Finally, there are clues on a non-contrasted CT of possible diffuse axonal injury; these include multiple areas of hemorrhagic or non-hemorrhagic shear injuries with focal edema, diffuse cerebral edema, and marker hemorrhagic lesions in the corpus callosum and/or in the brainstem. Therefore, non-contrasted head CT serves an irreplaceable function of early triage – to detect more serious injuries so that they can be treated as appropriate, and, simultaneously, to rule out the presence of visible signs of trauma so that a diagnosis of mild TBI can be made.

Disadvantages of non-contrasted head CT are primarily related to the fact that extensive injuries can be present that do not either produce enough characteristic hemorrhage - whether intraparenchymal, extra-axial, or intra-ventricular (within the fluid spaces or ventricles of the brain) - or enough edema, to be visible on CT. While some cases of diffuse axonal injury can be diagnosed on a non-contrasted head CT, there are other cases that lack evidence of focal hemorrhagic or non-hemorrhagic shear injuries, or lack the marker hemorrhages in the corpus callosum and brainstem, and these patients may present with an almost normal appearance or at worst minimal, and difficult to detect, diffuse edema. Finally, non-contrasted CT is essentially an anatomic imaging method, which is not capable of detecting or describing changes in the function of the central nervous system.

The first and prime indication to perform a non-contrasted head CT is for the initial emergent evaluation of an episode of traumatic brain injury, in which the modality's speed of detection and sensitivity too many acute injury findings of hemorrhage and edema is of paramount importance. However, non-contrasted head CT also has an important role in assessing the brain after the initial exam, especially in the first week or two after injury. It is often the first modality used to detect the complications that occur in this time period – delayed hemorrhages, developing edema and mass effect, and delayed regions of infarction (such as can occur after a time delay from vascular injuries or dissections). The clinical stimulus to perform this repeat examination can be a new alteration or further decline in mental status, the presence of new neurological deficits, decreasing level of consciousness, or continued un-explained failure to improve. It is also used to follow the results of surgical or medical therapy on a regular basis.

Contrasted head CT: Contrasted head CT scanning is performed exactly as is a non-contrasted head CT, with the addition of a sufficient amount of iodinated contrast agent administered intravenously immediately prior to and during the examination. In most settings of TBI the addition of contrast, without performing additional computations on the data acquired (such as CT perfusion or CT angiography, both discussed below), adds little if anything to the diagnostic information that can be obtained from a non-contrasted head CT. However, while there is little indication to perform only a contrasted head CT, the information contained within the source image set of CT images obtained for CTA is sufficient enough to generate a set of contrasted images.

The addition of iodinated contrast is performed for one of three primary reasons: 1) to detect regions of blood brain barrier disruption, 2) to obtain the source images necessary to compute CT perfusion maps of the brain, and 3) to opacify the blood vessels so that a high-resolution CT angiogram can be produced. As regarding reason number one, the blood brain barrier is most commonly disrupted in cases of trauma acutely; but in delayed cases, blood brain barrier disruption can occur from secondary complications such as infarctions, or from inflammation or infection. The advantages of the contrast CT is therefore the ability to detect these secondary complications of infarction and abscess, and to permit the performance of the CT perfusion and/or the CTA exam.

One of the major disadvantages of the contrasted CT examination is that it takes longer to perform a contrasted head CT than to perform a non-contrasted head CT. Also, individuals with poor renal function may have their renal function impaired even further by the administration of iodinated contrast agents. Therefore there is a subset of patients for whom contrasted study is contraindicated or had best ill-advised. Finally if a contrasted exam is performed without a preceding non-contrasted examination, small amounts of subarachnoid hemorrhage may be obscured, and consequently not recognized.

CT perfusion (CTP) of the brain: The technique for performing a CTP examination of the brain consists of rapid multi-slice sequential scanning of as much of the brain as can be included in the particular scanners scan volume, such that every portion of the included brain is scanned at least every 1 to 2 seconds over approximately a 60 second time window that begins before contrast is administered, and extends through the administration of the bolus, and into a washout period thereafter. At the end of the collection period, the scanner has obtained a set of images at each slice position that spans the entire scan time. Enough data is collected to produce a time-density curve for every voxel in the images, over the period of the scan. To further analyze this data, a prominent major feeding artery and large draining vein are identified, and using deconvolution theory, perfusion parameters can be computed for each voxel of the brain. Routinely, a series of color-coded maps are generated that show cerebral blood flow, cerebral blood volume, mean transit time, and time to peak of each voxel within the imaged volume of brain. The analysis software will designate ischemic regions based on variance of a computed perfusion parameter (for example, mean transit time more than 150% of the normal side); probable infarcted regions are similarly designated on the basis of a parameter falling below a threshold (for example, cerebral blood volume below 2 ml/100 gm of tissue).

CTP's major advantage is that it is a sensitive technique for the identification of regions of cerebral ischemia and regions of cerebral infarction. In the acute setting, these alterations can be due to direct traumatic injury to the blood vessels of the brain, or can be secondary to mass effects produced by regions of cerebral edema. If the regions of ischemia or infarction are due to direct vascular injury (which is best imaged on a usually near simultaneously performed CT angiogram), then therapy, whether intravenous thrombolytic, intra-arterial thrombolytic, or intra-arterial mechanical in nature can be administered. The technique is also useful, when performed in a serial fashion, to follow developing cerebral ischemia, and/or vasospasm. It can also be used as a means to assess the efficacy of medical or interventional therapy.

One of the disadvantages of CTP is that the performance of a high-quality exam places high demands on the CT scanner hardware and software. Ideally, a large proportion of the brain should be capable of being imaged without any table motion, or at worst, a jog or shuttle motion that still permits rapid and frequent coverage of the region of interest. Regardless of the specific slice acquisition method, CTP as an imaging tool is very sensitive to patient motion, as the technique requires good data, and good time activity curves for each voxel that can only occur when there is little if any motion over the period of data acquisition.

The indication therefore for CTP in the acute setting is any suspicion of regional cerebral ischemia or infarction. It is also indicated in the first week after injury when there is suspicion for new or developing ischemia, such as can occur from a delayed dissection of a carotid or vertebral artery. CTP may also be helpful in the assessment of cerebral vasospasm. This is a particularly interesting technique given reports that have emerged concerning the prevalence of vasospasm in moderate to severe military TBI. It is also indicated for the assessment of the efficacy of medical and/or interventional therapy. CTP may also be helpful in evaluating mild TBI patients with residual symptoms, as an aid to localize regions of abnormality and possibly guide therapy[109]. CTP also may play a role in determining the prognosis of patients with severe traumatic brain injury, by identifying brain that is very poorly perfused, despite less severe findings on non-contrasted CT.[110]

CT angiography (CTA): CTA consists of a single rapid scan through the brain, during the time that a dense bolus of iodinated contrast is passing through the brain, filling the intracranial vasculature. In reviewing a CTA, reformatted additional images in multiple additional planes are used to supplement the axial source images. Alternatively, more complex software can produce shaded 3-D surface images of the intracranial vessels. If the vascular bolus of contrast is sufficiently long, and the timing of the scan performed optimally, the same single injection of contrast and set of axial images also permits a simultaneous evaluation of the intracranial venous system (cortical veins, deep midline veins, and major dural venous sinuses).

The advantage of CTA is that it is the best (with less artifacts than MR angiography) noninvasive method to evaluate the intracranial and cervical venous and arterial vasculature. If the timing of the bolus is appropriate, relative to the scan timing, a CT venogram is also obtained simultaneously.

The disadvantages of CTA is that the examination is a very sensitive to a number of technical factors including patient motion, CT hardware and software capabilities, and a good vascular bolus of contrast material - in order to obtain optimal vascular opacification.

CTA is indicated in the acute setting when there is a high suspicion of vascular injury. It is also an excellent noninvasive way to detect delayed vascular injury, thrombus, or vasospasm.

Magnetic Resonance Imaging (MRI)

MRI Protocol: A typical MRI protocol for evaluating TBI must include a set of sequences designed to interrogate the structure, diffusion tensor, function, perfusion, angiography, and metabolite composition of the brain. Table 2 provides a typical set of sequences that may be used. Those sequences marked with an * are considered investigational as per a recent report from the American College of Radiology (ACR) Head Injury Institute[111].

Table 2. Typical Set of Sequences for Evaluating TBI

Type of Sequence	Typical Sequence Name	Typical Time
Structural sequences	MPRAGE T1W sequence	6-7min
	T2-weighted sequence	3-5min
	3-D SPACE Fluid Attenuation Inversion Recovery (FLAIR) sequence	3-5min
	Susceptibility-weighted Imaging (SWI)	4-5min
Diffusion Tensor Imaging*	60-direction, b1000 DTI	8-9min
Functional MRI*	BOLD MR imaging using either a task-based paradigm or resting-state paradigm	9-12min
	Hypercapnia BOLD imaging to assess cerebrovascular reserve (CVR)	9-12min
Perfusion & Angiography	Arterial Spin Labeling (3D ASL)	3-4min
	Time-of-Flight (TOF) Angiography	5-6min
MR Spectroscopy (MRS) & Chemical shift imaging (CSI)*	CSI for Lactate (e.g., spiral CSI_270ms)	3-4min
	CSI for other metabolites (e.g., spiral CSI_30ms)	3-4min

The structural sequences are designed to evaluate the gross morphology and injury to the brain. Examples of these sequences include T1-weighted, T2-weighted, T2-FLAIR, and T2*-GRE sequences. Susceptibility weighted images (SWI) should be included (perhaps in lieu of T*-GRE) as they increase the conspicuity of micro hemorrhages.[112,113] Generally, there is no need to administer intravenous contrast for the evaluation of TBI.

Diffusion Tensor imaging (discussed below) are an active area of research in TBI. However, normative data and tools for its implementation in the clinical setting are not yet available. The diffusion tensor is intimately related to the integrity of white matter tracts with in the brain.

The fMRI, detailed elsewhere in this document, interrogates the functional connectivity of the brain, using either a task-based paradigm, or a resting state paradigm. It is well known that this

connectivity pattern is altered by TBI, however; how this information could be used clinically is still an active area of research.

TBI may result in vascular injury both at micro and macroscopic levels. TBI is also associated with acute and delayed vasospasm. The microscopic injury to blood vessels can be visualized indirectly by assessing the associated foci of micro hemorrhages using the SQI sequence. The macroscopic vascular injury and vasospasm may be evaluated using MR angiography (MRA). Both contrast-enhanced and contrast-free paradigms for MRA, the latter leveraging the flow properties of blood to image a vessel, are available. TBI-associated vascular pathologies may result in alteration of blood perfusion to the brain parenchyma; this can be evaluated using MR Perfusion sequences. Once again, both contrast-enhanced and contrast-free perfusion sequences are available. Arterial Spin Labeling (ASL), a new sequence that tags in-flowing blood into the brain and then interrogates it to assess the perfusion of the brain, is a contrast-free paradigm for assessing brain perfusion this is gaining popularity because of its ease of use and contrast-free nature.

MR Spectroscopy (MRS) can be used to assess presence and relative concentrations of certain key neuro-metabolites such as lactate, choline, creatine, n-acetyl aspartate (NAA), and lipids. Multiple sequences, using chemical shift imaging, both in single voxel and multi-voxel versions, are available for this task and may be helpful in elucidating pathologies such as neuronal loss (NAA), rapid cell membrane turnover (choline), and anaerobic respiration (lactate).

It typically takes $60 - 70$ minutes of acquisition time to complete this regimen. The time can be longer if a task-based paradigm for fMRI is employed.

Positron Emission Tomography (PET)

There have been several recent reports of memory deficits, mood disorders, and motor symptoms resulting from TBI.[114–119] Coupled with increased public awareness, these studies have fueled scientific investigation into pathologic changes contributing to TBI-related neuropsychiatric symptoms including cognitive decline or affective changes (e.g., anxiety, mood swings, depression) in the absence of neurologic signs (e.g., slurred speech, parkinsonism). Positron emission tomography, or PET imaging, is a noninvasive imaging technology in which trace amounts of a radioactive ligand binds to a molecule of biological interest and subsequent radioactive decay is detected. In this way, PET is similar to SPECT, (see Single-Photon Emission Computed Tomography (SPECT)). However, because SPECT relies on a single camera to capture emitted gamma radiation, SPECT results in fewer photos detected and about 10 times lower sensitivity than PET.[120] PET has been applied to investigate TBI. At a broad level, researchers have used a glucose-analogue, fluorodexoxyglucose or FDG, to image changes in brain metabolism in response to TBI.[121] FDG PET may hold the potential of tracing how functional connections in the brain are affected by focal injury in one region through increasingly sophisticated analyses, but this area of TBI research, namely that which uses molecular imaging techniques such as PET, is only now emerging.

As noted earlier, in this report's section "Pathological Hallmarks of Neurotrauma," TBI occurs in two phases of injury. The first phase, of direct physical damage, is usually immediate and irreversible. The second phase consists of biochemical responses that might lead to cell death

and the neurocognitive impairments observed with TBI, see the earlier section "Microscopic Pathological Hallmarks of Neurotrauma." Secondary injury, this second phase, is an active area of research both for radiotracers, and for drug development, especially in the area of neuroinflammation.[122] Several proteins and receptor systems may play important roles in neuroinflammation and ligands that act as agonists or antagonists may be able to alter the neuroinflammatory response to minimize damage. At this stage, PET ligands suggest that TSPO, a translocator protein expressed in glial cells, can be used to track neuroinflammation in response to TBI, at least in animal models.[123] Similarly, animal models suggest that the α7 nicotinic acetylcholine receptor may play a role in neuroinflammation and possibly excitotoxicity, in which neurotransmitter excitatory response results in cell death, and the cannabinoid 2 receptor may also be activated for a neuroprotective role.[124,125]

Recent research also suggests that repeated TBI may result in the chronic neurodegenerative condition known as CTE, or chronic traumatic encephalopathy. CTE is a disease thought to result from the pathological deposition of tau protein, a protein that is hyperphosphoralated in its pathological state and associated with cognitive decline in other disease models, such as Alzheimer's disease.[126] Tau has been a challenge for which to develop PET radioligands, but because of its importance to the class of diseases called "tauopathies" (including Alzheimer's Disease and CTE), such ligands are actively being developed and implemented.[127]

Single-Photon Emission Computed Tomography (SPECT)

Single photon emission computed tomography (SPECT) involves the administration of a radioisotope, such as Tc99m, to a patient and performing two-dimensional slices, which are reconstructed into activity maps of the structure being imaged. In the case of brain SPECT, these images can be utilized to examine blood flow to regions of the brain. The most commonly used radiotracer for brain imaging is T99m-hexamethylpropylene amine oxide (HMPAO), which is seen at levels proportional to CBF within the brain. The resolution of SPECT scans is typically on the order of 128x128 and can be combined with conventional CT scans performed at the same time allowing for an anatomic/physiologic overlay which may be useful in the evaluation of traumatic brain injury.

As early as the mid-1980's[128], the potential for evaluating changes in blood flow in patients with traumatic brain injury was realized using SPECT. Patterns of decreased regional flow in patients with chronic head injury spurred further work to use this imaging tool as not only for diagnosis, but also prognosis. Longitudinal studies followed patients with TBI using SPECT, with the most convincing evidence of prognostic ability from a study of 136 patients over one year, with imaging taking place at four separate time points.[129] Clinical assessment was performed at each of the longitudinal scans, with final conclusions from this study stating that a normal SPECT study has a high negative predictive value for having persistent symptoms of mild TBI at one year. The intermediate scans were mixed in their prognostic ability, with larger perfusion lesions correlating to worse prognosis.

SPECT may also help identify regions of brain plasticity and reorganization. This is suggested by an article evaluating language and brain-discourse relationship in a pediatric population by Chiu Wong, et. al.[130] Their study demonstrates a paradoxical increase in perfusion patterns rather

than a decrease as reported in some of the prior TBI literature. This may be due to reorganization and plasticity changes within the brain to compensate for other areas damaged. This adds a complicated dimension to the use of SPECT in isolation to provide prognostic information to patients suffering from residual effects of TBI.

In a recent review, the use of SPECT was labeled as a "Level IIA" evidence for the value of SPECT in TBI.[131] The review encompasses both longitudinal and cross-sectional use of SPECT in TBI, highlighting regional consistency of perfusion abnormalities and high negative predictive values of normal SPECT scans. However, the article goes on to state that SPECT is superior to CT and MRI at both diagnosis and prognosis of TBI patients. The comparison used in the paper utilizes conventional anatomic sequences from lower field strength MRI and older generation CT technology which limits its value in comparing current advanced sequences and later generation CT. Perfusion technology is now readily available using the MRI sequences arterial spin labeling and BOLD resting state evaluation.

Other fields of study with SPECT: SPECT has a wide range of applications in whole body and neuroimaging which utilize various combinations of radioisotopes and ligands. The field is still evolving with applications to oncologic imaging, physiologic myocardial evaluation, as well as neurodegenerative diseases. Due to its physiologic applications, SPECT imaging will continue to be a useful tool in the evaluation of patients with TBI.

Ultrasound/Transcranial Doppler (TCD)

Excellent introductory texts on the basics of ultrasound include O'Brien (2007)[132], Leighton (1994)[133], ter Haar and Coussios (2007)[134], with Mourad (2013)[135] also including a survey of diagnostic and therapeutic ultrasound applied to the central and peripheral nervous systems.

In essence, most ultrasound for diagnostic purposes makes use of short pressure pulses with large amplitudes spaced fairly far apart in time, at frequencies low enough to propagate sufficiently yet high enough to resolve, via measurement of acoustic backscatter or derivatives of that backscatter, fine-scale biological structure with sufficient contrast in density (primarily) or relative movement. The specific choices of ultrasound parameters balance the need to maximize the backscattered signal strength and imaging resolution, generally by increasing the intensity and/or frequency of the sound, with the need to avoid harmful biological effects, achieved also by decreasing the length and increasing the spacing of the pulses to minimize the production of heat and mechanical forces within the interrogated tissue.

Diagnostic ultrasound shows great utility imaging peripheral tissue, giving rapid and real-time feedback to the trained user on tissue structure and blood flow. A classic book on the subject is by Kremkau (1998).[136]A wonderful example of the capacity of modern diagnostic ultrasound systems to image fine details in peripheral tissue is offered by Kermarrec et al (2010)[137], who demonstrated the likely surprising anatomical detail afforded by recent diagnostic ultrasound machines for imaging peripheral nerves and their associated diseases in a manner that compares favorably with MRI.

However, the skull limits the utility of diagnostic ultrasound for imaging. The skull severely attenuates the ultrasound signal at frequencies generally used for peripheral imaging (3-10

MHz). To compensate for this, most practitioners use cardiac imaging probes in 'penetration mode', thereby accessing the lower end of their 2-4 MHz frequency range. While this can produce images of brain, those images lack sufficient contrast under most circumstances to meet the needs of clinicians.

Diagnostic ultrasound for assay of blood flow into the brain (transcranial Doppler or TCD) represents, however, a mainstay of current clinical practice (e.g., the review of Tsivgoulis et al, 2009)[138]. Briefly, sufficient ultrasound at TCD frequencies (1.5-2.0 MHz) transmits through the skull at the temporal bone such that careful analysis of the measured return of that ultrasound (~1% of what was sent from the probe) offers measurements of the speed of blood flow towards or away from the probe in the major arteries that feed blood into the brain.

In the civilian sector TCD plays a critical role in the diagnosis and monitoring of ischemic stroke. The former is assayed by measurements of blood flow in the major cerebral arteries in which a clot may reside; the latter application of TCD focuses on the search for emboli entering the brain. Another critical application of TCD in the clinic is the assay of the reactivity of secondary cerebral arteries that allow the brain to regulate blood flow that enters the brain, otherwise known as cerebral autoregulation. Here, TCD-based assay of blood flow within the middle cerebral artery (MCA) tracks its changes after a challenge to the peripheral blood pressure through drugs or cuff-based procedures. For patients with intact cerebral autoregulation, their secondary arteries dilate sufficiently quickly (in a matter of seconds) to rapidly re-equilibrate adequate blood flow into the brain. Without intact cerebral autoregulation, blood flow takes a long time to renormalize (ten seconds or more), or it never does. Finally, civilian TCD finds common use in the assessment of the presence, extent, and evolution of cerebral vasospasm. Cerebral vasospasm consists of transient constriction of major arteries feeding the brain as well as secondary arterioles within the brain. Cerebral vasospasm often appears in the context of civilian TBI (e.g., Oertel et al, 2005)[139]. The gold standard for confirming the presence of vasospasm is CT- or MR-angiography. Since collecting that data requires moving the patient to an imaging facility, MDs use daily TCD-based measurements of blood flow in the major cerebral artieres, along with assay of clinical signs, to monitor for the onset of vasospasm as well as to track its clinical management.

Current Research Capabilities:

Computed Tomography (CT)

Dual and Multi Spectral CT

Conventional CT provides a single CT Number or Hounsfield Unit (HU) for each voxel. Prior knowledge about the anatomy and attenuation properties of different tissues is used to distinguish various materials such as fat, bone and muscle. There is overlap among the CT numbers of different tissues and conventional CT is unable to distinguish materials with similar HU. For example, intracranial hemorrhage may appear very similar to dilute contrast or diffuse parenchymal mineralization. Multi-spectral CT overcomes this limitation of single energy CT by utilizing energy dependence of CT numbers.

The mass-attenuation coefficient varies based on X-ray energies for different materials. Thus, Hounsfield units measured by CT are not absolute and change depending on the kVp used for image acquisition. In addition, the change in HU is material specific. This property is used by DECT for material decomposition by acquiring two image series with different kVp and assessing the change in HU to ascribe a tissue type to each voxel.

Dual energy CT can be implemented using one of the following four paradigms.

- Dual-spin Scanners: In these scanners, two independent acquisitions at a low and high energy kV setting are acquired sequentially.

- Fast kVp Switching: These scanners employ a special X-ray tube that is capable of rapidly switching between high and low voltage settings on a projection-by-projection basis.

- Dual-source Scanners: As the name implies, these scanners have two independent imaging chains mounted on a single CT gantry. One imaging chain is operated in the low-energy mode and the other imaging chain is operated in the high-energy mode.

- Dual-layer Detectors: The previous three paradigms operate the X-ray source at low and high energy in order to accomplish dual energy scanning. The X-ray source, however, is polychromatic. It is therefore possible to acquire a low and high-energy spectral band from a single exposure using a single, specialized detector.

Dual-energy CT can be used for material characterization for such applications as differentiating hemorrhage from iodine or calcification, characterizing plaque, and automatic bone removal. It can also be used as a quantitative tool, for example, for assessing the degree of enhancement of a tumor in oncologic applications, or for CT perfusion. Most DECT post-processing packages also allow generation of virtual monochromatic images that may be used for optimal contrast viewing, posterior fossa artifact reduction, and metal artifact reduction. In the literature, multiple clinical applications of DECT have been described; for combat care, the following are relevant and require further research.

- Differentiation of hemorrhage from iodinated-contrast staining

- Assessment of intracranial hemorrhage

- Reduction of posterior fossa artifacts

- Automatic bone subtraction in head and neck CTA

- Metal artifact reduction

Magnetic Resonance Imaging (MRI)

Functional MRI

Functional MRI (fMRI) is an attractive method for studying TBI because it uses deoxygenated blood as an endogenous contrast agent. It therefore avoids the risks of ionizing radiation and can

be used safely in longitudinal studies and on pediatric cases. In addition, measurements of brain function are arguably more closely linked than structural measures to the subjective symptoms experienced by patients and fMRI can reveal subtle changes in perception, emotion, and cognition.

Recent research provides ample evidence that fMRI is sensitive to brain changes caused by concussion. For example, youths with diagnosed concussion were found to have significantly worse performance and lower fMRI activation than controls in working memory task.[140] When performance on behavioral tasks is matched, patients who had experienced sports related concussions (SRC) had greater activation on a working memory (n-back) task than did controls.[141] Similarly, former NFL players who suffered three or more SRCs showed greater fMRI activation in several brain regions, including the medial temporal lobe, during a memory task than did former players with fewer than three SRCs, even though accuracy did not differ between groups.[142] High school football players who suffered collisions near the top of the head, but showed no clinical symptoms, had deficits on neurocognitive tests and abnormal activation in the dorsolateral prefrontal cortex (DLPFC) during a visual working memory task.[143] This suggests that fMRI is sensitive to brain changes in subclinical concussion as well. Resting state fMRI has revealed abnormal network patterns in mild TBI patients relative to controls and differences between patients with and without post-concussive syndrome (PCS).[144] fMRI may also be useful in evaluating treatment strategies. In a study of the effects of exercise on patients with PCS, aerobic exercise was shown to improve heart rate and PCS symptoms and increase fMRI activation during a math task relative to a PCS control group. The groups did not differ in performance on the math task.[145]

These and other studies suggest that fMRI is sensitive to changes in brain function that result from TBI, but basic questions of interpretation have yet to be settled. It is often assumed, for example, that fMRI activation reflects mental 'effort,' so low activation implies a relative inability to perform the task, while greater activation implies more effort is required to perform at the same level as controls. This interpretation is reasonable, but not proven. Another layer of uncertainty comes from the relation of the BOLD signal to neuronal activity. The BOLD signal reflects the total amount of deoxygenated blood in a voxel, and hence depends on blood flow, blood volume, and oxygen utilization by the tissue. Neurovascular coupling, the causal connection between neuronal activity and the vascular response, may be altered in TBI, however. If so, variations in neurovascular coupling would complicate the interpretation of fMRI studies of TBI.

Cerebrovascular reactivity (CVR) is the capacity of blood vessels to dilate. It can be assessed noninvasively using transcranial Doppler ultrasound or BOLD MRI during hypercapnia, for example by breathing 5% CO_2 alternating with room air.[146] It has been shown that brain injury affects cerebrovascular reactivity both in the acute[147] and chronic[148] phases. This may be a result of damage to the vascular endothelium, smooth muscle, perivascular nerve networks or some combination.[149] In any case, decreased vascular reactivity in TBI would confound comparisons of BOLD activation between patients and controls. Decreased BOLD signal could be due to less neuronal activity or to a smaller increase in blood flow evoked by a similar metabolic demand. Quantifying cerebral reactivity will be important for interpreting fMRI studies of TBI that is, distinguishing neuronal from vascular differences.

An important trend in fMRI research is the development of calibrated fMRI.[150] The goal is to devise methods to assess neuronal activity more directly. The BOLD signal change reflects cerebral blood flow, blood volume, and oxygen utilization. MRI methods exist to estimate blood flow and volume, so it is possible, in principle, to derive MR measures of local cerebral metabolic rate of oxygen consumption (CMRO2). Since individuals differ in resting blood flow and cerebrovascular reactivity, much of the intersubject variability in BOLD response is likely due to these variables, in addition to oxygen utilization. If successful, calibrated fMRI would improve the reproducibility of fMRI as well as provide estimate of oxygen consumption, which is a physiological quantity more directly related to neuronal energy metabolism.

Diffusion MRI

Diffusion MRI (dMRI) is a method to assess tissue microstructure. It measures the random (Brownian) motion of water molecules, which is constrained by low-permeability structures such as cell membranes, the cytoskeleton, and (in white matter) the myelin sheath surrounding axons.[151] For example, the mobility of intracellular water is restricted by the narrow confines of the plasma membrane. The diffusion of extracellular water is hindered by cells that molecules must travel around in order to move through the tortuous extracellular space. Changes in tissue microstructure, for example volume shifts between intra- and extracellular spaces, cell death, or disintegration of myelinated membranes, will likely change the net mobility of water in the tissue. Hence, dMRI is sensitive to brain injury, including edema, axonopathy, and demyelination.

The dMRI method most commonly used is Diffusion Tensor Imaging (DTI).[152] In DTI, the MRI signal is sensitized to the displacement of water molecules in each of several directions in space (at least 6, but typically 20-30). The signal measurements are fit to a mathematical ("tensor") model that describes the variation of diffusion with direction (if diffusion is the same in all directions in space, it is termed *isotropic*—otherwise it is *anisotropic*). The tensor specifies the diffusivity of water along three orthogonal axes, as well as the orientations of the axes, which correspond to the structural symmetry axes of the tissue. For example, in a white matter fiber bundle, axons are densely packed and nearly parallel. In this case, water diffusion is fastest along the axons (because water molecules moving in this direction encounter the lowest density of barriers and slowest diffusion is perpendicular to the axons. The variation of diffusivity over directions is usually quantified by the fractional anisotropy (FA) which equals 0 for isotropic diffusion (as in a glass of water) and equals 1 for (the idealized case of) diffusion in only one dimension. The diffusivity averaged over all directions is called the mean diffusivity (MD). It has been shown that the highest diffusivity (sometimes called *axial* diffusivity) is sensitive to axonal integrity and the mean of the two smaller diffusivities (the *radial* diffusivity) increases with demyelination.[153,154]

Reviews of the literature support the hypothesis that DTI is sensitive to white matter damage in TBI.[155–158] Recent studies have found widespread changes in DTI parameters as a result of sports related concussion (SRC), across a wide range of patient groups and analysis methods. For example, a whole-brain analysis found that FA was increased on average and mean diffusivity was decreased in concussed adolescent athletes, scanned within 2 months of concussion. Whole brain FA was significantly correlated with SCAT2 scores.[159] In a study comparing hockey players with and without concussion, FA and axial diffusivity were increased while radial and

mean diffusivity were decreased in multiple brain regions in the concussion group.[160] In a study of female athletes with SRC, mean diffusivity was higher in several major pathways relative to controls 7 months following injury. No differences in FA were observed in a similar voxelwise analysis (Tract-based Spatial Statistics, TBSS), however an ROI analysis in the corpus callosum showed significantly lower FA in fibers projecting to the primary motor region.[161] Other studies have related DTI changes to symptom severity. Reduced FA at the gray matter-white matter junction was shown to be significantly correlated with concussion symptom score while FA in the parahippocampal gyri was decreased in patients with sleep disturbances relative to those without sleep disturbances.[162]

Other studies find evidence for DTI changes from sub-clinical TBI. In a study over the course of a single high school football season (with no clinical concussions), FA changes were correlated with helmet telemetry and verbal memory score from the IMPACT test.[163] Similarly, a comparison between contact and non-contact sport athletes showed FA differences in multiple brain regions. These differences are more significant in post-season scans than in pre-season scans.[164] In a group of amateur soccer players, higher numbers of headings in the previous year were associated with lower FA values in temporo-occipital white matter regions, with a threshold of about 800 to 1500 headings per year, depending on the region. Lower FA values were associated with poorer memory scores.[165] In college football and hockey players, measures of head impact exposure (via instrumented helmets) correlated with DTI measures in several brain regions, including the corpus callosum, amygdala, hippocampus, and thalamus. The mean diffusivity change in the corpus callosum postseason was associated with performance in verbal learning and memory tests.[166] BBB disruption, assessed via serum levels of the astrocytic protein S100B and its auto-antibody, were measured both pre- and post-game in a group of college football players. No player experienced a clinical concussion, but BBB disruption was detected only in the players with the greatest number of head hits. Serum levels of S100B auto-antibodies predicted DTI abnormalities, which in turn were correlated with cognitive changes.[167]

Although many groups have reported DTI changes in TBI, these changes have not reached statistical significance in all studies. In a relatively large, homogenous sample of 75 mild TBI patients and 40 controls, Iwestmaki et al found no significant effect of acute mild TBI after controlling for age and gender (they did report trends that did not reach significance after correction for multiple comparisons). Post-acute (1 month) results were the same.[99]

There is similar interest in using DTI to study post-concussive symptoms (PCS). For example, DTI has been shown to differentiate pediatric mild TBI patients with and without persistent cognitive symptoms.[168] In a study of time to symptom-resolution (TSR), both sex and uncinate fasciculus FA independently correlated with TSR and were found to be stronger predictors of TSR than was initial symptom severity.[169] In a group of mild TBI patients with persistent symptoms, regions with abnormally high FA (compared to controls) were found in gray matter, possibly indicating gliosis, and regions with abnormally low FA were found in white matter.[100]

A fourth important line of research characterizes the differences between subtypes of mild TBI. In a study of US service members with blast or impact TBI, the most prominent microstructural abnormalities were shared between groups and included fronto-striatal, fronto-limbic, callosal and brainstem fibers. Beyond this, however, superior-inferior tracts were more vulnerable to

blast injury, while anterior-posterior tracts were more affected in impact injury. Post-concussion and PTSD symptoms were associated with lower FA in cortical-subcortical networks.[170]

Despite the sensitivity of DTI to subtle changes in brain tissue, there are several important limitations to the technique. The diffusion tensor has proved to be a valuable model of water diffusion in tissues with simple structure (e.g., where axons share a single orientation), but it cannot accurately describe more complicated cases, such as crossing or bending fibers. More general models are used in High Angular Resolution Diffusion Imaging (HARDI)[171] and Diffusion Spectrum Imaging (DSI).[172] While these newer methods successfully capture the angular dispersion of fibers, they do not simultaneously provide information on fiber-specific diffusivities (e.g., the fractional anisotropy for each of several crossing fibers). Until reliable information on both fiber orientation and integrity are provided by the generalized methods, their clinical utility will be limited. Hence, development of methods that provide both kinds of information should be a high priority.

Fiber orientation information is currently being exploited to track large bundles of axons in the brain. An ambitious goal of this work is to identify the entire set of large-scale connections between brain regions, a dataset that is termed the human connectome.[173] If networks of connected regions can be reliably determined and identified with specific cognitive systems, then measures of fiber integrity in the anatomical connections may be related to specific symptoms experienced by brain injury patients. A major challenge in this effort is to identify the correct cortical targets of white matter fibers. This is complicated by the complex geometry of fibers at many locations in the white matter, but especially directly under most cortical regions. Many axons at the gray/white matter interface bend with high curvature or cross "fibers of passage"— both features pose serious challenges for current tractography algorithms. In fact, the white matter directly under the cortex can have lower FA than the cortex due to the high dispersion of fibers. The accuracy of anatomical network models will depend on improvements in tractography wherever fibers are not all parallel within an image voxel—this represents another critical gap in technology.

A third significant gap in diffusion MRI is reproducibility. Poor reproducibility can make it difficult to interpret the literature, if for example little congruence exists between the results of different research studies. There are multiple potential explanations for poor reproducibility between studies: differences in data processing algorithms[174], choice of reported diffusion metrics (e.g., FA, mean, radial, or axial diffusivity), scanner platforms, and the heterogeneity of injuries in TBI all likely contribute. The situation would be improved if there was a consensus in the field on a near-optimal acquisition protocol, data analysis pipeline, and set of reported metrics.[175] Research groups eager to explore alternative methods should be encouraged to present results of both the consensus and their own novel methods. Similarly, measurements of diffusivity in standard phantoms can help to eliminate variability of results on different scanner platforms.[176]

Magnetic Resonance Angiography, Susceptibility Weighted Imaging, Perfusion Imaging and Oxygen Saturation Measurements

Following the initial traumatic insult, a series of vascular responses and perfusion changes are set in motion and the ultimate neurological outcome may well hinge on homeostasis modulated by

cerebral perfusion. Brain tissue architecture consists of a complex network of neurons and vasculature interspersed within a matrix of supporting cells. Insults to the cerebral vasculature such as microbleeding, local perfusion reduction or oxygen metabolism changes are known to cause devastating secondary complications after TBI.[177,178] Certainly for moderate to severe TBI, vascular damage in the form of shearing and stretching stress occurs. Although this vascular effect is well known, shearing damage of the vasculature may be important even for mild TBI patients. Using susceptibility weighted imaging (SWI)[179–182] and quantitative susceptibility mapping (QSM),[175,183] there is increasing evidence that there is not only major microbleeding that takes place after impact but also evidence of venous damage as well for mild TBI.[184] This venous vascular damage may be the cause of disrupted perfusion, with the hypothesis that the venous system is more vulnerable than arteries to traumatic stretching and shearing forces. This has been suggested recently by multiple investigations in a large number of TBI patients[185–191] and in subarachnoid patients,[192] as well as biomechanically.[193,194]

Evidence now exists that venous vascular damage can occur at much lower forces. This, in turn, can lead to thrombosis, shearing and perfusion loss in the local white matter being drained by these veins.[145] It has been suggested that neural damage may be secondary to vascular damage or obstruction resulting from increased extravascular pressure from petechial hemorrhage.[155] A similar thrust for the role of venous damage has recently been described for subarachnoid patients[156] where the argument is that increased intracranial pressure leads not to arterial problems but to compression of the veins and hence local reductions in blood flow.[154] One might expect that the pathophysiological responses to biomechanical insults at the time of trauma determine the sequence of secondary effects. For example, in an acceleration induced TBI model in primates, increased microvilli associated with metabolic activity of the endothelial cells in arterioles and venules has been shown to peak at 6 hours and this effect can persist up to 6 days.[157] As might be expected, vascular responses are a function of the severity of the trauma. A more recent paper has shown in an animal model that even for a lower magnitude injury, cerebral microbleeds (CMBs) gradually increased over the three months following injury.[158]

In this section, we review aspects of MR angiography, susceptibility weighted imaging, perfusion imaging, oxygen saturation measurements relevant to the study of traumatic brain injury.

MR Angiography (MRA): Investigating the anatomy and function of the vasculature can be done with MRA and quantitative flow imaging but currently the gold standard of angiography is intra-arterial digital subtraction angiography (IADSA).[159,160] However, imaging both arteries and veins rapidly and today for the most part without the use of contrast agents, lies in the purview of MRI. For non-contrast enhanced MRA, the 3D TOF method is most widely used for clinical exams for its potential to image small, tortuous arteries non-invasively. TOF MRA creates a positive artery-tissue contrast as a result of the in-flowing arterial blood being much less saturated than the static tissues. However, the in-flowing blood will gradually reach steady state and become saturated as it passes through the imaging slab, losing the contrast especially for smaller vessels with slow flow. There are several means to increase the contrast for small arteries, including using magnetization transfer contrast (MTC) RF pulse to suppress tissue signal,[161,162] multiple thinner slabs to reduce saturation effect,[163] TONE pulse for spatially varying flip angle excitation,[164] or acquiring an additional flow dephased image and then subtract it from the flow rephased

image.[165–169] The subtraction method is of particular interest as it can greatly reduce or even null the background tissue signal while retaining high vessel signal. Furthermore, a common dilemma for non-contrast enhanced MRAV imaging is the conflicting requirement on tissue signal, that TOF MRA requires low tissue signal while SWI based MRV requires high tissue signal. Today, time-of-flight MA can be done with resolutions on the order of 0.25 mm^3 to produce high quality M1 to M4 vessel information to look for the presence of stenosis or aneurysms without a contrast agent. More recent results have shown MRA in the brain with a resolution of 0.03 mm^3 using a T1 reducing contrast agent.[170] Future possibilities include the use of iron based contrast agents to visualize even smaller vessels.[171,172,173] The problem with using a contrast agent is that both arteries and veins are affected similarly. Using MRA with SWI, it will be possible to separate out arterial damage from venous damage in TBI.[170]

Flow Quantification: Revealing the flow pattern in the major vessels in the brain and the neck will provide a novel and critical insight to the brain's global hemodynamics. For vascular function, phase contrast (PC) flow quantification (FQ) sequences are available both with 2D and 3D methods.[174] The 3D phase PCFQ method offers the ability to monitor flow in 3 spatial dimensions as a function of the cardiac cycle. Currently, it is being used for velocity mapping in cardiovascular applications, using low resolution (typically 2×2×4 mm^3) and high velocity encoding (VENC) values (100 cm/s) to accommodate the need for fast scans to capture fast flows.[174] These data can be collected as a function of the cardiac cycle. This is a great capability but also limits the application to 3D since the effective phase encoding time is limited to the cardiac cycle. For 2D methods, a resolution of 0.5 mm in plane is viable today in just a few minutes, however, even with 1 mm in plane resolution, 3D FQ methods will take 10 to 20 minutes. Nevertheless, these high resolution MRA techniques are likely to become more viable clinically as new methods for faster imaging such as parallel imaging and compressed sensing continue to decrease acquisition time.[175] Combining both the SEPI readout and CS under sampling has the potential for 8 to 16 fold improvement[176,177] in imaging speed, and maintain the total imaging time at the 10 to 15 minute mark.

Susceptibility Weighted Imaging (SWI) and Quantitative Susceptibility Mapping (QSM): SWI has become one of the accepted standards in imaging TBI in the last few years.[142] Tong et al[178] reported that SWI is 3-6 times more sensitive than the clinical standard T2* GRE sequence in the detection of microhemorrhages. Similar results were found by Nandigam et al[179] in their study of CMBs in cerebral amyloid angiopathy (CAA) showing a factor of 3 improvement. SWI generally performs better than T2* methods bt this depends on the imaging parameters and the field strength used.[179–192] Of all these papers, only three papers have discussed using SWI in the spine.[193,194,195]

Although SWI can detect CMBs with exquisite detail, it cannot quantify their iron content. Even identifying the lesions can be difficult since the dark signal representing the CMBs in SWI can be air, blood or calcium for example. Some progress has been made in identifying CBMs from SWI data, but the algorithms are complicated and not widely available for public use.[196] But all three of these can be distinguished and separated with susceptibility maps. Using an iterative SWIM approach, it will be possible to not only visualize the veins but also quantify both the oxygen saturation in the veins as well as the iron content and volume of the CMBs. Other approaches to measure susceptibility and oxygen saturation include: susceptometry[139] and its

more modern form[197–200] as well as T(2) -Relaxation-Under-Spin-Tagging (TRUST)[201] and its more modern form T2-Relaxation-Under-Phase-Contrast (TRU-PC).[202] Both these methods focus on measuring the oxygen saturation in the macroscopic veins. The former uses phase while the latter uses T2 properties.

Future improvements in detecting and quantifying CMBs or detecting areas of ischemia with high levels of deoxyhemoglobin lies in the use of high resolution, high field imaging methods such as SWI and perfusion weighted imaging (PWI). As far as infarcted tissue is concerned, this is best studied using high resolution fluid attenuation inversion recovery (FLAIR) at high fields. A natural next step to monitor CMBs is to quantify the amount of iron present in a given lesion using QSM. This way, even if the bleed volume does not change, it will be possible to ascertain if there has been continued bleeding into the same lesion. This is a natural extension of using the same phase that is used to create the mask for SWI in the first place, but now this phase is used to create the source image instead. Along the lines of quantification of CMBs there has been some effort in this area by a few groups.[196,203,204]

The importance of cerebral microbleeds in TBI and cognitive function: CMBs appear as small punctuate hypo-intense lesions on gradient echo (GRE) imaging and SWI. They are very important in assessing damage in TBI.[157 189 205–217] CMBs are usually associated with small vessel disease such as cerebral amyloid angiopathy (CAA) but they can also appear in a variety of other conditions including but not limited to: hemorrhagic stroke, hypertensive vasculopathy, lacunar infracts, traumatic brain injury, and part of the natural aging process. They are often thought to imply an increased risk for intracranial hemorrhage and evidence is growing that the CMB lesion load is associated with cognitive decline, especially as this relates to dementia. However, their source and their role in neurovascular disease diagnosis and pathophysiology is still under investigation.[218–239] CMBs have been the subject of research papers in many different diseases[200, 240–249,250–267] and conditions including but not limited to: aldosteronosin, Alzheimer's disease, amyloid beta-related angiitis (ABRA), Binswangers disease, CAA, Cerebral autosomal dominant arteriopathy with subcortical infarcts and leukoencephalopathy (CADASIL), mutations, children with heart disease, dementia, Col4A1 mutation, hypertension, intra-cerebral hemorrhage, LPA2, moya-moya, Parkinson's disease, retinal bleeding, sleep apnea, subarachnoid hemorrhage, subdural hematoma, tumors and underweight persons. One of the most important aspects of CMBs is their relationship to cognitive decline and dementia[192,268–298] and Alzheimer's disease.[299–318] The source of a CMB is the hemosiderin left behind after extravasation of blood and after the hemorrhagic transformation process is complete. There are a number of CMB mimics, however, that can confound the situation and these are: a thrombus, iron deposition in the vessel wall as in CAA or a region of hypoxia where deoxyhemoglobin levels have increased beyond the usual 30% levels. All of these may appear the same in GRE or SWI data. Separating them will require the use of MRA, either time-of-flight or contrast enhanced MRA, perfusion imaging and QSM. Overall, the work that has been done on CMBs in other neurological diseases plays a key role in supporting TBI CMB studies.

The overall lesion load (volume and number) of CMBs has been reported to be associated with TBI patients' outcome. Tong et al reported the first study on this in moderate to severe TBI.[137] A study of chronic mild TBI patients also shows that depressive mild TBI patients have significantly higher lesion load (volume and number) of bleeding on SWI images.[215] These

differences in numbers and volume of CMBs were found only in the frontal, parietal and temporal lobes. Another study of single season Canadian Interuniversity Sports players show a statistically significant increase in the microbleeding compared to the beginning of season for male subjects with concussions at the 2-week postconcussion time point.[207] A smaller, non-significant rise in the burden for female subjects with concussions was also observed within the same time period.[207] There were no significant changes in burden for non-concussed subjects of either sex between the start and end of the season time points. CMBs can also be used as a marker of axonal injuries. In Grossman et al's classical neuroradiology text book, diffuse axonal injury could be diagnosed as multifoci hemorrhagic bleeding on major white matter tracts and the junction of gray and white matter.[70] In a study of CMBs using SWI,[211] Park et al reported that, in TBI patients, CMBs were located more frequently in white matter than in deep nucleus; and CMBs in TBI patients showed a characteristic regional distribution, and seemed to have an importance on the initial neurological status and the prognosis. SWI can provide etiologic evidence for some post-traumatic neurologic deficits which were unexplained with conventional MRI. A focal injury animal study has shown that evolving white matter degeneration following experimental TBI is associated with significantly delayed microvascular damage and focal microbleeds that are temporally and regionally associated with development of punctate BBB breakdown and progressive inflammatory responses.[158]

By using machine learning and pattern recognition analysis, a relative sophisticated analytical approach, another group used trained pattern classifiers to predict the presence of white matter damage in 25 TBI patients with microbleed evidence of traumatic axonal injury (TAI) compared to neurologically healthy age-matched controls.[206] The classifiers discriminated between patients with microbleeds and age-matched controls with a high degree of accuracy, and outperformed other methods. When the trained classifiers were applied to patients without microbleeds, patients having likely TAI showed evidence of greater cognitive impairment in information processing speed and executive function. The classifiers were also able to predict the extent of impairment in information processing speed and executive function. Regarding the location of bleeding, there are also substantial differences in locations of CMB development in trauma patients in comparison to stroke patients. Imaizumi et al compared the location of CMBs associated with cerebral microangiopathies with those associated with trauma (tCMBs).[195] They reported that tCMBs were frequently located in the mid portion of the subcortical area of the cerebrum, above the corpus callosum in axial slices, and were absent from the basal ganglia. In contrast, microangiopathic microbleeds were frequently located within the basal ganglia or thalamus.

The role of SWI in TBI treatment and recovery: With the quantification capability in QSM-SWIM, one could track the total CMB lesion load over time to monitor the patients' recovery process after injury. In a study of 146 patients without symptomatic intracranial hemorrhage on computed tomography after thrombolysis, the patients were allocated to two groups: group A (n = 72) received antiplatelets 24 h after recombinant tissue plasminogen activator, regardless of SWI-detected hemorrhage; group B (n = 74) received antiplatelets for patients without SWI-visualised hemorrhage.[196] The results indicated that SWI was an effective approach for the guidance of antiplatelet therapy in post-thrombolysis MB. In addition to CMB, venous thrombosis is often seen in TBI patients due to that veins are more vulnerable than arteries during traumatic event. On SWIM image, the thrombosed vein will show much higher

susceptibility measure than regular veins. This gives SWIM an opportunity to monitor future thrombolysis treatment. Jamjoom et al gave a systematic review on safety and efficacy of early pharmacological thromboprophylaxis (PTP) in traumatic brain injury. They conclude that early PTP (<72 h) reduces the risk of venous thromboembolic events without affecting progression of intracerebral hemorrhage. This could have significant impact in TBI treatment and SWI/SWIM could be used as a tool to guide clinical decision making.[185]

Perfusion Imaging: Cerebral perfusion and metabolism are less investigated areas in TBI.[197–200] Perfusion studies using either ASL[201] or DSC PWI[202] have demonstrated reduced CBF in moderate to severe TBI and in chronic mild TBI patients. Furthermore, experimental animal models in moderate to severe TBI have demonstrated a decrease in venous blood oxygenation that accompanies the decrease in arterial blood supply,[203] which is suggestive of brain tissue at risk for hypoxia. There are also a few studies indicating higher CBF immediately after trauma.[204–210] Marion et al[209] observed that CBF peaked to a significant high at the 24 hour time point after injury. They also studied a diverse range of injury pathologies at a wide range of times after injury. Obrist et al[211] studied the cerebral metabolic rate of oxygen ($CMRO_2$) and CBF in 75 severely-injured patients and observed a positive correlation between GCS score and CBF in patients with far lower GCS scores than ours. They also found that CBF reached its highest peak at 24 hours after injury, supporting the same timeline as seen in Marion's study. Muizelaar et al.[210] suggested that $CMRO_2$ is significantly positively correlated with GCS scores, though the study was limited to severe cases and did not include patients with high GCS scores. Bouma et al[204–206] observed that relative CBF reaches its peak between 24 to 48 hours after injury which was supported by the work of Mendelow et al[212] as well. In an animal study, Prat et al[213] observed that the animals impacted with less weight (producing a less severe injury) showed an increase in CBF acutely between the one and three hour time points after injury, which was followed by a decrease in CBF thereafter.

Improving CBF after TBI has been suggested as a target for drug treatment and neural intensive care management.[210] However, due to the decoupling between cerebral metabolic demand and blood supply after TBI, CBF is just part of the story. To make it worse, in addition to the deleterious effect of reduced perfusion, immediate reperfusion after trauma could be harmful to salvageable brain tissue as well. Recent clinical trials suggest the importance of increasing brain tissue oxygenation to improve moderate to severe TBI outcome. All these suggest that, instead of just CBF, $CMRO_2$ might be more important to serve as our treatment target. In terms of improving either CBF or brain tissue oxygenation, the final goal is to keep the brain tissue at reasonable $CMRO_2$ to maintain its homeostasis status. From a CBF treatment perspective, both timing and dose are critical issues that need to be considered in studying perfusion to the brain after TBI. In a recent study of TBI in an animal model by using caffeine as a neural protective agent to control the CBF, the data suggest that, subacute stage caffeine treatment rather than acute stage treatment results in more favorable outcome in traumatized animals.[214] Further, from a brain tissue oxygenation perspective, to maintaining a decent drainage of the venous system has the same importance as improving arterial blood supply. This could be the case of venous thrombosis after TBI.[185] Furthermore, the field still needs a better means to monitor regional brain tissue oxygenation to determine $CMRO_2$ in an non-invasive manner throughout the brain.[215] The current brain catheter probe offers continuous monitoring of brain tissue oxygenation for $CMRO_2$ determination. However, it is invasive and restricted to only one brain

region. The brain hemodynamics is region-specific. Patients with normal intracranial and cerebral perfusion pressure could still have regional hypoxia that could lead to worse outcomes.[216] From this perspective, MRI has the potential to solve the problem as described in the next section.

Conclusions and Future Directions: MRI with its many new tools offers the potential to investigate the full spectrum of vascular injury and its relationship with traumatic hemorrhage (neurovascular disruption), perfusion deficits, venous blood oxygen saturation changes and resultant tissue damage. The potential findings that could come from studying the disruption to the vasculature include: a better diagnosis of TBI; an improved understanding of the mechanisms behind TBI pathology; and potential neuro-protective and neuro-restorative approaches to treat TBI. These MRI methods make it possible to image the hemodynamics of the brain, monitor the damage, and show changes induced in the brain's function not only acutely but also longitudinally following treatment.

The three main knowledge gaps addressed in this material include:

- The role of reduced perfusion in mild TBI

- The duration of reduced perfusion and if it continues in persistent mild TBI

- The role of reduced perfusion and cerebral microbleeds leading to cognitive decline and dementia

The transformative technologies given here include perfusion weighted imaging, susceptibility weighted imaging and measuring oxygen saturation to estimate $CMRO_2$. The real unique aspect of these technologies is their marriage into a single imaging protocol to study mild TBI.

Magnetic Resonance Spectroscopy

Summary of MRS Studies: Magnetic resonance spectroscopy (MRS) differs from other imaging methods in traumatic brain injury in that it measures the concentration of chemicals in the brain. These chemicals are often involved in metabolic processes in the brain thus providing a window into the underlying pathological changes that can occur as a result of brain injury from acute to chronic stages.[217] This quantitative, non-invasive, and objective technique has demonstrated its value in diagnosis and prognosis, particularly in severe brain injury. Specific chemical changes identified by MRS are also amenable to targeted treatment and treatment-monitoring. Available across all MR scanners as a software option, this research technique shows great promise to be readily translated into clinical practice.

MRS can be acquired using several different methods.[218] The so-called single voxel method selects a region of interest (ROI) to interrogate metabolic concentrations using water-suppression pulses followed by a 90^0 refocusing pulse for a stimulated echo acquisition mode (STEAM) or 180^0 pulse for a spin-echo or point-resolved spectroscopy (PRESS) acquisition. Due to the overlap of chemicals within the spectrum, additional pulses can be used to obtain greater spectral specificity, such as the MEGA-PRESS method (REF), or to obtain a broader range of metabolites, such as the correlated spectroscopy method which provides two chemical shift domains.[219,220] Other pulse sequences can be used to also obtain greater spatial specificity, such

as chemical shift imaging (CSI) methods which utilize an additional phase encoding step to add a spatial dimension in slice (2D) or volume (3D). Similar to MRI, the choice of echo time affects which metabolites are visible based on their T2 relaxation such that short-echo (TE < 50 ms) can measure fast relaxing metabolites that are no longer visible in long echo acquisitions.

The major metabolites measured by MRS are the following:

- Lipid: Although lipids are present throughout the brain in the form of membranes, they are not "MR visible" unless liberated by a severe pathological process including brain trauma.[221]

- Lactate: Lactate is the end product of anaerobic glycolysis and therefore a direct indicator of hypoxic events in the brain. The presence of lactate in spectra indicates impairment of perfusion and is indicative of poor outcome.[222]

- N-acetyl aspartate (NAA): An amino-acid derivative synthesized in neurons and transported down axons, NAA is a marker of viable neurons, axons and dendrites. Brain injury is associated with decreased NAA.[223–225]

- Glutamate and glutamine (Glx): Glutamate is the primary excitatory neurotransmitter in the brain and is tightly coupled to glutamine which is found in the astrocytes. Studies have shown that the Glx resonance is predictive of outcome after severe TBI.[226] Glx is not visible at long echo.

- Cr (creatine): An energy marker that is often used as an internal reference for the measurement of other peaks. Earlier MRS TBI studies utilize ratios of metabolite to Cr. However, recent studies have shown changes in Cr as a result of head injury and therefore these ratios must be considered carefully.[227,228]

- Choline (Cho): Choline is a membrane marker used to measure the changes in brain tissue. Since the majority of choline-containing brain constituents are not normally soluble, pathological alterations in membrane turnover result in an increase in MRS visible Cho. In the context of head injury, Cho is often described as a marker of diffuse axonal injury.[229]

- mI (myo-inositol): mI is an astrocyte marker and osmolyte. It is also involved in the metabolism of phosphatidyl inositol, a membrane phospholipid, and, similar to choline, is expected to increase after TBI due to membrane damage. Another explanation for increased mI after TBI is that mI is a purported glial marker and increases as a result of reactive astrocytosis or glial scarring.[230] mI is not visible at long echo.

Early studies using MRS in severe traumatic brain injury[231] have demonstrated that there are changes in cerebral metabolites a strong correlation with clinical grade and patient outcome.[223] These studies have shown 1) a persistent reduction of the brain metabolite NAA indicative of neuronal and/or axonal injury, 2) presence of lipid and lactate, markers of hypoxia, and 3) elevated concentrations of cerebral osmolytes: choline (Cho), and myo-inositol (mI) in both grey (GM) and white matter (WM) regions of the brain in patients with traumatic brain injury when compared to age-matched controls. Typically the greatest changes were observed four days after

the injury.[384] These results have been confirmed in many other studies[46,226,229,232–238] that also demonstrate correlation of these MRS findings with neuro-psychological function.[46,234]

Mild TBI has shown similar findings although the results have been less consistent due to a number of different factors that influence the more subtle changes in concussions.[239] Age can be a factor as most studies in adults have shown reductions in NAA after concussion[227,228,236,240–245], whereas children have not[246], possibly demonstrating a potential developmental neuroprotective mechanism. Gender can also play a role with recent studies demonstrating differences in metabolic changes in women.[161,247] Variation in data acquisition methods including differences in pulse sequences and regions of interest which can be influenced by grey and white matter differences have also led to differences observed in Cho, Glx, and mI concentrations.[248] Heterogeneity of injury with regards to location as well as number of concussions also influence metabolic changes. Longitudinal MRS studies in mild TBI have also shown that metabolites can recover over time and therefore the time after injury (acute vs chronic) must also be taken into account when evaluating spectral differences.[228,243,244,247] In general, the studies show an initial decrease in NAA after injury which then recovers over time. Choline changes appear to be more variable and as it relates to membrane turnover or diffuse axonal injury may be dependent on the type and extent of the brain injury. Changes in Glx and mI, tied to excitoxicity and glial cell proliferation, respectively, appear to be more long-standing. It is important to note that both Glx and mI are only observed using short-echo spectroscopy which is the reason why other studies, which utilized long-echo methods, did not detect these changes. Similar findings have also been shown for repetitive brain injury such as those suffered by sports athletes[244,249] and military personnel.[250]

Recent Literature: There have been several recent reviews of brain injury that have focused on the use of magnetic resonance spectroscopy from mild[217] to severe[251] brain injury as well as more specific topics including repetitive brain injury[239], sports-related head injury[248] that provide a comprehensive list of relevant literature. In addition to that body of literature, the past two year have seen a dramatic increase in the number of MRS papers in TBI.[252–259,260] Recent new findings include the use of 3D chemical shift imaging methods[259,260] which provide greater spatial sensitivity of MRS to injury. Studies have also examined the impact that drug abuse[258] and aging[261] upon brain chemistry in the injured brain with both showing further decreases in NAA. Another study found that asymptomatic concussed athletes show normal levels of GABA, glutamate, and NAA but with a significant correlation between GABA and glutamate possibly indicative of a neurotransmitter imbalance.

Potential Clinical Applications: Given the heterogeneity of mild TBI, there still remains much work to be done before a viable diagnostic or prognostic tool can be utilized in the clinic, however the severe TBI work that has been done has demonstrated that metabolite measures can provide both diagnostic and more importantly prognostic measures. Current MRS methods such as single voxel spectroscopy and chemical shift imaging are clinically available across all MR manufacturers where an additional scan of 5-10 minutes can provide a wealth of information that can assist with outcome measures in the severely injured, particularly for patients in comas. There remains the need for large, prospective clinical trials to confirm the clinical utility of MRS in severe brain injury.

Existing Applications Outside of TBI: There are few studies that have utilized multinuclear MR spectroscopy methods such as ^{31}P, ^{13}C, and ^{23}Na in the field of TBI. ^{13}C MRS in TBI has been limited to animal studies however a recent review[262] describes how this technology can be used to investigate energy metabolism, neurotransmission, neuroglial compartmentation and other pathophysiological changes in brain injury. ^{13}C MRS has been applied in humans in various diseases such as Alzheimer's disease, metabolic disorders, and schizophrenia but has not yet been applied to brain injury.[263] Similarly, sodium imaging methods can provide additional pathophysiological information regarding tissue viability, intracellular changes, and cell integrity as has been shown in stroke[264] and other diseases[265] but not yet in brain injury.

Machine learning and pattern recognition methods have been increasingly utilized for both data acquisition methods as well as in diagnostic use. A recent comprehensive study by Luts et al[266] has shown that physics-based MRS quantitation techniques, do not offer any added value over purely numeric pattern recognition approaches in their effort to discriminate different tumor types. This was recognized early on who have long used pattern recognition techniques applied to MRS to discriminate between a wide range of different diseases.[267–275] Pattern recognition methods that enable the discovery of biomarkers to be used by classification algorithms have not yet been applied to MRS in mild TBI and could provide greater specificity and sensitivity to brain injury particularly in distinguishing comorbid conditions such as post-traumatic stress in military subjects which would influence spectroscopic results.

Knowledge Gaps: While the scientific evidence for the use of MRS in brain injury is strong, there remains the lack of large multicenter trial to demonstrate the efficacy of the technique in both severe and mild brain injury. Consensus as to how MRS data should be acquired and analyzed also remains elusive. Another knowledge gap is the paucity of studies that utilize a multimodal approach to determine how MRS can be complimentary and supportive of other imaging modalities thus enabling a more complete picture of the pathophysiology of brain injury. This would be particularly important when evaluating mild TBI within the context of comorbid conditions and where advanced MRS methods combined with other imaging methods can be used in conjunction to distinguish those changes specific to brain injury. Finally, the potential that subconcussive blows may also induce biochemical changes observed by MRS remains to be explored.

Optical Imaging

Introduction

Biomedical Optical imaging refers to a diverse array of imaging technologies that range from nanoscopic measurements of isolated cells to non-invasive measurements in humans. We limit the discussion here to technologies that are being used in humans with relevance to TBI. These technologies are near infrared spectroscopy (NIRS) and diffuse correlation spectroscopy (DCS). Confocal microscopy and two-photon microscopy and Optical Coherence Tomography are also used in humans, but presently their use for TBI in humans is not evident; although their assessment of blood brain barrier leakage[276] and microglia[277] and cerebral blood flow[278,279] responses to injury in animal models is impacting our understanding of injury evolution in animal models. As we review below, NIRS and DCS methods have been used in humans to measure cerebral hematomas, the impact of vasospasm and changes in intracranial pressure,

alterations of cerebral vascular reactivity and autoregulation, and the impact of TBI on cognitive function.

Near Infrared Spectroscopy (NIRS) and Diffuse Correlation Spectroscopy (DCS)

The dominant absorbers in the human body in the visible and near infrared wavelengths are oxygenated (HbO) and deoxygenated (HbR) hemoglobin and water (H_2O). Visible wavelengths of light are strongly absorbed by hemoglobin, decreasing significantly for near infrared wavelengths greater than 650 nm. Above 950 nm, water absorption increases significantly. Thus, there is a window between 650 and 950 nm where the absorption of light is small and, despite the strong scattering of light by tissue, the light is able to diffuse several centimeters through the tissue and still be detected.

It was first reported in 1977[280] that near infrared light could diffuse through the intact scalp and skull of an adult human to probe the hemoglobin concentrations in the brain. Because the absorption spectra of HbO and HbR differ, we can utilize measurements of the attenuation of light diffusely reflected by the brain at multiple wavelengths to perform a spectroscopic estimation of their concentrations in the brain. The challenge is that estimation of the absolute absorption coefficient, and thus absolute hemoglobin concentrations, requires knowledge of the path length of light through the tissue. The path length is not the physical distance from the source where light enters the tissue to the detector where it is measured exiting the tissue. Strong scattering of light by the tissue diffuses the light and increases the path length. Multiple strategies are employed to overcome this challenge with varying degrees of success. Typically, changes in the measured attenuation of light are related to changes in the hemoglobin concentrations. These measurements are made with simple continuous-wave NIRS devices.[281] More sophisticated frequency-domain (FD) and time-domain (TD)[282] instruments are used to estimate the path length of light through the tissue to enable estimation of the absolute hemoglobin concentrations. These instruments either intensity modulated the source at ~100MHz and resolve the amplitude and phase of the detected light, or picosecond pulse the laser and temporally resolve the detected light with ~100ps resolution. Light sources and detectors are typically connected to the head through fiber optical cables, but can also be placed directly on the surface of the head. On adults, the distance between source and detector is typically 3 cm or greater to increase sensitivity to the brain and reduce confounding influence from the scalp. The vast majority of NIRS studies in the literature are based on CW-NIRS devices, but recently more and more studies are beginning to appear with FD-NIRS and TD-NIRS devices as technology improvements make these more sophisticated devices more accessible.

Diffuse Correlation Spectroscopy also uses near infrared light to penetrate through several centimeters of tissue. Instead of measuring the attenuation of light, it measures the Doppler broadening of the light caused by light scattering from moving red blood cells.[283] DCS thus provides a measurement of cerebral blood flow (CBF), while NIRS provides measurements of total hemoglobin concentration (HbT = HbO + HbR) and hemoglobin oxygen saturation (SO2 = HbO / HbT). DCS measurements must be made with a laser with a coherence length longer than the distribution of path lengths of light through the tissue (typically 10's cm), and a detector that measures a single speckle of light usually through a single mode fiber. While NIRS

measurements can be made with >1mm detection fibers, DCS detection fibers are ~5um and thus collect 40,000x fewer photons.

The combination of NIRS and DCS provides a comprehensive measurement of oxygen delivery to the tissue, enabling estimation of the cerebral metabolic rate of oxygen, CMRO2. This has been demonstrated in healthy and brain injured infants[284,285], as well as in adults.[286]

Clinical Studies Relevant to TBI

The damage arising from TBI can be divided into primary and secondary types of injury. Primary injury arises at the moment of injury from mechanical forces directly damaging blood vessels and cells. This damage then leads to secondary injury arising from complex cellular, metabolic, and inflammatory reactions. Intracranial hematomas can result from the primary injury, many types of which can be detected by NIRS.[287,288] Insufficient oxygen delivery to the brain or oxygen utilization by the brain are common issues in TBI that lead to secondary injury.[289] While clinical protocols for maintaining oxygen delivery call for managing mean arterial blood pressure (MABP) and intracranial pressure (ICP), a more direct measure is provided by DCS and NIRS and would guide better management of the patient and likely help improve outcomes. Mild TBI is known to reduce cerebral blood flow and alter cerebral vascular reactivity, both of which are being measured with NIRS and DCS. Finally, the impact of TBI on brain function are being measured with NIRS as is the impact of cognitive rehabilitation.

Brain Hemorrhage

TBI can result in bleeding in the brain leading to epidural, subdural, and intra-parenchymal hematomas. This presents a large absorbing contrast target to be detected by NIRS. In 1993, Gopinath et al. first systematically investigated the ability of NIRS to detect these different types of hematomas.[287] They showed that NIRS detected less light on the hemisphere with the hematoma compared with the contralateral hemisphere. They measured 40 patients, 10 with epidural, 22 with subdural, and 8 with intra-parenchymal hematomas, and found optical density differences of 0.99 +/- 0.30, 0.87 +/- 0.31, and 0.41 +/- 0.11 respectively. The smaller difference for intra-parenchymal hematomas results because these are deeper in the brain and thus NIRS is less sensitive to them. This indicates the main limitation of NIRS for measuring hematomas, its limited penetration depth.

In subsequent papers, Gopinath and Robertson demonstrated that NIRS could be used to longitudinally follow TBI patients to determine if they develop a delayed hematoma not present at initial examination, or if it the hematoma worsens, thus providing important and timely information for optimally guiding the management of the patient.[290,290] Since these first studies, several other research groups have published comparable findings showing the ability of NIRS to reliably measure epidural and subdural hematomas.[291–295] The impact that a portable NIRS device could have on improving patient outcome by diagnosing this injury in the field needs to be determined, as well as the potential negative effects of reduced sensitivity to intra-parenchymal hematomas.

Vasospasm

Hematomas can lead to vasoconstriction of the arterioles supplying oxygen to the brain. This is known as vasospasm[296], frequently occurs following hematomas even after surgical evacuation

of the blood pool, and results in secondary ischemic damage of the brain. Vasospasm will result in reduced cerebral hemoglobin oxygenation (SO2) because of reduced blood flow. Using TD-NIRS, Yokose et al. reported observing significant reductions in SO2 due to vasospasm as confirmed by digital subtraction angiography.[297,298] The small study of 14 subarachnoid hemorrhage patients compared to 11 age matched controls provided evidence that NIRS could be an effective approach to continuously monitor a patient and promptly indicate the occurrence of vasospasm. This would then permit prompt pharmacological manipulations to increase blood flow and oxygen delivery to counteract the vasospasm and reduce the chance of ischemic damage. Indeed, Mutoh et al. has shown that NIRS could provide real-time feedback on the effectiveness of dobutamine for reversing the vasospasm induced reduction in blood flow.[299]

NIRS can also measure the occurrence of vasospasm through its impact on cerebral autoregulation. The impact on autoregulation has been extensively investigated with transcranial Doppler ultrasound by correlating slow variations in arterial blood pressure with blood flow velocity, and more recently with NIRS correlating pressure changes with hemoglobin oxygenation fluctuations.[296] An impaired autoregulation will permit pressure fluctuations to drive fluctuations in flow velocity and oxygenation and the two parameters will have a positive correlation. This correlation will become negative for intact autoregulation. Studies have shown that this correlation analysis can predict which patients will develop delayed cerebral ischemia from vasospasm.[300–302]

Intracranial Pressure

Increases in intracranial pressure (ICP) following TBI can result in reduced CBF and secondary ischemic damage to the brain. NIRS and DCS offer the ability to continuously monitor the brain to ensure adequate CBF and cerebral oxygenation is maintained and potentially provide evidence of increased ICP. Research has been published on using NIRS to monitor vasogeneic ICP waves following TBI. Slow oscillations in HbO and HbR were found to be negatively correlated with ICP of ~10mmHg, becoming positively correlated as ICP increased to 18 mmHg.[303] DCS is ideally suited to measure if CBF decreases with increasing ICP, but such a study has not yet been performed.

Head Position

In brain injured patients, it is common to raise the head of the bed to an angle of 30 degrees to reduce intracranial pressure allowing an increase in cerebral perfusion pressure and CBF. The effectiveness of this procedure is not well understood as it depends on a complex relationship between intracranial pressure, cerebral perfusion pressure, and cerebral vascular resistance and how they vary with the angle of the bed. It would be more effective to use a bedside optical method to obtain a direct measure of the impact of head of bed angle on CBF and cerebral oxygenation. This has recently been demonstrated in stroke and brain injured patients using NIRS and DCS measurements.[286,304–306] Using DCS, preliminary results demonstrate patient specific angles for maximizing blood flow and oxygen delivery.[286] The results are preliminary, but are an exciting indication of how continuous bedside optical measurements can be used to guide the management of patients to maintain sufficient CBF and oxygen delivery.

Cortical Spreading Depression

Cortical spreading depression (CSD) is a wave of neuronal depolarization that spreads through the cortex. In the context of brain injury, it is initiated by the inability of cells to maintain ionic balance and an excess of extracellular potassium triggers the release of more intracellular potassium leading to a spreading depolarization. This spreading depression is associated with strong changes in blood flow[307], oxygenation[308], and tissue scattering[309], all of which can be measured optically and non-invasively in humans. While CSD is normally associated with increases in blood flow, repeated CSD's in injured tissue have been observed to result in a vasoconstrictive response to reduces blood flow and oxygenation, producing ischemic conditions.[310–313]

Mild TBI

Increasing evidence is indicating that repeated concussions, or mild TBI, can lead to cumulative cognitive and psychiatric decline. Mild TBI is challenging to diagnose because it generally appears normal on standard imaging methods. Research is now focusing on the impact of mild TBI on the control and regulation of CBF as well as cerebrovascular reactivity.[314] Animal studies have revealed decreases in CBF from repeated blows to the head[315,316], a result that has recently confirmed using DCS in rodents (personal communication with David Boas and Maria Angela Franceschini). The observed decreases in CBF are significant and sufficiently large to measure in humans, as has been confirmed with transcranial Doppler ultrasound.[317] In addition to reducing resting CBF, the CO2 vascular reactivity has been shown to be impaired following mild TBI and to resolve after a few days.[318] Additional studies are now needed in humans to confirm if mild TBI causes a decrease in CBF and vascular reactivity and if this can then be used as a guide to determine mild TBI severity to help guide rehabilitation. Studies are also needed to investigate if these observed reductions are making the tissue more susceptible to ischemic damage that could be prevented by more aggressively managing cerebral oxygen delivery in these patients. Preliminary studies in humans have been reported to show that NIRS can resolve TBI induced changes in cerebral vascular reactivity.[319,320] (Zweifel, Castellani, Czosnyka, Helmy, et al. 2010; Highton et al. 2013).

Measuring Functional Brain Activity and the effect of TBI

NIRS has been used to measure brain activity for over 20 years, as recently reviewed in a special section of Neuroimage.[321] Several studies with NIRS have shown the effect of cognitive impairments on the brain activity measured by NIRS. Significant differences in the response of the dorsal lateral prefrontal cortex to verbal working memory and other cognitive tasks have been revealed in TBI patients compared with normal.[322–325] Further, it has been shown that NIRS can be used to monitor the cerebral responses to cognitive rehabilitation tasks to help monitor the effectiveness of therapy.[326]

Knowledge Gaps

While NIRS and DCS shows great promise for diagnosing TBI, guiding acute clinical management of the patient, and monitoring long-term response to therapy, there are two critical knowledge gaps. Primarily, the studies published to date have all been preliminary proof of principle studies indicating the promises. The technology has been evolving rapidly, overcoming several issues, and the time is mature for larger demonstrative clinical trials to be performed for targeted applications. None-the-less, there is still a major technical challenge that needs to be

considered when performing such clinical trials. NIRS and DCS measurements are more sensitive to the scalp than the brain and thus steps must be taken in analyzing the data to ensure that scalp hemodynamics are not confounding characterization of cerebral hemodynamics. Algorithmic advances are being made to better distinguish cerebral from extracerebral hemodynamics using short and long separation measurements[327] and time domain NIRS measurements can be gated at long photon transit times to increase sensitivity to the brain.[328,329] In addition, DCS has been shown to be fundamentally more sensitive to the brain than NIRS.[330]

Positron Emission Tomography (PET)

FDG PET in TBI:

- FDG-PET measures metabolic activity in the brain. In other brain disease states, such as Alzheimer's disease (AD), FDG-PET has enabled differential diagnoses of AD versus other neurological diseases.

- For TBI, FDG-PET has described physiological changes that underlie TBI symptoms.

- As of yet, FDG-PET studies have not demonstrated a consistent pattern of metabolic change that reliably characterizes TBI.

- FDG-PET may also image connections between specific brain regions such that patterns of altered metabolism might better enable diagnoses, but for TBI, further studies are necessary to determine if a pattern of functional connectivity can be discerned in the etiology of TBI.

[^{18}F]fluorodeoxyglucose (FDG) is a ^{18}F-labeled analog of deoxyglucose (DG); unlike glucose itself, deoxyglucose is only partly metabolized by hexokinase at the rate-limiting step in glycolysis.[120] FDG provides an inferred measure of glucose metabolism. Radiolabeled glucose has been used in PET studies for a more direct indication of glucose use, but because glucose metabolites enter many cellular pathways, radiolabeled glucose is more complex to quantify. FDG is clinically useful in indicating areas of hypo- or hypermetabolism in the brain, potentially indicating inflammation or cell death at early stages not detectable in other imaging modalities. Consistent patterns of altered metabolism in the brain have enabled clinical uses of FDG-PET. For example, FDG-PET is able to differentiate early AD cases from other dementing disorders. For TBI, FDG-PET is used to describe the physiological change that underlies TBI symptoms, as well as to distinguish symptoms arising from TBI from other, possibly comorbid conditions.

As Byrnes et al. (2014) note, MRGlc, the metabolic rate of glucose consumption, is not directly measured by FDG. Though analogous, FDG is not transported across the blood-brain barrier at the same rate as glucose and FDG must compete with DG. These complications mean that calculating MRGlc requires that nonradioactive glycemia must be measured in plasma and the lumped constant, a ratio that quantifies the differential binding of FDG versus glucose, must be determined. While the lumped constant is well established for healthy controls, pathological conditions, such as TBI, might well alter the lumped constant and necessitate robust studies that measure radioactivity and glucose concentration in blood.[121]
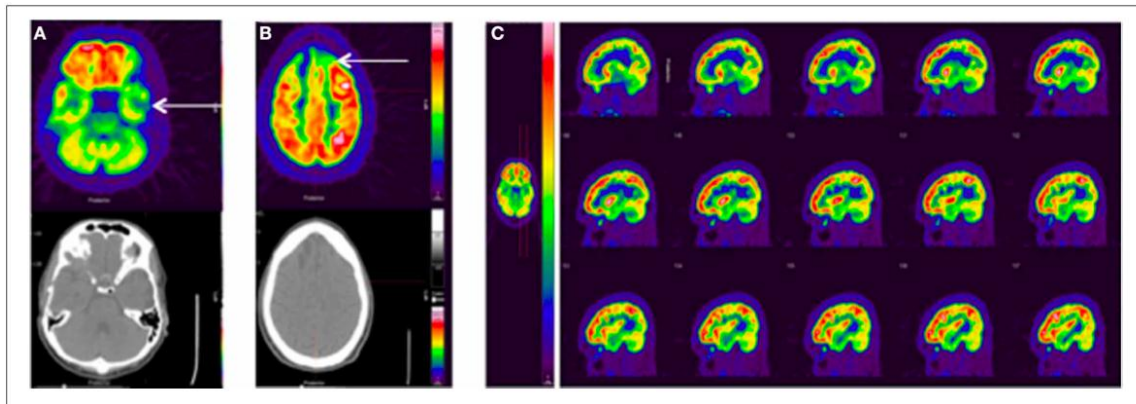
Figure 3. FDG-PET images from three cases of TBI, as reported in Byrnes et al., 2015. [121] The color bar in B applies to all images, with red indicating greater FDG uptake.

Because of these difficulties in quantitative FDG-PET, semiquantitative methods such as standardized uptake values are often used. SUVs calculate activity of FDG in relation to a reference region that does not have altered FDG uptake in a disease state versus control.[331] More sensitive semiquantitative methods are emerging that calculate PET radiotracer binding not in relation to region, but by voxel (a unit of resolution in 3 dimensions, like a pixel). García-Panach et al. (2011) apply a voxel-based approach in a semiquantitative FDG-PET study of TBI in 49 patients against 10 controls. The 49 TBI patients were divided into three groups: minimally conscious and vegetative patients, post-traumatic amnesia patients, and patients who have recovered from post-traumatic amnesia. The García-Panach group demonstrated that hypometabolism correlated to severity of injury in three cortical regions of interest (precuneus, and frontal and temporal lobes) and also in the thalamus. Thalamic hypometabolism is thought to result from either direct injury, diffuse axonal injury (DAI), or deafferentation.[332] García-Panach et al. suggest that deafferentation might best explain thalamic hypometabolism because their voxel-based approach seems to demonstrate functional connectivity between these regions. However, García-Panach's findings do not have the robust sample size to draw a more definitive conclusion regarding the connectivity of affected regions in TBI and whether a pattern of hypometabolism can emerge that would differentially characterize TBI.

Functional connectivity using FDG-PET has shown promise in enabling PET to differentiating a statistically consistent pattern of hypometabolism that characterizes ALS (amyotrophic lateral sclerosis) in contrast to controls, according to Pagani et al (2014) and in AD according to Toussaint et al (2012). That group emphasizes that use of FDG-PET in imaging the neural networks that underlie an observed pattern of hypometabolism requires a large number of study participants and statistical cross-validation.[333] Otherwise, voxel-based comparisons might overestimate model accuracy. In AD, Toussaint et al. used voxel-based analysis to show that patterns of hypometabolism in brain regions develop in early AD, but not in MCI (mild cognitive impairment), especially in areas that constitute the default mode network.[334] The potential that an observable pattern of hypometabolism might be functionally connected was hypothesized from past findings that showed consistent hypometabolism in parieto-temporal and posterior cingulate cortices in AD. These regions are thought to function in the default mode network. Functional

imaging is more common with MRI, as noted earlier in this report in the "Functional Imaging Overview."

Even without a statistically supported functional model, some studies have attempted to use FDG-PET to differentiate TBI from other comorbid conditions. Peskind et al. (2011) use FDG-PET to determine whether chronic symptoms such as cognitive deficits, fatigue, headache, and tinnitus indicate TBI or are associated with comorbid depression or post-traumatic stress disorder (PTSD) in Iraq War Veterans.[335] The Peskind group finds that TBI does have a consistent pattern of hypometabolism quantified by FDG-PET, notably in the cerebellum, vermis, pons, and medial temporal lobe. However, those findings are not consistent across other studies, as Byrnes et al. notes for a wider set of TBI studies.[121] Indeed, Mendez et al. (2013) control for PTSD and find hypometabolism in the left frontal and temporal regions and the thalamus. But unlike Peskind et al., they find hypermetabolism in the right caudate and temporal regions.[336] These studies suggest some clinical uses of FDG-PET for TBI, not only correlating symptoms with abnormal brain metabolism, but also for distinguishing TBI from other comorbid conditions.

Imaging with Ligands that Bind to Amyloid and Tau

- Chronic traumatic encephalopathy (CTE) is a neurodegenerative disease thought to arise from repeated instances of TBI. It is characterized by pathological accumulation of the tau protein, which normally functions to stabilize microtubules, especially in the brain.

- Tau has been challenging to image using PET because of its molecular properties—that it is expressed intracellularly, and occurs in six isoforms.

- Tau radioligand synthesis is an active area of research with at least six new classes of promising ligands.

- Preliminary case reports and first-in-man studies suggest the usefulness of T807 as a tau imaging agent, possibly in diagnosing CTE.

Autopsy studies of a limited number of patients who have suffered TBI have lead some researchers to diagnose chronic traumatic encephalopathy (CTE), a putative tauopathy—a neurodegenerative disease characterized by the aggregation of hyperphosphorylated tubulin associated unit protein or tau. In CTE, global brain atrophy with a thinned corpus callosum, enlarged ventricles, and cavum septum pellucidum have been observe.[337] The prevalence of CTE amongst subjects who have suffered TBI is unknown, as is the prevalence of other injury-associated brain pathologies, for example those associated with Alzheimer's disease or frontotemporal degeneration. Nevertheless, there are concerns that even mild, repetitive TBI leads to the development of one or more progressive pathologies causing the delayed emergence of these neuropsychiatric disturbance.[338–340] To best understand these relationships the development of *in vivo* tools, preferably utilizing brain imaging is essential.

Regarding CTE, it has been hypothesized that repetitive mild TBI leads to axonal damage and inflammation, followed by deposition and aggregation of hyperphosphorylated tau protein (p-tau) and the formation of neurofibrillary tangles (NFTs) in susceptible areas.[117,341] Thus CTE as a tauopathy would emerge as part of the secondary injury of TBI, or following secondary injury

as a chronic condition. CTE has been described in three stages. In stages I and II, foci of tau pathology are limited to the depths of cortical sulci and brainstem areas such as locus coeruleus. By stage III, NFTs have a more widespread distribution.[126] It is unclear whether the primary pathology of CTE is deposition of p-tau or whether dysregulated inflammation drives protein deposition.[342] Regional NFT distribution may promote chronic inflammation and neurotoxicity, resulting in underlying changes in local neuron morphology, more diffuse synaptic changes, and possibly changed cholinergic neurotransmission.[343,344] NFT accumulation may also promote aggregation and diminished clearance of other pathologic proteins including amyloid β, TDP-43, and alpha-synuclein, thereby fueling further neurodegeneration, inflammatory response, and associated cognitive decline.[341,342,345] Although neuroinflammation is not necessarily deleterious and could represent compensatory repair of these other degenerative processes, the ability to image inflammatory brain changes *in vivo* will contribute to putting together the complex puzzle involved.

The first PET radioligand developed to image tau, [^{18}F]FDDNP was initially touted for imaging both tau and beta amyloid (Aβ).[346] However, FDDNP's lack of specificity to tau complicates analyses, and it shows relatively low uptake.[127,347] Though tau is a challenging molecule to image – it is thought to be expressed intracellularly, which requires the corresponding ligand to cross the blood-brain barrier and enter the neuron, there are six distinct isoforms of tau, and tau occurs in lower concentrations than Aβ – a number of PET radioligands for tau have been developed.[127,347] Shah and Catafau (2014) review the tracer properties of six tau-specific ligands. They review the structure and binding characteristics, based on mouse brain uptake, cited below as Table 1.[127] A key parameter of tau ligands is their affinity for tau; the ligands [^{18}F]T807 and [^{18}F]T808 show promise due to their high affinities and suitable pharmacokinetics, and have begun to be used in clinical cases. One recent case study suggests how a PET methodology combining both the amyloid ligand Florbetapir, a ^{18}F-labelled ligand for Aβ , and a novel tau ligand, [^{18}F]T807.[125] Florbetapir was used to first eliminate AD as a diagnosis in two cases of suspected chronic traumatic encephalopathy; then using [^{18}F]T807 Mitsis et al. demonstrated that both cases exhibited tauopathies.[348] [^{18}F]T808 does show higher affinity as compared to [^{18}F]T807, but [^{18}F]T808 deflourinates into human bones at a high rate.[349] However, at this point tau imaging is still new, and which ligands will prove to be most useful clinically has yet to be established.
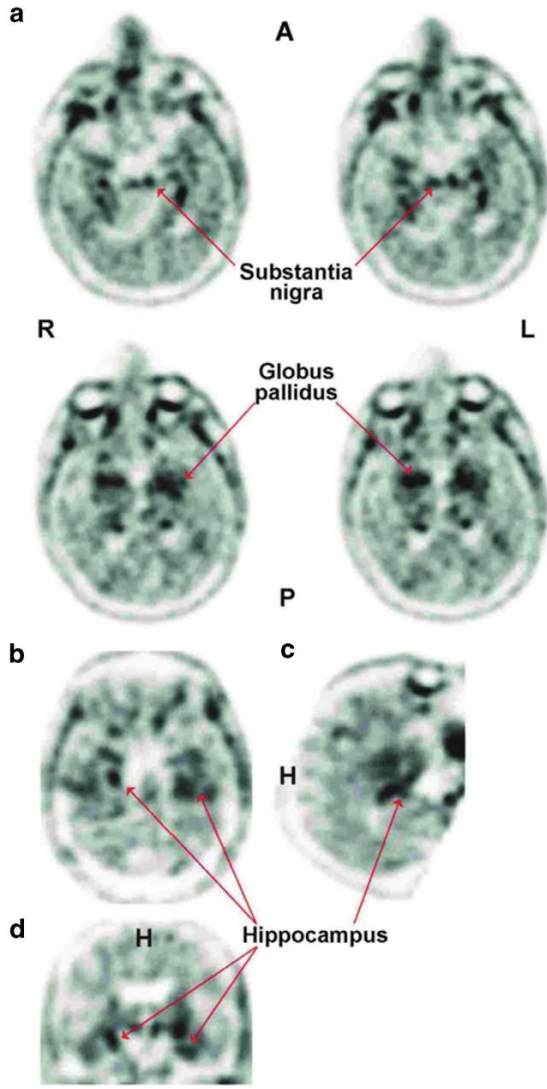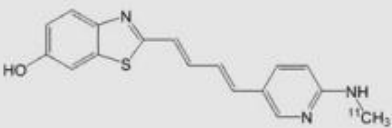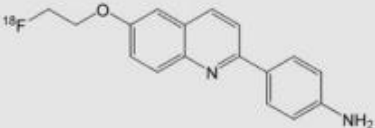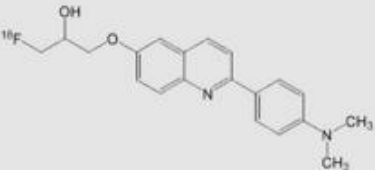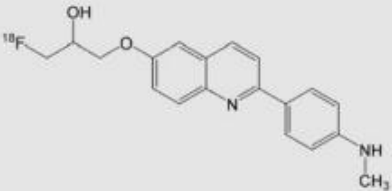
Figure 4. T807 PET imaging of pathological tau protein in an elderly former NFL player; signal is indicated by arrows. [348]

Table 3. Six tau radioligands summarized by Shah and Catafau (2014). [127]

Ligand	Structure	Affinity for Tau [nM]	Specificity for Tau relative to Aß	Mouse brain uptake at 2 min [%ID/g]	Mouse brain washout (2min/ 30 min)
[11]C-PBB3[(9)]		$K_{d1}=2.5^*$ $K_{d2}=100$	40-to-50-fold	NA	NA
^{18}F-THK523[(13, 15)]		$K_{d1}=1.99^†$ $K_{d2}=50.7$	15-fold	2.72	1.9
^{18}F-THK5105[(15)]		$K_{d1}=1.45^†$ $K_{d2}=7.40$	25-fold	9.2	2.6
^{18}F-THK5117[(15)]		$(K_i=10.5)^‡$	(NA)	6.06	10.3
[18]F-T807[(18)]		$K_d=14.6^*$	>25-fold	4.16	6.7
[18]F-T808[(17)]		$K_d=22^*$	27-fold	6.7[§]	2.9[ǀ]
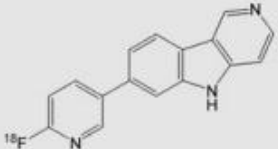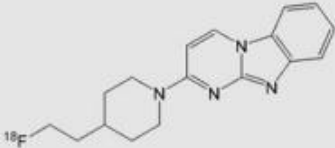
$^*K_d$ determined by ligand-binding to Tau-positive human brain sections
$^†K_d$ determined by ligand-binding to Tau-fibrils
$^‡K_i$ determined by competitive inhibition of ^{18}F-THK5105 to Tau-fibrils
§ 2.5 min; ^{ǀ} washout 2.5 min/20 min
NA= Not available; N.B. The affinity values for various ligands are generated from different types of experiments and may not always be directly comparable.

Apoptosis/Necrosis Ligands

Traumatic brain injury (TBI) is a complex disease process involving an initial physical perturbation of neurological tissues, followed by the activation of secondary biochemical injury cascades that result in progressive axonal and cell death. Axonal and cell death lead to diffuse downstream deafferentation of neuronal targets, resulting in manifestation of the morbidity and mortality associated with this disease process.

Mechanisms of cell death are largely preserved across neurological diseases and can be broadly categorized as apotosis or necrosis, with examples of cell death manifesting features of both pathways (e.g. necroptosis)[350]. Necrosis typically occurs in the setting of severe cellular injury, resulting in bioenergetic failure, loss of cell membrane integrity, and loss of normal cellular homeostasis. Cell contents are released into tissues, resulting in a local inflammatory response. Cellular mediators of necrosis include formation of mitochondrial reactive oxygen species (ROS), increased intracellular Ca^{2+}, activation of $\lceil$M and mM Ca^{2+} activated calpain neutral proteases, and disruption of pathways important for ATP production. Apoptosis represents a controlled process of cellular death, which may proceed through intrinsic (mitochondrial-mediated) or extrinsic (receptor mediated pathways). Both the intrinsic and extrinsic pathways of apoptosis converge on the caspase family of cysteine proteases, resulting in degradation intracellular components. Cathepsins are a class of powerful proteases found within lysosomes. Intracellular release of cathepsins have been observed in both apoptosis and necrosis, with large quantities of lysosomal cathepsin release associated with necrosis, while smaller amounts of cathepsin release may be seen in apoptosis.

Multiple previous studies have observed cell death through both apoptosis and necrosis in TBI. Excellent reviews on this topic are provided by Faden et al, 2000 and Sullivan et al, 2005. Additionally, both caspase activation and calpain activity have been observed in foci of axonal degeneration (Buki et al, 1999; Buki et al, 2000; Stone et al, 2002). Given the existing evidence illustrating the presence of apoptosis and necrotic cell death, along with activation of related proteolytic elements in axonal degeneration, components of these pathways may serve as targets for both molecular diagnostics and therapeutic intervention.

Apoptosis PET imaging
PET ligands for the detection of apoptosis have emerged in recent years in order to characterize this particular aspect of TBI in vivo. Radiotracers for apoptosis can be largely grouped into three categories, which include: (i) Membrane based, (ii) receptor based, and (iii) substrate based strategies.

Membrane-based apoptosis imaging
One of the most widely used membrane-based PET imaging strategies for detecting apoptosis detects the translocation of phosphatidylserine (PS) from the inner to outer membrane in the early phases of apotosis. Annexin-V forms trimer lattices in the setting of PS, resulting in its internalization. Although initially promising for the detection of cell death, its distribution profile is suboptimal with delayed clearance and a high level of nonspecific binding[351]. Additionally, externalization of PS occurs in necrosis, limiting the ability of annexin-V to detect necrosis alone. A number of compounds based upon Annexin5 are presently under development to improve properties of distribution and clearance while retaining PS binding capacity[352]. In

addition to Annexin-V, ^{18}F-ML10 is a compound that undergoes a conformational change in response to plasma membrane acidification and membrane depolarization, resulting in internalization and trapping of this compound within apoptotic cells[353].

Receptor based apoptosis imaging
Apoptosis may proceed through intrinsic or extrinsic pathways. The extrinsic pathway of apoptosis involves activation of a family of receptors known as the "death receptors". These include DR3, 4, and 5, along with Fas, and TNFR. CS-1008 (tigatuzumab) is an anti-DR5 antibody that has been successfully labeled with ^{111}In and is capable of labeling this receptor *in vivo*[354]. ^{64}Cu-DOTA-conatumumab is another monoclonal antibody that has been successfully labeled with a PET isotope, which is capable of labeling DR5 *in vivo*[355].

Substrate/Inhibitor based apoptosis imaging
^{18}F-CP18 is a synthetic peptide, which contains the tetrapeptide sequence Asp-Glu-Val-Asp (DEVD)[356]. The carboxyl-terminus of this peptide is linked to a PEG chain, allowing for improved cell membrane permeability, while the amino terminal has been labeled with [18]F. The DEVD sequence will be specifically cleaved by caspase-3. This radiotracer will move in and out of healthy and apoptosis cells alike. However, upon encountering the caspase-3 cysteine protease, ^{18}F-CP18 will be cleaved, with the subsequent trapping of the ^{18}F amino terminal fragment due to separation from the carboxy terminal PEG chain. In addition to substrate-based approaches, small molecule inhibitors of caspases have also been successfully radiolabeled (^{18}F-ICMT11, ^{11}C-WC-98, ^{18}F-WC-IV-3) and have shown promising results *in vitro*. However, *in vivo* studies have been challenged by the relatively high doses of compound required for imaging *in vivo*.

Apoptosis imaging and TBI
At present, studies exploring the utility of apoptosis imaging agents in TBI are quite limited. Reshef et al.[357] employed N,N'-Didansyl-L-cysteine (DDC), a fluorescent analog of ML-10 in a modified weight drop model of TBI in mice . Animals were allowed to survive 6h, 24h, 72h, and 7 days following injury. Tracer was administered IV 2 hours prior to sacrifice. Brains were prepared for multiple fluorescent label comparison with NeuN with semi-serial sections prepared with H&E to assess for morphologic features of apoptosis. At 6h following injury, uptake of DDC was noted, which peaked at 24 hours and had significantly diminished by 72 hours post-injury. Uptake was predominantly seen within NeuN stained neurons and correlated with regions demonstrating morphologic features of apoptosis by H&E.

Stone et al., explored both ^{18}F-ML10 and ^{18}F-CP18 uptake in the rodent controlled cortical impact model of TBI. Animals were allowed to survive 12h, 24h, or 48h following injury and received IV administration of radiotracer 2 hours before the predesignated post-injury survival time. Increased uptake was seen within the cortex, hippocampus, and corpus callosum ipsilateral to injury. Of note, hemispheric 18F-ML10 uptake peaked at 24h following injury, while ^{18}F-CP18 uptake was greatest at 48 hours following injury, suggesting differences in the potential temporal utility of these probes in the detection of TBI.

Necrosis imaging and TBI
Most existing PET approaches for the detection of necrosis focus upon strategies to differentiate radiation necrosis from viable cells in tumor imaging (Miwa et al, 2014). No strategies presently exist to directly image cellular mechanisms that specifically identifies the cellular features of necrosis and differentiates these mechanisms from those seen in apoptosis alone. The theoretical potential exists for the imaging of active calpain neutral proteases given the availability of calpain small molecule inhibitors. However, to date no published literature exists on successful attempts to do so.

Summary
Cellular death and axonal degeneration proceeds through pathways that have been relatively well characterized and contain multiple targets for PET imaging. Although multiple radiotracers have emerged in recent years for imaging key elements of cell death, the imaging of these features in the setting of TBI remains in the earliest of stages.

Inflammation Ligands

- Neuroinflammation, the immune response in the brain, may play a role in cell death, and with severe or repeated TBI might exacerbate debilitating cognitive symptoms.

- Translocator protein or TSPO is a mitochondrial membrane protein that is upregulated in microglia, cells responsible for immune response in the brain. The development of PET imaging agents for TSPO is an active area of research. A recent animal study of induced TBI and TSPO imaging was able to show a neuroinflammatory response to TBI through PET.

- Neuroinflammation can also be imaged via two anti-inflammatory systems in the brain: the α7 nicotinic acetylcholine receptor and cannabinoid receptor 2. Both of these systems have altered expression in TBI and might well offer, in addition to imaging capabilities, drug development possibilities.

The neuroinflammatory response, described in the "Microscopic Pathological Hallmarks of Neurotrauma" section above, is thought to work by inducing neuronal death to limit further injury following brain trauma.[122,358] Thus neuroinflammation should normally be neuroprotective, but with acute trauma, as in severe TBI—and, in recent research in mild TBI as well—evidence suggests the emergence of "gliopathy," pathological effects from neuroinflammation, contributes to the secondary tissue injury that follows primary physical injury in TBI.[358,359] Furthermore, severe, disabling symptoms of TBI such as neurocognitive decline may result from gliopathy.[360]

Neuroinflammation may be detected using FDG PET, but without specificity. During inflammation, glial cells should show increased metabolism, and cells that have been killed in response to neuroinflammation should be detected as hypometabolism, but because FDG is taken up by all cells, FDG PET is unable to resolve what cells are demonstrating increased metabolism.[121] Thus, more promising targets for PET imaging of neuroinflammation than deoxyglucose metabolism is an active area of research. As alluded to above, three receptor systems are currently undergoing research for PET imaging of neuroinflammation: translocator

protein, or TSPO, the α7 nicotinic acetylcholine receptor (7 nAChR), and the cannabinoid 2 receptor (CB2R).

TSPO is an 18-kDa outer membrane protein in mitochondria that is expressed at high levels in response to brain injury and inflammation in microglia, but otherwise is not highly expressed.[358] The precise biochemical function of TSPO is not known, indeed there is recent controversy on what had been assumed to be a basic function of TSPO, steroidogenesis.[361] However, as an area of active research for decades, TSPO has been associated with many cellular functions, such as cholesterol transport, steroid hormone synthesis, mitochondrial respiration, permeability transition pore opening, apoptosis, and cell proliferation.[358]

The classic radioligand for PET imaging of TSPO is [11]C-*R*-PK11195, which was developed in the mid-1980s.[338,362] While a vast body of research effectively uses [11]C-*R*-PK11195—and it is still currently used—[11]C-*R*-PK11195 has a low signal-to-noise ratio, and significant non-specific binding which complicates image analysis.[338,362] Because of these limitations, a great deal of novel radioligands with improved pharmacokinetics have been developed to bind to TSPO. Damont, Roeda and Dollé (2012) describe a variety of ligands belonging to 6 distinct chemical classes: 1. isoquinoline-3-carboxamides and quinoline-2-carboxamides (PK11195 and related molecules), 2. quinazoline-2-carbamates and quinazoline-4-carbamates (PK13162 and PK13168), 3. N-benzyl-N-(2-phenoxyaryl)acetamides (DAA1106, PBR28), 4. pyrazolo[1,5-a]pyrimidineacetamides (DPA-713, DPA-714), 5. indoleacetamides (SSR180575) and 6. 2-aryl-8-oxodihydropurines (FEDAC, FEAC).[362] While novel ligands belonging to these classes improve upon the radiotracer profile for PK11195, no review has been compiled that compares the binding properties and affinities for TSPO in new radioligands head to head.

PET imaging of TSPO in response to TBI is still a new area of inquiry. A recent report describes induced TBI in a rat model, and PET imaging with [^{18}F]DPA-714. In it, Wang et al. (2014) report significantly increased binding in the cortical area subjected to impact by day 2. Peak binding occurred at day 6, and binding decreased to normal levels by day 28. The most significant finding of this study was the feasibility of using DPA-714 to track the brain's inflammatory response noninvasively using PET. The Wang group also used FDG PET to evaluate the brain's response, finding a pattern of initially low FDG uptake (corresponding to disturbed blood flow and altered neural function), high uptake around day 5 and 9 (thought to correspond to elevated glycolysis following increased free-radical production known as oxidative burst, which is part of the neuroinflammatory response). By day 15 FDG binding in both the experimental and control groups were normal.[123]
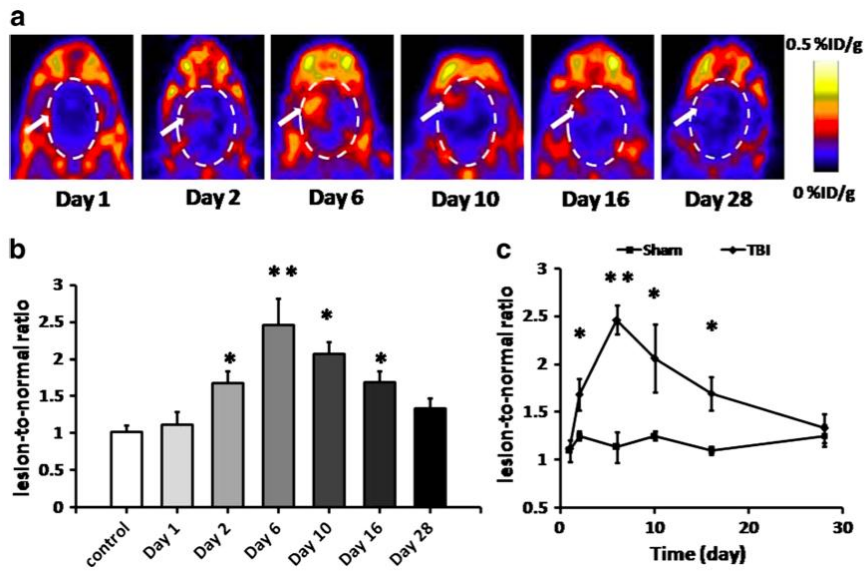
Figure 5. DPA-714 PET images of a mouse model shows TSPO binding at the site of induced TBI at day 6, corresponding to neuroinflammatory response. [123] Arrows in the brain images point to lesions, B and C graph DPA-714 uptake as lesion-to-normal ratios, compared to controls.

As Coughlin et al.[363] report, two prior studies in humans have suggested increased binding of TSPO after TBI, using the first generation tracer PK11195. As mentioned above, PK11195 is limited by a low signal and high levels of nonspecific binding.[363] Using DPA-713, Coughlin's group imaged 9 formal NFL players and 9 controls to show statistically significant, increased binding of DPA-713 in regions of the brain associated with atrophy in TBI and pathologic plaque formation in chronic traumatic encephalitis (CTE). These findings suggest that neuroinflammation and TSPO expression plays a role in the pathological effects of TBI.
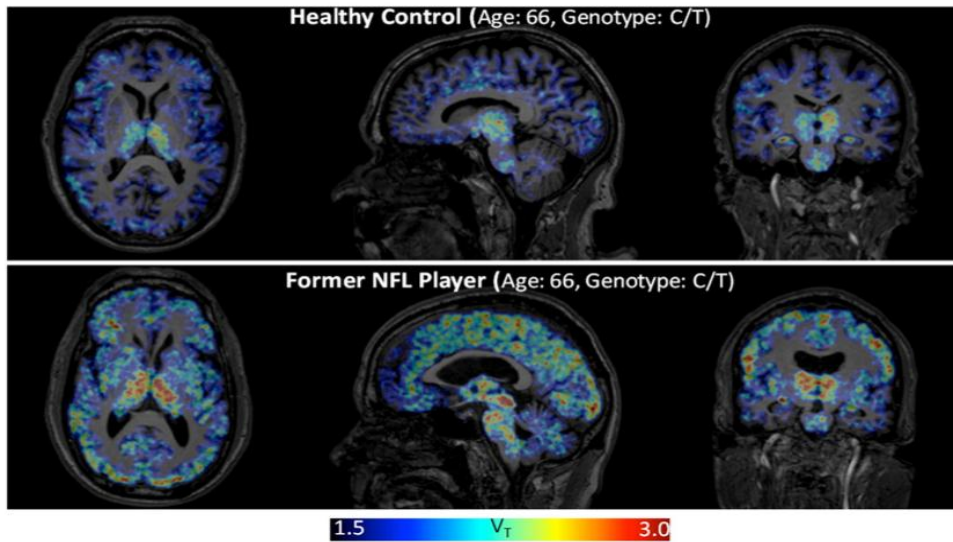
Figure 6. DPA-713 PET images show increased binding of TSPO in brain regions associated with TBI and CTE in a former NFL player, compared to healthy control, measured as total distribution volume (V_T).[363]

Animal studies have suggested other biochemical pathways for imaging neuroinflammation, including the α7 nAChR and CB2R. Controlled cortical impact in a mouse model resulted in decreased α7 nAChR expression.[124] Alpha 7 nicotinic receptors play an anti-inflammatory role, thought to activate a biochemical cascade of anti-inflammatory factors, such as Janus Kinase 2.[364] The observed decrease in α7 nAchR following TBI might result from negative feedback into the cholinergic anti-inflammatory pathway through markers in the blood that decrease vagus nerve tone.[364] Stimulation of the vagus nerve results in activation of the anti-inflammatory pathway, so loss of vagus nerve tone would result in increased inflammation and immune response. In TBI, Kelso and Oestreich (2012) also suggest that α7 nAchR may contribute to excitotoxicity, because of its high permeability to Ca^{2+} and because α7 nAchR stimulation contributes to the release of glutamate and the glutamate excitatory pathway. This nicotinic receptor subtype may represent a suitable target for neuroinflammation in the context of TBI[124].

Because TBI results in high levels of intracellular calcium[365], researchers have turned to the endocannabinoid system which is activated by high levels of intracellular calcium, but does not constitute a classical "neurotransmitter" system.[125] In a 2014 study of induced TBI in fetal pigs, Donat et al. demonstrated significant increases in CB2R density following injury at six hours. The Donat group was unable to conclude whether CB2R expression from primary injury or secondary injury. However, the strongest increase in CB2R expression was in the corpus callosum (+142%), which is a brain region that is vulnerable to axonal injury, and thus suggests that CB2R expression may respond to physical injury.[125] But then, CB2R may also (or alternatively) have been upregulated in response to inflammation. The precise mechanism is not clear despite these authors' attempt to pursue robust cardiovascular, metabolic, and neurophysiological monitoring.

Magnetoencephalography (MEG)

MEG sensitively demonstrates abnormal neuronal signals resulting from axonal injuries. Unlike *normal* spontaneous MEG data which is dominated by neuronal activity with frequencies above 8 Hz, injured neuronal tissues (due to head trauma, brain tumors, stroke, etc.) generate abnormal focal or multi-focal low-frequency neuronal magnetic signal (delta-band 1-4 Hz, or theta-band 5-7 Hz) that can be directly measured and localized using MEG.[366,367]

Pioneering studies by Lewine and colleagues showed that the brains of mild TBI patients generate abnormal low-frequency magnetic fields that can be measured and localized by MEG.[367,368] They also showed that MEG was more sensitive than conventional MRI or EEG for detecting abnormalities in mild TBI patients. Studying 20 normal subjects and 20 concussion patients with persistent postconcussive symptoms, Lewine et al[367] showed that MEG slow-waves were 65% sensitive in detecting symptomatic concussions, whereas EEG was only 20-25% sensitive, and MRI was only 20% sensitive in detecting lesions in patients with mild or moderate TBI. None of the 20 normal controls exhibited abnormal MEG slow-waves.

In a subsequent paper[368], Lewine et al performed a retrospective blinded review of 30 patients with persistent postconcussive symptoms more than 1 year after mild blunt head trauma, comparing the diagnostic utility of MEG, SPECT, and MRI. They found that MEG demonstrated abnormal dipolar slow-wave activity (DSWA) in 19 patients, compared with abnormal decreased SPECT uptake in 12, and abnormal MRI findings in 4 patients. No definite imaging associations were found with postconcussive *psychiatric* symptoms. However, in the subgroup of patients with postconcussive *cognitive* symptoms, MEG was abnormal in 86% of patients, compared with 40% of patients with abnormal SPECT, and 18% with abnormal MRIs (p < 0.01). In addition, MEG showed statistically significant (p < 0.01) associations between temporal lobe slow-waves (DSWA) and memory problems, parietal DSWA and attention problems, and frontal DSWA and executive-function problems.

A recent paper by Huang et al[369] examined the relationship between DTI abnormalities in white-matter fiber tracts and the generation of abnormal MEG slow-waves in mild TBI, in 10 human patients with persistent postconcussive symptoms after mild TBI. They found that MEG slow-waves in mild TBI patients originate from cortical gray-matter areas that experience de-afferentation due to axonal injuries in the white-matter fibers with reduced fractional anisotropy.

All 10 subjects showed abnormal slow-waves on MEG, but only one had any lesions on MRI or CT, and only 7 showed abnormalities on DTI. The DTI tractography patterns that link MEG and DTI findings fall into three categories.[369] Category 1: In six patients, slow-wave generating gray-matter areas were directly linked with nearby non-major fiber tracts showing abnormal diffusion (Figure 7). Category 2: In two patients, multiple slow-wave generating areas were linked with the same major fiber tracts showing abnormal diffusion (Figure 8). Category 3: In three patients, abnormal slow-waves were observed, but DTI were within normal range. One patient showed abnormalities in both Categories 1 and 2.

The findings of slow-waves in this MEG study are corroborated by prior animal studies of delta-wave generation in gray matter and axonal injuries in white matter, which have established a solid connection between pathological delta-wave generation in gray matter and axonal injuries

in white matter.[370-372] These experiments in cats concluded that partial cortical de-afferentation (due to axonal injury or disruption of afferent cholinergic axonal input) was an important factor in delta-wave production. The human MEG-DTI results were compatible with this conclusion, showing that MEG delta-waves in TBI patients are generated from gray-matter neurons that experience de-afferentation due to axonal injury in the underlying white-matter fiber tracts, or blockage of cholinergic transmission.[369]

Currently, MEG slow-wave detection and localization is usually manually performed by MEG analysts. However, to make MEG low-frequency source imaging an effective clinical tool for assisting in the diagnosis of mild TBI, it would be helpful to have an objective, automated and operator-independent MEG low-frequency source imaging method for detecting and localizing the MEG slow-waves.

To this end, VEctor-based Spatio-Temporal analysis using L1-minimum norm (VESTAL) is a high-resolution time-domain MEG source imaging solution [12] with the following properties: 1) can model many dipolar and non-dipolar sources; 2) requires no pre-determination of the number of sources (model order); 3) can resolve 100% temporally correlated sources. To more effectively image oscillatory MEG signals such as complicated MEG slow-waves, Huang et al expanded VESTAL from time-domain to frequency-domain[373]

Using such an automated MEG low-frequency source imaging approach which localized delta-waves to 96 standardized cortical regions, Huang et al[373] found abnormal delta-waves in 87% of 45 patients with mild TBI (23 with blast and 22 with non-blast causes); and 100% of 10 patients with moderate TBI (Fig. 8). These positive-finding rates are markedly higher than the ~9% and 20% rates using the conventional neuroimaging approaches (i.e., MRI) in the same mild and moderate TBI patients, respectively. At the threshold of 4.28 for the Zmax which is associated with p=0.01 after the Bonferroni correction, none of the 44 normal controls showed abnormal slow-waves. This result is consistent with the general conclusion from the MEG studies of concussions by Lewine and colleagues[367,368], except the true positive-finding rates in the Huang study[373] is higher.

One advantage of the above-described neuroimaging approach, shared with other MEG protocols which detect delta slow-waves, is that the resting-state MEG recording procedure is spontaneous, requiring almost no effort from TBI patients, and is thus independent of patients' performance and effort. With the wide availability of information about TBI symptomatology and commonly-used psychometric tests on the Internet, and the variety of motivations (i.e. legal, financial, as well as healthcare factors, etc.) for patients to exaggerate/understate symptoms and deficits, more objective diagnostic tests such as this resting-state MEG exam are invaluable, since they cannot be easily manipulated "gamed."

Note that abnormal slow/delta-waves are not specific to, nor pathognomonic of, traumatic brain injury[367], and are also found in neurological/psychiatric disorders such as infarcts, epilepsy, brain tumors, Alzheimer's disease[374], schizophrenia[375-377], and other organic brain disease. Hence in patients with these serious but readily diagnosable conditions, MEG cannot readily diagnose concussions, as distinguished from their other underlying serious brain disease. Also, the factors that may increase slow-wave power must be controlled in this MEG exam. These factors include neuroleptic, sedative, or hypnotic medications, or sleep deprivation.

The 2012 study by Huang et al[373] also revealed the diffuse nature of the neuronal injuries in TBI patients. On average, approximately 4-8 cortical gray-matter areas showed abnormal slow-wave generation in each TBI patient using the automated MEG low-frequency source imaging. Such findings are consistent with the mechanism of diffuse axonal injury in TBI due to a combination of linear and rotational acceleration and deceleration.[49,378,379] The findings are also consistent with Huang's 2009 MEG-DTI study in mild TBI[369], in which they found that abnormal MEG slow-waves are generated from cortical gray-matter areas that connect to white-matter fibers with reduced DTI fractional anisotropy due to axonal injury in patients with mild TBI. Specifically, the reduced DTI fractional anisotropy in *local* white-matter fiber tracts led to focal abnormal MEG slow-waves from neighboring gray matter in mild TBI. On the other hand, reduced anisotropy in *major* white-matter fiber tracts led to multi-focal or distributed patterns of abnormal slow-waves generated from cortical gray-matter areas that can be remote in location, but functionally and structurally linked by the injured major/long white-matter fiber tracts.[369] The diffuse nature of MEG slow-wave generation is also consistent with a recent DTI study in blast mild TBI subjects which showed reduced FA in a diffuse, widespread, and spatially variable pattern.[380]

The diffuse nature of abnormal MEG slow-wave generation in TBI also raises questions about the conventional neuroimaging analysis of group-averaging of source locations in space. Unlike abnormal slow-wave generation in patient populations with specific psychiatric and neurological disorders such as schizophrenia[375–377] and Alzheimer's disease[374] where group-averaging of source locations in space yielded meaningful information about dysfunctional neuronal networks, the loci that showed abnormal slow-wave generations in TBI patients tend to be highly variable in location. Hence, group-averaging of MEG slow-wave source locations in space is unlikely to be the most effective way to detect brain injuries. Instead, analyses of the MEG slow-wave generation characteristics of *individual* patients, such as that introduced in the Huang et al study[373], should provide more insights about the neuronal injuries in TBI.

Huang et al subsequently developed a *voxel-based* whole-brain MEG slow-wave imaging approach for detecting abnormality in patients with mild TBI on a single-subject basis[381], based on their fast-VESTAL MEG analysis technique.[382] A normative database of resting-state MEG source magnitude images (1–4 Hz) from 79 healthy control subjects was established for all brain voxels, using the recent Fast-VESTAL method. In 84 mild TBI patients with persistent post-concussive symptoms (36 from blasts, and 48 from non-blast causes), their method detected abnormalities with a positive detection rate of 84.5%, with no false-positives in the control subjects. Prefrontal, posterior parietal, inferior temporal, hippocampus, and cerebellar areas were particularly vulnerable to head trauma. The results also showed that MEG slow-wave generation in prefrontal areas positively correlated with personality change, trouble concentrating, affective lability, and depression symptoms.

Abnormal slow waves are not the only abnormal findings in TBI. A recent MEG study in a group with mixing mild, moderate, and severe TBI patients showed reduced functional connectivity in the alpha-band, primarily in bilateral frontal and left greater than right parieto-temporo-occipital regions as well as the right thalamus.[383] Another recent MEG study in sensor space also showed a reduced level of complexity in mild TBI patients.[384]

In summary, magnetoencephalographic (MEG) evaluation of abnormal brain slow delta-waves (1-4 Hz) is probably the most sensitive objective test to diagnose concussions. An automated MEG low-frequency (slow-wave) source imaging method, fast frequency-domain VEctor-based Spatio-Temporal analysis using L1-minimum norm (VESTAL), achieves a positive-finding rate of 85% for diagnosing concussions/mild TBI, with the threshold chosen so there were no false-positive diagnoses in the normal controls. Those recent studies also showed that the characteristics of slow-wave generation in mild blast-induced TBI and mild non-blast TBI patients are significantly correlated. Also, there were significant correlations between the number and locations of cortical regions that generated abnormal slow-waves, and the post-concussive symptoms in TBI patients.

Computational Processing

For the above-mentioned analyses, there are a few considerations to be made in formulating the actual processing pipeline including the focus of regional analysis, statistical testing, and ultimately the software tools to employ for data munging (i.e., cleaning, transformations, and other processing).

Preprocessing

Prior to extraction of quantitative information from images, certain preprocessing steps are necessary to remove processing confounds including artifacts due to the image acquisition protocols and variations in image gradient hardware. For example, the standard preprocessing workflow for images acquired under the Alzheimer's Disease Neuroimaging Initiative[385] includes 1) image geometric distortion correction, 2) B1, and 3) N3[386] intensity non-uniformity correction. Other preprocessing considerations for structural scans include noise reduction (e.g., SUSAN[387]), intensity standardization (e.g.,[388]), spatial normalization to a common coordinate system (such as the well-known Talaraich[389] or MNI[390] atlases, or one generated directly from the cohort[391]), and motion and eddy current correction[392] for DWI. Preprocessing for functional scans[393] may include motion correction[394], physiological noise correction methods (e.g., CompCor[395]), bandpass filtering, and spatial smoothing.

Structural analysis

Several imaging-derived features are potentially indicative of TBI severity. These include such quantities as cortical thickness and other cortical morphological features (e.g., surface area, volume, curvature) which are related to possible atrophic conditions. Similarly, spatial normalization to a common template can provide a related measurement (i.e., Jacobian-based morphometry) by calculating the Jacobian determinant[396] of the deformation. In addition other potential imaging features indicative of TBI severity include volumetry measures of discrete lesions. The presence of cerebral microbleeds, prominent Virchow-Robin spaces[397], and other unidentified bright objects are all related to neuropathology. Some effort has been made towards the automated identification of such lesion-based features.

Anatomical and functional connectivity

Recognition of the utility of identifying changes in anatomical and/or functional connectivity has motivated the use of DTI and fMRI for deriving additional feature sets for subsequent statistical analysis in characterizing TBI. Mathematical modeling of neural connectivity through the use of graph theory provides a formal language for characterizing complex brain networks.[398] Such anatomical or functional networks are composed of "nodes" (i.e., anatomical regions) which are linked together by "edges" (i.e., some form of functional, anatomical, or effective connectivity). From such graphical models, certain measures can be calculated which quantify, for example, a specific network's "centrality" or "resilience" which could possibly change with TBI.

Statistical analysis

The previously described image processing possibilities are meant to extract quantitative features for subsequent statistical analysis. Both the choice of imaging feature(s) and set of statistical tools play prominent roles in the success of any given study. Statistical analysis of TBI data includes multiple methodologies for a variety of applications including prediction of individual diagnoses to quantitative inference of population trends. Such methodologies include traditional statistical workhorses such as linear regression but also include much more recent developments in the machine learning community such as random forests, support vector machines, and deep learning. Although it is not a simple task in choosing which statistical framework to use for a particular study, facilitating the use of these modern techniques are open source packages such as the R statistical project[399] and imaging software which provide a direct interface to such statistical packages.

Software

Long-term scientific investment on the part of academic, industrial, and government groups (often working in tandem) has resulted in well-known computational tools for neuroimaging analysis with many having been applied to previously reported traumatic brain injury research. Some of the more popular packages include:

- FMRIB Software Library (FSL)[400]—set of freeware software analysis tools for both functional and structural neuroimaging developed at the University of Oxford.[401] Associated tools for DTI analysis, specifically tract-based spatial statistics (TBSS), have been particularly relevant for the TBI research community. Current large-scale projects using FSL include the Human Connectome Project.[402]

- Statistical Parametric Mapping (SPM)[403] —ongoing Matlab-based project originating in the early 1990's and presently supported and developed at the Wellcome Trust Centre for NeuroImaging.[404] Much of the foundational work for fMRI analysis, as well as seminal work in image registration and segmentation, was formulated by its developers and is currently distributed in SPM.

- FreeSurfer[405] set of analysis tools for constructing and analyzing brain surface models from structural (i.e. T1-weighted) MRI[406] with functional analysis tools also available (FsFast). This open source package is currently developed at the Center of Biomedical

Imaging at Mass General Hospital. Its cortical thickness component has demonstrated for TBI research.[407,408]

- AFNI[409]—an open source software package for fMRI display and analysis originating at the Medical College of Wisconsin and currently supported and developed at the NIH.[410]

- Advanced Normalization Tools (ANTs)[411]—a general suite of open source tools for such tasks as registration, segmentation, bias correction, and template construction [59]. It is built upon the Insight Toolkit (ITK)[412] of the National Library of Medicine with origins at the Penn Image Computing and Science Lab at the University of Pennsylvania. Related is the software interface between ANTs and the R statistical project called ANTsR.[413]

Several other ongoing and useful projects are more targeted to specific applications. For example, diffusion tensor image processing is greatly facilitated by such packages as the UCL Camino Diffusion MRI Toolkit[414], DTI-TK[415], and DTIstudio[416]. Widely used, comprehensive visualization and analysis packages include the java-based MIPAV[417] and ITK-based 3DSlicer[418]. Also, resources such as the XNAT informatics system, provide infrastructure for large-scale database management.

It should be noted that all these softwares have large developer and user communities which often overlap given the respective strengths and weaknesses of each. To enhance interoperability between packages and provide a common interface for analysis, meta-efforts such as Nipype[419] are currently under development. Additionally, the power of social networking has been utilized to increase information within the community regarding available resources. Websites such as NITRC (http://www.nitrc.org) provide a forum for sharing neuroimaging data and tools, answering inquiries, and access to computational resources. Finally, federally-supported, publicly available databases are essential for characterization of normal and pathological conditions as well as algorithmic testing. For example, the Federal Interagency Traumatic Brain Injury Research (FITBIR) informatics system[420] is a comprehensive NIH initiative to facilitate collaborative research endeavors specifically targeted to TBI.

Recent reviews also provide detailed sketches of current technologies and other discussion points related to the current state of neuroimaging and neuroinformatics issues within TBI research. Matthew et al., discuss neuroinformatics issues for the broad spectrum of relevant multimodal imaging techniques and current challenges facing the research community while the authors of[101] situate imaging biomarkers within the larger goal of identifying any and all physiological indicators of mild TBI. A more tailored review of research queries using fMRI specific to blast-related TBI is provided in. [421]

Ultrasound

Current research efforts on the use of ultrasound fall naturally into the same two categories as current clinical practice: imaging and non-imaging. Current research efforts still send ultrasound into brain and collect what scatters back from brain tissue or flowing blood. However, those efforts tend to analyze that data differently: they often generate diagnostically useful information based upon ultrasound tracking of endogenous movement of tissue or blood, or by inducing a

measurable exogenous movement of tissue that yields information on local, endogenous tissue properties.

Specifically, with important exceptions we note below, much research on ultrasound for TBI imaging or detection seeks to take advantage of ultrasound's sensitivity to differences in elasticity between healthy versus damaged brain along with its ability to detect small displacements of tissue. Differences in tissue elasticity (compressibility and/or resistance to shearing forces) can range over several orders of magnitude, whereas differences in tissue properties that generate backscatter ultrasound energy varies by less than a factor of two. Therefore, diagnostics based upon tissue elasticity can offer higher contrast than diagnostics based directly on ultrasound backscatter from tissue.

In its most general sense, to perform so-called 'sonoelastic' analysis one first collects baseline ultrasound data (an image for example) at a given moment. One then displaces the tissue and quickly collects additional ultrasound data. Representation of differences between the two data sets before and after the push highlights differences in different elastic properties, because softer tissue will move more for a given push than stiffer tissue. The source of the push and the means of analyzing its results distinguish between different ultrasound elasticity methodologies.

Regarding endogenous imaging methods, all rely on the 'push' on brain tissue generated by the arrival and passage of pulsatile blood flow into brain to generate usefully measurable brain-tissue displacement. Kucewicz et al (2008)[422] created images of endogenous brain tissue displacement in healthy humans using transcranially delivered ultrasound, images whose average amplitude varied with arterial CO_2 blood gas concentration, a known determinant of brain tissue pulsitilty. With that technique – tissue pulsatility imaging or TPI – Mourad and colleagues have produced transcranially derived images of the structure of traumatic brain injury (hence sTPI) in preliminary studies (Figure 7).
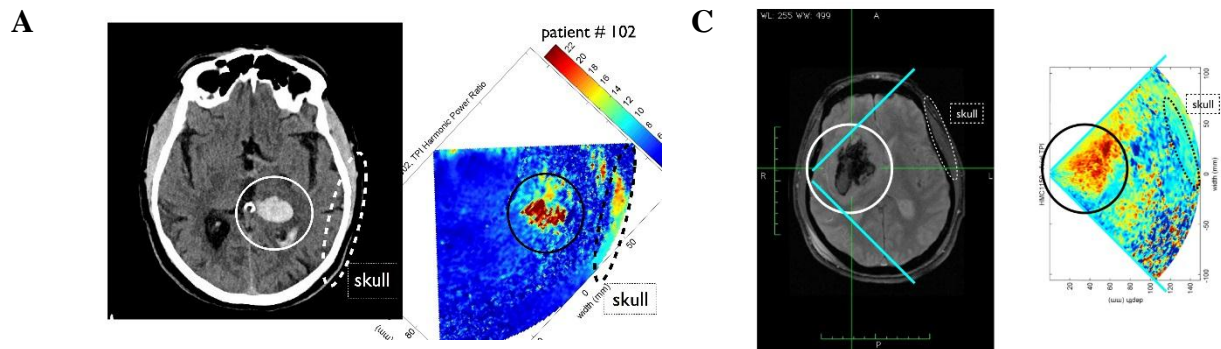
Figure 7. Comparison of MRI (gray) with structural TPI images (sTPI—hot colors). The same area of skull is identified in both sets of images to corroborate the location of the lesion and facilitate quantitative comparison of its size and structure

This same group has generated preliminary data supportive of transcranially derived TPI as a means to capture brain *function* (hence fTPI) in the context of emotional stimulation (frustration;

disgust), as shown in Figure 8, motivated by earlier studies by this same group[423] who imaged brain function under visual stimulation.

Figure 8. Sample results from the 'flanker' tasks
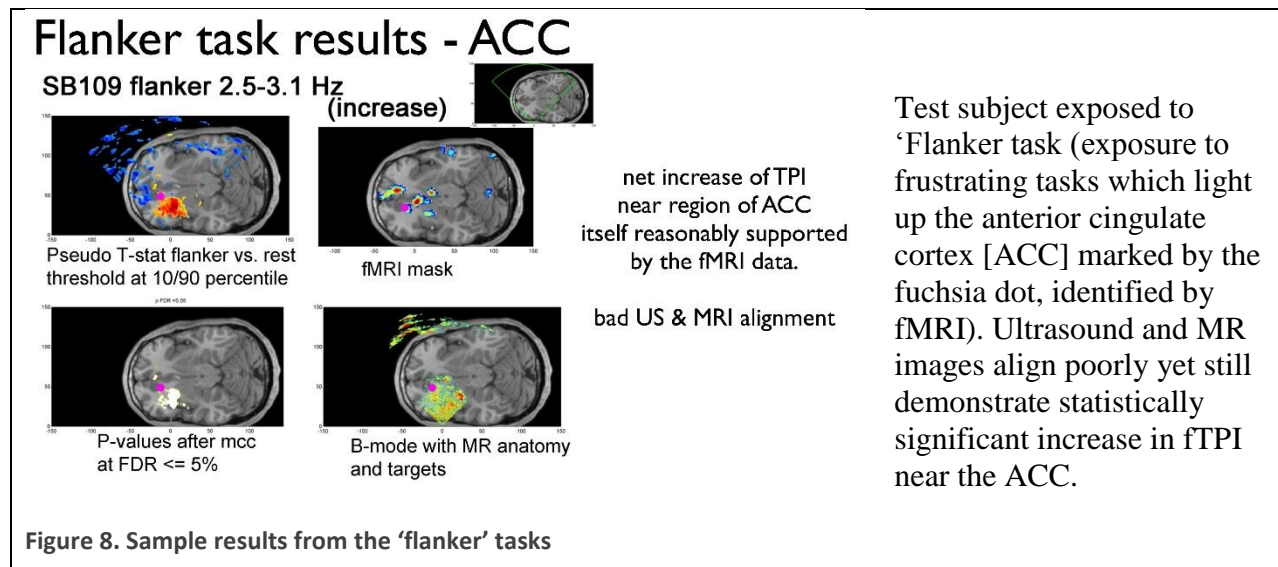
An exciting complement to tissue pulsatility imaging is the 'fast Doppler' approach pursued by Tanter, Fink and colleagues, applied to rat brain after craniectomy[424] and neonates through their fontanel.[425] The basis of their approach uses diagnostic ultrasound machines with very fast frame rates (thousands per second versus the usual 30-60), combined with peripheral tissue probes (hence high ultrasound frequencies not yet useful transcranially) to collect *Doppler* information (distributions of blood flow speed within a pixel) distributed on fine scales – that of small blood vessels over an image. Standard diagnostic ultrasound systems can create images of ultrasound backscatter or of average blood flow speed.

Regarding exogenous imaging methods, the dominant approach is offered by Tanter and colleagues[426] (Tanter et al, 2008 represents their earliest clinically oriented paper on this subject, applied to lesions within human breast). Tanter and colleagues (see their recent review)[427] track the propagation through tissue of artificially generated shear waves within tissue to create quantitative estimates of the shear modulus of that tissue. Here, specialized sequencing of a conventional US diagnostic probe generates a series of impulsive pushes of tissue via the acoustic radiation force associated with focused diagnostic ultrasound, thereby creating transient, propagating and non-destructive shear waves. While the shear waves propagate the device rapidly switches its ultrasound protocol to an ultrafast diagnostic image acquisition (on the order of thousands of images per second) to image the propagating shear wave. Local measurement of shear-wave propagation yields a direct estimate of the local shear modulus of the tissue through which the shear wave propagated. While used in humans for imaging peripheral tissue, published application to brain has focused on mouse and rat models of contusion-based TBI.[428,429] Changes in tissue stiffness inferred this way highlight in these animal models the structural evolution of the focal TBI. Specifically, over a time period of 1-3 days the increasing presence of edema and hemorrhage ipsilateral to injury decreases the measured stiffness of the brain while contralateral

reduction in cerebral hemodynamics increases the local stiffness of brain tissue. The main barrier to translation of this approach to humans use is both the complex anisotropy of human brains as well as difficulties faced by the need to generate robust shear waves via delivery of ultrasound through the human skull – much thicker, more spatially variable than that of rodents, of course.
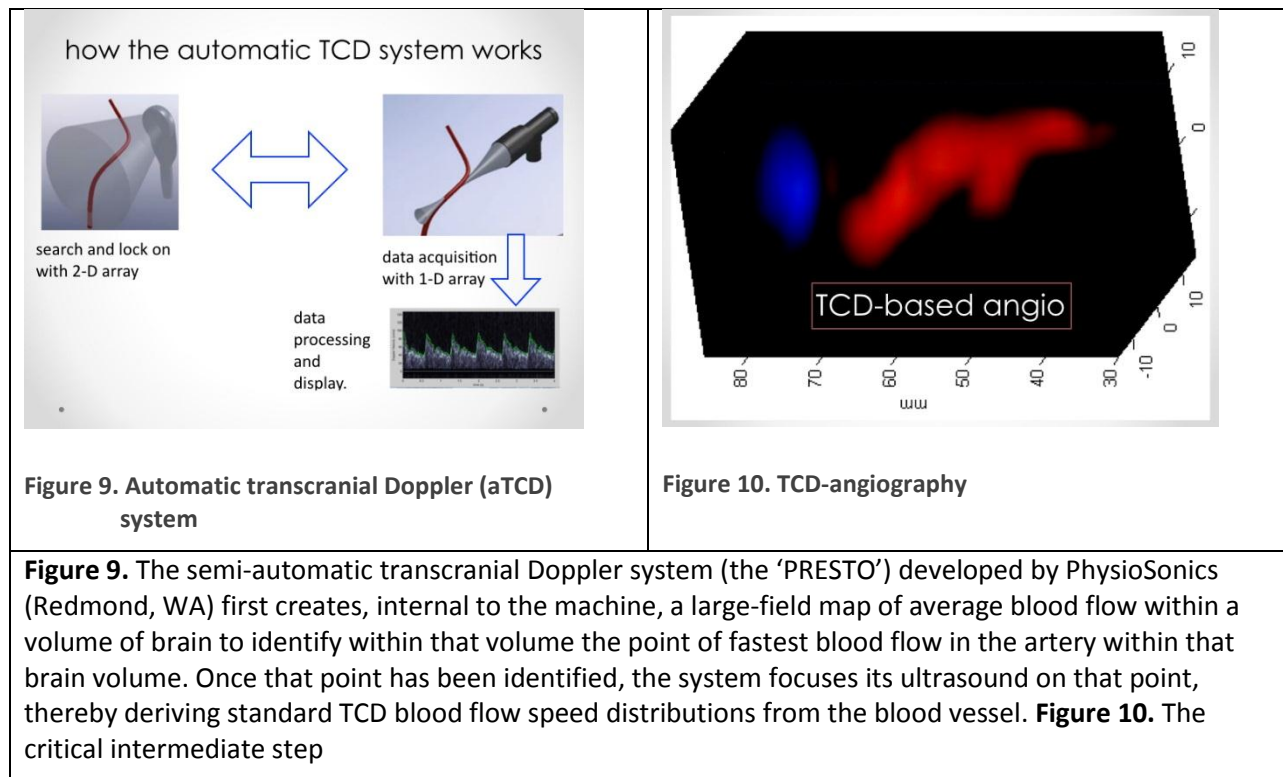
The skull represents a critical barrier between many peripheral imaging modalities and their application to brain. Clement and colleagues offer an interesting way around this barrier.[430] They, in essence, generate from outside of the skull an ultrasound shear wave that propagates through the skull and enters the brain as a standard ultrasound pressure wave, whose interaction with the brain generates a useful standard ultrasound image of brain structure sensitive to mid-line shift (a common diagnostic for the presence of a mass lesion in the context of TBI) and cerebral ventricle structure, relevant for hydrocephalus, for example.

Regarding endogenous non-imaging methods, almost all studies involve human-oriented research. They generally seek to develop an ultrasound-based proxy for the presence of TBI or for an important clinical variable associated with TBI, such as measures for cerebral vasospasm or elevated intracranial pressure.

An early example is called BAM (brain acoustic monitoring)[431] that does not send ultrasound into the brain. It acts instead as an acoustic stethoscope that listens to cerebral hemodynamics through the skull. The creators of this device have demonstrated the sensitivity of these measures to the status of cerebral autoregulation and seek to use it as a diagnostic for the presence of mild TBI, with, regrettably, mixed success.

TCD plays a vital role in the assay of traumatic cerebral vasospasm (TCV). TCV reduces blood flow into the brain, producing ischemia and neuronal damage then death. TCV is a major contributor to morbidity and mortality experienced by blast-induced TBI patients, having been observed in nearly 50% of cases after blast-induced TBI.[432] Aggressive neurosurgical treatment motivated by early diagnosis appears to improve the clinical outcome for these military patients[432] as well as their civilian counterparts.[139] Moreover, on-going TCD exams allow for continuing monitoring of patients with vasospasm during their treatment.

However, the skill necessary to successfully deploy a TCD and thereby extract the appropriate data from it and limitations on available personnel with this skill, all conspire to limit the use of TCD for vasospasm relative to its need. A device that could automatically, or with minimal skill, extract the necessary Doppler data would address this need. Also, vasospasm is often intermittent in time, and we can expect improved detection and monitoring of TCV if there exists a device that can hold the TCD beam in place for long periods of time, although this has been studied in only a limited fashion. (Mackinnon et al, 2004). Mourad and colleagues have on-going research to address this problem, through the testing and refinement of an automatic transcranial Doppler (aTCD) system (Figure 9). An especially promising aspect of this research is the prospect of creating TCD-angiography – maps of cerebral blood vessel structure (Figure 10). This would facilitate bedside *imaging* of cerebral arteries in spasm, an adjunct to CT- or MR-angiography, without requiring patient movement. TCD angiography would also allow identification of patients (most likely those with polytrauma that includes vasospasm) whose TCD-derived fast blood flow arises due to reduced hematocrit, hence reduced effective viscosity of blood rather than a narrowing of cerebral arteries.

| Figure 9. Automatic transcranial Doppler (aTCD) system | Figure 10. TCD-angiography |

Figure 9. The semi-automatic transcranial Doppler system (the 'PRESTO') developed by PhysioSonics (Redmond, WA) first creates, internal to the machine, a large-field map of average blood flow within a volume of brain to identify within that volume the point of fastest blood flow in the artery within that brain volume. Once that point has been identified, the system focuses its ultrasound on that point, thereby deriving standard TCD blood flow speed distributions from the blood vessel. **Figure 10.** The critical intermediate step

As noted above head trauma can produce extra fluid within the cranium due to bleeding and edema formation. This, in turn, elevates the pressure within the cranium, otherwise known as intracranial pressure or ICP. Much medical and surgical management of brain trauma follows guidelines based on measurements of patient's ICP, performed currently by (necessarily invasive) placement within the cranium of a pressure sensor. A number of investigators have tried to replace this invasive measurement with analysis of various combinations of blood pressure, TCD-based measurements of blood flow speed into the middle cerebral artery, among other variables. The majority of these models employ *features* of arterial blood pressure (ABP) and TCD time series as predictors of ICP. For example, Kim et al. (2011 & 2013)[433,434] construct complex features from the peaks and troughs of the ABP and TCD-derived waveforms across a cardiac cycle. Other complex features are inferred from examining the time series of ABP and TCD time series across multiple cardiac cycles, and in turn mapping the results to ICP as in Schmidt et al (1997) – see the review of Hawthorne and Piper (2014)[435]. All of these models involve the identification of the morphology (i.e., shape or wave-form) of the time series across one or multiple cardiac cycles of ABP and/or TCD time series. Sadly, these and other TCD-based methods have met with only statistical success, not clinical success. These approaches include Marzban et al (2013, and citations within)[436], who also use TCD and arterial blood pressure in a purely statistical way based on the 'zero closing pressure' hypothesis. Finally, methods based on optical (not ultrasound – see the intriguing though not yet definitive results of Ragauskas and colleagues[437] measurements of diameter of the optic nerve have achieved some recent success in identifying those patients with high versus normal ICP values.[438,439]

Gaps: There exists a pressing need for portable diagnostics to address two critical needs of TBI patients in and near the battlefield. One specific need centers on rapid identification of structural damage to brain in the moderate to severe class to facilitate triage. Of particular interest is quantifying epidural and subdural (but extra-axial) bleeds given that rapid, generally surgical treatment of these bleeds can profoundly affect clinical outcome.

Another important gap is quantification of mild TBI in and near the battlefield, where only the most sophisticated imaging modalities plus clinical exams and neuropsychological evaluations can thus far highlight structural damage due to mild TBI, as reviewed elsewhere in this article.

Capability Gaps

Computational tools for advanced analysis of imaging data in patient care

The availability of computational tools for advanced neuromaging analysis has greatly facilitated population studies for exploring neuroscience hypotheses. Certain software packages have sufficiently evolved that any interested researcher, even one without formal computational science training, can use such tools to perform complex analyses. However, despite these significant advancements, there continues to be capability gaps in terms of computational application to TBI research.

As mentioned previously, parameter choices significantly affect analysis results when passed through the TBSS pipeline.[95] Such variation is certainly not restricted to this particular pipeline but extends, to varying degrees, to all software tools with a set of user-specified parameters. Although analysis protocol standardization would be ideal (e.g., a set of optimal parameters), the "No Free Lunch Thereom"[440] formalizes the difficulty of finding a single set of optimal parameters underscoring the importance of prior knowledge of a particular application in tuning a given algorithm. Consequently, researchers need to be explicit in specifying parameter choices in experimental descriptions. This would facilitate reproducibility of experimental findings[441] and aid other researchers looking for guidance in using similar tools. Towards the latter, researchers also need to provide feedback to developers of said tools regarding usage and findings for improved documentation and, possibly, performance. Related, the various methodological issues (e.g., type I errors in fMRI and voxel-based analysis, motion correction in DTI and fMRI, small sample sizes) described previously need to be better understood by the community at large.

Previously mentioned research concerned the development of novel neuroimaging metrics which account for the possible lack of spatial correspondence of TBI effects within a given cohort. This research direction needs to continue for the development of new analysis methods and statistical frameworks specific for TBI. Also, and similar to other areas of neuroimaging research, individual subject assessment is essential for translating research knowledge to patient care. A first step towards such an assessment is the search for a comprehensive neuroimaging signature of TBI. Perhaps if such a signature existed, derived from multimodal acquisition, sophisticated machine learning concepts could be used to predict or classify TBI in individual subjects such as are currently being investigated in neuropathologies such as Alzheimer's disease.[442]

High-resolution imaging of cortical layers

Clinical MRI scans, with typical 1 mm in-plane resolution and 5 mm slice thickness, clearly visualize the gray-white margins of the cerebral cortex but not the interior cortical structure. Nevertheless, the ability to discern the gray-white interface and the cortical surface has been used to map cortical thickness over the whole brain.[103] When combined with automatic cortical surface reconstructions to enable quantitative morphometric analyses of brain anatomy,

sensitivity to changes in cortical thickness have been used to track or detect brain atrophy, plasticity, and development.[443–447]

The cortex is a highly folded, layered structure, and there is a need for more detailed imaging especially in clinically vulnerable areas. Ex vivo MRI-based structural imaging can visualize the cortical layers,[448–451] however acquisition times may take hours or days. More recently ex vivo DTI tractography[452,453] has been used to provide insight in the cortical layer interconnections.

Studies combining ex vivo MRI with histology,[454,455] and most recently using high channel number MRI coil technology[456] provide very high resolution structural scans with detailed structure consistent with the histological sections.

As ex vivo measurements do not allow functional information to be combined with structural imaging, it is critical to meet to the challenge of in vivo cortical imaging. The keys to successfully implementing such methods in the living human cortex are high spatial resolution and high SNR. The additional SNR made available through the use of higher field (3T and above) magnets and multi-coil head arrays now allows the direct visualization of the cortical layers, for example work at 7 T.[457–459] Continued improvements in multi-coil technology, high field MRI scanners and pulse sequence design are crucial to meeting this challenge.

In addition to the push towards every increasing field strengths, improvements in motion correction have become essential technology to obtain high resolution cortical images in vivo.[460] In the case of rigid skull motion, tremendous gains in resolution by the use of prospective motion correction. In particular, intra-cortical imaging with a remarkable 350 μm isotropic resolution over the whole brain was recently obtained using navigator-based motion correction,[461] the highest resolution in vivo neuroanatomical imaging to date. Camera-based prospective motion correction strategies have also been explored.[462] Motion control strategies also need to be developed to mitigate the small non-rigid brain motion due to cardiac pulsatility if cortical imaging is to be pushed to its limits.[463,464]

A capability gap exists in the understanding of the true sources of intracortical contrast. The mapping between subtle anatomical features and contrast in MRI data is not entirely understood[465,466] with considerable ambiguity about the source of laminar contrast.[467] In many cortical areas, features such as increased capillary density and increased iron deposition occur in the same layer[465,468] so it is difficult to tease apart the contribution from each effect. Although the relationship between the features and the contrast in areas of the brain such as the primary visual cortex have been widely studied[449,457] it is very difficult to generalize these relationships to other parts of the brain.

Perhaps the biggest capability gap in cortical imaging is that no single technology combines the whole-brain field-of-view of MRI with the resolution of optical microscopy. Boas and Fischl have been trying to fill this need using Optical Coherence Tomography (OCT).[469–471] This work has the potential to propagate the fine details of cell types obtained from OCT to statistical atlases of whole brains constructed with MRI, including their laminar location, local connections and long distance projections, allowing inferences about cellular architecture to be made in vivo. This technical methodology is scalable to the goal of building a cellular census of the entire human brain, given automated acquisition and analysis algorithms. OCT can enable the building

of undistorted 3D models of large portions of the human brain, with the resolution to distinguish cell types, cortical layers and architectonic boundaries. This will enable population studies of normal and pathological variations in the number, type and spatial distribution of cells in the human brain.

High spatial and temporal resolution of functional circuits

A longstanding belief in the fMRI community contends that that improvement in spatio-temporal resolution of beyond ~ 2 mm and ~ 6 s is unlikely to provide significant gains, as the BOLD response itself is spatially and temporally imprecise. These limits are thought to limit the resolution of any functional imaging methods that rely on hemodynamic-based signal, including not only fMRI signals like BOLD and ASL but also invasive optical imaging. Recent studies have challenged these ideas, arguing that the biological resolution, in space and in time, is actually far tighter than what is commonly believed.

Hemodynamic changes at the capillary level were believed to simply be a consequence of upstream regulation at the feeding arterioles with the capillaries themselves having no ability to regulate blood flow on their own. However, studies have identified evidence for extremely fine-scale regulation within a capillary network,[472] as well as mechanisms for rapid and precise blood flow regulation *at capillary length scales*, including the observed direct neural control of vascular sphincters via interneurons or coordinated regulation of capillary diameter by pericytes.[473–475]

Several recent fMRI studies have clearly demonstrated that, while the BOLD impulse response peaks 6 s post-stimulus, the BOLD response itself has *a high degree of temporal precision* trial-to-trial and the signal presents promptly, 1 s or less after the stimulus onset.[476] Using the Inverse Imaging method, which samples the fMRI signal across the entire brain at temporal sampling intervals at or below 100 ms, Chang et al., and Lin et al. have recently demonstrated that the temporal precision of the BOLD signal is high enough to detect difference in onset time in cortical responses to visual stimuli presented 100 ms apart.[477,478]

On the heels of these findings, a clear capability gap exists in the need for smaller voxels and more rapid sampling in fMRI in order to achieve the ultimate goal of improving spatiotemporal resolution down to its biological limits. Ultra-high resolution human MRI can now resolve columnar[479] and laminar functional units[480] at the length scales where the emergent properties of local neural circuits should manifest. Thus, advances to extend the efficiency of MRI acquisitions to allow for high spatiotemporal whole brain coverage, and efforts to improve imaging of small brainstem and other deep brain nuclei connecting cortical with subcortical organization, are especially relevant. As pointed out in a partial volume analysis by Polimeni et. al, laminar analysis requires isotropic voxels due to cortical curvature, and high isotropic spatial resolution will reduce partial volume effects in the folded cortex and avoid the non-isotropic voxels that have plagued high-resolution functional studies over large areas of folding cortex.[480] Pushing fMRI methodology to the biological limits will provide *far more information regarding the underlying neuronal dynamics*.

High spatiotemporal fMRI is becoming more widely available because of advances in receive coil technology, higher-field magnets, and strong, fast gradient coils An important new development from the pulse sequence side is the *Simultaneous Multi-Slice (SMS)* parallel imaging technique that utilizes multi-band RF pulses for EPI. SMS-EPI allows the fMRI signal to be sampled at a faster rate by acquiring multiple slices at the same time. The region of interest is covered in fewer steps, and parallel imaging reconstruction techniques are used to separate the multiple slices.[481–485] Blipped-CAIPI, in addition to SMS-EPI acquisition,[574] enables higher acceleration factors by controlling the aliasing pattern between the collapsed slices. For a typical 32-channel head coil at 3 T, this can dramatically reduce the time to acquire high quality SMS-EPI data by factors of up to 8-fold.[486]

The advantage of SMS-EPI for resting-state fMRI was first demonstrated by Feinberg *et al.*, where finer parcellation of global brain networks was provided by sampling the resting-state fMRI data more rapidly, suggesting that the increased sampling rate provided functional connectivity estimates with increased spatial specificity either because of the larger amount of data acquired in a single experimental session, or because of the higher temporal resolution. These substantial improvements to fMRI methodology will have a lasting impact on routine scientific, translational, and clinical studies of functional circuits.

Although previous fMRI studies have laid the foundation by investigating the temporal characteristics and resolution of the BOLD response, these studies achieved either whole-brain coverage by sacrificing spatial resolution,[477,478,487,488] where spatial resolutions of about 5–8 mm were required), or very limited brain coverage (where a single imaging slice was employed).[489] The SMS-EPI technique allows for conventional imaging protocols with 1–3 mm resolution to sample the entire brain $10\times$ faster, and therefore allows us to build upon this previous work without sacrificing spatial resolution or coverage. SMS-EPI is essentially conventional imaging sped up, which is in part why the field has been so quick to adopt this method, and why it is poised to change how fMRI studies are performed. Therefore due to the emergence of evidence that the fMRI signal may reflect information that is relevant to neuronal function at very short temporal scales, there is an untapped potential for a new class of studies utilizing rapid fMRI.

The increases in sensitivity and BOLD contrast at 7 T together with the of highly parallel arrays for reducing distortion in high-resolution EPI has enabled dramatic decreased voxel sizes for fMRI studies (~ 0.75mm to 1mm isotropic).[490–492] Together with new surface-based techniques for laminar analysis over large extents of cortex,[480,490] this finer spatial sampling can probe laminar organization of neural connectivity in brain networks.

Additionally, as pointed out by Wald,[493] the desire for high spatial resolution in fMRI not just motivated by a desire to better localize activation within cortical regions, but also by the need to reduce systematic effects and image distortion. Contemporary MRI technology development has been moving more towards the needs of diffusion imaging, i.e. increases in gradient strength. But to address the needs of fMRI, increases in gradient slew rate along with the development of GPAs capable of high duty cycle operation are also needed to reduce single shot EPI image distortion performance.[494] Concern over peripheral nerve stimulation is one of the primary issues blocking further gradient improvements along these lines.[495,496] A move toward smaller, head-sized gradient coils can help to reduce peripheral nerve stimulation compared to whole body

gradients. Head-only gradient designs such as those described by Poole et al. can slew faster without nerve stimulation since their fields do not extend much beyond the head.[497]

Imaging Theragnostics for TBI

Theragnostics is a term that represents combined strategy of disease detection and application of a specific therapeutic strategy depending upon the outcome of a specific diagnostic test.[498] This term was first used by John Funkhouser, CEO of PharmaNetics to describe a strategic approach of developing diagnostic tests that may be specifically linked to treatment strategies. Since this initial description, the term has evolved to describe individualized patient therapy, where genetic, genomic, proteomic, and imaging examinations will be performed which may be predictive of not only the presence of a specific disease state, but also to determine whether features of this disease are present that may predict response to a given therapy.[499] In 1998 the United States Food and Drug Administration (FDA) simultaneously approved the trastuzumab (Herceptin, Roche, Switzerland) and the human epidermal growth factor receptor 2 (HER2) diagnostic test (HercepTest, Dako, Ca) for treatment of HER2neu positive breast cancer. This represented an early key landmark in the evolution of the theragnostic approach, and has led to the co-development of subsequent diagnostic-therapeutic paired applications.

Traumatic brain injury (TBI) is a disease process that is well suited for theragnostic approaches. This is a highly complcex, heterogenous condition with differing macroscopic, microscopic, and molecular features depending upon the mechanism of injury, severity of injury, and individual patient factors contributing to a response to an initial mechanical insult. Secondary injury cascades have been associated with TBI, which include: (i) oxidative stress, (ii) inflammation, (iii) blood brain barrier disruption, (iv) excitotoxicity, (v) mitochondrial dysfunction, (vi) delayed axonal degeneration, and (vii) cell death.[500] Each of these major categories involves temporal cascades of events, which culminate in progressive injury and loss of function. Interruption of these cascades within a therapeutic window may offer the opportunity to diminish the degree of morbidity or prevent mortality associated with this disease state. Mechanisms of axonal degeneration are further discussed below as a case example for potential targets for theragnostic development.

TBI invokes widespread alterations in the axonal cytoskeleton, including microtubule dissolution, neurofilament sidearm alteration, and neurofilament compaction. As it is posited that these profound cytoskeletal changes lead to the impaired axoplasmic transport and axonal disconnection associated with TAI, it is important to further understand the factors involved in the generation of such cytoskeletal change. Based upon an understanding of the normal cellular biology of the cytoskeleton, it is known that phosphatases can decrease the phosphorylation of neurofilament sidearms, thus causing a reduction in sidearm extension, degree of charge, and subsequent interfilament spacing.[501–503] It is possible such mechanisms are ongoing within traumatically injured axons, allowing for the visualization of neurofilament rod domains that are normally immunocytochemically undetectable, however further studies are required to definitively address this issue. In addition to the action of kinases and phosphatases, it is also known that Ca2+ may act to directly depolymerize the actin filamentous network, and cold-labile microtubular network,[504,505] while Ca2+ activated calmodulin will modulate the disassembly of

cold-stable microtubules.[506] Further, a Ca^{2+} activated calmodulin domain present on the spectrin molecule will contribute to the disassembly of the cytoskeleton by inhibiting the ability for spectrin to cross-link actin filaments.[507,508]

In addition to the direct and indirect action of Ca^{2+} on cytoskeletal disassembly, Ca^{2+} also activates proteases that may irreversibly degrade specific components of the cytoskeleton. One such family of proteases are the calpains, which are Ca^{2+}-activated cysteine proteases that are ubiquitously expressed in axons, dendrites, neurons, and glial cells.[509,510] Calpains are typically designated as either μ-calpain (active at μM Ca^{2+} concentrations) or m-calpain (activated at mM Ca^{2+} concentrations). These two forms of calpain are differentially expressed in the brain, with μ-calpain found in neurons, dendrites, and axons, while m-calpain is typically found in glial cells, with minimal presence in axons. In its inactive form, calpain exists as a pro-enzyme heterodimer, with a large calcium-dependent catalytic subunit (80kD) and a small regulatory subunit (30kD). The catalytic subunit contains four sites that may specifically bind Ca^{2+}. An important event in the conversion of the calpain proenzyme to activated calpain appears to be binding of Ca^{2+} to the catalytic subunit, with the subsequent autolysis of the catalytic subunit to 76kD and the regulatory subunit to 19kD. Following this autolysis, calpains will cleave a specific set of intracellular proteins including neurofilaments, microtubule-associated protein 2 (MAP2), spectrin, and tau. Additionally, calpains have been implicated in the cleavage of calmodulin-binding proteins, protein kinase C, calcineurin, phospholipase C, and transcription factors. Interestingly, calpains typically cleave their substrates into limited fragments, with little further degradation, unlike digestive proteases such as trypsin. Such limited cleavage typically leaves behind a "fingerprint" of calpain-mediated breakdown products that may be used to measure the activity of the enzyme.[509]

Antibodies specifically targeting the breakdown products of calpain mediated ⟨-spectrin proteolysis have provided important insight into the activation of calpains following global cerebral ischemia. Additionally, the development of this methodology provided researchers with a powerful tool to investigate calpain activity in settings that previously did not lend themselves to study. Specifically, calpains have been posited to contribute to the cytoskeletal damage associated with TAI, based upon observations that the axolemma of traumatically injured axons becomes permeable to large molecular weight species such as HRP, and thus, should become permeable to Ca^{2+} as well. However, prior to the development of antibodies specific for the breakdown products of calpain mediated proteolysis, the methodology did not exist to assess calpain activation within diffusely scattered sites of traumatically induced axonal damage. In this context, Buki and colleagues[511] conducted a set of experiments in traumatically injured animals, to study whether calpain activation occurred within traumatically injured axonal segments, and if so, how this calpain activity compared with markers of traumatically injured cytoskeletal damage. This study was conducted in rats that were allowed to survive from 15 min to 2 h following administration of impact acceleration TBI. The antibody Ab38, targeting the NH_2 terminal fragment of calpain mediated ⟨-spectrin proteolysis, was used to study calpain activation, while the antibody RM014, targeting the rod domain of the NF-M neurofilament, was used to visualize sites of traumatically compacted neurofilaments. Immunocytochemical visualization of these markers illustrated the appearance of Ab38 within focally damaged axons by 15 minutes post-injury, and within swollen and disconnected axonal profiles by 2 hours post-injury. Additionally, dual label Ab38/RM014 immunocytochemistry illustrated an overlap

between sites of Ab38 and RM014 immunoreactivity at all studied time-points. Further, ultrastructural analysis of Ab38 immunopositive traumatically injured axons revealed sites of neurofilament compaction that exhibited subaxolemmal Ab38 immunoreactivity early post-injury and diffuse Ab38 throughout the axonal cylinder at later time-points following trauma. Thus, this study concluded that calpains are activated in traumatically injured axons early post-injury, and correlate with sites of traumatically induced neurofilament compaction. As neurofilaments are a known substrate of calpain proteolysis, it is possible that this calpain activation may contribute to the neurofilament damage observed within traumatically injured axons. Further, as calpain immunoreactivity is seen to progress from the subaxolemmal compartment to internal portions of the axonal cylinder, it is possible that calpain activation, and subsequent proteolysis is part of a progressive event occurring within traumatically injured axons.

Another set of enzymes that have been implicated in the genesis of traumatically induced axonal change are the caspases. Caspases are a group of enzymes that participate in the process of programmed cell death, or apoptosis, through the cleavage of substrates that are important for the maintained integrity of the cell. While the bulk of caspase research has been performed in the cell body, recent evidence has suggested that the caspase-associated cascade of events may take place within traumatically injured axons, involving the caspase-mediated cleavage of a substrates that are remarkably similar to those cleaved by calpains.[511] Caspases were initially postulated to be involved in TAI based upon observations that intra-axonal mitochondria will become swollen and disrupted within traumatically injured axons.[17,30,512] It was thought that this disruption of intra-axonal mitochondria could lead to the release of cytochrome-c into the cytosol. This cytochrome-c could then bind to apaf-1, and complex to caspase-9, after which caspase-9 could be autolytically cleaved, forming a dimer that converts procaspase-3 to caspase-3. Activated caspase-3 could then cleave its designated substrates, including spectrin, neurofilaments, and tau, potentially causing a disruption of the cytoskeleton, leading to impaired axoplasmic transport, swelling, and disconnection of the axon. Similar to calpains, caspases cleave their substrates in a highly specific manner, leaving a "fingerprint" of substrate breakdown products[510] that may be immunocytochemically detected similar to the methodology described above in relation to the immunodetection of calpain-mediated proteolytic activity. In order to explore whether the caspase cell death cascade is associated with TAI, Büki and colleagues conducted an LM and EM immunocytochemical study, whereby the distribution of cytochrome-c was compared to caspase-3 activation and the subsequent caspase-3-mediated breakdown of spectrin.[511] The results of this study found that antibodies to cytochrome-c label traumatically injured axons as early as 15 minutes post-injury. Further, this cytochrome-c release was associated with immunoreactivity for the active form of caspase, and generation of the specific 120kD breakdown products of caspase-3-mediated spectrin proteolysis. Interestingly, the numbers of traumatically injured axons immunoreactive for all antibodies increased over time, suggesting that the progressive axonal failure associated with TAI may show a more delayed time-course within less severely damaged axons. Ultrastructural analysis of antibodies to cytochrome-c revealed immunoreactivity associated with regions of mitochondrial disruption and swelling early post-injury, and general regions of cytoskeletal damage at later time-points post-injury, suggesting that cytochrome-c is being released from the mitochondria into the cytosol under conditions of traumatically induced axonal change. Further, antibodies to the caspase-3-mediated 120kD breakdown product of spectrin proteolysis revealed immunoreactivity associated with

perimitochondrial regions and cytoskeletal elements early post-injury, and associated with regions of progressive cytoskeletal failure later post-injury. Thus, the findings of these studies concluded that cytochrome-c is released from the damaged mitochondria of traumatically injured axons. Further, this cytochrome-c release is found in those axons exhibiting the activation of caspase-3, and presence of caspase-3-mediated breakdown products, both of which are ultrastructurally associated with progressive cytoskeletal failure. Thus, it was concluded that the caspase cell death cascade is operant within traumatically injured axons, and may contribute to the pathobiological changes found within these damaged axonal foci.

The above discussion provides evidence supporting calpain and caspase cysteine protease activity within sites of traumatically induced axonal damage. As the cytoskeleton is a known substrate for these proteases, and both calpain and caspase activity has been associated with progressive cytoskeletal damage, these proteases may potentially play a role in inducing the cytoskeletal failure that leads to a focal impairment of axoplasmic transport, axonal swelling, and ultimate axonal disconnection. Recently, a variety of calpain and caspase small molecule inhibitors have emerged to influence the activity of these enzymes in TBI. Additionally, PET agents are emerging to detect the activity of caspase proteases in TBI. A caspase small molecule inhibitor and caspase PET imaging probe is one example of a potential theragnostic strategy in TBI. Additional focus should be directed towards the development of imaging tools to diagnose aspects of TBI for which therapies may be available. Given the failure of more than 30 phase III clinical trials to date in the treatment of patients with TBI,[500] the field may benefit from the subselection of patients with specific pathologic features implicating the presence of the specific mechanism that a given therapy may influence.

Pre-Hospital Imaging Tools for Triage of the TBI Patient

Neuroimaging studies are an invaluable tool for patient management, from the determination of presence and extent of brain injury for acute surgical intervention to the identification of chronic sequelae and guidance of rehabilitation therapies. Lee and Newberg[513] have extensively reviewed the significant role of neuroimaging tools play in the care of the TBI patient.

X-ray CT has emerged as a ubiquitous hospital-based triage tool for acute head injury in large measure due to the ability to scan rapidly (< 5 minute) in the presence of life support equipment, and CT is often the first tool used for evaluation in these cases.[514] Nowhere is the role that the rapid availability of neuroimaging tools can play in pre-hospital decision making of acute brain injury patients more abundantly clear then in the recent example of mobile CT scanners for use in acute stroke.[515] Early treatment of stroke is long known to be associated with better outcomes, in the timely dosing with a throbolytic for ischemic stroke after critical exclusion of hemorrhagic stroke.[516] In this study, the deployment of an ambulance-based CT scanner accompanied with a care team consisting of a neurologist, paramedic, and radiology technician were able to confirm the presence of acute ischemic stroke and begin treatment with tPA before transport to the hospital, greatly improving patient outcome.

Despite the widespread use of CT, MRI has been demonstrated to have clear advantages over CT for the evaluation of head injury.[517,518] MRI techniques such as DTI, are far more sensitive to white matter injury than CT,[519] and often reveal injury pathology while CT scans of the same

subject are inconclusive or negative.[520] Indeed, MRI provides the undisputed standard of care for the diagnosis and monitoring of neurological disorders and injuries including traumatic brain injury (TBI).[517] MRI has been shown to have greater sensitivity to edema,[521,522] diffuse axonal injury, nonhemorrhagic cortical contusions, intraventricular hemorrhage, intra-axial lesions, and brain stem injury.[522,523]

MRI is not widely deployable because high-strength magnetic fields (of order 1 T) are necessary to obtain useful brain images. These systems involve large, heavy, fragile, and expensive equipment (such as superconducting magnets) that is incompatible with operation outside the strict hospital infrastructure, and as a result high-field MRI instruments offer limited utility for imaging in these contexts. A tragic consequence of this situation is that soldiers do not have access to MRI when it counts, which is in the first hours or days after a trauma such as a blast that may cause TBI.

Recently, non-cryogenic low-magnetic-field implementations of MRI are beginning to emerge to allow **robust**, **transportable** imaging modalities well suited to triage and manage the types of injuries prevalent in TBI, and practical for field operation. These robust low-field MRI scanners are either high performance electromagnets with high-efficiency MRI pulse sequences[524,525] or lightweight (~ 100 lb) permanent magnets with reduced homogeneity using novel encoding schemes.[526] This work has been rethinking conventional approaches to MRI scanner construction, and is focused on brain imaging in deployable scanners with high diagnostic impact and low power and siting requirements. These scanners, by their ubiquity, will lead to entirely new ways of informing and practicing pre-hospital decision making for the TBI patient.

Ultrasound as a tool has demonstrated a large variety of potential applications to many medical fields; applications to brain representing the earliest (see the papers cited from the 1940s in Jagannathan et al, 2009).[527] With the same orientation as written above for recently developed portable MRI systems, we briefly list a variety of potential applications of ultrasound. Among the significant advantages for ultrasound's use in the field is that ultrasound as a structural and functional imaging modality can readily deploy in the field, given its commercial embodiment within lap-top (e.g., Sonosite) and tablet (e.g., Philips, GE, Mobisante) form factors.

We have noted preliminary work on functional and structural tissue pulsatility imaging. These pilot studies, while offering reason for optimism, still require extensive refinement and validation. The fast Doppler approach of Tanter, Fink and colleagues show tremendous facility where applicable, but the skull thus far represents a substantial barrier to its use in the context of adult TBI, due to the small wavelengths require to resolve the features of interest with fast Doppler, wavelengths that do not readily penetrate the skull. Perhaps it and their 'shear-wave' imaging modality will one day benefit of the clever technique of Clement and colleagues for transmission of sufficient ultrasound across the skull.

Vasospasm after blast TBI tends to manifest acutely, or after several days. Given the importance of screening and monitoring these patients for the first quantitative signs of vasospasm, any advance in easing the technical burden required to make TCD measurements would help these patients; TCD-angiography would help in all cases, at least to reduce patient movement. This interesting approach will require substantially more work, however, to make a clinical impact.

Thinking further into the future, we note that Meairs et al.,(2000)[528] used ultrasound, in combination with acoustic contrast agents (micron-sized bubbles introduced into the vasculature) to highlight changes in brain perfusion within the penumbra of acute stroke, in pilot clinical studies. This remains an entirely untested application in the context of TBI and merits further exploration.

A variety of recent studies point towards the use of transcranially delivered ultrasound to transiently alter brain function. For example, Tyler and colleagues[529,530] have demonstrated that low intensity, pulsed, low-frequency unfocused ultrasound, delivered transcranially, can activate neural circuits within mouse brain, as evidenced by direct measurement of action potentials within intact brain as well as by direct observation of peripheral motor function. Yoo et al. (2011)[531] demonstrated that low intensity, pulsed focused ultrasound with a carrier frequency of 0.69 MHz created functional changes in rabbit brain, including excitatory effects when applied to motor cortex, measurable with fMRI. Then, in a flurry of work this last year, we have Deffieux et al. (2013)[532], who demonstrated reversible changes in macaque visual function after application of focused 0.32 MHz ultrasound to their prefrontal cortex. A second paper by the Stanford group (King et al. 2014)[533] demonstrated rostral to caudal anatomical specificity (on the order of a centimeter) in motor function responses in mice to transcranially delivered, pulsed unfocused ultrasound at 0.5 MHz. Moreover, Mehic et al. (2014)[534] embodied a means of generating very low-frequency ultrasound within a system capable of focused delivery of that ultrasound ('modulated focused ultrasound [mFU] and used it to demonstrate focal (on length scales of a mm) and transcranial activation of brain circuits of mice. Finally, Legon et al (2014)[535] showed modulation of the function of human primary somatosensory cortex with transcranial and focused ultrasound delivered at 0.5 MHz. Perhaps one day these 'neuromodulatory' ultrasound techniques may find use in transiently modulating function as an assay for the correct function of brain or for its vulnerability to future insult. Alternatively or additionally, therapeutic modulation of brain function in conjunction with psychotherapy and/or medications may help change brain function.

The availability of computational tools for advanced neuromaging analysis has greatly facilitated population studies for exploring neuroscience hypotheses. Certain software packages have sufficiently evolved that any interested researcher, even one without formal computational science training, can use such tools to perform complex analyses. However, despite these significant advancements, there continues to be capability gaps in terms of computational application to TBI research.

As mentioned previously, parameter choices significantly affect analysis results when passed through the TBSS pipeline.[102] Such variation is certainly not restricted to this particular pipeline but extends, to varying degrees, to all software tools with a set of user-specified parameters. Although analysis protocol standardization would be ideal (e.g., a set of optimal parameters), the "No Free Lunch Thereom"[529] formalizes the difficulty of finding a single set of optimal parameters underscoring the importance of prior knowledge of a particular application in tuning a given algorithm. Consequently, researchers need to be explicit in specifying parameter choices in experimental descriptions. This would facilitate reproducibility of experimental findings[530] and aid other researchers looking for guidance in using similar tools. Towards the latter, researchers also need to provide feedback to developers of said tools regarding usage and

findings for improved documentation and, possibly, performance. Related, the various methodological issues (e.g., type I errors in fMRI and voxel-based analysis, motion correction in DTI and fMRI, small sample sizes) described previously need to be better understood by the community at large.

Previously mentioned research concerned the development of novel neuroimaging metrics which account for the possible lack of spatial correspondence of TBI effects within a given cohort. This research direction needs to continue for the development of new analysis methods and statistical frameworks specific for TBI. Also, and similar to other areas of neuroimaging research, individual subject assessment is essential for translating research knowledge to patient care. A first step towards such an assessment is the search for a comprehensive neuroimaging signature of TBI. Perhaps if such a signature existed, derived from multimodal acquisition, sophisticated machine learning concepts could be used to predict or classify TBI in individual subjects such as are currently being investigated in neuropathologies such as Alzheimer's disease.[531]

Lack of consensus for standardized imaging protocols

Problem: The advanced neuroimaging methods described in this report have demonstrated that they are sensitive to the acute, sub-acute, and/or chronic sequelae of traumatic brain injury by providing quantitative insight into the morphological, pathophysiological, or functional changes in the brain. Studies demonstrating group or even individualized differences demonstrate that these methods could be used for diagnosis, prognosis, and treatment monitoring. However, very few of these tools are used regularly in clinical practice. One of the reasons for these technologies have not been translated into the clinic is due to the lack of consensus for standardized imaging protocols. Multiple reviews and meta-analysis all agree that the lack of imaging standardization in TBI research across almost all modalities including DTI[217–219], fMRI[220], MRS[221,222] and others[223] is one of the major barriers to adaption (see also Magnetic Resonance Imaging and Magnetic Resonance Spectroscopy sections). This problem lies not only in different data acquisition methods, but also different methods of data analysis and post-processing, and as a result differences in imaging metrics throughout the literature. This not only makes it difficult to compare studies, but perhaps more importantly, does not satisfy the evidenced-based medicine criteria utilized by health insurance companies to determine reimbursement.

Gaps: There are several reasons for the lack of consensus for standardization. First and foremost, these advanced imaging methods are in a constant state of development with improvements and refinements to the pulse sequences and data acquisition methods that evolve with time. Similarly, the second issue is that hardware used for imaging also evolves but at different rates depending on the imaging site. For example, major academic centers have the capability to stay at the cutting-edge of imaging platforms whereas tertiary sites or standalone clinics do not have the resources to be constantly updating their hardware. Since many of the imaging method improvements are dependent upon the hardware, arriving at a consensus for standardization must also take into consideration the availability of hardware. Encumbered into this problem are differences between different manufacturers of the hardware. Proprietary technology and the need to stay competitive results in an inability to compare methods and data between different

manufacturers. Finally, many of these advanced imaging methods require sophisticated post-processing methods. This often serves the advantage of providing quantitative results but introduces the difficulty of comparing those results if different data analysis methods are used. Therefore there also needs to be a consensus as to how to process the data and how to present it. Acquisition parameters, post-processing methods, vendor-related hardware differences, and choice of phantoms all need to be standardized in order to compare results from different studies.

In addition, to problems with cross-study comparisons, it is important to note that traumatic brain injuries vary a great deal across a number of factors such as severity of injury (severe, moderate, to mild) as well as type of injury (open vs closed head wound, subconcussive vs. concussive, blast vs collision, etc). As a result the effect size of different measures across the multiple modalities discussed in this report will differ greatly such that these differences in acquisition methods or vendor-related hardware could be greater than the differences in injured subjects and healthy controls. Mild TBIs, particularly subconcussive injuries, have inherently lower effect sizes which would be greatly influenced by the differences in methodology. There is also a lack of data examining the effect of differences in methods.

Solution: This capability gap has long been recognized within the imaging community. In 2010, the Common Data Elements Neuroimaging Working Group was formed and published two papers describing the common data elements (CDEs) for MRI and CT [8, 9]. Subsequent workshops have also been conducted such as the "Developing Standards for Diffusion Tensor Imaging (DTI) and Diffusion Spectrum Imaging (DSI) through Public-Private Partnerships", sponsored by the Institute of Medicine's Forum on Neuroscience and Nervous System Disorders, Health Arm of the National Academy of Science for specific discussions on methods such as DTI. Most recently, the "Joint ASNR-ACR HII-ASFNR Traumatic Brain Injury (TBI) Workshop: Bringing Advanced Neuroimaging for TBI into the Clinic" was held on May 23, 2014 in Montreal, Canada where similar discussions were held. The results of these discussions have provided potential solutions to the problem of reaching consensus for standardizing imaging protocols.

The first solution that arose from the initial discussions was to utilize NINDS CDE that arose from the consensus of scientific experts. These ensure that the outcome measures utilized by studies will allow for data pooling. As a direct result, the development of national data repositories followed naturally. The FITBIR Informatics System provides a national resource for the storage and sharing of TBI research studies for which imaging can then be documented. The American College of Radiology has developed tools such as the Data Archive and Research Toolkit (DART) that provides de-identification, automated data validation, and quality control measures. The Joint ASNR-ACR HII-ASFNR workshop produce a white paper that provides details on developing a normative database utilizing these resources and where advanced imaging protocols have been recommended. The recommended protocols takes into account issues such as differences in hardware platforms by providing different tiers of protocols that allow for both the lowest common denominator in terms of technology.

However, this approach may result in compromising the availability of more advanced systems and protocols. The individual differences in data acquisition, post-processing, and hardware need to be evaluated yet there are few studies that have examined this cohesively and within the context of brain injury. Studies need to be conducted within the context of head injury where

rigorous testing of different acquisition variables can be conducted to better understand the effects of changing these variables in a given protocol. One part of this solution is to develope 'phantoms', a mock-up of the brain which contains various components that can be used for testing. If a model of brain injury were available, the effects of different variables could be tested to determine the ideal protocol for neuroimaging. In addition, phantoms can be used across all imaging sites will help ensure image and data quality. The difficulty with this approach, much like some of the difficulties with translating methods from animal experiments, is that idealized approaches provide only a general solution. Ultimately, there needs to be a roadmap developed to determine the effect of these variables so that their importance can be determined.

Future long-term approaches include the use of the so-called 'big data' methods where computational modeling can be used for data harmonization and methods of fusing the different modalities to provide an integrated diagnostic imaging tool. One potential solution is presented in a recent paper that examined the reproducibility of multi-parametric neuroimaging[536] where scan-rescan reproducibility was obtained using different modalities. Their results found that structural reproducibility was high but other measures such as diffusion and were higher. In addition, measures in certain brain structures also resulted in greater variability. One key component to this study was that the data was made available online at the Neuroimaging Informatics Tools and Resources Clearinghouse (NITRC) for further analysis. By making these resources available, different fusion and modeling approaches can be tested on human data that would be superior to models and simulated data.

Future Directions

The Neuroimaging Working Group identified critical areas that must be addressed in the near term to advance the field of neuroimaging. Specifically, the need exists for improvement of correlational data of anatomic and functional networks of the brain. An improved understanding of the anatomic and functional networks of the brain can be achieved by creating and implementing novel algorithms to evaluate brain network connectivity and pairing these with functional studies. In addition, non-invasive advanced imaging techniques are required to improve the identification of post injury damage. An optimal end state in the field of neuroimaging is development of reliable biomarkers for detection of TBI.

The working group also identified long term, future directions for the field of neuroimaging, which require transformative technologies. The transformative technology section that follows describes the impact and long term advancements that can occur with transformative technology.

Big Data Approaches to the Neuroimaging of TBI
Given the heterogeneity of TBI, it is difficult to generalize neuroimaging findings within current computational analysis frameworks in contrast, for example, to such pathologies as Alzheimer's disease.[537] Further methodological and statistical development is needed to integrate the multiple aspects of TBI manifestation, particularly within neuroimaging data, while simultaneously regressing out confounding effects such as comorbidity (e.g., PTSD) and aging. This heterogeneity also necessitates large-scale, publicly available data sets across populations of interest to tease out potential differentiating characteristics of TBI-related pathologies. However, such data accessibility is certainly not sufficient— the additional requirements of 1) making data

manipulation programs (e.g., cortical thickness a la FreeSurfer) available, 2) processing the data with minimal computational overhead given the projected cohort sizes and, most importantly, 3) ensuring that such data transformations are well-vetted and meaningful within the TBI context are also necessary. Given all the complex issues associated with computational neuroimage processing, collaborative endeavors on the part of image data and neuroscientists resulting in a central computational infrastructure might be worth the effort. Specifically, a "one-stop-shop" where groups or individuals can submit data to be analyzed using one or multiple algorithmic pipelines with a simple click of a button might facilitate discovery and development.

Neuroimaging of Secondary Injury Cascades

TBI is a complex disease, involving not only a primary injury that includes direct disruption of brain parenchyma, but also a secondary injury characterized by a cascade of biochemical, cellular, and molecular events in the evolution of secondary damage. Secondary brain injury is damage to the brain after the initial trauma, and is an indirect result of the insult. Secondary injury plays a large role in the brain damage and death that results from TBI. In particular, the time course of secondary injury may span days to weeks after the initial insult, resulting in deterioration of neuronal regions that were unharmed in the primary injury.[538] Thus efforts to reduce disability and death from TBI are thought to be best focused on elucidating the pathophysiology of secondary injury and determining the various biomarkers and observables in the hopes of improving final outcome by minimizing secondary injury.[539]

Nitric oxide is a universal mediator of biological effects in the brain, and has been implicated in many of the pathophysiological processes of secondary traumatic brain injury.[540] In particular, overproduction of free radical nitroxides is thought to play an active role in the pathophysiology of secondary injury in TBI.[541] Although pharmacological interventions with nitroxide scavengers have proven to be effective in experimental TBI models[542], critical work is needed to clarify the therapeutic potential of these compounds because nitroxides can be either neuroprotective or destructive depending on its spatiotemporal distribution and concentration.[541] Because the morbidity and mortality associated with secondary injury mechanisms is high, the best patient outcomes are associated with early and aggressive interventions.[543]

The identification and characterization of the mechanisms of TBI-induced secondary brain injury would significantly reduce morbidity and mortality, and improve recovery and quality of life. In particular, direct monitoring of the damage-inducing radical production processes would allow the important mechanisms associated with injury and recovery to be directly monitored and enable effective pharmacological intervention to mitigate brain damage, and reduce disability and death from secondary injury following TBI.

Conventional MRI offers no window into the presence and progression of the fundamental processes of oxidative stress injury following TBI since no known NMR contrast mechanism can reveal increased levels of destructive endogenous radicals. Recent advancements, however, have led to a new approach to brain imaging that may revolutionize the use of MRI for the assessment and treatment of pathologies including secondary brain injury following traumatic brain injury (TBI), non-invasive tomographic detection of endogenous free radicals in vivo as an early marker of injury. A high-resolution approach for imaging free radicals with low field MRI has been recently demonstrated: free radical sensitive Overhauser-enhanced MRI (OMRI).[544] The

use of technology in vivo[545] has the potential to become a powerful tool to obtain pathophysiologic insight into the spatiotemporal kinetics of free radical generation following brain injury, monitor the impact of therapies directed to alleviate free radical-mediated cell damage, and ultimately aid in clinical evaluation and treatment of acute TBI. Indeed, timely and non-invasive tomographic detection of free radical production and oxidative stress can guide therapeutic interventions to be tailored for each patient, in purpose-built portable "injury imagers" based around low-field OMRI.

Future Directions in CT Technology

Fifth-Generation CT

CT is one of the most commonly used diagnostic imaging modalities in modern medicine enabling rapid, non-invasive image acquisition of the brain at high resolutions. Efficacy of CT imaging in diagnosing a variety of traumatic conditions typical of battlefront injuries is unquestioned. It is well known that early imaging, image-guided intervention and triage can significantly reduce mortality and morbidity associated with severe traumatic injury. In a recent study, Huber-Wagner et al. 2009[546] shows the importance of CT imaging in early stage trauma treatments. Specifically, they showed that the probability of survival for 4621 patients with blunt trauma was significantly lower given whole-body CT compared to non-whole-body CT.

CT can be used for managing a variety of battlefront injuries including intracranial hemorrhage, fractures and image-guided interventions. This, however, require availability of a 3rd- generation CT scanner consisting of a rotating gantry fitted with an X-ray tube and a detector assembly. The current, 3rd generation CT architecture is unsuitable for forward deployment because of its weight, power requirements, need for sophisticated control hardware and specially trained personnel. Importantly, a small failure in one of the components, which can occur anytime in the envisioned operational environment, will render the entire system to be inoperable.

With rapid advances in the technologies for X-ray sources, detectors, and reconstruction algorithms, it may be feasible to build a motion-free, completely solid-state 5th generation CT scanner. Also, using flexible substrates for the sources, detectors, and the electronics, it may be possible to have a modular device that can be easily transported, assembled, and serviced in the field. Therefore, a transformative technology in management of combat trauma would be development of a new generation of X-ray CT systems that can be used in a far-forward military environment. Such an instrument must eliminate large, heavy rotating gantries, and drastically reduce size, weight and power compared to the existing CT scanner, and use cutting-edge computational imaging techniques for low-dose operation.

Included in this effort is the development of reconstruction algorithms that provide fast, accurate and robust reconstruction. Simplifying the acquisition protocols and removing "bells and whistles" must make the scanner made smart, compact and so easy to use that a non-specialist can operate it after a simple training or online instruction.

Development of such a novel concept is essential for forward deployment of CT scanners. Such a development will make CT imaging available under real-life military constraints for monitoring and management of severely injured casualties both acutely as well as during episodes of delayed or protracted evacuation. Such a portable, fully static CT scanner may be used in a variety of

settings including forward deployment, triage and en route care for early intervention in life-threatening battle injuries. This research topic relates directly to the Combat Casualty Care Research Program (CCCRP) as it provides integrated imaging capabilities for far-forward medical care to reduce the mortality and morbidity associated with major battlefield wounds and injuries. Immediate clinical benefits, which go beyond TBI, are summarized below:

- Assess Neuro Trauma for rapid triage and transport: Intracranial Hematomas are hard to assess without imaging.

- Minimize Unnecessary Exploratory Laparotomies (ExLaps): Large number of unnecessary ExLaps to investigate deep bleeders, which can be lethal during transport. A simple CT with vascular capability, especially in the retroperitoneal area, can avoid them.

- Use high-negative predictive value of CT: Figure out very early on who needs no surgery; High negative predictive value of CT is an asset in combat imaging.

- Differentiate well-compensated shock from normal: Young soldiers can look normal early on, and then decompensate during transport.

- Evaluate Areas Missed by clinical exam: E.g., Pelvis can hide large quantities of blood and pelvic hematomas are not evaluated by ex-laps. Currently, there is no way to look: ultrasound is less than ideal as most clinicians on the front line, unless they are a radiologist, are not trained in it.

Dual and Multi Spectral CT

Conventional CT provides a single CT Number or Hounsfield Unit (HU) for each voxel. Prior knowledge about the anatomy and attenuation properties of different tissues is used to distinguish various materials such as fat, bone and muscle. There is overlap among the CT numbers of different tissues and conventional CT is unable to distinguish materials with similar HU. For example, intracranial hemorrhage may appear very similar to dilute contrast or diffuse parenchymal mineralization. Multi-spectral CT overcomes this limitation of single energy CT by utilizing energy dependence of CT numbers.

The mass-attenuation coefficient varies based on X-ray energies for different materials. Thus, Hounsfield units measured by CT are not absolute and change depending on the kVp used for image acquisition. In addition, the change in HU is material specific. This property is used by DECT for material decomposition by acquiring two image series with different kVp and assessing the change in HU to ascribe a tissue type to each voxel.

Dual energy CT can be implemented using one of the following four paradigms.

- Dual-spin Scanners: In these scanners, two independent acquisitions at a low and high energy kV setting are acquired sequentially.

- Fast kVp Switching: These scanners employ a special X-ray tube that is capable of rapidly switching between high and low voltage settings on a projection-by-projection basis.

- Dual-source Scanners: As the name implies, these scanners have two independent imaging chains mounted on a single CT gantry. One imaging chain is operated in the low-energy mode and the other imaging chain is operated in the high-energy mode.

- Dual-layer Detectors: The previous three paradigms operate the X-ray source at low and high energy in order to accomplish dual energy scanning. The X-ray source, however, is polychromatic. It is therefore possible to acquire a low and high-energy spectral band from a single exposure using a single, specialized detector.

Dual-energy CT can be used for material characterization for such applications as differentiating hemorrhage from iodine or calcification, characterizing plaque, and automatic bone removal. It can also be used as a quantitative tool, for example, for assessing the degree of enhancement of a tumor in oncologic applications, or for CT perfusion. Most DECT post-processing packages also allow generation of virtual monochromatic images that may be used for optimal contrast viewing, posterior fossa artifact reduction, and metal artifact reduction. In the literature, multiple clinical applications of DECT have been described; for combat care, the following are relevant and require further research.

Photon Counting Detectors

While dual-energy scanners acquire images in two separate spectral bands, photon counting detectors segregate incoming photons into two different bins according to the photon energy. Anywhere from 2 to 8 bins may be used, allowing decomposition of each projection into that many spectral bands. By appropriately setting the noise threshold, one can nearly completely eliminate the electronic noise using these detectors. Different spectral bands can also be appropriately weighted according to their information content so as to improve contrast resolution. One can think of these scanners as true multi-spectral CT scanners.

CT scanners based on photon counting detectors have been experimentally demonstrated and have been shown to have significant contrast improvement, noise reduction, dose reduction, and multi-energy imaging. Multiple challenges, however, persist in building a stable prototype. These challenges include photon pile-up, charge sharing between detector elements, detector polarization after prolonged operation, and inability to properly deal with high peak photon flux typical of CT scanning. For these reasons, these scanners are still under development and commercial versions are not available.

How Photon-counting CT scanners may be used in combat care, and whether they offer any additional features beyond dual energy scanners that may be useful in this environment, are currently open questions.

Iterative Reconstruction Algorithms

In theory, conventional filtered Fourier back projection algorithms provide exact solutions to the inverse problem of CT image reconstruction, under the assumption that a complete set of noiseless transmission measurements is available, which represent linear functions of the attenuation line integral through the patient.[547] However, in actual practice, noise, scatter, beam-hardening, and high-contrast edge effects undermine this assumption. This leads to data nonlinearity and artifacts such as streaking and cupping in the reconstructed image.[547] In addition, since noise is inversely proportional to the square root of the radiation dose, less noisy

images can be obtained by increasing the mAs. However, in clinical practice it is desirable to minimize radiation dose without compromising image quality.

The expectation-maximization algorithm of Lange and Carson accounts for the nonlinear signal-formation processes that introduce noise in x-ray CT data and forms the basis of statistically motivated reconstruction algorithms. Although such mathematical models have actually been used in positron-emission tomography for many years, these algorithms could not be implemented in CT until recently because the computational power necessary could only be achieved with high-performance computer processors. Consequently, several iterative reconstruction software packages are commercially available for use in CT, including ASIR (GE Healthcare, Milwaukee, Wisconsin), IRIS (Siemens, Erlagen, Germany), Adaptive Iterative Dose Reduction (Toshiba, Tochigi, Japan), and iDose (Philips Healthcare, Best, the Netherlands).

The iterative reconstruction algorithm essentially consists of a "trial and error" correction loop that is introduced in the image reconstruction process. A filtered Fourier back projection image reconstruction is initially performed in the raw data domain in order to generate a master reconstruction. Since the filtered back projection is an approximate reconstruction, there is discordance between the measured and calculated projections. This difference is used to derive correction projections, reconstruct a correction image, and update the original image. This process is repeated until the deviation between measured and calculated projections is smaller than a predefined limit. Nonlinear image processing algorithms are used to stabilize the resolution every time the original image is updated. Thus, this regularization loop exploits prior image information with the aim of reducing image noise.[548] Indeed, implementation of iterative reconstruction can yield diagnostic-quality images at 20%–66% lower volume CT dose index (CTDIvol) values than those obtained with filtered Fourier back projection techniques for head CT as well as the chest and abdomen.[549–553,553,554]

Besides dose reduction, iterative reconstruction algorithms may also be used for eliminating structured noise such as metal streak artifacts. Such artifacts are especially prevalent in combat imaging because of the presence of shrapnel, bullets, and other foreign bodies. The extent of this reduction, and how these algorithms can be tailored for combat environment, is an open area of research.

Phase-contrast CT
Conventional X-ray imaging is sensitive to attenuation differences arising primarily from photoelectric effect and Compton scattering. Contrast arising from these effects cannot adequately differentiate various types of soft tissues. For example, various cortical layers with in the gray matter are essentially indistinguishable at X-ray CT. Conventional X-ray imaging does not account for ultra-small angle refraction and other processes that alter the phase of the X-ray beam due to differences in the refractive index of various tissues along the X-ray propagation path. As such, all X-ray modalities, including fluoroscopy, angiography, mammography, and CT, are sensitive to atomic number difference but not to differences in electron density.

X-ray phase-contrast imaging (PCI) holds great promise in improving soft-tissue contrast of traditional X-ray imaging. Like any material, the complex refractive index of tissue (n) can be expressed as $n=1-\delta-i\beta$, where the real term δ is responsible for phase alterations and the imaginary term β for attenuation. Imaging based on the phase-contrast term δ produces much

greater contrast in the case of biological soft tissues, which are primarily composed of low Z elements, than imaging based on the absorption term β.

A variety of imaging methods have been proposed to image phase.[555,556] Majority of these techniques require a synchrotron, a powerful, coherent source of X-rays with high brilliance. Phase contrast X-ray imaging can also be performed using traditional X-ray sources. The most commonly used configuration employs a sequence of gratings to implement a Talbot-Lau interferometer. Tapfer et al.[557] recently reported on a preclinical phase-contrast CT system, similar to those using a synchrotron source. This system showed that X-ray CT using phase contrast can produce images with superior soft-tissue contrast in comparison to conventional attenuation-based CT.

Although feasibility of phase contrast imaging has been demonstrated, both with synchrotron-based and laboratory X-ray sources, there is no phase-contrast imaging system that is currently available for clinical use. These systems, when fully developed, have the potential to open a new window on the morphology and pathophysiology of TBI. Further development of these systems is awaited.

Future Directions in MRI Technology

Quantitative Diffusion Tensor Imaging
Current clinical tests and methods for predicting long-term outcome after TBI are inaccurate and unreliable. This confounds decisions regarding therapeutic intensity and goals of care. Such decisions are commonly made on the basis of limited evidence, leading to a potential mismatch between outcomes and resources mobilized to care for a patient, with associated psychological and financial burdens on patients, their families, and society.[558]

White matter damage, a key feature of TBI, can be identified and quantified with diffusion tensor imaging (DTI). Single-center studies have demonstrated the diagnostic and prognostic value of DTI in TBI patients.[559–561] However, for these results to be widely applicable, quantitative MRI methods must account for hardware and software disparities within and across institutions.

Despite intense research activity, no guidelines exist on how to interpret the DTI images in the setting of TBI. A part of the difficulty lies in lack of standardization in the numerical values associated with the diffusion tensor. Sensitivity of these numerical parameters to patient motion, artifacts, field strength, age, and the echo time (TE) poses another problem in coming up with a standardized algorithm.[562] Due these difficulties, at the current time, DTI in the setting of trauma remains a research topic and is not a part of the routine clinical practice. An algorithm for outcome prediction in TBI that can work for a variety of MRI instruments at multiple centers will represent a key transformative technology in this space.

Blood Oxygen-level Dependent (BOLD) Function MRI
fMRI, sometimes referred to blood-oxygen dependent level (BOLD) imaging, relies on changes in blood flow in response to increased neuronal activity.[563–566] As the neuronal activity increases, if the standard physiological response of the brain is preserved, the cerebral blood flow increases in response to increased metabilic demand. This increase in CBF, which is regional, out strips the metabolic demand. In fact, the ratio of oxy to deoxy hemoglobin increases in the areas of the brain where there is increased demand and consumption of oxygen. This change in oxy/deoxy

hemoglobin can be detected and mapped by MRI because these two states of hemoglobin affect the local magnetic environment differently. Hence the name "BOLD" imaging. The temporal resolution of BOLD of fMRI imaging is slow because the hemodynamic processes it is trying to measure are slow. The changes, however, can be plotted on a fine grid with millimeter scale resolution.

One can sequentially acquire BOLD signal in all parts of the brain, while the brain is at "rest", i.e., when no active motor, memory, visual, or other paradigm is prescribed. These datasets consist of time-series data points of BOLD signal over a certain time period. This task-free resting-state paradigm is attractive for TBI studies, as it does not require any active participation from the patient. It relies on the low-frequency fluctuations in the resting brain that reflect underlying sequence of neuronal activity. It turns out that this so-called resting-state fMRI, rs-fMRI for short, is far from random. There are repeatable and reliable activation patterns and sequences that can be found in this time-series of BOLD data. Researchers have defined the concept of "functional connectivity" between regions of brain where there is high inter-regional correlation in the BOLD waveform. This has given rise to the concept of functional networks within the brain that are composed of spatially distributed regions that have highly correlated BOLD activity pattern. A variety of research techniques have been applied to identify and characterize these networks from a graph theoretical point of view.

In addition of rs-fMRI, task-based paradigms have also been studied. These paradigms require active participation from the subject. During fMRI acquisition, simple tasks are prescribed to the patient and the BOLD signal in response to the prescribed task (e.g., finger tapping), is recorded. This paradigm can be used to activate individual portions or circuits with in the brain.

Both task-based and task-free fMRI paradigms are being actively studied and a number of brain networks have been identified. The data to date, however, is inconclusive and routine use of fMRI in the setting of acute TBI is not recommended. The use of fMRI has the potential to represent a transformative technology in TBI management.

Future improvements in detecting and quantifying CMBs or detecting areas of ischemia with high levels of deoxyhemoglobin lies in the use of high resolution, high field imaging methods such as SWI and perfusion weighted imaging (PWI). As far as infarcted tissue is concerned, this is best studied using high resolution fluid attenuation inversion recovery (FLAIR) at high fields. A natural next step to monitor CMBs is to quantify the amount of iron present in a given lesion using QSM. This way, even if the bleed volume does not change, it will be possible to ascertain if there has been continued bleeding into the same lesion. This is a natural extension of using the same phase that is used to create the mask for SWI in the first place, but now this phase is used to create the source image instead. Along the lines of quantification of CMBs there has been some effort in this area by a few groups.[567,568,569]

Mapping hemodynamics of the brain: The regulation of oxygen supply and its consumption by the brain is a complex and dynamic process. One of the underlying pathophysiological mechanisms of injury to the brain tissue and vasculature is believed to involve impairment of oxygen supply at the site of vascular damage. More interestingly, recent studies have shown that there are positive effects of increased brain tissue oxygenation in severe TBI patients.[570] Therefore, there is a need to provide multi-modal methods for monitoring changes not just for

perfusion but also for oxygen saturation in TBI patients. The amount of oxygen delivered is dependent on the tissue metabolic requirement and on physiologic parameters such as the arterial oxygen content, cerebral blood flow rate and hematocrit (Hct). The difference in oxygen content between the afferent arterial blood (Ya) and the efferent venous blood (Yv) reflects the amount of oxygen utilized by the tissue for its metabolic processes. Under various physiological challenges, the body maintains a balance between oxygen supply and consumption via modulation of the CBF and OEF (defined as (Ya-Yv)/Ya).[571,572] Methods of measuring oxygen metabolism in the brain have been important areas of study in a number of neurological diseases.[573–582] A reliable means to obtain high-resolution venous blood oxygen saturation measurements non-invasively would provide valuable prognostic information about the patient's condition.

There have been a few attempts to extract oxygen saturation using T2, T2* or T2' approaches.[583–599] For example, Graham Wright and others[595–597] have made pioneering efforts to use the T2 of blood in major vessels in the heart and brain to extract blood oxygen saturation. Debiao Li and others[586,591,592,598] have tried a similar approach using T2* based methods. A T2* approach with partial volume effects for small vessels has been proposed by Sedlacik et al.[600,601] Lin[583–585] and He[588,589] have used the theory from Yablonskiy and Haacke[602] to extract oxygen saturation and blood volume of the underlying capillary network using T2'.[603,604] Lastly, MR phase based methods[180,605–609], have also been used on single vessels in an attempt to extract venous susceptibility and oxygen saturation from veins. And finally, QSM provides a map of oxygen extraction fraction.[183,610] Current QSM algorithms have considerable errors in estimating the absolute value of oxygen saturation due to the limited resolution available to study small veins. It is important to note that recent work using QSM in stroke patients shows abnormally dark veins on the side of the stroke.[611]

The correlation between perfusion and venous oxygenation level may reveal the underlying metabolism of brain tissue. Having a local measure of CBV will help answer this critical question. Since local CBV is available in PWI data, its effects can then be accounted for and for the first time it will become possible to predict the local changes in oxygen saturation by using PWI and SWIM together. Using PWI in stroke patients, we found that areas of dark veins corresponded generally to areas of lower flow. The question is whether this is caused by a reduction in blood flow and the accompanying change in deoxyhemoglobin levels or something else. Changes in susceptibility can come from four sources for small veins: changes in oxygen saturation; changes in venous blood volume, thrombosis or extravasted blood in or around the vessel wall. Given CBF, CBV and MTT from perfusion imaging, it should be possible to disentangle these four sources of susceptibility change. Finally, given both flow and OEF, it may be possible to calculate the cerebral metabolic rate of oxygen utilization (CMRO2). To be able to draw conclusions about perfusion, OEF and CMRO2 as measured with MRI, it will be necessary to validate the methodologies quantitatively with appropriate phantoms and to compare these results with a large group of normal controls to account for age related hemodynamic changes.

Magnetic Resonance Spectroscopy (MRS)

MRI provides anatomic maps of T1 and T2 relaxation times. MR spectroscopy (MRS), unlike MRI, is a spectrum of the signal intensities of different metabolites with the brain as a function of their Larmor resonance frequency. This can be done for a single voxel, a matrix of voxels in

two or three dimensions (designated as single-voxel spectroscopy or SVS, and 2D/3D multi-voxel chemical shift imaging or CSI, respectively). The brain metabolites that are commonly imaged include: N-acetyl aspartate (NAA) for neuronal integrity, creatine (Cr) for cellular energy/density, choline (Cho) for membrane turnover, and lactate (Lac) for anaerobic metabolism. By varying the echo times, other metabolites such as glutamate/glutamine excitatory amino acids reseased after TBI[612], and Myoinositol, a marker of astroglial proliferation[237], can also be quantified.

Because TBI is a heterogeneous disease, there is considerable heterogeneity in the published MRS studies on TBI. The sensitivity and specificity of MRS in TBI has never been confirmed by any large, prospective controlled trial. While ample evidence exists that TBI affects the underlying metabolic mix and the metabolites. However, MRS remains an experimental tool and is not recommended for routine work-up of TBI patients. Nonetheless, the ability of MRS to map different metabolites within the brain represents a key potential of this modality that is unique. With proper tools for interpreting the MRS signal, there is a possibility that MRS may hold the key to TBI assessment of acute and chronic TBI for management, triage, rehab planning, and prognostication.

Conclusions

TBI is an increasingly prevalent and complex challenge for the U.S. military. The JPC-6 has been charged with managing a neurotrauma research portfolio that focuses on improving the health and survivability of warfighters injured by TBI. To effectively achieve this goal, it is necessary to fund studies that evaluate neuroimaging approaches, which are among the most promising methods for diagnosing TBI.

To identify the critical issues that must be addressed in order to advance the field of neuroimaging, four working group teleconferences and one in person working group meeting were held from June through October 2014. Working group participants discussed the state of the field, focusing on identification of critical areas in need of additional research investment. The working group agreed that neuroimaging approaches must be developed which improve the role of imaging in the setting of mild TBI. Additionally, the working group agreed that foundational work must be performed to bridge the gap between advanced neuroimaging currently employed for TBI research and the clinical utilization of these tools. The group recognized the significant evolution of advanced neuroimaging tools that has occurred over the past decade. However, longitudinal studies employing these tools must be supported to allow for the identification of features predictive of diagnosis and prognosis.

Collectively, these efforts may provide clinicians with practical tools to objectively diagnose brain injury, provide earlier intervention, and prescribe more precise follow on therapy for brain injuries. There is great hope that neuroimaging may be used to guide more personalized medicine with targeted interventions for treatment of TBI.

Appendix: Working Group Participants

Working Group Participants
Adam Anderson, Ph.D., M.S. *Associate Professor* *Biomedical Engineering* *Radiology and Radiological Sciences* Vanderbilt University
Jeff Creasy, M.D. *Professor* *Radiology and Radiological Sciences* Vanderbilt University
Rajiv Gupta, M.D., Ph.D. *Associate Radiologist, Massachusetts General Hospital* *Assistant Professor, Harvard Medical School* Harvard Medical School Massachusetts General Hospital
Mark Haacke, Ph.D., M.S. *Professor of Radiology, Wayne State University* *Professor and Associate Chair, Department of Biomedical Engineering Wayne State University* *Adjunct Professor of Physics, Case Western Reserve University* *Adjunct Professor of Electrical and Computer Engineering, McMaster University* *Adjunct Professor of Diagnostic Imaging, Loma Linda University* *Distinguished Foreign Professor, Northeastern University, China* Wayne State University
Iren Horkayne-Szakaly, Ph.D. *Adjunct Investigator* *National Institute of Child Health and Human Development* Armed Forces Institute of Pathology
Zhifeng Kou, Ph.D. *Assistant Professor* *Biomedical Engineering and Radiology* Wayne State University
Roland Lee, M.D. *Professor in Residence of Radiology* University of California San Diego
Alexander Lin, Ph.D. *Clinical Spectroscopist, Center for Clinical Spectroscopy, Brigham and Women's Hospital* *Instructor of Radiology, Harvard Medical School* Bringham and Women's Hospital Harvard Medical School

Pierre Mourad, Ph.D., M.S.
Associate Professor
Department of Neurological Surgery
Department of Engineering and Mathematics
Adjunct Associate Professor in the Departments of Bioengineering, Radiology and Pediatric Dentistry
University of Washington

Srini Mukundan, M.D., Ph.D.
Radiologist, Brigham and Women's Hospital
Associate Professor of Radiology, Harvard Medical School
Brigham and Women's Hospital

Martin Pomper, M.D., Ph.D.
Professor
Radiology and Radiological Science
Johns Hopkins School of Medicine

Matthew Rosen, Ph.D.
Instructor in Radiology, Harvard Medical School
Assistant in Biomedical Engineering, Massachusetts General Hospital
Senior Research Scientist, Department of Physics, Harvard University
Harvard University
Massachusetts General Hospital

James Stone, M.D., Ph.D.
Associate Professor
Radiology and Medical Imaging
Neurological Surgery
University of Virginia
Co-Chair of Working Group

Nick Tustison, DSc
Assistant Professor
Radiology and Medical Imaging
University of Virginia

Gerald York, M.D.
Director of TBI Imaging
Imaging Associates of Providence
Providence Alaska Medical Center
Co-Chair of Working Group

References

1. (2008). Guidance for Development of the Force Task Force- Program and Budget Assessment A4.16: Medical Research and Development Investments.

2. Wojcik, B.E., Stein, C.R., Bagg, K., Humphrey, R.J., and Orosco, J. (2010). Traumatic brain injury hospitalizations of U.S. army soldiers deployed to Afghanistan and Iraq. Am J Prev Med 38, S108–116.

3. Blumbergs, P., Reilly, P., and Vink, R. (2008). Chapter 11: Trauma., in: *Greenfield's Neuropathology*, 8th ed. Hadder Arnold, pp. 7330832.

4. Troncoso, J., Rubio, A., and Fowler, D. (2010). Essential Forensic Neuropathology. LWW Wolters Kluwer Health.

5. Frati, A., Salvati, M., Mainiero, F., Ippoliti, F., Rocchi, G., Raco, A., Caroli, E., Cantore, G., and Delfini, R. (2004). Inflammation markers and risk factors for recurrence in 35 patients with a posttraumatic chronic subdural hematoma: a prospective study. J. Neurosurg. 100, 24–32.

6. Adams, J.H., Scott, G., Parker, L.S., Graham, D.I., and Doyle, D. (1980). The contusion index: a quantitative approach to cerebral contusions in head injury. Neuropathol. Appl. Neurobiol. 6, 319–324.

7. Adams, J.H., Doyle, D., Graham, D.I., Lawrence, A.E., McLellan, D.R., Gennarelli, T.A., Pastuszko, M., and Sakamoto, T. (1985). The contusion index: a reappraisal in human and experimental non-missile head injury. Neuropathol. Appl. Neurobiol. 11, 299–308.

8. Unterberg, A.W., Stover, J., Kress, B., and Kiening, K.L. (2004). Edema and brain trauma. Neuroscience 129, 1021–1029.

9. Powner, D.J., Boccalandro, C., Alp, M.S., and Vollmer, D.G. (2006). Endocrine failure after traumatic brain injury in adults. Neurocrit Care 5, 61–70.

10. Graham, D.I., Adams, J.H., and Doyle, D. (1978). Ischaemic brain damage in fatal non-missile head injuries. J. Neurol. Sci. 39, 213–234.

11. Graham, D.I., Ford, I., Adams, J.H., Doyle, D., Teasdale, G.M., Lawrence, A.E., and McLellan, D.R. (1989). Ischaemic brain damage is still common in fatal non-missile head injury. J. Neurol. Neurosurg. Psychiatr. 52, 346–350.

12. Bouma, G.J., Muizelaar, J.P., Choi, S.C., Newlon, P.G., and Young, H.F. (1991). Cerebral circulation and metabolism after severe traumatic brain injury: the elusive role of ischemia. J. Neurosurg. 75, 685–693.

13. Della Corte, F., Giordano, A., Pennisi, M.A., Barelli, A., Caricato, A., Campioni, P., and Galli, G. (1997). Quantitative cerebral blood flow and metabolism determination in the first 48 hours after severe head injury with a new dynamic SPECT device. Acta Neurochir (Wien) 139, 636–641; discussion 641–642.

14. Coles, J.P., Fryer, T.D., Smielewski, P., Chatfield, D.A., Steiner, L.A., Johnston, A.J., Downey, S.P.M.J., Williams, G.B., Aigbirhio, F., Hutchinson, P.J., Rice, K., Carpenter, T.A., Clark, J.C., Pickard, J.D., and Menon, D.K. (2004). Incidence and mechanisms of cerebral ischemia in early clinical head injury. J. Cereb. Blood Flow Metab. 24, 202–211.

15. Coles, J.P., Leary, T.S., Monteiro, J.N., Brazier, P., Summors, A., Doyle, P., Matta, B.F., and Gupta, A.K. (2000). Propofol anesthesia for craniotomy: a double-blind comparison of remifentanil, alfentanil, and fentanyl. J Neurosurg Anesthesiol 12, 15–20.

16. Kobrine, A.I., Timmins, E., Rajjoub, R.K., Rizzoli, H.V., and Davis, D.O. (1977). Demonstration of massive traumatic brain swelling within 20 minutes after injury. Case report. J. Neurosurg. 46, 256–258.

17. Martin, N.A., Patwardhan, R.V., Alexander, M.J., Africk, C.Z., Lee, J.H., Shalmon, E., Hovda, D.A., and Becker, D.P. (1997). Characterization of cerebral hemodynamic phases following severe head trauma: hypoperfusion, hyperemia, and vasospasm. J. Neurosurg. 87, 9–19.

18. Martin, N.A., Doberstein, C., Zane, C., Caron, M.J., Thomas, K., and Becker, D.P. (1992). Posttraumatic cerebral arterial spasm: transcranial Doppler ultrasound, cerebral blood flow, and angiographic findings. J. Neurosurg. 77, 575–583.

19. Hoshino, S., Tamaoka, A., Takahashi, M., Kobayashi, S., Furukawa, T., Oaki, Y., Mori, O., Matsuno, S., Shoji, S., Inomata, M., and Teramoto, A. (1998). Emergence of immunoreactivities for phosphorylated tau and amyloid-beta protein in chronic stage of fluid percussion injury in rat brain. Neuroreport 9, 1879–1883.

20. Smith, D.H., Chen, X.H., Nonaka, M., Trojanowski, J.Q., Lee, V.M., Saatman, K.E., Leoni, M.J., Xu, B.N., Wolf, J.A., and Meaney, D.F. (1999). Accumulation of amyloid beta and tau and the formation of neurofilament inclusions following diffuse brain injury in the pig. J. Neuropathol. Exp. Neurol. 58, 982–992.

21. Zemlan, F.P., Rosenberg, W.S., Luebbe, P.A., Campbell, T.A., Dean, G.E., Weiner, N.E., Cohen, J.A., Rudick, R.A., and Woo, D. (1999). Quantification of axonal damage in traumatic brain injury: affinity purification and characterization of cerebrospinal fluid tau proteins. J. Neurochem. 72, 741–750.

22. Nakamura, M., Raghupathi, R., Merry, D.E., Scherbel, U., Saatman, K.E., and Mcintosh, T.K. (1999). Overexpression of Bcl-2 is neuroprotective after experimental brain injury in transgenic mice. J. Comp. Neurol. 412, 681–692.

23. Zhang, X., Chen, J., Graham, S.H., Du, L., Kochanek, P.M., Draviam, R., Guo, F., Nathaniel, P.D., Szabó, C., Watkins, S.C., and Clark, R.S.B. (2002). Intranuclear localization of apoptosis-inducing factor (AIF) and large scale DNA fragmentation after traumatic brain injury in rats and in neuronal cultures exposed to peroxynitrite. J. Neurochem. 82, 181–191.

24. Volbracht, C., Leist, M., Kolb, S.A., and Nicotera, P. (2001). Apoptosis in caspase-inhibited neurons. Mol. Med. 7, 36–48.

25. Zipfel, G.J., Babcock, D.J., Lee, J.M., and Choi, D.W. (2000). Neuronal apoptosis after CNS injury: the roles of glutamate and calcium. J. Neurotrauma 17, 857–869.

26. Stone, J.R., Singleton, R.H., and Povlishock, J.T. (2001). Intra-axonal Neurofilament Compaction Does Not Evoke Local Axonal Swelling in all Traumatically Injured Axons. Experimental Neurology 172, 320–331.

27. Stone, J.R., Okonkwo, D.O., Dialo, A.O., Rubin, D.G., Mutlu, L.K., Povlishock, J.T., and Helm, G.A. (2004). Impaired axonal transport and altered axolemmal permeability occur in distinct populations of damaged axons following traumatic brain injury. Exp. Neurol. 190, 59–69.

28. Gwag, B.J., Canzoniero, L.M., Sensi, S.L., Demaro, J.A., Koh, J.Y., Goldberg, M.P., Jacquin, M., and Choi, D.W. (1999). Calcium ionophores can induce either apoptosis or necrosis in cultured cortical neurons. Neuroscience 90, 1339–1348.

29. Evan, G., and Littlewood, T. (1998). A matter of life and cell death. Science 281, 1317–1322.

30. Vamvakas, S., Vock, E.H., and Lutz, W.K. (1997). On the role of DNA double-strand breaks in toxicity and carcinogenesis. Crit. Rev. Toxicol. 27, 155–174.

31. Oehmichen, M., Theuerkauf, I., and Meissner, C. (1999). Is traumatic axonal injury (AI) associated with an early microglial activation? Application of a double-labeling technique for simultaneous detection of microglia and AI. Acta Neuropathol. 97, 491–494.

32. Vaz, R., Sarmento, A., Borges, N., Cruz, C., and Azevedo, T. (1998). Experimental traumatic cerebral contusion: morphological study of brain microvessels and characterization of the oedema. Acta Neurochir (Wien) 140, 76–81.

33. Castejón, O.J. (2014). Ultrastructural alterations of human cortical capillary basement membrane in human brain oedema. Folia Neuropathol 52, 10–21.

34. Lin, B., Ginsberg, M.D., Zhao, W., Alonso, O.F., Belayev, L., and Busto, R. (2001). Quantitative analysis of microvascular alterations in traumatic brain injury by endothelial barrier antigen immunohistochemistry. J. Neurotrauma 18, 389–397.

35. Sangiorgi, S., De Benedictis, A., Protasoni, M., Manelli, A., Reguzzoni, M., Cividini, A., Dell'orbo, C., Tomei, G., and Balbi, S. (2013). Early-stage microvascular alterations of a new model of controlled cortical traumatic brain injury: 3D morphological analysis using scanning electron microscopy and corrosion casting. J. Neurosurg. 118, 763–774.

36. Terpolilli, N.A., Kim, S.-W., Thal, S.C., Kuebler, W.M., and Plesnila, N. (2013). Inhaled nitric oxide reduces secondary brain damage after traumatic brain injury in mice. J. Cereb. Blood Flow Metab. 33, 311–318.

37. Petrov, T., and Rafols, J.A. (2001). Acute alterations of endothelin-1 and iNOS expression and control of the brain microcirculation after head trauma. Neurol. Res. 23, 139–143.

38. Rochfort, K.D., Collins, L.E., Murphy, R.P., and Cummins, P.M. (2014). Downregulation of blood-brain barrier phenotype by proinflammatory cytokines involves NADPH oxidase-dependent ROS generation: consequences for interendothelial adherens and tight junctions. PLoS ONE 9, e101815.

39. Lawther, B.K., Kumar, S., and Krovvidi, H. (2011). Blood–brain barrier. Contin Educ Anaesth Crit Care Pain 11, 128–132.

40. Hadass, O., Tomlinson, B.N., Gooyit, M., Chen, S., Purdy, J.J., Walker, J.M., Zhang, C., Giritharan, A.B., Purnell, W., Robinson, C.R., Shin, D., Schroeder, V.A., Suckow, M.A., Simonyi, A., Y Sun, G., Mobashery, S., Cui, J., Chang, M., and Gu, Z. (2013). Selective inhibition of matrix metalloproteinase-9 attenuates secondary damage resulting from severe traumatic brain injury. PLoS ONE 8, e76904.

41. Lohmann, C., Krischke, M., Wegener, J., and Galla, H.J. (2004). Tyrosine phosphatase inhibition induces loss of blood-brain barrier integrity by matrix metalloproteinase-dependent and -independent pathways. Brain Res. 995, 184–196.

42. Wang, X., Jung, J., Asahi, M., Chwang, W., Russo, L., Moskowitz, M.A., Dixon, C.E., Fini, M.E., and Lo, E.H. (2000). Effects of matrix metalloproteinase-9 gene knock-out on morphological and motor outcomes after traumatic brain injury. J. Neurosci. 20, 7037–7042.

43. Lobato, R.D., Sarabia, R., Cordobes, F., Rivas, J.J., Adrados, A., Cabrera, A., Gomez, P., Madera, A., and Lamas, E. (1988). Posttraumatic cerebral hemispheric swelling. Analysis of 55 cases studied with computerized tomography. J. Neurosurg. 68, 417–423.

44. Gómez, P.A., de-la-Cruz, J., Lora, D., Jiménez-Roldán, L., Rodríguez-Boto, G., Sarabia, R., Sahuquillo, J., Lastra, R., Morera, J., Lazo, E., Dominguez, J., Ibañez, J., Brell, M., de-la-Lama, A., Lobato, R.D., and Lagares, A. (2014). Validation of a prognostic score for early mortality in severe head injury cases. J. Neurosurg. , 1–9.

45. Marmarou, A., Fatouros, P.P., Barzó, P., Portella, G., Yoshihara, M., Tsuji, O., Yamamoto, T., Laine, F., Signoretti, S., Ward, J.D., Bullock, M.R., and Young, H.F.

(2000). Contribution of edema and cerebral blood volume to traumatic brain swelling in head-injured patients. J. Neurosurg. 93, 183–193.

46. Friedman, S.D., Brooks, W.M., Jung, R.E., Hart, B.L., and Yeo, R.A. (1998). Proton MR spectroscopic findings correspond to neuropsychological function in traumatic brain injury. AJNR Am J Neuroradiol 19, 1879–1885.

47. Verweij, B.H., Muizelaar, J.P., Vinas, F.C., Peterson, P.L., Xiong, Y., and Lee, C.P. (2000). Impaired cerebral mitochondrial function after traumatic brain injury in humans. J. Neurosurg. 93, 815–820.

48. Graham, D.I., Maxwell, W.L., Adams, J.H., and Jennett, B. (2005). Novel aspects of the neuropathology of the vegetative state after blunt head injury. Prog. Brain Res. 150, 445–455.

49. Adams, J.H., Doyle, D., Ford, I., Gennarelli, T.A., Graham, D.I., and McLellan, D.R. (1989). Diffuse axonal injury in head injury: definition, diagnosis and grading. Histopathology 15, 49–59.

50. Andrews, K. (1998). Prediction of recovery from post-traumatic vegetative state. Lancet 351, 1751.

51. Adams, J.H., Jennett, B., McLellan, D.R., Murray, L.S., and Graham, D.I. (1999). The neuropathology of the vegetative state after head injury. J. Clin. Pathol. 52, 804–806.

52. Strittmatter, W., and Hill, C. (2002). Molecular biology of apolipoprotein E. Current Opinion in Lipidology 13, 119–123.

53. Graham, D.I., Horsburgh, K., Nicoll, J.A., and Teasdale, G.M. (1999). Apolipoprotein E and the response of the brain to injury. Acta Neurochir. Suppl. 73, 89–92.

54. Teasdale, G.M., Nicoll, J.A., Murray, G., and Fiddes, M. (1997). Association of apolipoprotein E polymorphism with outcome after head injury. Lancet 350, 1069–1071.

55. Guo, Z., Cupples, L.A., Kurz, A., Auerbach, S.H., Volicer, L., Chui, H., Green, R.C., Sadovnick, A.D., Duara, R., DeCarli, C., Johnson, K., Go, R.C., Growdon, J.H., Haines, J.L., Kukull, W.A., and Farrer, L.A. (2000). Head injury and the risk of AD in the MIRAGE study. Neurology 54, 1316–1323.

56. Lye, T.C., and Shores, E.A. (2000). Traumatic brain injury as a risk factor for Alzheimer's disease: a review. Neuropsychol Rev 10, 115–129.

57. Luukinen, H., Viramo, P., Koski, K., Laippala, P., and Kivelä, S.L. (1999). Head injuries and cognitive decline among older adults: a population-based study. Neurology 52, 557–562.

58. Mehta, K.M., Ott, A., Kalmijn, S., Slooter, A.J., van Duijn, C.M., Hofman, A., and Breteler, M.M. (1999). Head trauma and risk of dementia and Alzheimer's disease: The Rotterdam Study. Neurology 53, 1959–1962.

59. Irving, E.A., Nicoll, J., Graham, D.I., and Dewar, D. (1996). Increased tau immunoreactivity in oligodendrocytes following human stroke and head injury. Neurosci. Lett. 213, 189–192.

60. Smith, C., Graham, D.I., Murray, L.S., and Nicoll, J. a. R. (2003). Tau immunohistochemistry in acute brain injury. Neuropathol. Appl. Neurobiol. 29, 496–502.

61. Geddes, J.F., Vowles, G.H., Nicoll, J.A., and Révész, T. (1999). Neuronal cytoskeletal changes are an early consequence of repetitive head injury. Acta Neuropathol. 98, 171–178.

62. Giza, C.C., and Hovda, D.A. (2001). The Neurometabolic Cascade of Concussion. J Athl Train 36, 228–235.

63. Binder, D.R., Dunn, W.H., and Swerdlow, R.H. (2005). Molecular characterization of mtDNA depleted and repleted NT2 cell lines. Mitochondrion 5, 255–265.

64. Serbest, G., Burkhardt, M.F., Siman, R., Raghupathi, R., and Saatman, K.E. (2007). Temporal profiles of cytoskeletal protein loss following traumatic axonal injury in mice. Neurochem. Res. 32, 2006–2014.

65. Bigler, E.D., and Maxwell, W.L. (2012). Neuropathology of mild traumatic brain injury: relationship to neuroimaging findings. Brain Imaging Behav 6, 108–136.

66. Cushman, J.G., Agarwal, N., Fabian, T.C., Garcia, V., Nagy, K.K., Pasquale, M.D., Salotto, A.G., and EAST Practice Management Guidelines Work Group. (2001). Practice management guidelines for the management of mild traumatic brain injury: the EAST practice management guidelines work group. J Trauma 51, 1016–1026.

67. Jagoda, A.S., Bazarian, J.J., Bruns, J.J., Cantrill, S.V., Gean, A.D., Howard, P.K., Ghajar, J., Riggio, S., Wright, D.W., Wears, R.L., Bakshy, A., Burgess, P., Wald, M.M., Whitson, R.R., American College of Emergency Physicians, and Centers for Disease Control and Prevention. (2008). Clinical policy: neuroimaging and decisionmaking in adult mild traumatic brain injury in the acute setting. Ann Emerg Med 52, 714–748.

68. Tavender, E.J., Bosch, M., Green, S., O'Connor, D., Pitt, V., Phillips, K., Bragge, P., and Gruen, R.L. (2011). Quality and consistency of guidelines for the management of mild traumatic brain injury in the emergency department. Acad Emerg Med 18, 880–889.

69. National Collaborating Centre for Acute Care (UK). (2007). Head Injury: Triage, Assessment, Investigation and Early Management of Head Injury in Infants, Children and Adults. London: National Collaborating Centre for Acute Care (UK).

70. Galanaud, D., Perlbarg, V., Gupta, R., Stevens, R.D., Sanchez, P., Tollard, E., de Champfleur, N.M., Dinkel, J., Faivre, S., Soto-Ares, G., Veber, B., Cottenceau, V., Masson, F., Tourdias, T., André, E., Audibert, G., Schmitt, E., Ibarrola, D., Dailler, F., Vanhaudenhuyse, A., Tshibanda, L., Payen, J.-F., Le Bas, J.-F., Krainik, A., Bruder, N., Girard, N., Laureys, S., Benali, H., Puybasset, L., and Neuro Imaging for Coma Emergence and Recovery Consortium. (2012). Assessment of white matter injury and outcome in severe brain trauma: a prospective multicenter cohort. Anesthesiology 117, 1300–1310.

71. Añon, J., Remonda, L., Spreng, A., Scheurer, E., Schroth, G., Boesch, C., Thali, M., Dirnhofer, R., and Yen, K. (2008). Traumatic extra-axial hemorrhage: correlation of postmortem MSCT, MRI, and forensic-pathological findings. J Magn Reson Imaging 28, 823–836.

72. Friston, K.J. (1994). Statistical parametric maps in functional imaging: a general linear approach. Hum Brain Mapp 2, 189–210.

73. Worsley, K.J., Marrett, S., Neelin, P., Vandal, A.C., Friston, K.J., and Evans, A.C. (1996). A unified statistical approach for determining significant signals in images of cerebral activation. Hum Brain Mapp 4, 58–73.

74. Genovese, C.R., Lazar, N.A., and Nichols, T. (2002). Thresholding of statistical maps in functional neuroimaging using the false discovery rate. Neuroimage 15, 870–878.

75. Ashburner, J., and Friston, K.J. (2000). Voxel-based morphometry--the methods. Neuroimage 11, 805–821.

76. Jones, D.K., Symms, M.R., Cercignani, M., and Howard, R.J. (2005). The effect of filter size on VBM analyses of DT-MRI data. Neuroimage 26, 546–554.

77. Jorge, R.E., Acion, L., White, T., Tordesillas-Gutierrez, D., Pierson, R., Crespo-Facorro, B., and Magnotta, V.A. (2012). White matter abnormalities in veterans with mild traumatic brain injury. Am J Psychiatry 169, 1284–1291.

78. Gale, S.D., Baxter, L., Roundy, N., and Johnson, S.C. (2005). Traumatic brain injury and grey matter concentration: a preliminary voxel based morphometry study. J. Neurol. Neurosurg. Psychiatr. 76, 984–988.

79. Lull, N., Noé, E., Lull, J.J., García-Panach, J., Chirivella, J., Ferri, J., López-Aznar, D., Sopena, P., and Robles, M. (2010). Voxel-based statistical analysis of thalamic glucose metabolism in traumatic brain injury: relationship with consciousness and cognition. Brain Inj 24, 1098–1107.

80. Wilde, E.A., Merkley, T.L., Bigler, E.D., Max, J.E., Schmidt, A.T., Ayoub, K.W., McCauley, S.R., Hunter, J.V., Hanten, G., Li, X., Chu, Z.D., and Levin, H.S. (2012). Longitudinal changes in cortical thickness in children after traumatic brain injury and their

relation to behavioral regulation and emotional control. Int. J. Dev. Neurosci. 30, 267–276.

81. Tustison, N.J., Avants, B.B., Cook, P.A., Kim, J., Whyte, J., Gee, J.C., and Stone, J.R. (2014). Logical circularity in voxel-based analysis: normalization strategy may induce statistical bias. Hum Brain Mapp 35, 745–759.

82. Smith, S.M., Jenkinson, M., Johansen-Berg, H., Rueckert, D., Nichols, T.E., Mackay, C.E., Watkins, K.E., Ciccarelli, O., Cader, M.Z., Matthews, P.M., and Behrens, T.E.J. (2006). Tract-based spatial statistics: voxelwise analysis of multi-subject diffusion data. Neuroimage 31, 1487–1505.

83. Good, C.D., Johnsrude, I.S., Ashburner, J., Henson, R.N., Friston, K.J., and Frackowiak, R.S. (2001). A voxel-based morphometric study of ageing in 465 normal adult human brains. Neuroimage 14, 21–36.

84. Scarpazza, C., Sartori, G., De Simone, M.S., and Mechelli, A. (2013). When the single matters more than the group: very high false positive rates in single case Voxel Based Morphometry. Neuroimage 70, 175–188.

85. Tustison, N.J., Johnson, H.J., Rohlfing, T., Klein, A., Ghosh, S.S., Ibanez, L., and Avants, B.B. (2013). Instrumentation bias in the use and evaluation of scientific software: recommendations for reproducible practices in the computational sciences. Front Neurosci 7, 162.

86. Bacchetti, P. (2010). Current sample size conventions: flaws, harms, and alternatives. BMC Med 8, 17.

87. Zeineh, M.M., Holdsworth, S., Skare, S., Atlas, S.W., and Bammer, R. (2012). Ultra-high resolution diffusion tensor imaging of the microscopic pathways of the medial temporal lobe. Neuroimage 62, 2065–2082.

88. Lauzon, C.B., Asman, A.J., Esparza, M.L., Burns, S.S., Fan, Q., Gao, Y., Anderson, A.W., Davis, N., Cutting, L.E., and Landman, B.A. (2013). Simultaneous analysis and quality assurance for diffusion tensor imaging. PLoS ONE 8, e61737.

89. Power, J.D., Barnes, K.A., Snyder, A.Z., Schlaggar, B.L., and Petersen, S.E. (2012). Spurious but systematic correlations in functional connectivity MRI networks arise from subject motion. Neuroimage 59, 2142–2154.

90. Goh, S.Y.M., Irimia, A., Torgerson, C.M., and Horn, J.D.V. (2014). Neuroinformatics challenges to the structural, connectomic, functional and electrophysiological multimodal imaging of human traumatic brain injury. Front Neuroinform 8, 19.

91. Poldrack, R.A. (2007). Region of interest analysis for fMRI. Soc Cogn Affect Neurosci 2, 67–70.

92. Wang, H., and Yushkevich, P.A. (2013). Multi-atlas segmentation with joint label fusion and corrective learning-an open source implementation. Front Neuroinform 7, 27.

93. Klein, A., and Tourville, J. (2012). 101 labeled brain images and a consistent human cortical labeling protocol. Front Neurosci 6, 171.

94. Jovicich, J., Marizzoni, M., Bosch, B., Bartrés-Faz, D., Arnold, J., Benninghoff, J., Wiltfang, J., Roccatagliata, L., Picco, A., Nobili, F., Blin, O., Bombois, S., Lopes, R., Bordet, R., Chanoine, V., Ranjeva, J.-P., Didic, M., Gros-Dagnac, H., Payoux, P., Zoccatelli, G., Alessandrini, F., Beltramello, A., Bargalló, N., Ferretti, A., Caulo, M., Aiello, M., Ragucci, M., Soricelli, A., Salvadori, N., Tarducci, R., Floridi, P., Tsolaki, M., Constantinidis, M., Drevelegas, A., Rossini, P.M., Marra, C., Otto, J., Reiss-Zimmermann, M., Hoffmann, K.-T., Galluzzi, S., Frisoni, G.B., and PharmaCog Consortium. (2014). Multisite longitudinal reliability of tract-based spatial statistics in diffusion tensor imaging of healthy elderly subjects. Neuroimage 101, 390–403.

95. Madhyastha, T., Mérillat, S., Hirsiger, S., Bezzola, L., Liem, F., Grabowski, T., and Jäncke, L. (2014). Longitudinal reliability of tract-based spatial statistics in diffusion tensor imaging. Hum. Brain Mapp. 35, 4544–4555.

96. Mohammadi, S., Keller, S.S., Glauche, V., Kugel, H., Jansen, A., Hutton, C., Flöel, A., and Deppe, M. (2012). The Influence of Spatial Registration on Detection of Cerebral Asymmetries Using Voxel-Based Statistics of Fractional Anisotropy Images and TBSS. PLoS ONE 7, e36851.

97. Keihaninejad, S., Ryan, N.S., Malone, I.B., Modat, M., Cash, D., Ridgway, G.R., Zhang, H., Fox, N.C., and Ourselin, S. (2012). The Importance of Group-Wise Registration in Tract Based Spatial Statistics Study of Neurodegeneration: A Simulation Study in Alzheimer's Disease. PLoS ONE 7, e45996.

98. Rosenbaum, S.B., and Lipton, M.L. (2012). Embracing chaos: the scope and importance of clinical and pathological heterogeneity in mTBI. Brain Imaging Behav 6, 255–282.

99. Ilvesmäki, T., Luoto, T.M., Hakulinen, U., Brander, A., Ryymin, P., Eskola, H., Iverson, G.L., and Ohman, J. (2014). Acute mild traumatic brain injury is not associated with white matter change on diffusion tensor imaging. Brain 137, 1876–1882.

100. Bouix, S., Pasternak, O., Rathi, Y., Pelavin, P.E., Zafonte, R., and Shenton, M.E. (2013). Increased gray matter diffusion anisotropy in patients with persistent post-concussive symptoms following mild traumatic brain injury. PLoS ONE 8, e66205.

101. Palacios, E.M., Sala-Llonch, R., Junque, C., Roig, T., Tormos, J.M., Bargallo, N., and Vendrell, P. (2013). Resting-state functional magnetic resonance imaging activity and connectivity and cognitive outcome in traumatic brain injury. JAMA Neurol 70, 845–851.

102. Graner, J., Oakes, T.R., French, L.M., and Riedy, G. (2013). Functional MRI in the investigation of blast-related traumatic brain injury. Front Neurol 4, 16.

103. Fischl, B., and Dale, A.M. (2000). Measuring the thickness of the human cerebral cortex from magnetic resonance images. Proc. Natl. Acad. Sci. U.S.A. 97, 11050–11055.

104. Albers, C.E., von Allmen, M., Evangelopoulos, D.S., Zisakis, A.K., Zimmermann, H., and Exadaktylos, A.K. (2013). What is the incidence of intracranial bleeding in patients with mild traumatic brain injury? A retrospective study in 3088 Canadian CT head rule patients. Biomed Res Int 2013, 453978.

105. Isokuortti, H., Luoto, T.M., Kataja, A., Brander, A., Siironen, J., Liimatainen, S., Iverson, G.L., Ylinen, A., and Ohman, J. (2014). Necessity of monitoring after negative head CT in acute head injury. Injury 45, 1340–1344.

106. Jacobs, B., Beems, T., Stulemeijer, M., van Vugt, A.B., van der Vliet, T.M., Borm, G.F., and Vos, P.E. (2010). Outcome prediction in mild traumatic brain injury: age and clinical variables are stronger predictors than CT abnormalities. J. Neurotrauma 27, 655–668.

107. Lannsjö, M., Backheden, M., Johansson, U., Af Geijerstam, J.L., and Borg, J. (2013). Does head CT scan pathology predict outcome after mild traumatic brain injury? Eur. J. Neurol. 20, 124–129.

108. Jacobs, B., Beems, T., van der Vliet, T.M., van Vugt, A.B., Hoedemaekers, C., Horn, J., Franschman, G., Haitsma, I., van der Naalt, J., Andriessen, T.M.J.C., Borm, G.F., and Vos, P.E. (2013). Outcome prediction in moderate and severe traumatic brain injury: a focus on computed tomography variables. Neurocrit Care 19, 79–89.

109. Metting, Z., Spikman, J.M., Rödiger, L.A., and van der Naalt, J. (2014). Cerebral perfusion and neuropsychological follow up in mild traumatic brain injury: acute versus chronic disturbances? Brain Cogn 86, 24–31.

110. Bendinelli, C., Bivard, A., Nebauer, S., Parsons, M.W., and Balogh, Z.J. (2013). Brain CT perfusion provides additional useful information in severe traumatic brain injury. Injury 44, 1208–1212.

111. Wintermark, M., Sanelli, P.C., Anzai, Y., Tsiouris, A.J., and Whitlow, C.T. (2015). Imaging Evidence and Recommendations for Traumatic Brain Injury: Conventional Neuroimaging Techniques. Journal of the American College of Radiology 12, e1–e14.

112. Davis, P.C., Drayer, B.P., Anderson, R.E., Braffman, B., Deck, M.D., Hasso, A.N., Johnson, B.A., Masaryk, T., Pomeranz, S.J., Seidenwurm, D., Tanenbaum, L., and Masdeu, J.C. (2000). Head trauma. American College of Radiology. ACR Appropriateness Criteria. Radiology 215 Suppl, 507–524.

113. Le, T.H., and Gean, A.D. (2009). Neuroimaging of traumatic brain injury. Mt. Sinai J. Med. 76, 145–162.

114. Guskiewicz, K.M., Marshall, S.W., Bailes, J., McCrea, M., Harding, H.P., Matthews, A., Mihalik, J.R., and Cantu, R.C. (2007). Recurrent concussion and risk of depression in retired professional football players. Med Sci Sports Exerc 39, 903–909.

115. Guskiewicz, K.M., Marshall, S.W., Bailes, J., McCrea, M., Cantu, R.C., Randolph, C., and Jordan, B.D. (2005). Association between recurrent concussion and late-life cognitive impairment in retired professional football players. Neurosurgery 57, 719–726; discussion 719–726.

116. Hart, J., Kraut, M.A., Womack, K.B., Strain, J., Didehbani, N., Bartz, E., Conover, H., Mansinghani, S., Lu, H., and Cullum, C.M. (2013). Neuroimaging of cognitive dysfunction and depression in aging retired National Football League players: a cross-sectional study. JAMA Neurol 70, 326–335.

117. McKee, A.C., Daneshvar, D.H., Alvarez, V.E., and Stein, T.D. (2014). The neuropathology of sport. Acta Neuropathol. 127, 29–51.

118. Pearce, A.J., Hoy, K., Rogers, M.A., Corp, D.T., Maller, J.J., Drury, H.G.K., and Fitzgerald, P.B. (2014). The long-term effects of sports concussion on retired Australian football players: a study using transcranial magnetic stimulation. J. Neurotrauma 31, 1139–1145.

119. Seichepine, D.R., Stamm, J.M., Daneshvar, D.H., Riley, D.O., Baugh, C.M., Gavett, B.E., Tripodis, Y., Martin, B., Chaisson, C., McKee, A.C., Cantu, R.C., Nowinski, C.J., and Stern, R.A. (2013). Profile of self-reported problems with executive functioning in college and professional football players. J. Neurotrauma 30, 1299–1304.

120. Turkheimer, F., Veronese, M., and Dunn, J. (2014). Experimental Design and Practical Data Analysis in Positron Emission Tomography., in: *CreateSpace Independent Publishing Platform*. pp. 114.

121. Byrnes, K.R., Wilson, C.M., Brabazon, F., von Leden, R., Jurgens, J.S., Oakes, T.R., and Selwyn, R.G. (2014). FDG-PET imaging in mild traumatic brain injury: a critical review. Front Neuroenergetics 5, 13.

122. Ching, A.S.C., Kuhnast, B., Damont, A., Roeda, D., Tavitian, B., and Dollé, F. (2012). Current paradigm of the 18-kDa translocator protein (TSPO) as a molecular target for PET imaging in neuroinflammation and neurodegenerative diseases. Insights Imaging 3, 111–119.

123. Wang, Y., Yue, X., Kiesewetter, D.O., Niu, G., Teng, G., and Chen, X. (2014). PET imaging of neuroinflammation in a rat traumatic brain injury model with radiolabeled TSPO ligand DPA-714. Eur. J. Nucl. Med. Mol. Imaging 41, 1440–1449.

124. Kelso, M.L., and Oestreich, J.H. (2012). Traumatic brain injury: central and peripheral role of α7 nicotinic acetylcholine receptors. Curr Drug Targets 13, 631–636.

125. Donat, C.K., Fischer, F., Walter, B., Deuther-Conrad, W., Brodhun, M., Bauer, R., and Brust, P. (2014). Early increase of cannabinoid receptor density after experimental traumatic brain injury in the newborn piglet. Acta Neurobiol Exp (Wars) 74, 197–210.

126. Stein, T.D., Alvarez, V.E., and McKee, A.C. (2014). Chronic traumatic encephalopathy: a spectrum of neuropathological changes following repetitive brain trauma in athletes and military personnel. Alzheimers Res Ther 6, 4.

127. Shah, M., and Catafau, A.M. (2014). Molecular Imaging Insights into Neurodegeneration: Focus on Tau PET Radiotracers. J. Nucl. Med. 55, 871–874.

128. Barclay, L., Zemcov, A., Reichert, W., and Blass, J.P. (1985). Cerebral blood flow decrements in chronic head injury syndrome. Biol. Psychiatry 20, 146–157.

129. Jacobs, A., Put, E., Ingels, M., Put, T., and Bossuyt, A. (1996). One-year follow-up of technetium-99m-HMPAO SPECT in mild head injury. J. Nucl. Med. 37, 1605–1609.

130. Chiu Wong, S.B., Chapman, S.B., Cook, L.G., Anand, R., Gamino, J.F., and Devous, M.D. (2006). A SPECT study of language and brain reorganization three years after pediatric brain injury. Prog. Brain Res. 157, 173–185.

131. Raji, C.A., Tarzwell, R., Pavel, D., Schneider, H., Uszler, M., Thornton, J., van Lierop, M., Cohen, P., Amen, D.G., and Henderson, T. (2014). Clinical utility of SPECT neuroimaging in the diagnosis and treatment of traumatic brain injury: a systematic review. PLoS ONE 9, e91088.

132. O'Brien, W.D. (2007). Ultrasound-biophysics mechanisms. Prog. Biophys. Mol. Biol. 93, 212–255.

133. Leighton, T.G. (1994). The Acoustic Bubble. Academic Press, 640 p.

134. Haar, G.T., and Coussios, C. (2007). High intensity focused ultrasound: physical principles and devices. Int J Hyperthermia 23, 89–104.

135. Mourad, P. (2013). Therapeutic Ultrasound, with an emphasis on applications to the brain., in: *Ultrasonic Transducers - Materials Design and Applications*. Woodhead Publishing Ltd, pps. 545–568.

136. Kremkau, F. (1998). Diagnostic Ultrasound: Principles and Instruments, 5th edition, 5th edition. Philadelphia, PA: W. B. Saunders, 304 p.

137. Kermarrec, E., Demondion, X., Khalil, C., Le Thuc, V., Boutry, N., and Cotten, A. (2010). Ultrasound and magnetic resonance imaging of the peripheral nerves: current techniques, promising directions, and open issues. Semin Musculoskelet Radiol 14, 463–472.

138. Tsivgoulis, G., Alexandrov, A.V., and Sloan, M.A. (2009). Advances in transcranial Doppler ultrasonography. Curr Neurol Neurosci Rep 9, 46–54.

139. Oertel, M., Boscardin, W.J., Obrist, W.D., Glenn, T.C., McArthur, D.L., Gravori, T., Lee, J.H., and Martin, N.A. (2005). Posttraumatic vasospasm: the epidemiology, severity, and time course of an underestimated phenomenon: a prospective study performed in 299 patients. J. Neurosurg. 103, 812–824.

140. Keightley, M.L., Saluja, R.S., Chen, J.-K., Gagnon, I., Leonard, G., Petrides, M., and Ptito, A. (2014). A functional magnetic resonance imaging study of working memory in youth after sports-related concussion: is it still working? J. Neurotrauma 31, 437–451.

141. Dettwiler, A., Murugavel, M., Putukian, M., Cubon, V., Furtado, J., and Osherson, D. (2014). Persistent differences in patterns of brain activation after sports-related concussion: a longitudinal functional magnetic resonance imaging study. J. Neurotrauma 31, 180–188.

142. Ford, J.H., Giovanello, K.S., and Guskiewicz, K.M. (2013). Episodic memory in former professional football players with a history of concussion: an event-related functional neuroimaging study. J. Neurotrauma 30, 1683–1701.

143. Talavage, T.M., Nauman, E.A., Breedlove, E.L., Yoruk, U., Dye, A.E., Morigaki, K.E., Feuer, H., and Leverenz, L.J. (2014). Functionally-detected cognitive impairment in high school football players without clinically-diagnosed concussion. J. Neurotrauma 31, 327–338.

144. Messé, A., Caplain, S., Pélégrini-Issac, M., Blancho, S., Lévy, R., Aghakhani, N., Montreuil, M., Benali, H., and Lehéricy, S. (2013). Specific and evolving resting-state network alterations in post-concussion syndrome following mild traumatic brain injury. PLoS ONE 8, e65470.

145. Leddy, J.J., Cox, J.L., Baker, J.G., Wack, D.S., Pendergast, D.R., Zivadinov, R., and Willer, B. (2013). Exercise treatment for postconcussion syndrome: a pilot study of changes in functional magnetic resonance imaging activation, physiology, and symptoms. J Head Trauma Rehabil 28, 241–249.

146. Yezhuvath, U.S., Lewis-Amezcua, K., Varghese, R., Xiao, G., and Lu, H. (2009). On the assessment of cerebrovascular reactivity using hypercapnia BOLD MRI. NMR Biomed 22, 779–786.

147. Len, T.K., Neary, J.P., Asmundson, G.J.G., Candow, D.G., Goodman, D.G., Bjornson, B., and Bhambhani, Y.N. (2013). Serial monitoring of CO2 reactivity following sport concussion using hypocapnia and hypercapnia. Brain Inj 27, 346–353.

148. Bailey, D.M., Jones, D.W., Sinnott, A., Brugniaux, J.V., New, K.J., Hodson, D., Marley, C.J., Smirl, J.D., Ogoh, S., and Ainslie, P.N. (2013). Impaired cerebral haemodynamic function associated with chronic traumatic brain injury in professional boxers. Clin. Sci. 124, 177–189.

149. Ueda, Y., Walker, S.A., and Povlishock, J.T. (2006). Perivascular nerve damage in the cerebral circulation following traumatic brain injury. Acta Neuropathol. 112, 85–94.

150. Hoge, R.D. (2012). Calibrated FMRI. Neuroimage 62, 930–937.

151. Beaulieu, C., and Allen, P.S. (1994). Determinants of anisotropic water diffusion in nerves. Magn Reson Med 31, 394–400.

152. Basser, P.J., Mattiello, J., and LeBihan, D. (1994). Estimation of the effective self-diffusion tensor from the NMR spin echo. J Magn Reson B 103, 247–254.

153. Song, S.-K., Sun, S.-W., Ju, W.-K., Lin, S.-J., Cross, A.H., and Neufeld, A.H. (2003). Diffusion tensor imaging detects and differentiates axon and myelin degeneration in mouse optic nerve after retinal ischemia. Neuroimage 20, 1714–1722.

154. Song, S.-K., Sun, S.-W., Ramsbottom, M.J., Chang, C., Russell, J., and Cross, A.H. (2002). Dysmyelination revealed through MRI as increased radial (but unchanged axial) diffusion of water. Neuroimage 17, 1429–1436.

155. Gardner, A., Kay-Lambkin, F., Stanwell, P., Donnelly, J., Williams, W.H., Hiles, A., Schofield, P., Levi, C., and Jones, D.K. (2012). A systematic review of diffusion tensor imaging findings in sports-related concussion. J. Neurotrauma 29, 2521–2538.

156. Hulkower, M.B., Poliak, D.B., Rosenbaum, S.B., Zimmerman, M.E., and Lipton, M.L. (2013). A decade of DTI in traumatic brain injury: 10 years and 100 articles later. AJNR Am J Neuroradiol 34, 2064–2074.

157. Kou, Z., Wu, Z., Tong, K.A., Holshouser, B., Benson, R.R., Hu, J., and Haacke, E.M. (2010). The role of advanced MR imaging findings as biomarkers of traumatic brain injury. J Head Trauma Rehabil 25, 267–282.

158. Shenton, M.E., Hamoda, H.M., Schneiderman, J.S., Bouix, S., Pasternak, O., Rathi, Y., Vu, M.-A., Purohit, M.P., Helmer, K., Koerte, I., Lin, A.P., Westin, C.-F., Kikinis, R., Kubicki, M., Stern, R.A., and Zafonte, R. (2012). A review of magnetic resonance imaging and diffusion tensor imaging findings in mild traumatic brain injury. Brain Imaging Behav 6, 137–192.

159. Virji-Babul, N., Borich, M.R., Makan, N., Moore, T., Frew, K., Emery, C.A., and Boyd, L.A. (2013). Diffusion tensor imaging of sports-related concussion in adolescents. Pediatr. Neurol. 48, 24–29.

160. Sasaki, T., Pasternak, O., Mayinger, M., Muehlmann, M., Savadjiev, P., Bouix, S., Kubicki, M., Fredman, E., Dahlben, B., Helmer, K.G., Johnson, A.M., Holmes, J.D., Forwell, L.A., Skopelja, E.N., Shenton, M.E., Echlin, P.S., and Koerte, I.K. (2014). Hockey Concussion Education Project, Part 3. White matter microstructure in ice hockey players with a history of concussion: a diffusion tensor imaging study. J. Neurosurg. 120, 882–890.

161. Chamard, E., Lassonde, M., Henry, L., Tremblay, J., Boulanger, Y., De Beaumont, L., and Théoret, H. (2013). Neurometabolic and microstructural alterations following a sports-related concussion in female athletes. Brain Inj 27, 1038–1046.

162. Fakhran, S., Yaeger, K., and Alhilali, L. (2013). Symptomatic white matter changes in mild traumatic brain injury resemble pathologic features of early Alzheimer dementia. Radiology 269, 249–257.

163. Davenport, E.M., Whitlow, C.T., Urban, J.E., Espeland, M.A., Jung, Y., Rosenbaum, D.A., Gioia, G.A., Powers, A.K., Stitzel, J.D., and Maldjian, J.A. (2014). Abnormal white matter integrity related to head impact exposure in a season of high school varsity football. J. Neurotrauma 31, 1617–1624.

164. Gajawelli, N., Lao, Y., Apuzzo, M.L.J., Romano, R., Liu, C., Tsao, S., Hwang, D., Wilkins, B., Lepore, N., and Law, M. (2013). Neuroimaging changes in the brain in contact versus noncontact sport athletes using diffusion tensor imaging. World Neurosurg 80, 824–828.

165. Lipton, M.L., Kim, N., Zimmerman, M.E., Kim, M., Stewart, W.F., Branch, C.A., and Lipton, R.B. (2013). Soccer heading is associated with white matter microstructural and cognitive abnormalities. Radiology 268, 850–857.

166. McAllister, T.W., Ford, J.C., Flashman, L.A., Maerlender, A., Greenwald, R.M., Beckwith, J.G., Bolander, R.P., Tosteson, T.D., Turco, J.H., Raman, R., and Jain, S. (2014). Effect of head impacts on diffusivity measures in a cohort of collegiate contact sport athletes. Neurology 82, 63–69.

167. Marchi, N., Bazarian, J.J., Puvenna, V., Janigro, M., Ghosh, C., Zhong, J., Zhu, T., Blackman, E., Stewart, D., Ellis, J., Butler, R., and Janigro, D. (2013). Consequences of repeated blood-brain barrier disruption in football players. PLoS ONE 8, e56805.

168. Bartnik-Olson, B.L., Holshouser, B., Wang, H., Grube, M., Tong, K., Wong, V., and Ashwal, S. (2014). Impaired neurovascular unit function contributes to persistent symptoms after concussion: a pilot study. J. Neurotrauma 31, 1497–1506.

169. Fakhran, S., Yaeger, K., Collins, M., and Alhilali, L. (2014). Sex differences in white matter abnormalities after mild traumatic brain injury: localization and correlation with outcome. Radiology 272, 815–823.

170. Yeh, P.-H., Wang, B., Oakes, T.R., French, L.M., Pan, H., Graner, J., Liu, W., and Riedy, G. (2014). Postconcussional disorder and PTSD symptoms of military-related traumatic brain injury associated with compromised neurocircuitry. Hum Brain Mapp 35, 2652–2673.

171. Frank, L.R. (2001). Anisotropy in high angular resolution diffusion-weighted MRI. Magn Reson Med 45, 935–939.

172. Wedeen, V.J., Hagmann, P., Tseng, W.-Y.I., Reese, T.G., and Weisskoff, R.M. (2005). Mapping complex tissue architecture with diffusion spectrum magnetic resonance imaging. Magn Reson Med 54, 1377–1386.

173. Hagmann, P., Cammoun, L., Gigandet, X., Gerhard, S., Grant, P.E., Wedeen, V., Meuli, R., Thiran, J.-P., Honey, C.J., and Sporns, O. (2010). MR connectomics: Principles and challenges. J. Neurosci. Methods 194, 34–45.

174. Jones, D.K., and Cercignani, M. (2010). Twenty-five pitfalls in the analysis of diffusion MRI data. NMR Biomed 23, 803–820.

175. Haacke, E.M., Duhaime, A.C., Gean, A.D., Riedy, G., Wintermark, M., Mukherjee, P., Brody, D.L., DeGraba, T., Duncan, T.D., Elovic, E., Hurley, R., Latour, L., Smirniotopoulos, J.G., and Smith, D.H. (2010). Common data elements in radiologic imaging of traumatic brain injury. J Magn Reson Imaging 32, 516–543.

176. Walker, L., Curry, M., Nayak, A., Lange, N., Pierpaoli, C., and Brain Development Cooperative Group. (2013). A framework for the analysis of phantom data in multicenter diffusion tensor imaging studies. Hum Brain Mapp 34, 2439–2454.

177. Barnes, S.R.S., and Haacke, E.M. (2009). Susceptibility-weighted imaging: clinical angiographic applications. Magn Reson Imaging Clin N Am 17, 47–61.

178. Tong, K.A., Ashwal, S., Holshouser, B.A., Nickerson, J.P., Wall, C.J., Shutter, L.A., Osterdock, R.J., Haacke, E.M., and Kido, D. (2004). Diffuse axonal injury in children: clinical correlation with hemorrhagic lesions. Ann. Neurol. 56, 36–50.

179. Haacke, E.M., Xu, Y., Cheng, Y.-C.N., and Reichenbach, J.R. (2004). Susceptibility weighted imaging (SWI). Magn. Reson. Med. 52, 612–618.

180. Haacke, E.M., Lai, S., Reichenbach, J.R., Kuppusamy, K., Hoogenraad, F.G., Takeichi, H., and Lin, W. (1997). In vivo measurement of blood oxygen saturation using magnetic resonance imaging: a direct validation of the blood oxygen level-dependent concept in functional brain imaging. Hum Brain Mapp 5, 341–346.

181. Haacke, E.M., Mittal, S., Wu, Z., Neelavalli, J., and Cheng, Y.-C.N. (2009). Susceptibility-weighted imaging: technical aspects and clinical applications, part 1. AJNR Am J Neuroradiol 30, 19–30.

182. Mittal, S., Wu, Z., Neelavalli, J., and Haacke, E.M. (2009). Susceptibility-weighted imaging: technical aspects and clinical applications, part 2. AJNR Am J Neuroradiol 30, 232–252.

183. Tang, J., Liu, S., Neelavalli, J., Cheng, Y.C.N., Buch, S., and Haacke, E.M. (2013). Improving susceptibility mapping using a threshold-based K-space/image domain iterative reconstruction approach. Magn Reson Med 69, 1396–1407.

184. Haacke, E.M., Raza, W., Wu, B., and Kou, Z. (2013). The Presence of Venous Damage and Microbleeds in Traumatic Brain Injury and the Potential Future Role of Angiographic and Perfusion Magnetic Resonance Imaging., in: Kreipke, C.W., and Rafols, J.A. (eds). *Cerebral Blood Flow, Metabolism, and Head Trauma*. Springer New York, pps. 75–94.

185. Jamjoom, A.A.B., and Jamjoom, A.B. (2013). Safety and efficacy of early pharmacological thromboprophylaxis in traumatic brain injury: systematic review and meta-analysis. J. Neurotrauma 30, 503–511.

186. Ito, H., Ishii, K., Onuma, T., Kawashima, R., and Fukuda, H. (1997). Cerebral perfusion changes in traumatic diffuse brain injury; IMP SPECT studies. Ann Nucl Med 11, 167–172.

187. Yamauchi, H., Okazawa, H., Kishibe, Y., Sugimoto, K., and Takahashi, M. (2003). The effect of acetazolamide on the changes of cerebral blood flow and oxygen metabolism during visual stimulation. Neuroimage 20, 543–549.

188. Kabasawa, H., Ogawa, T., Iida, A., and Matsubara, M. (2002). [Cerebral circulation and metabolism in the patients with higher brain dysfunction caused by chronic minor traumatic brain injury: a study by the positron emission tomography in twenty subjects with normal MRI findings]. Rinsho Shinkeigaku 42, 512–518.

189. Kato, T., Nakayama, N., Yasokawa, Y., Okumura, A., Shinoda, J., and Iwama, T. (2007). Statistical image analysis of cerebral glucose metabolism in patients with cognitive impairment following diffuse traumatic brain injury. J. Neurotrauma 24, 919–926.

190. Kim, J., Whyte, J., Patel, S., Avants, B., Europa, E., Wang, J., Slattery, J., Gee, J.C., Coslett, H.B., and Detre, J.A. (2010). Resting cerebral blood flow alterations in chronic traumatic brain injury: an arterial spin labeling perfusion FMRI study. J. Neurotrauma 27, 1399–1411.

191. Iwamura, A., Taoka, T., Fukusumi, A., Sakamoto, M., Miyasaka, T., Ochi, T., Akashi, T., Okuchi, K., and Kichikawa, K. (2012). Diffuse vascular injury: convergent-type hemorrhage in the supratentorial white matter on susceptibility-weighted image in cases of severe traumatic brain damage. Neuroradiology 54, 335–343.

192. Wu, Z., Li, S., Lei, J., An, D., and Haacke, E.M. (2010). Evaluation of traumatic subarachnoid hemorrhage using susceptibility-weighted imaging. AJNR Am J Neuroradiol 31, 1302–1310.

193. Monson, K.L., Goldsmith, W., Barbaro, N.M., and Manley, G.T. (2005). Significance of source and size in the mechanical response of human cerebral blood vessels. J Biomech 38, 737–744.

194. Monson, K.L., Goldsmith, W., Barbaro, N.M., and Manley, G.T. (2003). Axial mechanical properties of fresh human cerebral blood vessels. J Biomech Eng 125, 288–294.

195. Imaizumi, T., Miyata, K., Inamura, S., Kohama, I., Nyon, K.S., and Nomura, T. (2011). The difference in location between traumatic cerebral microbleeds and microangiopathic microbleeds associated with stroke. J Neuroimaging 21, 359–364.

196. Yan, L., Li, Y.-D., Li, Y.-H., Li, M.-H., Zhao, J.-G., and Chen, S.-W. (2014). Outcomes of antiplatelet therapy for haemorrhage patients after thrombolysis: a prospective study based on susceptibility-weighted imaging. Radiol Med 119, 175–182.

197. Deibler, A.R., Pollock, J.M., Kraft, R.A., Tan, H., Burdette, J.H., and Maldjian, J.A. (2008). Arterial spin-labeling in routine clinical practice, part 1: technique and artifacts. AJNR Am J Neuroradiol 29, 1228–1234.

198. Deibler, A.R., Pollock, J.M., Kraft, R.A., Tan, H., Burdette, J.H., and Maldjian, J.A. (2008). Arterial spin-labeling in routine clinical practice, part 2: hypoperfusion patterns. AJNR Am J Neuroradiol 29, 1235–1241.

199. Deibler, A.R., Pollock, J.M., Kraft, R.A., Tan, H., Burdette, J.H., and Maldjian, J.A. (2008). Arterial spin-labeling in routine clinical practice, part 3: hyperperfusion patterns. AJNR Am J Neuroradiol 29, 1428–1435.

200. McGehee, B.E., Pollock, J.M., and Maldjian, J.A. (2012). Brain perfusion imaging: How does it work and what should I use? J Magn Reson Imaging 36, 1257–1272.

201. Ge, Y., Patel, M.B., Chen, Q., Grossman, E.J., Zhang, K., Miles, L., Babb, J.S., Reaume, J., and Grossman, R.I. (2009). Assessment of thalamic perfusion in patients with mild traumatic brain injury by true FISP arterial spin labelling MR imaging at 3T. Brain Inj 23, 666–674.

202. Liu, W., Wang, B., Wolfowitz, R., Yeh, P.-H., Nathan, D.E., Graner, J., Tang, H., Pan, H., Harper, J., Pham, D., Oakes, T.R., French, L.M., and Riedy, G. (2013). Perfusion deficits in patients with mild traumatic brain injury characterized by dynamic susceptibility contrast MRI. NMR Biomed 26, 651–663.

203. Shen, Y., Kou, Z., Kreipke, C.W., Petrov, T., Hu, J., and Haacke, E.M. (2007). In vivo measurement of tissue damage, oxygen saturation changes and blood flow changes after experimental traumatic brain injury in rats using susceptibility weighted imaging. Magn Reson Imaging 25, 219–227.

204. Bouma, G.J., and Muizelaar, J.P. (1992). Cerebral blood flow, cerebral blood volume, and cerebrovascular reactivity after severe head injury. J. Neurotrauma 9 Suppl 1, S333–348.

205. Bouma, G.J., and Muizelaar, J.P. (1995). Cerebral blood flow in severe clinical head injury. New Horiz 3, 384–394.

206. Bouma, G.J., and Muizelaar, J.P. (1993). Evaluation of regional cerebral blood flow in acute head injury by stable xenon-enhanced computerized tomography. Acta Neurochir Suppl (Wien) 59, 34–40.

207. Kelly, D.F., Martin, N.A., Kordestani, R., Counelis, G., Hovda, D.A., Bergsneider, M., McBride, D.Q., Shalmon, E., Herman, D., and Becker, D.P. (1997). Cerebral blood flow as a predictor of outcome following traumatic brain injury. J. Neurosurg. 86, 633–641.

208. Kelly, D.F., Kordestani, R.K., Martin, N.A., Nguyen, T., Hovda, D.A., Bergsneider, M., McArthur, D.L., and Becker, D.P. (1996). Hyperemia following traumatic brain injury: relationship to intracranial hypertension and outcome. J. Neurosurg. 85, 762–771.

209. Marion, D.W., Darby, J., and Yonas, H. (1991). Acute regional cerebral blood flow changes caused by severe head injuries. J. Neurosurg. 74, 407–414.

210. Muizelaar, J.P., Marmarou, A., DeSalles, A.A., Ward, J.D., Zimmerman, R.S., Li, Z., Choi, S.C., and Young, H.F. (1989). Cerebral blood flow and metabolism in severely head-injured children. Part 1: Relationship with GCS score, outcome, ICP, and PVI. J. Neurosurg. 71, 63–71.

211. Obrist, W.D., Langfitt, T.W., Jaggi, J.L., Cruz, J., and Gennarelli, T.A. (1984). Cerebral blood flow and metabolism in comatose patients with acute head injury. Relationship to intracranial hypertension. J. Neurosurg. 61, 241–253.

212. Mendelow, A.D., Teasdale, G.M., Russell, T., Flood, J., Patterson, J., and Murray, G.D. (1985). Effect of mannitol on cerebral blood flow and cerebral perfusion pressure in human head injury. J. Neurosurg. 63, 43–48.

213. Prat, R., Markiv, V., Dujovny, M., and Misra, M. (1997). Evaluation of cerebral autoregulation following diffuse brain injury in rats. Neurol. Res. 19, 393–402.

214. Kallakuri, S. (2012). Traumatic Brain Injury and potential role of Caffeine in alleviating secondary injury changes in an animal model. Wayne State University.

215. Muizelaar, J.P., and Schröder, M.L. (1994). Overview of monitoring of cerebral blood flow and metabolism after severe head injury. Can J Neurol Sci 21, S6–11.

216. Oddo, M., Levine, J.M., Mackenzie, L., Frangos, S., Feihl, F., Kasner, S.E., Katsnelson, M., Pukenas, B., Macmurtrie, E., Maloney-Wilensky, E., Kofke, W.A., and LeRoux, P.D. (2011). Brain hypoxia is associated with short-term outcome after severe traumatic brain injury independently of intracranial hypertension and low cerebral perfusion pressure. Neurosurgery 69, 1037–1045; discussion 1045.

217. Lin, A.P., Liao, H.J., Merugumala, S.K., Prabhu, S.P., Meehan, W.P., and Ross, B.D. (2012). Metabolic imaging of mild traumatic brain injury. Brain Imaging Behav 6, 208–223.

218. Mountford, C.E., Stanwell, P., Lin, A., Ramadan, S., and Ross, B. (2010). Neurospectroscopy: the past, present and future. Chem. Rev. 110, 3060–3086.

219. Ramadan, S., Andronesi, O.C., Stanwell, P., Lin, A.P., Sorensen, A.G., and Mountford, C.E. (2011). Use of in Vivo Two-dimensional MR Spectroscopy to Compare the Biochemistry of the Human Brain to That of Glioblastoma. Radiology 259, 540–549.

220. Thomas, M.A., Yue, K., Binesh, N., Davanzo, P., Kumar, A., Siegel, B., Frye, M., Curran, J., Lufkin, R., Martin, P., and Guze, B. (2001). Localized two-dimensional shift correlated MR spectroscopy of human brain. Magn. Reson. Med. 46, 58–67.

221. Haseler, L.J., Arcinue, E., Danielsen, E.R., Bluml, S., and Ross, B.D. (1997). Evidence From Proton Magnetic Resonance Spectroscopy for a Metabolic Cascade of Neuronal Damage in Shaken Baby Syndrome. Pediatrics 99, 4–14.

222. Makoroff, K.L., Cecil, K.M., Care, M., and Jr, W.S.B. (2005). Elevated lactate as an early marker of brain injury in inflicted traumatic brain injury. Pediatr Radiol 35, 668–676.

223. Ross, B.D., Ernst, T., Kreis, R., Haseler, L.J., Bayer, S., Danielsen, E., Blüml, S., Shonk, T., Mandigo, J.C., Caton, W., Clark, C., Jensen, S.W., Lehman, N.L., Arcinue, E., Pudenz, R., and Shelden, C.H. (1998). 1H MRS in acute traumatic brain injury. J. Magn. Reson. Imaging 8, 829–840.

224. Signoretti, S., Marmarou, A., Tavazzi, B., Lazzarino, G., Beaumont, A., and Vagnozzi, R. (2001). N-Acetylaspartate Reduction as a Measure of Injury Severity and Mitochondrial Dysfunction Following Diffuse Traumatic Brain Injury. Journal of Neurotrauma 18, 977–991.

225. Moffett, J.R., Arun, P., Ariyannur, P.S., and Namboodiri, A.M.A. (2013). N-Acetylaspartate reductions in brain injury: impact on post-injury neuroenergetics, lipid synthesis, and protein acetylation. Front Neuroenergetics 5, 11.

226. Shutter, L., Tong, K.A., and Holshouser, B.A. (2004). Proton MRS in Acute Traumatic Brain Injury: Role for Glutamate/Glutamine and Choline for Outcome Prediction. Journal of Neurotrauma 21, 1693–1705.

227. Gasparovic, C., Yeo, R., Mannell, M., Ling, J., Elgie, R., Phillips, J., Doezema, D., and Mayer, A.R. (2009). Neurometabolite Concentrations in Gray and White Matter in Mild Traumatic Brain Injury: An 1H–Magnetic Resonance Spectroscopy Study. Journal of Neurotrauma 26, 1635–1643.

228. Yeo, R.A., Gasparovic, C., Merideth, F., Ruhl, D., Doezema, D., and Mayer, A.R. (2010). A Longitudinal Proton Magnetic Resonance Spectroscopy Study of Mild Traumatic Brain Injury. Journal of Neurotrauma 28, 1–11.

229. Holshouser, B.A., Tong, K.A., and Ashwal, S. (2005). Proton MR Spectroscopic Imaging Depicts Diffuse Axonal Injury in Children with Traumatic Brain Injury. AJNR Am J Neuroradiol 26, 1276–1285.

230. Ashwal, S., Holshouser, B., Tong, K., Serna, T., Osterdock, R., Gross, M., and Kido, D. (2004). Proton Spectroscopy Detected Myoinositol in Children with Traumatic Brain Injury. Pediatr Res 56, 630–638.

231. oss, B., C. Enriquez, and A. Lin,. ([date unknown]). MR spectroscopy of hypoxic brain injury, in Clinical MR Neuroimaging: Diffusion, Perfusion and Spectroscopy,. Cambridge University Press, 690-705 p.

232. Ashwal, S., Holshouser, B.A., Shu, S.K., Simmons, P.L., Perkin, R.M., Tomasi, L.G., Knierim, D.S., Sheridan, C., Craig, K., Andrews, G.H., and Hinshaw, D.B. (2000). Predictive value of proton magnetic resonance spectroscopy in pediatric closed head injury. Pediatr. Neurol. 23, 114–125.

233. Brooks, W.M., Friedman, S.D., and Gasparovic, C. (2001). Magnetic resonance spectroscopy in traumatic brain injury. J Head Trauma Rehabil 16, 149–164.

234. Brooks, W.M., Stidley, C.A., Petropoulos, H., Jung, R.E., Weers, D.C., Friedman, S.D., Barlow, M.A., Sibbitt, W.L., and Yeo, R.A. (2000). Metabolic and cognitive response to human traumatic brain injury: a quantitative proton magnetic resonance study. J. Neurotrauma 17, 629–640.

235. Friedman, S.D., Brooks, W.M., Jung, R.E., Chiulli, S.J., Sloan, J.H., Montoya, B.T., Hart, B.L., and Yeo, R.A. (1999). Quantitative proton MRS predicts outcome after traumatic brain injury. Neurology 52, 1384–1391.

236. Garnett, M.R., Blamire, A.M., Corkill, R.G., Cadoux-Hudson, T.A., Rajagopalan, B., and Styles, P. (2000). Early proton magnetic resonance spectroscopy in normal-appearing brain correlates with outcome in patients following traumatic brain injury. Brain 123 (Pt 10), 2046–2054.

237. Garnett, M.R., Blamire, A.M., Rajagopalan, B., Styles, P., and Cadoux-Hudson, T.A. (2000). Evidence for cellular damage in normal-appearing white matter correlates with injury severity in patients following traumatic brain injury: A magnetic resonance spectroscopy study. Brain 123 (Pt 7), 1403–1409.

238. Holshouser, B.A., Tong, K.A., Ashwal, S., Oyoyo, U., Ghamsary, M., Saunders, D., and Shutter, L. (2006). Prospective longitudinal proton magnetic resonance spectroscopic imaging in adult traumatic brain injury. J Magn Reson Imaging 24, 33–40.

239. Ng, T.S., Lin, A.P., Koerte, I.K., Pasternak, O., Liao, H., Merugumala, S., Bouix, S., and Shenton, M.E. (2014). Neuroimaging in repetitive brain trauma. Alzheimers Res Ther 6, 10.

240. Cecil, K.M., Hills, E.C., Sandel, M.E., Smith, D.H., McIntosh, T.K., Mannon, L.J., Sinson, G.P., Bagley, L.J., Grossman, R.I., and Lenkinski, R.E. (1998). Proton magnetic

resonance spectroscopy for detection of axonal injury in the splenium of the corpus callosum of brain-injured patients. J. Neurosurg. 88, 795–801.

241. Cohen, B.A., Inglese, M., Rusinek, H., Babb, J.S., Grossman, R.I., and Gonen, O. (2007). Proton MR spectroscopy and MRI-volumetry in mild traumatic brain injury. AJNR Am J Neuroradiol 28, 907–913.

242. Kirov, I., Fleysher, L., Babb, J.S., Silver, J.M., Grossman, R.I., and Gonen, O. (2007). Characterizing "mild" in traumatic brain injury with proton MR spectroscopy in the thalamus: Initial findings. Brain Inj 21, 1147–1154.

243. Vagnozzi, R., Signoretti, S., Tavazzi, B., Floris, R., Ludovici, A., Marziali, S., Tarascio, G., Amorini, A.M., Di Pietro, V., Delfini, R., and Lazzarino, G. (2008). Temporal window of metabolic brain vulnerability to concussion: a pilot 1H-magnetic resonance spectroscopic study in concussed athletes--part III. Neurosurgery 62, 1286–1295; discussion 1295–1296.

244. Henry, L.C., Tremblay, S., Leclerc, S., Khiat, A., Boulanger, Y., Ellemberg, D., and Lassonde, M. (2011). Metabolic changes in concussed American football players during the acute and chronic post-injury phases. BMC Neurol 11, 105.

245. Johnson, B., Gay, M., Zhang, K., Neuberger, T., Horovitz, S.G., Hallett, M., Sebastianelli, W., and Slobounov, S. (2012). The use of magnetic resonance spectroscopy in the subacute evaluation of athletes recovering from single and multiple mild traumatic brain injury. J. Neurotrauma 29, 2297–2304.

246. Maugans, T.A., Farley, C., Altaye, M., Leach, J., and Cecil, K.M. (2012). Pediatric sports-related concussion produces cerebral blood flow alterations. Pediatrics 129, 28–37.

247. Chamard, E., Théoret, H., Skopelja, E.N., Forwell, L.A., Johnson, A.M., and Echlin, P.S. (2012). A prospective study of physician-observed concussion during a varsity university hockey season: metabolic changes in ice hockey players. Part 4 of 4. Neurosurg Focus 33, E4: 1–7.

248. Gardner, A., Iverson, G.L., and Stanwell, P. (2014). A systematic review of proton magnetic resonance spectroscopy findings in sport-related concussion. J. Neurotrauma 31, 1–18.

249. Lin AP, Ramadan S, Box H, Stanwell P, Stern R. (2010). Neurochemical Changes in Athletes with Chronic Traumatic Encephalopathy,.

250. Hetherington, H.P., Hamid, H., Kulas, J., Ling, G., Bandak, F., de Lanerolle, N.C., and Pan, J.W. (2014). MRSI of the medial temporal lobe at 7 T in explosive blast mild traumatic brain injury. Magn Reson Med 71, 1358–1367.

251. Marino, S., Ciurleo, R., Bramanti, P., Federico, A., and De Stefano, N. (2011). 1H-MR spectroscopy in traumatic brain injury. Neurocrit Care 14, 127–133.

252. Tremblay, S., Beaulé, V., Proulx, S., Tremblay, S., Marjańska, M., Doyon, J., Lassonde, M., and Théoret, H. (2014). Multimodal assessment of primary motor cortex integrity following sport concussion in asymptomatic athletes. Clin Neurophysiol 125, 1371–1379.

253. Sivák, Š., Bittšanský, M., Grossmann, J., Nosál', V., Kantorová, E., Siváková, J., Demková, A., Hnilicová, P., Dobrota, D., and Kurča, E. (2014). Clinical correlations of proton magnetic resonance spectroscopy findings in acute phase after mild traumatic brain injury. Brain Inj 28, 341–346.

254. Kierans, A.S., Kirov, I.I., Gonen, O., Haemer, G., Nisenbaum, E., Babb, J.S., Grossman, R.I., and Lui, Y.W. (2014). Myoinositol and glutamate complex neurometabolite abnormality after mild traumatic brain injury. Neurology 82, 521–528.

255. George, E.O., Roys, S., Sours, C., Rosenberg, J., Zhuo, J., Shanmuganathan, K., and Gullapalli, R.P. (2014). Longitudinal and prognostic evaluation of mild traumatic brain injury: A 1H-magnetic resonance spectroscopy study. J. Neurotrauma 31, 1018–1028.

256. Du, Y., Li, Y., and Lan, Q. (2011). 1H-Magnetic resonance spectroscopy correlates with injury severity and can predict coma duration in patients following severe traumatic brain injury. Neurol India 59, 679–684.

257. Vagnozzi, R., Signoretti, S., Floris, R., Marziali, S., Manara, M., Amorini, A.M., Belli, A., Di Pietro, V., D'urso, S., Pastore, F.S., Lazzarino, G., and Tavazzi, B. (2013). Decrease in N-acetylaspartate following concussion may be coupled to decrease in creatine. J Head Trauma Rehabil 28, 284–292.

258. O'Phelan, K., Ernst, T., Park, D., Stenger, A., Denny, K., Green, D., Chang, C., and Chang, L. (2013). Impact of methamphetamine on regional metabolism and cerebral blood flow after traumatic brain injury. Neurocrit Care 19, 183–191.

259. Kirov, I.I., Tal, A., Babb, J.S., Reaume, J., Bushnik, T., Ashman, T.A., Flanagan, S., Grossman, R.I., and Gonen, O. (2013). Proton MR spectroscopy correlates diffuse axonal abnormalities with post-concussive symptoms in mild traumatic brain injury. J. Neurotrauma 30, 1200–1204.

260. Kirov, I.I., Tal, A., Babb, J.S., Lui, Y.W., Grossman, R.I., and Gonen, O. (2013). Diffuse axonal injury in mild traumatic brain injury: a 3D multivoxel proton MR spectroscopy study. J. Neurol. 260, 242–252.

261. Tremblay, S., De Beaumont, L., Henry, L.C., Boulanger, Y., Evans, A.C., Bourgouin, P., Poirier, J., Théoret, H., and Lassonde, M. (2013). Sports concussions and aging: a neuroimaging investigation. Cereb. Cortex 23, 1159–1166.

262. Bartnik-Olson, B.L., Harris, N.G., Shijo, K., and Sutton, R.L. (2013). Insights into the metabolic response to traumatic brain injury as revealed by (13)C NMR spectroscopy. Front Neuroenergetics 5, 8.

263. Ross, B., Lin, A., Harris, K., Bhattacharya, P., and Schweinsburg, B. (2003). Clinical experience with 13C MRS in vivo. NMR Biomed 16, 358–369.

264. Thulborn, K.R., Davis, D., Snyder, J., Yonas, H., and Kassam, A. (2005). Sodium MR imaging of acute and subacute stroke for assessment of tissue viability. Neuroimaging Clin. N. Am. 15, 639–653, xi–xii.

265. Madelin, G., and Regatte, R.R. (2013). Biomedical applications of sodium MRI in vivo. J Magn Reson Imaging 38, 511–529.

266. Luts, J., Poullet, J.-B., Garcia-Gomez, J.M., Heerschap, A., Robles, M., Suykens, J.A.K., and Van Huffel, S. (2008). Effect of feature extraction for brain tumor classification based on short echo time 1H MR spectra. Magn Reson Med 60, 288–298.

267. Mountford, C.E., Doran, S., Lean, C.L., and Russell, P. (2004). Proton MRS can determine the pathology of human cancers with a high level of accuracy. Chem. Rev. 104, 3677–3704.

268. Mountford, C., Lean, C., Malycha, P., and Russell, P. (2006). Proton spectroscopy provides accurate pathology on biopsy and in vivo. J Magn Reson Imaging 24, 459–477.

269. Dzendrowskyj, T.E., Dolenko, B., Sorrell, T.C., Somorjai, R.L., Malik, R., Mountford, C.E., and Himmelreich, U. (2005). Diagnosis of cerebral cryptococcoma using a computerized analysis of 1H NMR spectra in an animal model. Diagn. Microbiol. Infect. Dis. 52, 101–105.

270. Himmelreich, U., Accurso, R., Malik, R., Dolenko, B., Somorjai, R.L., Gupta, R.K., Gomes, L., Mountford, C.E., and Sorrell, T.C. (2005). Identification of Staphylococcus aureus brain abscesses: rat and human studies with 1H MR spectroscopy. Radiology 236, 261–270.

271. Baumgartner, R., Somorjai, R., Bowman, C., Sorrell, T.C., Mountford, C.E., and Himmelreich, U. (2004). Unsupervised feature dimension reduction for classification of MR spectra. Magn Reson Imaging 22, 251–256.

272. Himmelreich, U., Somorjai, R.L., Dolenko, B., Lee, O.C., Daniel, H.-M., Murray, R., Mountford, C.E., and Sorrell, T.C. (2003). Rapid identification of Candida species by using nuclear magnetic resonance spectroscopy and a statistical classification strategy. Appl. Environ. Microbiol. 69, 4566–4574.

273. Doran, S.T., Falk, G.L., Somorjai, R.L., Lean, C.L., Himmelreich, U., Philips, J., Russell, P., Dolenko, B., Nikulin, A.E., and Mountford, C.E. (2003). Pathology of Barrett's esophagus by proton magnetic resonance spectroscopy and a statistical classification strategy. Am. J. Surg. 185, 232–238.

274. Soper, R., Himmelreich, U., Painter, D., Somorjai, R.L., Lean, C.L., Dolenko, B., Mountford, C.E., and Russell, P. (2002). Pathology of hepatocellular carcinoma and its

precursors using proton magnetic resonance spectroscopy and a statistical classification strategy. Pathology 34, 417–422.

275. Mountford, C.E., Somorjai, R.L., Malycha, P., Gluch, L., Lean, C., Russell, P., Barraclough, B., Gillett, D., Himmelreich, U., Dolenko, B., Nikulin, A.E., and Smith, I.C. (2001). Diagnosis and prognosis of breast cancer by magnetic resonance spectroscopy of fine-needle aspirates analysed using a statistical classification strategy. Br J Surg 88, 1234–1240.

276. Cho, E.E., Drazic, J., Ganguly, M., Stefanovic, B., and Hynynen, K. (2011). Two-photon fluorescence microscopy study of cerebrovascular dynamics in ultrasound-induced blood-brain barrier opening. J. Cereb. Blood Flow Metab. 31, 1852–1862.

277. Nimmerjahn, A. (2012). Two-photon imaging of microglia in the mouse cortex in vivo. Cold Spring Harb Protoc 2012.

278. Srinivasan, V.J., Atochin, D.N., Radhakrishnan, H., Jiang, J.Y., Ruvinskaya, S., Wu, W., Barry, S., Cable, A.E., Ayata, C., Huang, P.L., and Boas, D.A. (2011). Optical coherence tomography for the quantitative study of cerebrovascular physiology. J. Cereb. Blood Flow Metab. 31, 1339–1345.

279. Srinivasan, V.J., Mandeville, E.T., Can, A., Blasi, F., Climov, M., Daneshmand, A., Lee, J.H., Yu, E., Radhakrishnan, H., Lo, E.H., Sakadžić, S., Eikermann-Haerter, K., and Ayata, C. (2013). Multiparametric, longitudinal optical coherence tomography imaging reveals acute injury and chronic recovery in experimental ischemic stroke. PLoS ONE 8, e71478.

280. Jöbsis, F.F. (1977). Noninvasive, infrared monitoring of cerebral and myocardial oxygen sufficiency and circulatory parameters. Science 198, 1264–1267.

281. Scholkmann, F., Kleiser, S., Metz, A.J., Zimmermann, R., Mata Pavia, J., Wolf, U., and Wolf, M. (2014). A review on continuous wave functional near-infrared spectroscopy and imaging instrumentation and methodology. Neuroimage 85 Pt 1, 6–27.

282. Torricelli, A., Contini, D., Pifferi, A., Caffini, M., Re, R., Zucchelli, L., and Spinelli, L. (2014). Time domain functional NIRS imaging for human brain mapping. Neuroimage 85 Pt 1, 28–50.

283. Durduran, T., and Yodh, A.G. (2014). Diffuse correlation spectroscopy for non-invasive, micro-vascular cerebral blood flow measurement. Neuroimage 85 Pt 1, 51–63.

284. Grant, P.E., Roche-Labarbe, N., Surova, A., Themelis, G., Selb, J., Warren, E.K., Krishnamoorthy, K.S., Boas, D.A., and Franceschini, M.A. (2009). Increased cerebral blood volume and oxygen consumption in neonatal brain injury. J. Cereb. Blood Flow Metab. 29, 1704–1713.

285. Dehaes, M., Aggarwal, A., Lin, P.-Y., Rosa Fortuno, C., Fenoglio, A., Roche-Labarbe, N., Soul, J.S., Franceschini, M.A., and Grant, P.E. (2014). Cerebral oxygen metabolism in neonatal hypoxic ischemic encephalopathy during and after therapeutic hypothermia. J. Cereb. Blood Flow Metab. 34, 87–94.

286. Mesquita, R.C., Durduran, T., Yu, G., Buckley, E.M., Kim, M.N., Zhou, C., Choe, R., Sunar, U., and Yodh, A.G. (2011). Direct measurement of tissue blood flow and metabolism with diffuse optics. Philos Trans A Math Phys Eng Sci 369, 4390–4406.

287. Robertson, C.S., Gopinath, S.P., and Chance, B. (1995). A new application for near-infrared spectroscopy: detection of delayed intracranial hematomas after head injury. J. Neurotrauma 12, 591–600.

288. Gopinath, S.P., Robertson, C.S., Grossman, R.G., and Chance, B. (1993). Near-infrared spectroscopic localization of intracranial hematomas. J. Neurosurg. 79, 43–47.

289. Haitsma, I.K., and Maas, A.I.R. (2007). Monitoring cerebral oxygenation in traumatic brain injury. Prog. Brain Res. 161, 207–216.

290. Gopinath, S.P., Robertson, C.S., Contant, C.F., Narayan, R.K., Grossman, R.G., and Chance, B. (1995). Early detection of delayed traumatic intracranial hematomas using near-infrared spectroscopy. J. Neurosurg. 83, 438–444.

291. Kahraman, S., Kayali, H., Atabey, C., Acar, F., and Gocmen, S. (2006). The accuracy of near-infrared spectroscopy in detection of subdural and epidural hematomas. J Trauma 61, 1480–1483.

292. Kessel, B., Jeroukhimov, I., Ashkenazi, I., Khashan, T., Oren, M., Haspel, J., Medvedev, M., Nesterenko, V., Halevy, A., and Alfici, R. (2007). Early detection of life-threatening intracranial haemorrhage using a portable near-infrared spectroscopy device. Injury 38, 1065–1068.

293. Ghalenoui, H., Saidi, H., Azar, M., Yahyavi, S.T., Borghei Razavi, H., and Khalatbari, M. (2008). Near-infrared laser spectroscopy as a screening tool for detecting hematoma in patients with head trauma. Prehosp Disaster Med 23, 558–561.

294. Leon-Carrion, J., Dominguez-Roldan, J.M., Leon-Dominguez, U., and Murillo-Cabezas, F. (2010). The Infrascanner, a handheld device for screening in situ for the presence of brain haematomas. Brain Inj 24, 1193–1201.

295. Weatherall, A., Skowno, J., Lansdown, A., Lupton, T., and Garner, A. (2012). Feasibility of cerebral near-infrared spectroscopy monitoring in the pre-hospital environment. Acta Anaesthesiol Scand 56, 172–177.

296. Budohoski, K.P., Guilfoyle, M., Helmy, A., Huuskonen, T., Czosnyka, M., Kirollos, R., Menon, D.K., Pickard, J.D., and Kirkpatrick, P.J. (2014). The pathophysiology and

treatment of delayed cerebral ischaemia following subarachnoid haemorrhage. J. Neurol. Neurosurg. Psychiatr. 85, 1343–1353.

297. Yokose, N., Sakatani, K., Murata, Y., Awano, T., Igarashi, T., Nakamura, S., Hoshino, T., and Katayama, Y. (2010). Bedside monitoring of cerebral blood oxygenation and hemodynamics after aneurysmal subarachnoid hemorrhage by quantitative time-resolved near-infrared spectroscopy. World Neurosurg 73, 508–513.

298. Poon, W.S., Wong, G.K.C., and Ng, S.C.P. (2010). The quantitative time-resolved near infrared spectroscopy (TR-NIRs) for bedside cerebrohemodynamic monitoring after aneurysmal subarachnoid hemorrhage: can we predict delayed neurological deficits? World Neurosurg 73, 465–466.

299. Mutoh, T., Ishikawa, T., Suzuki, A., and Yasui, N. (2010). Continuous cardiac output and near-infrared spectroscopy monitoring to assist in management of symptomatic cerebral vasospasm after subarachnoid hemorrhage. Neurocrit Care 13, 331–338.

300. Zweifel, C., Castellani, G., Czosnyka, M., Carrera, E., Brady, K.M., Kirkpatrick, P.J., Pickard, J.D., and Smielewski, P. (2010). Continuous assessment of cerebral autoregulation with near-infrared spectroscopy in adults after subarachnoid hemorrhage. Stroke 41, 1963–1968.

301. Budohoski, K.P., Czosnyka, M., Smielewski, P., Kasprowicz, M., Helmy, A., Bulters, D., Pickard, J.D., and Kirkpatrick, P.J. (2012). Impairment of cerebral autoregulation predicts delayed cerebral ischemia after subarachnoid hemorrhage: a prospective observational study. Stroke 43, 3230–3237.

302. Budohoski, K.P., Czosnyka, M., Smielewski, P., Varsos, G.V., Kasprowicz, M., Brady, K.M., Pickard, J.D., and Kirkpatrick, P.J. (2013). Cerebral autoregulation after subarachnoid hemorrhage: comparison of three methods. J. Cereb. Blood Flow Metab. 33, 449–456.

303. Weerakkody, R.A., Czosnyka, M., Zweifel, C., Castellani, G., Smielewski, P., Brady, K., Pickard, J.D., and Czosnyka, Z. (2012). Near infrared spectroscopy as possible non-invasive monitor of slow vasogenic ICP waves. Acta Neurochir. Suppl. 114, 181–185.

304. Kim, M.N., Edlow, B.L., Durduran, T., Frangos, S., Mesquita, R.C., Levine, J.M., Greenberg, J.H., Yodh, A.G., and Detre, J.A. (2014). Continuous optical monitoring of cerebral hemodynamics during head-of-bed manipulation in brain-injured adults. Neurocrit Care 20, 443–453.

305. Hargroves, D., Tallis, R., Pomeroy, V., and Bhalla, A. (2008). The influence of positioning upon cerebral oxygenation after acute stroke: a pilot study. Age Ageing 37, 581–585.

306. Favilla, C.G., Mesquita, R.C., Mullen, M., Durduran, T., Lu, X., Kim, M.N., Minkoff, D.L., Kasner, S.E., Greenberg, J.H., Yodh, A.G., and Detre, J.A. (2014). Optical bedside monitoring of cerebral blood flow in acute ischemic stroke patients during head-of-bed manipulation. Stroke 45, 1269–1274.

307. Dunn, A.K., Bolay, H., Moskowitz, M.A., and Boas, D.A. (2001). Dynamic imaging of cerebral blood flow using laser speckle. J. Cereb. Blood Flow Metab. 21, 195–201.

308. Yuzawa, I., Sakadžić, S., Srinivasan, V.J., Shin, H.K., Eikermann-Haerter, K., Boas, D.A., and Ayata, C. (2012). Cortical spreading depression impairs oxygen delivery and metabolism in mice. J. Cereb. Blood Flow Metab. 32, 376–386.

309. Sato, S., Kawauchi, S., Okuda, W., Nishidate, I., Nawashiro, H., and Tsumatori, G. (2014). Real-time optical diagnosis of the rat brain exposed to a laser-induced shock wave: observation of spreading depolarization, vasoconstriction and hypoxemia-oligemia. PLoS ONE 9, e82891.

310. Dreier, J.P., Woitzik, J., Fabricius, M., Bhatia, R., Major, S., Drenckhahn, C., Lehmann, T.-N., Sarrafzadeh, A., Willumsen, L., Hartings, J.A., Sakowitz, O.W., Seemann, J.H., Thieme, A., Lauritzen, M., and Strong, A.J. (2006). Delayed ischaemic neurological deficits after subarachnoid haemorrhage are associated with clusters of spreading depolarizations. Brain 129, 3224–3237.

311. Dreier, J.P., Major, S., Manning, A., Woitzik, J., Drenckhahn, C., Steinbrink, J., Tolias, C., Oliveira-Ferreira, A.I., Fabricius, M., Hartings, J.A., Vajkoczy, P., Lauritzen, M., Dirnagl, U., Bohner, G., Strong, A.J., and COSBID study group. (2009). Cortical spreading ischaemia is a novel process involved in ischaemic damage in patients with aneurysmal subarachnoid haemorrhage. Brain 132, 1866–1881.

312. Bosche, B., Graf, R., Ernestus, R.-I., Dohmen, C., Reithmeier, T., Brinker, G., Strong, A.J., Dreier, J.P., Woitzik, J., and Members of the Cooperative Study of Brain Injury Depolarizations (COSBID). (2010). Recurrent spreading depolarizations after subarachnoid hemorrhage decreases oxygen availability in human cerebral cortex. Ann. Neurol. 67, 607–617.

313. Woitzik, J., Dreier, J.P., Hecht, N., Fiss, I., Sandow, N., Major, S., Winkler, M., Dahlem, Y.A., Manville, J., Diepers, M., Muench, E., Kasuya, H., Schmiedek, P., Vajkoczy, P., and COSBID study group. (2012). Delayed cerebral ischemia and spreading depolarization in absence of angiographic vasospasm after subarachnoid hemorrhage. J. Cereb. Blood Flow Metab. 32, 203–212.

314. Len, T.K., and Neary, J.P. (2011). Cerebrovascular pathophysiology following mild traumatic brain injury. Clin Physiol Funct Imaging 31, 85–93.

315. Yuan, X.Q., Prough, D.S., Smith, T.L., and Dewitt, D.S. (1988). The effects of traumatic brain injury on regional cerebral blood flow in rats. J. Neurotrauma 5, 289–301.

316. Golding, E.M., Steenberg, M.L., Contant, C.F., Krishnappa, I., Robertson, C.S., and Bryan, R.M. (1999). Cerebrovascular reactivity to CO_2 and hypotension after mild cortical impact injury. Am. J. Physiol. 277, H1457–1466.

317. McQuire, J.C., Sutcliffe, J.C., and Coats, T.J. (1998). Early changes in middle cerebral artery blood flow velocity after head injury. J. Neurosurg. 89, 526–532.

318. Len, T.K., Neary, J.P., Asmundson, G.J.G., Candow, D.G., Goodman, D.G., Bjornson, B., and Bhambhani, Y.N. (2013). Serial monitoring of CO_2 reactivity following sport concussion using hypocapnia and hypercapnia. Brain Inj 27, 346–353.

319. Zweifel, C., Castellani, G., Czosnyka, M., Helmy, A., Manktelow, A., Carrera, E., Brady, K.M., Hutchinson, P.J.A., Menon, D.K., Pickard, J.D., and Smielewski, P. (2010). Noninvasive monitoring of cerebrovascular reactivity with near infrared spectroscopy in head-injured patients. J. Neurotrauma 27, 1951–1958.

320. Highton, D., Panovska-Griffiths, J., Smith, M., and Elwell, C.E. (2013). Mathematical modelling of near-infrared spectroscopy signals and intracranial pressure in brain-injured patients. Adv. Exp. Med. Biol. 789, 345–351.

321. Boas, D.A., Elwell, C.E., Ferrari, M., and Taga, G. (2014). Twenty years of functional near-infrared spectroscopy: introduction for the special issue. Neuroimage 85 Pt 1, 1–5.

322. Rodriguez Merzagora, A.C., Izzetoglu, M., Onaral, B., and Schultheis, M.T. (2014). Verbal working memory impairments following traumatic brain injury: an fNIRS investigation. Brain Imaging Behav 8, 446–459.

323. Amyot, F., Zimmermann, T., Riley, J., Kainerstorfer, J.M., Chernomordik, V., Mooshagian, E., Najafizadeh, L., Krueger, F., Gandjbakhche, A.H., and Wassermann, E.M. (2012). Normative database of judgment of complexity task with functional near infrared spectroscopy--application for TBI. Neuroimage 60, 879–883.

324. Hashimoto, K., Uruma, G., and Abo, M. (2008). Activation of the prefrontal cortex during the wisconsin card sorting test (Keio Version) as measured by two-channel near-infrared spectroscopy in patients with traumatic brain injury. Eur. Neurol. 59, 24–30.

325. Bhambhani, Y., Maikala, R., Farag, M., and Rowland, G. (2006). Reliability of near-infrared spectroscopy measures of cerebral oxygenation and blood volume during handgrip exercise in nondisabled and traumatic brain-injured subjects. J Rehabil Res Dev 43, 845–856.

326. Hibino, S., Mase, M., Shirataki, T., Nagano, Y., Fukagawa, K., Abe, A., Nishide, Y., Aizawa, A., Iida, A., Ogawa, T., Abe, J., Hatta, T., Yamada, K., and Kabasawa, H. (2013). Oxyhemoglobin changes during cognitive rehabilitation after traumatic brain injury using near infrared spectroscopy. Neurol. Med. Chir. (Tokyo) 53, 299–303.

327. Gagnon, L., Cooper, R.J., Yücel, M.A., Perdue, K.L., Greve, D.N., and Boas, D.A. (2012). Short separation channel location impacts the performance of short channel regression in NIRS. Neuroimage 59, 2518–2528.

328. Selb, J., Joseph, D.K., and Boas, D.A. (2006). Time-gated optical system for depth-resolved functional brain imaging. J Biomed Opt 11, 044008.

329. Pifferi, A., Torricelli, A., Spinelli, L., Contini, D., Cubeddu, R., Martelli, F., Zaccanti, G., Tosi, A., Dalla Mora, A., Zappa, F., and Cova, S. (2008). Time-resolved diffuse reflectance using small source-detector separation and fast single-photon gating. Phys. Rev. Lett. 100, 138101.

330. Selb, J., Boas, D.A., Chan, S.-T., Evans, K.C., Buckley, E.M., and Carp, S.A. (2014). Sensitivity of near-infrared spectroscopy and diffuse correlation spectroscopy to brain hemodynamics: simulations and experimental findings during hypercapnia. Neurophotonics 1.

331. Shokouhi, S., Claassen, D., and Riddle, W. (2014). Imaging Brain Metabolism and Pathology in Alzheimer's Disease with Positron Emission Tomography. J Alzheimers Dis Parkinsonism 4.

332. García-Panach, J., Lull, N., Lull, J.J., Ferri, J., Martínez, C., Sopena, P., Robles, M., Chirivella, J., and Noé, E. (2011). A voxel-based analysis of FDG-PET in traumatic brain injury: regional metabolism and relationship between the thalamus and cortical areas. J. Neurotrauma 28, 1707–1717.

333. Pagani, M., Chiò, A., Valentini, M.C., Öberg, J., Nobili, F., Calvo, A., Moglia, C., Bertuzzo, D., Morbelli, S., De Carli, F., Fania, P., and Cistaro, A. (2014). Functional pattern of brain FDG-PET in amyotrophic lateral sclerosis. Neurology 83, 1067–1074.

334. Toussaint, P.-J., Perlbarg, V., Bellec, P., Desarnaud, S., Lacomblez, L., Doyon, J., Habert, M.-O., Benali, H., and Benali, for the Alzheimer's Disease Neuroimaging Initiative. (2012). Resting state FDG-PET functional connectivity as an early biomarker of Alzheimer's disease using conjoint univariate and independent component analyses. Neuroimage 63, 936–946.

335. Peskind, E.R., Petrie, E.C., Cross, D.J., Pagulayan, K., McCraw, K., Hoff, D., Hart, K., Yu, C.-E., Raskind, M.A., Cook, D.G., and Minoshima, S. (2011). Cerebrocerebellar hypometabolism associated with repetitive blast exposure mild traumatic brain injury in 12 Iraq war Veterans with persistent post-concussive symptoms. Neuroimage 54 Suppl 1, S76–82.

336. Mendez, M.F., Owens, E.M., Reza Berenji, G., Peppers, D.C., Liang, L.-J., and Licht, E.A. (2013). Mild traumatic brain injury from primary blast vs. blunt forces: post-concussion consequences and functional neuroimaging. NeuroRehabilitation 32, 397–407.

337. Jordan, B.D. (2013). The clinical spectrum of sport-related traumatic brain injury. Nat Rev Neurol 9, 222–230.

338. Endres, C.J., Pomper, M.G., James, M., Uzuner, O., Hammoud, D.A., Watkins, C.C., Reynolds, A., Hilton, J., Dannals, R.F., and Kassiou, M. (2009). Initial evaluation of 11C-DPA-713, a novel TSPO PET ligand, in humans. J. Nucl. Med. 50, 1276–1282.

339. Collins, M.W., Grindel, S.H., Lovell, M.R., Dede, D.E., Moser, D.J., Phalin, B.R., Nogle, S., Wasik, M., Cordry, D., Daugherty, K.M., Sears, S.F., Nicolette, G., Indelicato, P., and McKeag, D.B. (1999). Relationship between concussion and neuropsychological performance in college football players. JAMA 282, 964–970.

340. Matser, E.J., Kessels, A.G., Lezak, M.D., Jordan, B.D., and Troost, J. (1999). Neuropsychological impairment in amateur soccer players. JAMA 282, 971–973.

341. Shively, S., Scher, A.I., Perl, D.P., and Diaz-Arrastia, R. (2012). Dementia resulting from traumatic brain injury: what is the pathology? Arch. Neurol. 69, 1245–1251.

342. Hazrati, L.-N., Tartaglia, M.C., Diamandis, P., Davis, K.D., Green, R.E., Wennberg, R., Wong, J.C., Ezerins, L., and Tator, C.H. (2013). Absence of chronic traumatic encephalopathy in retired football players with multiple concussions and neurological symptomatology. Front Hum Neurosci 7, 222.

343. Smith, D.H., Johnson, V.E., and Stewart, W. (2013). Chronic neuropathologies of single and repetitive TBI: substrates of dementia? Nat Rev Neurol 9, 211–221.

344. Hellström-Lindahl, E., Moore, H., and Nordberg, A. (2000). Increased levels of tau protein in SH-SY5Y cells after treatment with cholinesterase inhibitors and nicotinic agonists. J. Neurochem. 74, 777–784.

345. McKee, A.C., Stern, R.A., Nowinski, C.J., Stein, T.D., Alvarez, V.E., Daneshvar, D.H., Lee, H.-S., Wojtowicz, S.M., Hall, G., Baugh, C.M., Riley, D.O., Kubilus, C.A., Cormier, K.A., Jacobs, M.A., Martin, B.R., Abraham, C.R., Ikezu, T., Reichard, R.R., Wolozin, B.L., Budson, A.E., Goldstein, L.E., Kowall, N.W., and Cantu, R.C. (2013). The spectrum of disease in chronic traumatic encephalopathy. Brain 136, 43–64.

346. Rubio, A., Pérez, M., and Avila, J. (2006). Acetylcholine receptors and tau phosphorylation. Curr. Mol. Med. 6, 423–428.

347. Shin, J., Kepe, V., Barrio, J.R., and Small, G.W. (2011). The merits of FDDNP-PET imaging in Alzheimer's disease. J. Alzheimers Dis. 26 Suppl 3, 135–145.

348. Mitsis, E.M., Riggio, S., Kostakoglu, L., Dickstein, D.L., Machac, J., Delman, B., Goldstein, M., Jennings, D., D'Antonio, E., Martin, J., Naidich, T.P., Aloysi, A., Fernandez, C., Seibyl, J., DeKosky, S.T., Elder, G.A., Marek, K., Gordon, W., Hof, P.R., Sano, M., and Gandy, S. (2014). Tauopathy PET and amyloid PET in the diagnosis of

chronic traumatic encephalopathies: studies of a retired NFL player and of a man with FTD and a severe head injury. Transl Psychiatry 4, e441.

349. Chien, D.T., Szardenings, A.K., Bahri, S., Walsh, J.C., Mu, F., Xia, C., Shankle, W.R., Lerner, A.J., Su, M.-Y., Elizarov, A., and Kolb, H.C. (2014). Early clinical PET imaging results with the novel PHF-tau radioligand [F18]-T808. J. Alzheimers Dis. 38, 171–184.

350. Galluzzi, L., Kepp, O., Krautwald, S., Kroemer, G., and Linkermann, A. (2014). Molecular mechanisms of regulated necrosis. Semin. Cell Dev. Biol. 35, 24–32.

351. Cheng, A.-L., Batool, S., McCreary, C.R., Lauzon, M.L., Frayne, R., Goyal, M., and Smith, E.E. (2013). Susceptibility-weighted imaging is more reliable than T2*-weighted gradient-recalled echo MRI for detecting microbleeds. Stroke 44, 2782–2786.

352. Oltmanns, D., Zitzmann-Kolbe, S., Mueller, A., Bauder-Wuest, U., Schaefer, M., Eder, M., Haberkorn, U., and Eisenhut, M. (2011). Zn(II)-bis(cyclen) complexes and the imaging of apoptosis/necrosis. Bioconjug. Chem. 22, 2611–2624.

353. De Saint-Hubert, M., Bauwens, M., and Mottaghy, F.M. (2014). Molecular imaging of apoptosis for early prediction of therapy efficiency. Curr. Pharm. Des. 20, 2319–2328.

354. Burvenich, I.J.G., Lee, F.T., Cartwright, G.A., O'Keefe, G.J., Makris, D., Cao, D., Gong, S., Chueh, A.C., Mariadason, J.M., Brechbiel, M.W., Beckman, R.A., Fujiwara, K., von Roemeling, R., and Scott, A.M. (2013). Molecular imaging of death receptor 5 occupancy and saturation kinetics in vivo by humanized monoclonal antibody CS-1008. Clin. Cancer Res. 19, 5984–5993.

355. Rossin, R., Kohno, T., Hagooly, A., Sharp, T., Gliniak, B., Arroll, T., Chen, Q., Hewig, A., Kaplan-Lefko, P., Friberg, G., Radinsky, R., Evelhoch, J.L., Welch, M.J., and Hwang, D.-R. (2011). Characterization of 64Cu-DOTA-conatumumab: a PET tracer for in vivo imaging of death receptor 5. J. Nucl. Med. 52, 942–949.

356. Su, H., Chen, G., Gangadharmath, U., Gomez, L.F., Liang, Q., Mu, F., Mocharla, V.P., Szardenings, A.K., Walsh, J.C., Xia, C.-F., Yu, C., and Kolb, H.C. (2013). Evaluation of [(18)F]-CP18 as a PET imaging tracer for apoptosis. Mol Imaging Biol 15, 739–747.

357. Reshef, A., Shirvan, A., Shohami, E., Grimberg, H., Levin, G., Cohen, A., Trembovler, V., and Ziv, I. (2008). Targeting cell death in vivo in experimental traumatic brain injury by a novel molecular probe. J. Neurotrauma 25, 569–580.

358. Papadopoulos, V., and Lecanu, L. (2009). Translocator protein (18 kDa) TSPO: an emerging therapeutic target in neurotrauma. Exp. Neurol. 219, 53–57.

359. Mechtler, L.L., Shastri, K.K., and Crutchfield, K.E. (2014). Advanced neuroimaging of mild traumatic brain injury. Neurol Clin 32, 31–58.

360. Kou, Z., and VandeVord, P.J. (2014). Traumatic white matter injury and glial activation: from basic science to clinics. Glia 62, 1831–1855.

361. Tu, L.N., Morohaku, K., Manna, P.R., Pelton, S.H., Butler, W.R., Stocco, D.M., and Selvaraj, V. (2014). Peripheral benzodiazepine receptor/translocator protein global knock-out mice are viable with no effects on steroid hormone biosynthesis. J. Biol. Chem. 289, 27444–27454.

362. Damont, A., Roeda, D., and Dollé, F. (2013). The potential of carbon-11 and fluorine-18 chemistry: illustration through the development of positron emission tomography radioligands targeting the translocator protein 18 kDa. J Labelled Comp Radiopharm 56, 96–104.

363. Coughlin, J.M., Wang, Y., Munro, C.A., Ma, S., Yue, C., Chen, S., Airan, R., Kim, P.K., Adams, A.V., Garcia, C., Higgs, C., Sair, H.I., Sawa, A., Smith, G., Lyketsos, C.G., Caffo, B., Kassiou, M., Guilarte, T.R., and Pomper, M.G. (2014). Neuroinflammation and brain atrophy in former NFL players: An in vivo multimodal imaging pilot study. Neurobiol. Dis. 74C, 58–65.

364. Kox, M., Pompe, J.C., Pickkers, P., Hoedemaekers, C.W., van Vugt, A.B., and van der Hoeven, J.G. (2008). Increased vagal tone accounts for the observed immune paralysis in patients with traumatic brain injury. Neurology 70, 480–485.

365. Weber, J.T. (2004). Calcium homeostasis following traumatic neuronal injury. Curr Neurovasc Res 1, 151–171.

366. Vieth, J.B., Kober, H., and Grummich, P. (1996). Sources of spontaneous slow waves associated with brain lesions, localized by using the MEG. Brain Topogr 8, 215–221.

367. Lewine, J.D., Davis, J.T., Sloan, J.H., Kodituwakku, P.W., and Orrison, W.W. (1999). Neuromagnetic assessment of pathophysiologic brain activity induced by minor head trauma. AJNR Am J Neuroradiol 20, 857–866.

368. Lewine, J.D., Davis, J.T., Bigler, E.D., Thoma, R., Hill, D., Funke, M., Sloan, J.H., Hall, S., and Orrison, W.W. (2007). Objective documentation of traumatic brain injury subsequent to mild head trauma: multimodal brain imaging with MEG, SPECT, and MRI. J Head Trauma Rehabil 22, 141–155.

369. Huang, M.-X., Theilmann, R.J., Robb, A., Angeles, A., Nichols, S., Drake, A., D'Andrea, J., Levy, M., Holland, M., Song, T., Ge, S., Hwang, E., Yoo, K., Cui, L., Baker, D.G., Trauner, D., Coimbra, R., and Lee, R.R. (2009). Integrated imaging approach with MEG and DTI to detect mild traumatic brain injury in military and civilian patients. J. Neurotrauma 26, 1213–1226.

370. Gloor, P., Ball, G., and Schaul, N. (1977). Brain lesions that produce delta waves in the EEG. Neurology 27, 326–333.

371. Schaul, N., Gloor, P., Ball, G., and Gotman, J. (1978). The electromicrophysiology of delta waves induced by systemic atropine. Brain Res. 143, 475–486.

372. Ball, G.J., Gloor, P., and Schaul, N. (1977). The cortical electromicrophysiology of pathological delta waves in the electroencephalogram of cats. Electroencephalogr Clin Neurophysiol 43, 346–361.

373. Huang, M.-X., Nichols, S., Robb, A., Angeles, A., Drake, A., Holland, M., Asmussen, S., D'Andrea, J., Chun, W., Levy, M., Cui, L., Song, T., Baker, D.G., Hammer, P., McLay, R., Theilmann, R.J., Coimbra, R., Diwakar, M., Boyd, C., Neff, J., Liu, T.T., Webb-Murphy, J., Farinpour, R., Cheung, C., Harrington, D.L., Heister, D., and Lee, R.R. (2012). An automatic MEG low-frequency source imaging approach for detecting injuries in mild and moderate TBI patients with blast and non-blast causes. Neuroimage 61, 1067–1082.

374. Fernández, A., Maestú, F., Amo, C., Gil, P., Fehr, T., Wienbruch, C., Rockstroh, B., Elbert, T., and Ortiz, T. (2002). Focal temporoparietal slow activity in Alzheimer's disease revealed by magnetoencephalography. Biol. Psychiatry 52, 764–770.

375. Wienbruch, C., Moratti, S., Elbert, T., Vogel, U., Fehr, T., Kissler, J., Schiller, A., and Rockstroh, B. (2003). Source distribution of neuromagnetic slow wave activity in schizophrenic and depressive patients. Clin Neurophysiol 114, 2052–2060.

376. Rockstroh, B.S., Wienbruch, C., Ray, W.J., and Elbert, T. (2007). Abnormal oscillatory brain dynamics in schizophrenia: a sign of deviant communication in neural network? BMC Psychiatry 7, 44.

377. Cañive, J.M., Lewine, J.D., Edgar, J.C., Davis, J.T., Torres, F., Roberts, B., Graeber, D., Orrison, W.W., and Tuason, V.B. (1996). Magnetoencephalographic assessment of spontaneous brain activity in schizophrenia. Psychopharmacol Bull 32, 741–750.

378. Basser, P.J. (1995). Inferring microstructural features and the physiological state of tissues from diffusion-weighted images. NMR Biomed 8, 333–344.

379. Xu, J., Rasmussen, I.-A., Lagopoulos, J., and Håberg, A. (2007). Diffuse axonal injury in severe traumatic brain injury visualized using high-resolution diffusion tensor imaging. J. Neurotrauma 24, 753–765.

380. Davenport, N.D., Lim, K.O., Armstrong, M.T., and Sponheim, S.R. (2012). Diffuse and spatially variable white matter disruptions are associated with blast-related mild traumatic brain injury. Neuroimage 59, 2017–2024.

381. Huang, M.-X., Nichols, S., Baker, D.G., Robb, A., Angeles, A., Yurgil, K.A., Drake, A., Levy, M., Song, T., McLay, R., Theilmann, R.J., Diwakar, M., Risbrough, V.B., Ji, Z., Huang, C.W., Chang, D.G., Harrington, D.L., Muzzatti, L., Canive, J.M., Christopher Edgar, J., Chen, Y.-H., and Lee, R.R. (2014). Single-subject-based whole-brain MEG

slow-wave imaging approach for detecting abnormality in patients with mild traumatic brain injury. Neuroimage Clin 5, 109–119.

382. Huang, M.-X., Huang, C.W., Robb, A., Angeles, A., Nichols, S.L., Baker, D.G., Song, T., Harrington, D.L., Theilmann, R.J., Srinivasan, R., Heister, D., Diwakar, M., Canive, J.M., Edgar, J.C., Chen, Y.-H., Ji, Z., Shen, M., El-Gabalawy, F., Levy, M., McLay, R., Webb-Murphy, J., Liu, T.T., Drake, A., and Lee, R.R. (2014). MEG source imaging method using fast L1 minimum-norm and its applications to signals with brain noise and human resting-state source amplitude images. Neuroimage 84, 585–604.

383. Tarapore, P.E., Findlay, A.M., LaHue, S.C., Lee, H., Honma, S.M., Mizuiri, D., Luks, T.L., Manley, G.T., Nagarajan, S.S., and Mukherjee, P. (2013). Resting state magnetoencephalography functional connectivity in traumatic brain injury. J Neurosurg 118, 1306–1316.

384. Luo, Q., Xu, D., Roskos, T., Stout, J., Kull, L., Cheng, X., Whitson, D., Boomgarden, E., Gfeller, J., and Bucholz, R.D. (2013). Complexity analysis of resting state magnetoencephalography activity in traumatic brain injury patients. J. Neurotrauma 30, 1702–1709.

385. ([date unknown]). ADNI | MRI Pre-processing.

386. Sled, J.G., Zijdenbos, A.P., and Evans, A.C. (1998). A nonparametric method for automatic correction of intensity nonuniformity in MRI data. IEEE Trans Med Imaging 17, 87–97.

387. Smith, S.M., and Brady, J.M. (1997). SUSAN—A New Approach to Low Level Image Processing. International Journal of Computer Vision 23, 45–78.

388. Nyúl, L.G., Udupa, J.K., and Zhang, X. (2000). New variants of a method of MRI scale standardization. IEEE Trans Med Imaging 19, 143–150.

389. Talairach, J., and Tournoux, P. (1988). Co-planar stereotaxic atlas of the human brain. 3-Dimensional proportional system: an approach to cerebral imaging. Thieme.

390. Collins, D.L., Neelin, P., Peters, T.M., and Evans, A.C. (1994). Automatic 3D intersubject registration of MR volumetric data in standardized Talairach space. J Comput Assist Tomogr 18, 192–205.

391. Avants, B.B., Yushkevich, P., Pluta, J., Minkoff, D., Korczykowski, M., Detre, J., and Gee, J.C. (2010). The optimal template effect in hippocampus studies of diseased populations. Neuroimage 49, 2457–2466.

392. Jezzard, P., Barnett, A.S., and Pierpaoli, C. (1998). Characterization of and correction for eddy current artifacts in echo planar diffusion imaging. Magn Reson Med 39, 801–812.

393. Murphy, K., Birn, R.M., and Bandettini, P.A. (2013). Resting-state fMRI confounds and cleanup. Neuroimage 80, 349–359.

394. Oakes, T.R., Johnstone, T., Ores Walsh, K.S., Greischar, L.L., Alexander, A.L., Fox, A.S., and Davidson, R.J. (2005). Comparison of fMRI motion correction software tools. Neuroimage 28, 529–543.

395. Behzadi, Y., Restom, K., Liau, J., and Liu, T.T. (2007). A component based noise correction method (CompCor) for BOLD and perfusion based fMRI. Neuroimage 37, 90–101.

396. Avants, B.B., Tustison, N.J., Stauffer, M., Song, G., Wu, B., and Gee, J.C. (2014). The Insight ToolKit image registration framework. Front Neuroinform 8, 44.

397. Inglese, M., Grossman, R.I., Diller, L., Babb, J.S., Gonen, O., Silver, J.M.A., and Rusinek, H. (2006). Clinical significance of dilated Virchow-Robin spaces in mild traumatic brain injury. Brain Inj 20, 15–21.

398. Rubinov, M., and Sporns, O. (2010). Complex network measures of brain connectivity: uses and interpretations. Neuroimage 52, 1059–1069.

399. ([date unknown]). The R Project for Statistical Computing. [cited 2015 Jan 30] Available from: http://www.r-project.org/.

400. ([date unknown]). FSL - FslWiki. [cited 2014 Aug 13] Available from: http://fsl.fmrib.ox.ac.uk/fsl/fslwiki/.

401. Jenkinson, M., Beckmann, C.F., Behrens, T.E.J., Woolrich, M.W., and Smith, S.M. (2012). FSL. Neuroimage 62, 782–790.

402. ([date unknown]). Human Connectome Project | Mapping the human brain connectivity.

403. ([date unknown]). SPM - Statistical Parametric Mapping. [cited 2014 Aug 13] Available from: http://www.fil.ion.ucl.ac.uk/spm/.

404. Ashburner, J. (2012). SPM: A history. Neuroimage 62, 791–800.

405. ([date unknown]). FreeSurfer. [cited 2014 Aug 13] Available from: http://surfer.nmr.mgh.harvard.edu/.

406. Fischl, B. (2012). FreeSurfer. Neuroimage 62, 774–781.

407. Lindemer, E.R., Salat, D.H., Leritz, E.C., McGlinchey, R.E., and Milberg, W.P. (2013). Reduced cortical thickness with increased lifetime burden of PTSD in OEF/OIF Veterans and the impact of comorbid TBI. Neuroimage Clin 2, 601–611.

408. Tate, D.F., York, G.E., Reid, M.W., Cooper, D.B., Jones, L., Robin, D.A., Kennedy, J.E., and Lewis, J. (2014). Preliminary findings of cortical thickness abnormalities in blast injured service members and their relationship to clinical findings. Brain Imaging Behav 8, 102–109.

409. ([date unknown]). Welcome to the AFNI/NIfTI Server — AFNI and NIfTI Server for NIMH/NIH/PHS/DHHS/USA/Earth. [cited 2014 Aug 13] Available from: http://afni.nimh.nih.gov/.

410. Cox, R.W. (2012). AFNI: what a long strange trip it's been. Neuroimage 62, 743–747.

411. ([date unknown]). ANTs by stnava. [cited 2014 Aug 13] Available from: http://stnava.github.io/ANTs/.

412. ([date unknown]). ITK - Segmentation & Registration Toolkit. [cited 2014 Aug 13] Available from: http://www.itk.org/.

413. Tustison, N.J., Avants, B.B., Cook, P.A., Gee, J.C., and Stone, J.R. (2013). Statistical bias in optimized VBM. pp. 86720U–86720U–4.

414. ([date unknown]). Camino | UCL Camino Diffusion MRI Toolkit. [cited 2014 Aug 13] Available from: http://cmic.cs.ucl.ac.uk/camino/.

415. ([date unknown]). DTI-TK Home Page. [cited 2014 Aug 13] Available from: http://dti-tk.sourceforge.net/pmwiki/pmwiki.php.

416. ([date unknown]). DTI software/data/atlas brain human/animal. [cited 2014 Aug 13] Available from: http://cmrm.med.jhmi.edu/.

417. ([date unknown]). Main Page - MIPAV. [cited 2014 Aug 13] Available from: http://mipav.cit.nih.gov/pubwiki/index.php/Main_Page.

418. ([date unknown]). 3D Slicer. [cited 2014 Aug 13] Available from: http://www.slicer.org/.

419. ([date unknown]). Neuroimaging in Python - Pipelines and Interfaces — nipy pipeline and interfaces package. [cited 2014 Aug 13] Available from: http://nipy.sourceforge.net/nipype/.

420. ([date unknown]). FITBIR: Federal Interagency Traumatic Brain Injury Research Informatics System. [cited 2014 Aug 13] Available from: https://fitbir.nih.gov/.

421. Bullmore, E., and Sporns, O. (2009). Complex brain networks: graph theoretical analysis of structural and functional systems. Nat. Rev. Neurosci. 10, 186–198.

422. Kucewicz, J.C., Dunmire, B., Giardino, N.D., Leotta, D.F., Paun, M., Dager, S.R., and Beach, K.W. (2008). Tissue pulsatility imaging of cerebral vasoreactivity during hyperventilation. Ultrasound Med Biol 34, 1200–1208.

423. Kucewicz, J.C., Dunmire, B., Leotta, D.F., Panagiotides, H., Paun, M., and Beach, K.W. (2007). Functional tissue pulsatility imaging of the brain during visual stimulation. Ultrasound Med Biol 33, 681–690.

424. Mace, E., Montaldo, G., Osmanski, B.-F., Cohen, I., Fink, M., and Tanter, M. (2013). Functional ultrasound imaging of the brain: theory and basic principles. IEEE Trans Ultrason Ferroelectr Freq Control 60, 492–506.

425. Demené, C., Pernot, M., Biran, V., Alison, M., Fink, M., Baud, O., and Tanter, M. (2014). Ultrafast Doppler reveals the mapping of cerebral vascular resistivity in neonates. J. Cereb. Blood Flow Metab. 34, 1009–1017.

426. Tanter, M., Bercoff, J., Athanasiou, A., Deffieux, T., Gennisson, J.-L., Montaldo, G., Muller, M., Tardivon, A., and Fink, M. (2008). Quantitative assessment of breast lesion viscoelasticity: initial clinical results using supersonic shear imaging. Ultrasound Med Biol 34, 1373–1386.

427. Nahas, A., Tanter, M., Nguyen, T.-M., Chassot, J.-M., Fink, M., and Claude Boccara, A. (2013). From supersonic shear wave imaging to full-field optical coherence shear wave elastography. J Biomed Opt 18, 121514.

428. Xu, Z.S., Yao, A., Chu, S.S., Paun, M.K., McClintic, A.M., Murphy, S.P., and Mourad, P.D. (2014). Detection of mild traumatic brain injury in rodent models using shear wave elastography: preliminary studies. J Ultrasound Med 33, 1763–1771.

429. Xu, Z.S., Lee, R.J., Chu, S.S., Yao, A., Paun, M.K., Murphy, S.P., and Mourad, P.D. (2013). Evidence of changes in brain tissue stiffness after ischemic stroke derived from ultrasound-based elastography. J Ultrasound Med 32, 485–494.

430. White, P.J., Whalen, S., Tang, S.C., Clement, G.T., Jolesz, F., and Golby, A.J. (2009). An intraoperative brain shift monitor using shear mode transcranial ultrasound: preliminary results. J Ultrasound Med 28, 191–203.

431. Dutton, R.P., Prior, K., Cohen, R., Wade, C., Sewell, J., Fouche, Y., Stein, D., Aarabi, B., and Scalea, T.M. (2011). Diagnosing mild traumatic brain injury: where are we now? J Trauma 70, 554–559.

432. Armonda, R.A., Bell, R.S., Vo, A.H., Ling, G., DeGraba, T.J., Crandall, B., Ecklund, J., and Campbell, W.W. (2006). Wartime traumatic cerebral vasospasm: recent review of combat casualties. Neurosurgery 59, 1215–1225; discussion 1225.

433. Kim, S., Hu, X., McArthur, D., Hamilton, R., Bergsneider, M., Glenn, T., Martin, N., and Vespa, P. (2011). Inter-subject correlation exists between morphological metrics of cerebral blood flow velocity and intracranial pressure pulses. Neurocrit Care 14, 229–237.

434. Kim, S., Hamilton, R., Pineles, S., Bergsneider, M., and Hu, X. (2013). Noninvasive intracranial hypertension detection utilizing semisupervised learning. IEEE Trans Biomed Eng 60, 1126–1133.

435. Hawthorne, C., and Piper, I. (2014). Monitoring of intracranial pressure in patients with traumatic brain injury. Front Neurol 5, 121.

436. Marzban, C., Illian, P.R., Morison, D., Moore, A., Kliot, M., Czosnyka, M., and Mourad, P.D. (2013). A method for estimating zero-flow pressure and intracranial pressure. J Neurosurg Anesthesiol 25, 25–32.

437. Ragauskas, A., Daubaris, G., Dziugys, A., Azelis, V., and Gedrimas, V. (2005). Innovative non-invasive method for absolute intracranial pressure measurement without calibration. Acta Neurochir. Suppl. 95, 357–361.

438. Kimberly, H.H., Shah, S., Marill, K., and Noble, V. (2008). Correlation of optic nerve sheath diameter with direct measurement of intracranial pressure. Acad Emerg Med 15, 201–204.

439. Soldatos, T., Karakitsos, D., Chatzimichail, K., Papathanasiou, M., Gouliamos, A., and Karabinis, A. (2008). Optic nerve sonography in the diagnostic evaluation of adult brain injury. Crit Care 12, R67.

440. Wolpert, D.H., and Macready, W.G. (1997). No Free Lunch Theorems for Optimization. Trans. Evol. Comp 1, 67–82.

441. (2010). Reproducible Research. Computing in Science & Engineering 12, 8–13.

442. Gray, K.R., Aljabar, P., Heckemann, R.A., Hammers, A., Rueckert, D., and Alzheimer's Disease Neuroimaging Initiative. (2013). Random forest-based similarity measures for multi-modal classification of Alzheimer's disease. Neuroimage 65, 167–175.

443. Kuperberg, G.R., Broome, M.R., McGuire, P.K., David, A.S., Eddy, M., Ozawa, F., Goff, D., West, W.C., Williams, S.C.R., van der Kouwe, A.J.W., Salat, D.H., Dale, A.M., and Fischl, B. (2003). Regionally localized thinning of the cerebral cortex in schizophrenia. Arch. Gen. Psychiatry 60, 878–888.

444. Rosas, H.D., Liu, A.K., Hersch, S., Glessner, M., Ferrante, R.J., Salat, D.H., van der Kouwe, A., Jenkins, B.G., Dale, A.M., and Fischl, B. (2002). Regional and progressive thinning of the cortical ribbon in Huntington's disease. Neurology 58, 695–701.

445. Salat, D.H., Lee, S.Y., van der Kouwe, A.J., Greve, D.N., Fischl, B., and Rosas, H.D. (2009). Age-associated alterations in cortical gray and white matter signal intensity and gray to white matter contrast. Neuroimage 48, 21–28.

446. Sowell, E.R., Thompson, P.M., Leonard, C.M., Welcome, S.E., Kan, E., and Toga, A.W. (2004). Longitudinal mapping of cortical thickness and brain growth in normal children. J. Neurosci. 24, 8223–8231.

447. Raz, N., Rodrigue, K.M., and Haacke, E.M. (2007). Brain Aging and Its Modifiers. Annals of the New York Academy of Sciences 1097, 84–93.

448. Walters, N.B., Egan, G.F., Kril, J.J., Kean, M., Waley, P., Jenkinson, M., and Watson, J.D.G. (2003). In vivo identification of human cortical areas using high-resolution MRI: an approach to cerebral structure-function correlation. Proc. Natl. Acad. Sci. U.S.A. 100, 2981–2986.

449. Barbier, E.L., Marrett, S., Danek, A., Vortmeyer, A., van Gelderen, P., Duyn, J., Bandettini, P., Grafman, J., and Koretsky, A.P. (2002). Imaging cortical anatomy by high-resolution MR at 3.0T: detection of the stripe of Gennari in visual area 17. Magn Reson Med 48, 735–738.

450. Waehnert, M.D., Dinse, J., Weiss, M., Streicher, M.N., Waehnert, P., Geyer, S., Turner, R., and Bazin, P.-L. (2014). Anatomically motivated modeling of cortical laminae. Neuroimage 93 Pt 2, 210–220.

451. Hinds, O., Polimeni, J.R., Rajendran, N., Balasubramanian, M., Wald, L.L., Augustinack, J.C., Wiggins, G., Rosas, H.D., Fischl, B., and Schwartz, E.L. (2008). The intrinsic shape of human and macaque primary visual cortex. Cereb. Cortex 18, 2586–2595.

452. McNab, J.A., Jbabdi, S., Deoni, S.C.L., Douaud, G., Behrens, T.E.J., and Miller, K.L. (2009). High resolution diffusion-weighted imaging in fixed human brain using diffusion-weighted steady state free precession. Neuroimage 46, 775–785.

453. Leuze, C.W.U., Anwander, A., Bazin, P.-L., Dhital, B., Stüber, C., Reimann, K., Geyer, S., and Turner, R. (2014). Layer-specific intracortical connectivity revealed with diffusion MRI. Cereb. Cortex 24, 328–339.

454. Augustinack, J.C., van der Kouwe, A.J.W., Blackwell, M.L., Salat, D.H., Wiggins, C.J., Frosch, M.P., Wiggins, G.C., Potthast, A., Wald, L.L., and Fischl, B.R. (2005). Detection of entorhinal layer II using 7Tesla [corrected] magnetic resonance imaging. Ann. Neurol. 57, 489–494.

455. Geyer, S., Weiss, M., Reimann, K., Lohmann, G., and Turner, R. (2011). Microstructural Parcellation of the Human Cerebral Cortex - From Brodmann's Post-Mortem Map to in vivo Mapping with High-Field Magnetic Resonance Imaging. Front Hum Neurosci 5, 19.

456. Mareyam, A., Polimeni, J.R., Alagappan, V., Fischl, B., and Wald, L. (2009). A 30 channel receive-only 7T array for ex vivo brain hemisphere imaging. Proceedings of International Society for Magnetic Resonance in Medicine 17, 106.

457. Duyn, J.H., van Gelderen, P., Li, T.-Q., de Zwart, J.A., Koretsky, A.P., and Fukunaga, M. (2007). High-field MRI of brain cortical substructure based on signal phase. Proc. Natl. Acad. Sci. U.S.A. 104, 11796–11801.

458. Trampel, R., Ott, D.V.M., and Turner, R. (2011). Do the congenitally blind have a stria of Gennari? First intracortical insights in vivo. Cereb. Cortex 21, 2075–2081.

459. Heidemann, R.M., Ivanov, D., Trampel, R., Fasano, F., Meyer, H., Pfeuffer, J., and Turner, R. (2012). Isotropic submillimeter fMRI in the human brain at 7 T: combining reduced field-of-view imaging and partially parallel acquisitions. Magn Reson Med 68, 1506–1516.

460. Maclaren, J., Armstrong, B.S.R., Barrows, R.T., Danishad, K.A., Ernst, T., Foster, C.L., Gumus, K., Herbst, M., Kadashevich, I.Y., Kusik, T.P., Li, Q., Lovell-Smith, C., Prieto, T., Schulze, P., Speck, O., Stucht, D., and Zaitsev, M. (2012). Measurement and correction of microscopic head motion during magnetic resonance imaging of the brain. PLoS ONE 7, e48088.

461. Tisdall, M., Polimeni, J.R., and van der Kouwe, A. (2013). Motion-corrected 350 μm isotropic MPRAGE at 3 T using volumetric navigators (vNavs). Proceedings of International Society for Magnetic Resonance in Medicine 21, 0268.

462. Zaitsev, M., Dold, C., Sakas, G., Hennig, J., and Speck, O. (2006). Magnetic resonance imaging of freely moving objects: prospective real-time motion correction using an external optical motion tracking system. Neuroimage 31, 1038–1050.

463. Enzmann, D.R., and Pelc, N.J. (1992). Brain motion: measurement with phase-contrast MR imaging. Radiology 185, 653–660.

464. Poncelet, B.P., Wedeen, V.J., Weisskoff, R.M., and Cohen, M.S. (1992). Brain parenchyma motion: measurement with cine echo-planar MR imaging. Radiology 185, 645–651.

465. Fukunaga, M., Li, T.-Q., van Gelderen, P., de Zwart, J.A., Shmueli, K., Yao, B., Lee, J., Maric, D., Aronova, M.A., Zhang, G., Leapman, R.D., Schenck, J.F., Merkle, H., and Duyn, J.H. (2010). Layer-specific variation of iron content in cerebral cortex as a source of MRI contrast. Proc. Natl. Acad. Sci. U.S.A. 107, 3834–3839.

466. Zhong, K., Leupold, J., von Elverfeldt, D., and Speck, O. (2008). The molecular basis for gray and white matter contrast in phase imaging. Neuroimage 40, 1561–1566.

467. Lee, J., Hirano, Y., Fukunaga, M., Silva, A.C., and Duyn, J.H. (2010). On the contribution of deoxy-hemoglobin to MRI gray-white matter phase contrast at high field. Neuroimage 49, 193–198.

468. Weber, B., Keller, A.L., Reichold, J., and Logothetis, N.K. (2008). The microvascular system of the striate and extrastriate visual cortex of the macaque. Cereb. Cortex 18, 2318–2330.

469. Magnain, C., Augustinack, J.C., Reuter, M., Wachinger, C., Frosch, M.P., Ragan, T., Akkin, T., Wedeen, V.J., Boas, D.A., and Fischl, B. (2014). Blockface histology with optical coherence tomography: a comparison with Nissl staining. Neuroimage 84, 524–533.

470. Augustinack, J.C., Magnain, C., Reuter, M., van der Kouwe, A.J.W., Boas, D., and Fischl, B. (2014). MRI parcellation of ex vivo medial temporal lobe. Neuroimage 93 Pt 2, 252–259.

471. Wang, H., Zhu, J., Reuter, M., Vinke, L.N., Yendiki, A., Boas, D.A., Fischl, B., and Akkin, T. (2014). Cross-validation of serial optical coherence scanning and diffusion tensor imaging: A study on neural fiber maps in human medulla oblongata. Neuroimage 100C, 395–404.

472. Chaigneau, E., Oheim, M., Audinat, E., and Charpak, S. (2003). Two-photon imaging of capillary blood flow in olfactory bulb glomeruli. Proc. Natl. Acad. Sci. U.S.A. 100, 13081–13086.

473. Murphy, D.D., and Wagner, R.C. (1994). Differential contractile response of cultured microvascular pericytes to vasoactive agents. Microcirculation 1, 121–128.

474. Peppiatt, C.M., Howarth, C., Mobbs, P., and Attwell, D. (2006). Bidirectional control of CNS capillary diameter by pericytes. Nature 443, 700–704.

475. Hamilton, N.B., Attwell, D., and Hall, C.N. (2010). Pericyte-mediated regulation of capillary diameter: a component of neurovascular coupling in health and disease. Front Neuroenergetics 2.

476. Silva, A.C., and Koretsky, A.P. (2002). Laminar specificity of functional MRI onset times during somatosensory stimulation in rat. Proc. Natl. Acad. Sci. U.S.A. 99, 15182–15187.

477. Chang, W.-T., Setsompop, K., Ahveninen, J., Belliveau, J.W., Witzel, T., and Lin, F.-H. (2014). Improving the spatial resolution of magnetic resonance inverse imaging via the blipped-CAIPI acquisition scheme. Neuroimage 91, 401–411.

478. Lin, F.-H., Witzel, T., Raij, T., Ahveninen, J., Tsai, K.W.-K., Chu, Y.-H., Chang, W.-T., Nummenmaa, A., Polimeni, J.R., Kuo, W.-J., Hsieh, J.-C., Rosen, B.R., and Belliveau, J.W. (2013). fMRI hemodynamics accurately reflects neuronal timing in the human brain measured by MEG. Neuroimage 78, 372–384.

479. Yacoub, E., Harel, N., and Ugurbil, K. (2008). High-field fMRI unveils orientation columns in humans. Proc. Natl. Acad. Sci. U.S.A. 105, 10607–10612.

480. Polimeni, J.R., Fischl, B., Greve, D.N., and Wald, L.L. (2010). Laminar analysis of 7T BOLD using an imposed spatial activation pattern in human V1. Neuroimage 52, 1334–1346.

481. Larkman, D., and Nunes, R. (2007). Parallel magnetic resonance imaging. Physics in Medicine and Biology 52, R15–R55.

482. Feinberg, D.A., Moeller, S., Smith, S.M., Auerbach, E., Ramanna, S., Gunther, M., Glasser, M.F., Miller, K.L., Ugurbil, K., and Yacoub, E. (2010). Multiplexed echo planar imaging for sub-second whole brain FMRI and fast diffusion imaging. PLoS ONE 5, e15710.

483. Moeller, S., Yacoub, E., Olman, C.A., Auerbach, E., Strupp, J., Harel, N., and Uğurbil, K. (2010). Multiband multislice GE-EPI at 7 tesla, with 16-fold acceleration using partial parallel imaging with application to high spatial and temporal whole-brain fMRI. Magn Reson Med 63, 1144–1153.

484. Setsompop, K., Gagoski, B.A., Polimeni, J.R., Witzel, T., Wedeen, V.J., and Wald, L.L. (2012). Blipped-controlled aliasing in parallel imaging for simultaneous multislice echo planar imaging with reduced g-factor penalty. Magn Reson Med 67, 1210–1224.

485. Setsompop, K., Cohen-Adad, J., Gagoski, B.A., Raij, T., Yendiki, A., Keil, B., Wedeen, V.J., and Wald, L.L. (2012). Improving diffusion MRI using simultaneous multi-slice echo planar imaging. Neuroimage 63, 569–580.

486. Feinberg, D.A., and Setsompop, K. (2013). Ultra-fast MRI of the human brain with simultaneous multi-slice imaging. J. Magn. Reson. 229, 90–100.

487. Witzel, T., Polimeni, J.R., Wiggins, G., Lin, F., Biber, S., Hamm, M., Seethamraju, R., and Wald, L. (2008). Single-shot echo-volumar imaging using highly parallel detection,. Proceedings of International Society for Magnetic Resonance in Medicine 1387, 2367.

488. Lee, H.-L., Zahneisen, B., Hugger, T., LeVan, P., and Hennig, J. (2013). Tracking dynamic resting-state networks at higher frequencies using MR-encephalography. Neuroimage 65, 216–222.

489. Pfeuffer, J., McCullough, J.C., Van de Moortele, P.F., Ugurbil, K., and Hu, X. (2003). Spatial dependence of the nonlinear BOLD response at short stimulus duration. Neuroimage 18, 990–1000.

490. De Martino, F., Zimmermann, J., Muckli, L., Ugurbil, K., Yacoub, E., and Goebel, R. (2013). Cortical depth dependent functional responses in humans at 7T: improved specificity with 3D GRASE. PLoS ONE 8, e60514.

491. Siero, J.C.W., Petridou, N., Hoogduin, H., Luijten, P.R., and Ramsey, N.F. (2011). Cortical depth-dependent temporal dynamics of the BOLD response in the human brain. J. Cereb. Blood Flow Metab. 31, 1999–2008.

492. Sánchez-Panchuelo, R.M., Francis, S.T., Schluppeck, D., and Bowtell, R.W. (2012). Correspondence of human visual areas identified using functional and anatomical MRI in vivo at 7 T. J Magn Reson Imaging 35, 287–299.

493. Wald, L.L. (2012). The future of acquisition speed, coverage, sensitivity, and resolution. Neuroimage 62, 1221–1229.

494. Landis, S.C., Amara, S.G., Asadullah, K., Austin, C.P., Blumenstein, R., Bradley, E.W., Crystal, R.G., Darnell, R.B., Ferrante, R.J., Fillit, H., Finkelstein, R., Fisher, M., Gendelman, H.E., Golub, R.M., Goudreau, J.L., Gross, R.A., Gubitz, A.K., Hesterlee, S.E., Howells, D.W., Huguenard, J., Kelner, K., Koroshetz, W., Krainc, D., Lazic, S.E., Levine, M.S., Macleod, M.R., McCall, J.M., Moxley, R.T., 3rd, Narasimhan, K., Noble, L.J., Perrin, S., Porter, J.D., Steward, O., Unger, E., Utz, U., and Silberberg, S.D. (2012). A call for transparent reporting to optimize the predictive value of preclinical research. Nature 490, 187–191.

495. Schenck, J.F. (2005). Physical interactions of static magnetic fields with living tissues. Prog. Biophys. Mol. Biol. 87, 185–204.

496. Schenck, J.F. (2000). Safety of strong, static magnetic fields. J Magn Reson Imaging 12, 2–19.

497. Poole, M., and Bowtell, R. (2007). Novel gradient coils designed using a boundary element method. Concepts Magn. Reson. 31B, 162–175.

498. Pene, F., Courtine, E., Cariou, A., and Mira, J.-P. (2009). Toward theragnostics. Crit. Care Med. 37, S50–58.

499. Jeelani, S., Reddy, R.C.J., Maheswaran, T., Asokan, G.S., Dany, A., and Anand, B. (2014). Theranostics: A treasured tailor for tomorrow. J Pharm Bioallied Sci 6, S6–8.

500. Loane, D.J., and Faden, A.I. (2010). Neuroprotection for traumatic brain injury: translational challenges and emerging therapeutic strategies. Trends Pharmacol. Sci. 31, 596–604.

501. Goldstein, M.E., Sternberger, N.H., and Sternberger, L.A. (1987). Phosphorylation protects neurofilaments against proteolysis. J. Neuroimmunol. 14, 149–160.

502. Nixon, R.A., and Sihag, R.K. (1991). Neurofilament phosphorylation: a new look at regulation and function. Trends Neurosci. 14, 501–506.

503. Hall, G.F., and Lee, V.M. (1995). Neurofilament sidearm proteolysis is a prominent early effect of axotomy in lamprey giant central neurons. J. Comp. Neurol. 353, 38–49.

504. Gaskin, F., Cantor, C.R., and Shelanski, M.L. (1975). Biochemical studies on the in vitro assembly and disassembly of microtubules. Ann. N. Y. Acad. Sci. 253, 133–146.

505. Nishida, E., and Sakai, H. (1977). Calcium-sensitivity of the microtubule reassembly system. Difference between crude brain extract and purified microtubular proteins. J. Biochem. 82, 303–306.

506. Job, D., Fischer, E.H., and Margolis, R.L. (1981). Rapid disassembly of cold-stable microtubules by calmodulin. Proc. Natl. Acad. Sci. U.S.A. 78, 4679–4682.

507. Burns, N.R., and Gratzer, W.B. (1985). Interaction of calmodulin with the red cell and its membrane skeleton and with spectrin. Biochemistry 24, 3070–3074.

508. Sobue, K., Kanda, K., Adachi, J., and Kakiuchi, S. (1983). Calmodulin-binding proteins that interact with actin filaments in a Ca2+-dependent flip-flop manner: survey in brain and secretory tissues. Proc. Natl. Acad. Sci. U.S.A. 80, 6868–6871.

509. Kampfl, A., Posmantur, R.M., Zhao, X., Schmutzhard, E., Clifton, G.L., and Hayes, R.L. (1997). Mechanisms of calpain proteolysis following traumatic brain injury: implications for pathology and therapy: implications for pathology and therapy: a review and update. J. Neurotrauma 14, 121–134.

510. Wang, K.K. (2000). Calpain and caspase: can you tell the difference? Trends Neurosci. 23, 20–26.

511. Büki, A., Okonkwo, D.O., Wang, K.K., and Povlishock, J.T. (2000). Cytochrome c release and caspase activation in traumatic axonal injury. J. Neurosci. 20, 2825–2834.

512. Pettus, E.H., and Povlishock, J.T. (1996). Characterization of a distinct set of intra-axonal ultrastructural changes associated with traumatically induced alteration in axolemmal permeability. Brain Res. 722, 1–11.

513. Lee, B., and Newberg, A. (2005). Neuroimaging in Traumatic Brain Imaging. NeuroRx 2, 372–383.

514. Smits, M., Dippel, D.W.J., de Haan, G.G., Dekker, H.M., Vos, P.E., Kool, D.R., Nederkoorn, P.J., Hofman, P.A.M., Twijnstra, A., Tanghe, H.L.J., and Hunink, M.G.M. (2005). External validation of the Canadian CT Head Rule and the New Orleans Criteria for CT scanning in patients with minor head injury. JAMA 294, 1519–1525.

515. Ebinger, M., Winter, B., Wendt, M., Weber, J.E., Waldschmidt, C., Rozanski, M., Kunz, A., Koch, P., Kellner, P.A., Gierhake, D., Villringer, K., Fiebach, J.B., Grittner, U., Hartmann, A., Mackert, B.-M., Endres, M., Audebert, H.J., and STEMO Consortium. (2014). Effect of the use of ambulance-based thrombolysis on time to thrombolysis in acute ischemic stroke: a randomized clinical trial. JAMA 311, 1622–1631.

516. Saver, J.L., Fonarow, G.C., Smith, E.E., Reeves, M.J., Grau-Sepulveda, M.V., Pan, W., Olson, D.M., Hernandez, A.F., Peterson, E.D., and Schwamm, L.H. (2013). Time to treatment with intravenous tissue plasminogen activator and outcome from acute ischemic stroke. JAMA 309, 2480–2488.

517. Kim, D.S., Kong, M.H., Jang, S.Y., Kim, J.H., Kang, D.S., and Song, K.Y. (2013). The usefulness of brain magnetic resonance imaging with mild head injury and the negative findings of brain computed tomography. J Korean Neurosurg Soc 54, 100–106.

518. Coles, J.P. (2007). Imaging after brain injury. Br J Anaesth 99, 49–60.

519. Narayana, P.A., Yu, X., Hasan, K.M., Wilde, E.A., Levin, H.S., Hunter, J.V., Miller, E.R., Patel, V.K.S., Robertson, C.S., and McCarthy, J.J. ([date unknown]). Multi-modal MRI of mild traumatic brain injury. NeuroImage: Clinical .

520. Niogi, S.N., and Mukherjee, P. (2010). Diffusion tensor imaging of mild traumatic brain injury. J Head Trauma Rehabil 25, 241–255.

521. Langfitt, T.W., Obrist, W.D., Alavi, A., Grossman, R.I., Zimmerman, R., Jaggi, J., Uzzell, B., Reivich, M., and Patton, D.R. (1986). Computerized tomography, magnetic resonance imaging, and positron emission tomography in the study of brain trauma. Preliminary observations. J. Neurosurg. 64, 760–767.

522. Kim, H.J. (2012). The prognostic factors related to traumatic brain stem injury. J Korean Neurosurg Soc 51, 24–30.

523. Karantanas, A.H., Komnos, A., Paterakis, K., and Hadjigeorgiou, G. (2005). Differences between CT and MR imaging in acute closed head injuries. CMIG Extra: Cases 29, 1–8.

524. Cristen D. LaPierre, Mathieu Sarracanie, Jonathan Polimeni, Lawrence L. Wald, and Matthew S. Rosen. ([date unknown]). Parallel Imaging and Acceleration in the Johnson Noise Dominated Regime.

525. Mathieu Sarracanie. ([date unknown]). Low-cost MRI enable by Sparse Sampling and Quantum Control. In preparation .

526. Cooley, C.Z., Stockmann, J.P., Armstrong, B.D., Sarracanie, M., Lev, M.H., Rosen, M.S., and Wald, L.L. (2014). Two-dimensional imaging in a lightweight portable MRI scanner without gradient coils. Magn Reson Med .

527. Jagannathan, J., Sanghvi, N.T., Crum, L.A., Yen, C.-P., Medel, R., Dumont, A.S., Sheehan, J.P., Steiner, L., Jolesz, F., and Kassell, N.F. (2009). High-intensity focused ultrasound surgery of the brain: part 1--A historical perspective with modern applications. Neurosurgery 64, 201–210; discussion 210–211.

528. Meairs, S., Daffertshofer, M., Neff, W., Eschenfelder, C., and Hennerici, M. (2000). Pulse-inversion contrast harmonic imaging: ultrasonographic assessment of cerebral perfusion. Lancet 355, 550–551.

529. Tyler, W.J., Tufail, Y., Finsterwald, M., Tauchmann, M.L., Olson, E.J., and Majestic, C. (2008). Remote excitation of neuronal circuits using low-intensity, low-frequency ultrasound. PLoS ONE 3, e3511.

530. Tufail, Y., Matyushov, A., Baldwin, N., Tauchmann, M.L., Georges, J., Yoshihiro, A., Tillery, S.I.H., and Tyler, W.J. (2010). Transcranial pulsed ultrasound stimulates intact brain circuits. Neuron 66, 681–694.

531. Yoo, S.-S., Bystritsky, A., Lee, J.-H., Zhang, Y., Fischer, K., Min, B.-K., McDannold, N.J., Pascual-Leone, A., and Jolesz, F.A. (2011). Focused ultrasound modulates region-specific brain activity. Neuroimage 56, 1267–1275.

532. Deffieux, T., Younan, Y., Wattiez, N., Tanter, M., Pouget, P., and Aubry, J.-F. (2013). Low-intensity focused ultrasound modulates monkey visuomotor behavior. Curr. Biol. 23, 2430–2433.

533. King, R.L., Brown, J.R., and Pauly, K.B. (2014). Localization of ultrasound-induced in vivo neurostimulation in the mouse model. Ultrasound Med Biol 40, 1512–1522.

534. Mehić, E., Xu, J.M., Caler, C.J., Coulson, N.K., Moritz, C.T., and Mourad, P.D. (2014). Increased anatomical specificity of neuromodulation via modulated focused ultrasound. PLoS ONE 9, e86939.

535. Legon, W., Sato, T.F., Opitz, A., Mueller, J., Barbour, A., Williams, A., and Tyler, W.J. (2014). Transcranial focused ultrasound modulates the activity of primary somatosensory cortex in humans. Nat. Neurosci. 17, 322–329.

536. Landman, B.A., Huang, A.J., Gifford, A., Vikram, D.S., Lim, I.A.L., Farrell, J.A.D., Bogovic, J.A., Hua, J., Chen, M., Jarso, S., Smith, S.A., Joel, S., Mori, S., Pekar, J.J., Barker, P.B., Prince, J.L., and van Zijl, P.C.M. (2011). Multi-parametric neuroimaging reproducibility: a 3-T resource study. Neuroimage 54, 2854–2866.

537. Khan, U.A., Liu, L., Provenzano, F.A., Berman, D.E., Profaci, C.P., Sloan, R., Mayeux, R., Duff, K.E., and Small, S.A. (2014). Molecular drivers and cortical spread of lateral entorhinal cortex dysfunction in preclinical Alzheimer's disease. Nat. Neurosci. 17, 304–311.

538. Narayan, R.K., Michel, M.E., Ansell, B., Baethmann, A., Biegon, A., Bracken, M.B., Bullock, M.R., Choi, S.C., Clifton, G.L., Contant, C.F., Coplin, W.M., Dietrich, W.D., Ghajar, J., Grady, S.M., Grossman, R.G., Hall, E.D., Heetderks, W., Hovda, D.A., Jallo, J., Katz, R.L., Knoller, N., Kochanek, P.M., Maas, A.I., Majde, J., Marion, D.W., Marmarou, A., Marshall, L.F., McIntosh, T.K., Miller, E., Mohberg, N., Muizelaar, J.P., Pitts, L.H., Quinn, P., Riesenfeld, G., Robertson, C.S., Strauss, K.I., Teasdale, G., Temkin, N., Tuma, R., Wade, C., Walker, M.D., Weinrich, M., Whyte, J., Wilberger, J., Young, A.B., and Yurkewicz, L. (2002). Clinical trials in head injury. J. Neurotrauma 19, 503–557.

539. Armin, S.S., Colohan, A.R.T., and Zhang, J.H. (2006). Traumatic subarachnoid hemorrhage: our current understanding and its evolution over the past half century. Neurol. Res. 28, 445–452.

540. Gahm, C., Holmin, S., and Mathiesen, T. (2002). Nitric oxide synthase expression after human brain contusion. Neurosurgery 50, 1319–1326.

541. Silver, J.M., McAllister, T.W., and Yudofsky, S.C. (2011). Textbook of Traumatic Brain Injury. American Psychiatric Pub, 688 p.

542. Khaldi, A., Chiueh, C.C., Bullock, M.R., and Woodward, J.J. (2002). The significance of nitric oxide production in the brain after injury. Ann. N. Y. Acad. Sci. 962, 53–59.

543. Whitmore, R.G., Thawani, J.P., Grady, M.S., Levine, J.M., Sanborn, M.R., and Stein, S.C. (2012). Is aggressive treatment of traumatic brain injury cost-effective? J. Neurosurg. 116, 1106–1113.

544. Sarracanie, M., Armstrong, B.D., Stockmann, J., and Rosen, M.S. (2013). High speed 3D overhauser-enhanced MRI using combined b-SSFP and compressed sensing. Magn Reson Med .

545. Matthew Rosen, Mathieu Sarracanie, Brandon Armstrong, Fanny Herisson, Najat Salameh, and Cenk Ayata. ([date unknown]). Overhauser-enhanced MRI as a Non-invasive Probe of BBB Breakdown and Redox State in Stroke.

546. Huber-Wagner, S., Lefering, R., Qvick, L.-M., Körner, M., Kay, M.V., Pfeifer, K.-J., Reiser, M., Mutschler, W., Kanz, K.-G., and Working Group on Polytrauma of the German Trauma Society. (2009). Effect of whole-body CT during trauma resuscitation on survival: a retrospective, multicentre study. Lancet 373, 1455–1461.

547. Evans, J.D., Politte, D.G., Whiting, B.R., O'Sullivan, J.A., and Williamson, J.F. (2011). Noise-resolution tradeoffs in x-ray CT imaging: a comparison of penalized alternating minimization and filtered backprojection algorithms. Med Phys 38, 1444–1458.

548. Renker, M., Nance, J.W., Schoepf, U.J., O'Brien, T.X., Zwerner, P.L., Meyer, M., Kerl, J.M., Bauer, R.W., Fink, C., Vogl, T.J., and Henzler, T. (2011). Evaluation of heavily calcified vessels with coronary CT angiography: comparison of iterative and filtered back projection image reconstruction. Radiology 260, 390–399.

549. Rapalino, O., Kamalian, S., Kamalian, S., Payabvash, S., Souza, L.C.S., Zhang, D., Mukta, J., Sahani, D.V., Lev, M.H., and Pomerantz, S.R. (2012). Cranial CT with adaptive statistical iterative reconstruction: improved image quality with concomitant radiation dose reduction. AJNR Am J Neuroradiol 33, 609–615.

550. Korn, A., Fenchel, M., Bender, B., Danz, S., Hauser, T.K., Ketelsen, D., Flohr, T., Claussen, C.D., Heuschmid, M., Ernemann, U., and Brodoefel, H. (2012). Iterative reconstruction in head CT: image quality of routine and low-dose protocols in comparison with standard filtered back-projection. AJNR Am J Neuroradiol 33, 218–224.

551. Vorona, G.A., Zuccoli, G., Sutcavage, T., Clayton, B.L., Ceschin, R.C., and Panigrahy, A. (2013). The use of adaptive statistical iterative reconstruction in pediatric head CT: a feasibility study. AJNR Am J Neuroradiol 34, 205–211.

552. Hara, A.K., Paden, R.G., Silva, A.C., Kujak, J.L., Lawder, H.J., and Pavlicek, W. (2009). Iterative reconstruction technique for reducing body radiation dose at CT: feasibility study. AJR Am J Roentgenol 193, 764–771.

553. Prakash, P., Kalra, M.K., Ackman, J.B., Digumarthy, S.R., Hsieh, J., Do, S., Shepard, J.-A.O., and Gilman, M.D. (2010). Diffuse lung disease: CT of the chest with adaptive statistical iterative reconstruction technique. Radiology 256, 261–269.

554. Sagara, Y., Hara, A.K., Pavlicek, W., Silva, A.C., Paden, R.G., and Wu, Q. (2010). Abdominal CT: comparison of low-dose CT with adaptive statistical iterative reconstruction and routine-dose CT with filtered back projection in 53 patients. AJR Am J Roentgenol 195, 713–719.

555. Somenkov, V., Tkalich, A., and Shil'shtein, S. (1997). Refraction contrast in x-ray introscopy. Soviet Physics. Technical Physics 36, 2015–2025.

556. Momose, A., Takeda, T., Itai, Y., and Hirano, K. (1996). Phase-contrast X-ray computed tomography for observing biological soft tissues. Nat. Med. 2, 473–475.

557. Tapfer, A., Bech, M., Velroyen, A., Meiser, J., Mohr, J., Walter, M., Schulz, J., Pauwels, B., Bruyndonckx, P., Liu, X., Sasov, A., and Pfeiffer, F. (2012). Experimental results from a preclinical X-ray phase-contrast CT scanner. Proc. Natl. Acad. Sci. U.S.A. 109, 15691–15696.

558. Grubb, A., Walsh, P., Lambe, N., Murrells, T., and Robinson, S. (1996). Survey of British clinicians' views on management of patients in persistent vegetative state. Lancet 348, 35–40.

559. Mac Donald, C.L., Johnson, A.M., Cooper, D., Nelson, E.C., Werner, N.J., Shimony, J.S., Snyder, A.Z., Raichle, M.E., Witherow, J.R., Fang, R., Flaherty, S.F., and Brody, D.L. (2011). Detection of blast-related traumatic brain injury in U.S. military personnel. N. Engl. J. Med. 364, 2091–2100.

560. Sidaros, A., Engberg, A.W., Sidaros, K., Liptrot, M.G., Herning, M., Petersen, P., Paulson, O.B., Jernigan, T.L., and Rostrup, E. (2008). Diffusion tensor imaging during recovery from severe traumatic brain injury and relation to clinical outcome: a longitudinal study. Brain 131, 559–572.

561. Tollard, E., Galanaud, D., Perlbarg, V., Sanchez-Pena, P., Le Fur, Y., Abdennour, L., Cozzone, P., Lehericy, S., Chiras, J., and Puybasset, L. (2009). Experience of diffusion tensor imaging and 1H spectroscopy for outcome prediction in severe traumatic brain injury: Preliminary results. Crit. Care Med. 37, 1448–1455.

562. Pagani, E., Hirsch, J.G., Pouwels, P.J.W., Horsfield, M.A., Perego, E., Gass, A., Roosendaal, S.D., Barkhof, F., Agosta, F., Rovaris, M., Caputo, D., Giorgio, A., Palace, J., Marino, S., De Stefano, N., Ropele, S., Fazekas, F., and Filippi, M. (2010). Intercenter differences in diffusion tensor MRI acquisition. J Magn Reson Imaging 31, 1458–1468.

563. Logothetis, N.K., Pauls, J., Augath, M., Trinath, T., and Oeltermann, A. (2001). Neurophysiological investigation of the basis of the fMRI signal. Nature 412, 150–157.

564. Heeger, D.J., and Ress, D. (2002). What does fMRI tell us about neuronal activity? Nat. Rev. Neurosci. 3, 142–151.

565. Arthurs, O.J., and Boniface, S. (2002). How well do we understand the neural origins of the fMRI BOLD signal? Trends Neurosci. 25, 27–31.

566. Jantzen, K.J. (2010). Functional magnetic resonance imaging of mild traumatic brain injury. J Head Trauma Rehabil 25, 256–266.

567. Barnes, S.R.S., Haacke, E.M., Ayaz, M., Boikov, A.S., Kirsch, W., and Kido, D. (2011). Semiautomated detection of cerebral microbleeds in magnetic resonance images. Magn Reson Imaging 29, 844–852.

568. Kuijf, H.J., Brundel, M., de Bresser, J., van Veluw, S.J., Heringa, S.M., Viergever, M.A., Biessels, G.J., and Vincken, K.L. (2013). Semi-Automated Detection of Cerebral Microbleeds on 3.0 T MR Images. PLoS ONE 8, e66610.

569. Kuijf, H.J., de Bresser, J., Geerlings, M.I., Conijn, M.M.A., Viergever, M.A., Biessels, G.J., and Vincken, K.L. (2012). Efficient detection of cerebral microbleeds on 7.0 T MR images using the radial symmetry transform. Neuroimage 59, 2266–2273.

570. Diaz-Arrastia, R. (2014). Brain Oxygen Optimization in Severe TBI. Miami.

571. Powers, W.J., Grubb, R.L., Darriet, D., and Raichle, M.E. (1985). Cerebral blood flow and cerebral metabolic rate of oxygen requirements for cerebral function and viability in humans. J. Cereb. Blood Flow Metab. 5, 600–608.

572. Powers, W.J. (1991). Cerebral hemodynamics in ischemic cerebrovascular disease. Ann. Neurol. 29, 231–240.

573. Beaney, R.P., Lammertsma, A.A., Jones, T., McKenzie, C.G., and Halnan, K.E. (1984). Positron emission tomography for in-vivo measurement of regional blood flow, oxygen utilisation, and blood volume in patients with breast carcinoma. Lancet 1, 131–134.

574. Benaron, D.A., Benitz, W.E., Ariagno, R.L., and Stevenson, D.K. (1992). Noninvasive methods for estimating in vivo oxygenation. Clin Pediatr (Phila) 31, 258–273.

575. Buxton, D.B., Nienaber, C.A., Luxen, A., Ratib, O., Hansen, H., Phelps, M.E., and Schelbert, H.R. (1989). Noninvasive quantitation of regional myocardial oxygen

consumption in vivo with [1-11C]acetate and dynamic positron emission tomography. Circulation 79, 134–142.

576. Derdeyn, C.P. (2005). Positron emission tomography imaging of cerebral ischemia. Neuroimaging Clin. N. Am. 15, 341–350, x–xi.

577. Khan, N., Williams, B.B., Hou, H., Li, H., and Swartz, H.M. (2007). Repetitive tissue pO2 measurements by electron paramagnetic resonance oximetry: current status and future potential for experimental and clinical studies. Antioxid. Redox Signal. 9, 1169–1182.

578. Madsen, P.L., and Secher, N.H. (1999). Near-infrared oximetry of the brain. Prog. Neurobiol. 58, 541–560.

579. Schelbert, H.R. (1994). Blood flow and metabolism by PET. Cardiol Clin 12, 303–315.

580. Thorniley, M.S., Houston, R., Wickramasinghe, Y.A., and Rolfe, P. (1990). Application of near-infrared spectroscopy for the assessment of the oxygenation level of myoglobin and haemoglobin in cardiac muscle in vivo. Biochem. Soc. Trans. 18, 1195–1196.

581. Thorniley, M.S., Livera, L.N., Wickramasinghe, Y.A., Spencer, S.A., and Rolfe, P. (1990). The non-invasive monitoring of cerebral tissue oxygenation. Adv. Exp. Med. Biol. 277, 323–334.

582. Torres Filho, I.P., Terner, J., Pittman, R.N., Proffitt, E., and Ward, K.R. (2008). Measurement of hemoglobin oxygen saturation using Raman microspectroscopy and 532-nm excitation. J. Appl. Physiol. 104, 1809–1817.

583. An, H., and Lin, W. (2000). Quantitative measurements of cerebral blood oxygen saturation using magnetic resonance imaging. J. Cereb. Blood Flow Metab. 20, 1225–1236.

584. An, H., and Lin, W. (2002). Cerebral oxygen extraction fraction and cerebral venous blood volume measurements using MRI: effects of magnetic field variation. Magn Reson Med 47, 958–966.

585. An, H., Lin, W., Celik, A., and Lee, Y.Z. (2001). Quantitative measurements of cerebral metabolic rate of oxygen utilization using MRI: a volunteer study. NMR Biomed 14, 441–447.

586. Chien, D., Levin, D.L., and Anderson, C.M. (1994). MR gradient echo imaging of intravascular blood oxygenation: T2* determination in the presence of flow. Magn Reson Med 32, 540–545.

587. Golay, X., Silvennoinen, M.J., Zhou, J., Clingman, C.S., Kauppinen, R.A., Pekar, J.J., and van Zij, P.C. (2001). Measurement of tissue oxygen extraction ratios from venous blood T(2): increased precision and validation of principle. Magn Reson Med 46, 282–291.

588. He, X., Zhu, M., and Yablonskiy, D.A. (2008). Validation of oxygen extraction fraction measurement by qBOLD technique. Magn Reson Med 60, 882–888.

589. He, X., and Yablonskiy, D.A. (2007). Quantitative BOLD: mapping of human cerebral deoxygenated blood volume and oxygen extraction fraction: default state. Magn Reson Med 57, 115–126.

590. Hoppel, B.E., Weisskoff, R.M., Thulborn, K.R., Moore, J.B., Kwong, K.K., and Rosen, B.R. (1993). Measurement of regional blood oxygenation and cerebral hemodynamics. Magn Reson Med 30, 715–723.

591. Li, D., Waight, D.J., and Wang, Y. (1998). In vivo correlation between blood T2* and oxygen saturation. J Magn Reson Imaging 8, 1236–1239.

592. Li, D., Wang, Y., and Waight, D.J. (1998). Blood oxygen saturation assessment in vivo using T2* estimation. Magn Reson Med 39, 685–690.

593. Lu, H., and Ge, Y. (2008). Quantitative evaluation of oxygenation in venous vessels using T2-Relaxation-Under-Spin-Tagging MRI. Magn Reson Med 60, 357–363.

594. Qin, Q., Grgac, K., and van Zijl, P.C.M. (2011). Determination of whole-brain oxygen extraction fractions by fast measurement of blood T(2) in the jugular vein. Magn Reson Med 65, 471–479.

595. Oja, J.M., Gillen, J.S., Kauppinen, R.A., Kraut, M., and van Zijl, P.C. (1999). Determination of oxygen extraction ratios by magnetic resonance imaging. J. Cereb. Blood Flow Metab. 19, 1289–1295.

596. Van Zijl, P.C., Ulug, A.M., Eleff, S.M., Ulatowski, J.A., Traystman, R.J., Oja, J.M., and Kauppinen, R.A. (1998). [Quantitative assessment of blood flow, blood volume and blood oxygenation effects in functional magnetic resonance imaging]. Duodecim 114, 808–809.

597. Wright, G.A., Hu, B.S., and Macovski, A. (1991). 1991 I.I. Rabi Award. Estimating oxygen saturation of blood in vivo with MR imaging at 1.5 T. J Magn Reson Imaging 1, 275–283.

598. Weisskoff, R., Kiihne, S., Cohen, M., and Thulborn, K. (1991). Quantitative in vivo blood oxygenation measurements by echo planar imaging at 1.5 Tesla. San Francisco, CA.

599. Xu, F., Ge, Y., and Lu, H. (2009). Noninvasive quantification of whole-brain cerebral metabolic rate of oxygen (CMRO2) by MRI. Magn Reson Med 62, 141–148.

600. Sedlacik, J., Rauscher, A., and Reichenbach, J.R. (2009). Quantification of modulated blood oxygenation levels in single cerebral veins by investigating their MR signal decay. Z Med Phys 19, 48–57.

601. Sedlacik, J., and Reichenbach, J.R. (2010). Validation of quantitative estimation of tissue oxygen extraction fraction and deoxygenated blood volume fraction in phantom and in vivo experiments by using MRI. Magn Reson Med 63, 910–921.

602. Yablonskiy, D.A., and Haacke, E.M. (1994). Theory of NMR signal behavior in magnetically inhomogeneous tissues: the static dephasing regime. Magn Reson Med 32, 749–763.

603. Yablonskiy, D.A., and Haacke, E.M. (1997). An MRI method for measuring T2 in the presence of static and RF magnetic field inhomogeneities. Magn Reson Med 37, 872–876.

604. Yablonskiy, D.A., Reinus, W.R., Stark, H., and Haacke, E.M. (1997). Quantitation of T2' anisotropic effects on magnetic resonance bone mineral density measurement. Magn Reson Med 37, 214–221.

605. Fernández-Seara, M.A., Techawiboonwong, A., Detre, J.A., and Wehrli, F.W. (2006). MR susceptometry for measuring global brain oxygen extraction. Magn Reson Med 55, 967–973.

606. Langham, M.C., Magland, J.F., Epstein, C.L., Floyd, T.F., and Wehrli, F.W. (2009). Accuracy and precision of MR blood oximetry based on the long paramagnetic cylinder approximation of large vessels. Magn Reson Med 62, 333–340.

607. Langham, M.C., Magland, J.F., Floyd, T.F., and Wehrli, F.W. (2009). Retrospective correction for induced magnetic field inhomogeneity in measurements of large-vessel hemoglobin oxygen saturation by MR susceptometry. Magn Reson Med 61, 626–633.

608. Liu, Y., Pu, Y., Fox, P.T., and Gao, J.H. (1999). Quantification of dynamic changes in cerebral venous oxygenation with MR phase imaging at 1.9 T. Magn Reson Med 41, 407–411.

609. Langham, M.C., Floyd, T.F., Mohler, E.R., Magland, J.F., and Wehrli, F.W. (2010). Evaluation of cuff-induced ischemia in the lower extremity by magnetic resonance oximetry. J. Am. Coll. Cardiol. 55, 598–606.

610. Haacke, E.M., Tang, J., Neelavalli, J., and Cheng, Y.C.N. (2010). Susceptibility mapping as a means to visualize veins and quantify oxygen saturation. J Magn Reson Imaging 32, 663–676.

611. Jensen-Kondering, U., and Böhm, R. (2013). Asymmetrically hypointense veins on T2*w imaging and susceptibility-weighted imaging in ischemic stroke. World J Radiol 5, 156–165.

612. Bullock, R., Zauner, A., Woodward, J.J., Myseros, J., Choi, S.C., Ward, J.D., Marmarou, A., and Young, H.F. (1998). Factors affecting excitatory amino acid release following severe human head injury. J. Neurosurg. 89, 507–518.